The Roles of the Robo2 and Robo3 Receptors in the Development of Cortical Interneurons

A thesis submitted to University College London for the degree of Doctor of Philosophy

by

Melissa Barber

Department of Cell and Developmental Biology
University College London
London WC1E 6BT
United Kingdom

March 2009

I, Melissa Barber, confirm that the
work presented here in this thesis is my own.
Where information has been derived from other sources,
I confirm that this has been indicated in the thesis.

……

ABSTRACT

This thesis focuses on the putative roles of the Robo2 and Robo3 receptors in regulating the development of cortical interneurons and Cajal-Retzius cells in the embryonic mouse forebrain. A detailed analysis of the expression patterns of the Robo3 receptor is elucidated for the first time. Further comparison of all three Robos with interneuron markers confirms that different populations of cortical interneurons express these receptors during development. The putative roles of the Robo2 and Robo3 receptors in specifying the total number and distribution of cortical interneurons during development is investigated *in vivo,* using transgenic mice deficient in these receptors. This analysis shows that removal of the Robo2 or Robo3 receptors alone does not result in significant changes in the total numbers or positioning of interneurons within the cortex, suggesting that these receptors are not involved in the ventral-dorsal tangential migration of interneurons from their origins within the ganglionic eminences to the cortex. However, both Robo2 and Robo3 receptors significantly regulate the morphology of migrating interneurons during development. Preliminary analysis in triple Robo mutant mice points to a complex interplay between these receptors, and highlights the importance of understanding the functional relationship between these. In addition, a population of pioneering Cajal-Retzius cells express Robo receptors during preplate stages of development. Analysis in single Robo mutant animals suggests that Robo2 has a role in determining the total numbers of (reelin immunopositive) Cajal-Retzius cells within the hippocampal cortex.

DEDICATIONS

For my loving and
supportive parents,
Richard and Anjali Barber,
and for my beautiful sister, Rowena.

ACKNOWLEDGEMENTS

I am sincerely grateful to Professor John G. Parnavelas, for his continuous supervision, inspiration and unwavering support, and for allowing me to carry out this work in his laboratory.

It is with deep gratitude and great fondness that I wish to thank Dr. William Andrews, for his ever-enduring help, guidance, and insight throughout the duration of my time within the laboratory. The animals used in this study were provided by Dr W. Andrews. The work presented here for the morphological analysis of migrating interneurons within the Robo3 and Robo triple mutants was carried out by Dr. W. Andrews.

Mary Antypa, Ana Carriboni, Francesca Chiara, Clare Faux, Gaelle Friocourt, Luis-Hernandez Rodrigo Miranda and Sonjia Rakić, I could not thank you enough for all your encouragement, continuous advice, discussions and friendships. Thanks to Dr. Sonjia Rakić for carrying out the carbocyanine dye injections in the investigations of the development of the thalamocortical and corticofugal tracts in Robo2 mutants; and to Luis-Hernández Miranda for preparing and staining the dissociated GAD67-GFP cultures.

I'm also grateful to Marg and Christine, Daniel, Chris and Jane at confocal, everyone at the AH, and Ian for their help and support and for making this study possible.

Thanks to Professor Murakami for his generous gift of the Robo antibodies and Dr. Alain Chédotal and Thomas Di Megglio for genotyping and supplying the Robo3 mutant and triple Robo mutant material used in this study.

Much acknowledgement is also given to the BBSRC for funding this studentship.

Last, but not least, thanks to Rowena and Julia for their reassurance, positive outlook and belief in me.

TABLE OF CONTENTS

INDEX OF FIGURES

INDEX OF TABLES

ABBREVIATIONS

Ab	Antibody
BrdU	5-bromo-2-deoxyuridine
BSA	Bovine serum albumen
CC	Copus callosum
CC(number)	Cytoplasmic conserved sequence
CF	Corticofugal
CGE	Caudal ganglionic eminence
CH	Cortical hem
ChP	Choroid plexus
CNS	Central nervous system
Comm	Commissural
CP	Cortical plate
CR	Cajal-Retzius
Cx	Cortex
DAPI	4',6-diamidino-2-phenylindole
DiA	4-(dihexadecylamino)styryl)-N-methylpyridium iodide
DiI	1, 1- dioctadecyl –3, 3, 3', 3'-tetramethylindocarbocyanine perchlorate
Dlx	Distal-less homeobox
DNA	Deoxyribonucleic acid
DRG	Dorsal root ganglion
dTh	Dorsal Thalamus
E(number)	Embryonic day
FCS	Fetal calf serum
Fx	Fornix
GABA	Gamma-amino-butyric acid
GAD	Glutamic acid decarboxylase
GE	Ganglionic eminence
GFP	Green fluorescent protein
H	Hippocampus
IC	Internal capsule
Ig	Immunoglobulin

IP	Intermediate progenitors
IZ	Intermediate zone
LGE	Lateral ganglionic eminence
LIZ	Lower intermediate zone
LOT	Lateral olfactory tract
LPOA	Lateral preoptic area
LRR	Leucine rich repeats
LV	Lateral ventricle
NAcc	Nucleus accumbens
NIH	National Institute of Health
NGS	Normal goat serum
NPY	Neuro-peptide Y
MGE	Medial ganglionic eminence
mRNA	Messenger ribonucleic acid
MS	Medial septum
MZ	Marginal zone
P<	Probability
P(number)	Postnatal day
PB	Phosphate buffer
PBS	Phosphate buffer saline
PCR	Polymerase chain reaction
PFA	Paraformaldehyde
Pir	Piriform cortex
POA	Preoptic area
PPL	Preplate layer
PV	Parvalbumin
Rb	Retinoblastoma
RGC	Radial glial cells
RNA	Ribonucleic acid
RT	Room temperature
S	Septum
SEM	Standard error mean
SP	Subplate

Str	Striatum
SVZ	Subventricular zone
TC	Thalamocortical
UIZ	Upper intermediate zone
µg	Microgram
µm	Micrometer
µM	Micromolar
vTh	Ventral thalamus
VZ	Ventricular zone

CHAPTER 1: INTRODUCTION

1.1 THE ADULT CEREBRAL CORTEX

The telencephalon is a highly organised and complex neuronal structure in the mammalian central nervous system (CNS). This constitutes the anterior portion of the forebrain (the prosencephalon) and is molecularly, and, histologically, divided into the pallium (dorsal forebrain) and subpallium (ventral forebrain). Regional expression of homeodomain proteins and other transcription factors, molecularly define the pallium (eg. Pax6, Emx1,2, Tbr1,2) and subpallium (eg. Gsh2, Nkx 2.1, Dlx1,2) (Stoykova & Gruss, 1994; Bulfone et al., 1995; Liu et al., 1997; Eisenstat et al., 1999; Puelles et al., 2000; Mallacami & Stoykova, 2006). The pallium is further molecularly subdivided into the medial, dorsal, lateral and ventral pallium, which will give rise to the hippocampus, neocortex, olfactory cortex and some nuclei of the amygdala, as well as to the calustrum-amygdalar complex, respectively. The subpallium comprises three main evaginations, the medial, lateral and caudal ganglionic eminences, which will give rise to the striatum, pallidum and amygdala respectively (Puelles et al., 2000, 2001; Donoghue et al., 1999).

A defining histological feature of the mammalian pallium is that, unlike the nuclear arrangement of cell bodies within the subpallium, neurons are organised into horizontal layers or laminae. Variations in the patterns of lamination further distinguish the pallial archicortex (hippocampal cortex), paleocortex (olfactory cortex) and neocortex; while the archicortex and paleocortex consist of two to three cell layers, neurons in the neocortex are arranged into six layers (Ramón y

Cajal, 1909, 1911; Puelles et al., 2000; Molnár et al., 2006). It is the evolution of the neocortex that specifically underlies, and is unique to, mammalian evolution.

Each cortical layer is distinguished by the composition, morphology, and density of its constituent neurons. Neurons within each lamina further exhibit specific patterns of connectivity. Thus, whilst neurons in layer V/VI of the neocortex predominately project to subcortical structures such as the thalamus, superior colliculus, spinal cord and pons, neurons in layers II/III project within the cortex of the same and contra-lateral hemispheres (Ram□n y Cajal, 1909, 1911; Jones, 1985; Peters & Jones, 1985). Another defining feature of the mammalian neocortex is its parcellation into distinct areas characterised by cytoarchitecture and function (Brodman, 1909; Donghue et al., 1999; Lukaszewicz et al., 2005).

Comparative anatomical studies in rodent, primate and human forebrain have shown an expansion and an associated increase in the cellular complexity of the cerebral cortex across mammalian species (Ramón y Cajal, 1909, 1911; Rakić, 2000, 2005; Molnár et al., 2006, 2007; Reviewed in Abdel-Mannan et al., 2008). An increase in the diversification of cortical areas is further correlated with the acquisition of more complex behaviours and higher cognitive abilities in mammals (Karlen & Krubitzer, 2006). This is poignant to the evolution of *homo sapiens*, in which the surface area of the neocortex expanded one thousand fold (Smart et al., 2002). The neocortex was divided into 47 distinct cortical areas by Brodmann in 1909. The neocortex is thought to underlie the acquisition of abilities such as language and consciousness which are so characteristic of

being human. Despite these intra- and inter-species differences in cortical cytoarchitecture, the cellular organisation of the adult neocortex is largely conserved across mammals.

1.1.1 The adult neocortex

Investigations into the cytoarchitecture of the mammalian neocortex were made possible by the refinement of the Golgi technique by Ramon y Cajal in the mid 1800's. These studies showed that what appeared to be a contiguous mass of connected neurons actually comprised separate neuronal entities, which were intricately interconnected through small extra cellular spaces or synapses (Ramon y Cajal, 1909, 1911). It is now well established that the six-layered neocortex indeed comprises assemblies of two major populations of neurons: the pyramidal projection neurons and the non-pyramidal interneurons.

1.1.1.1 Glutamatergic pyramidal neurons

Pyramidal neurons comprise approximately 70-80% of the total cortical neuronal population, and are morphologically characterised by their pyramidal shaped soma, apical dendrites and their extensive efferent axonal processes. These project over long distances reaching subcortical and distant cortical targets, and predominately use the excitatory neurotransmitter glutamate in their signalling (Parnavelas et al., 1989).

1.1.1.2 GABAergic interneurons

Interneurons comprise 20-30% of the total population of cortical neurons, however, these constitute a highly heterogeneous group. These are extremely

diverse in terms of their morphology, connectivity, chemical composition and electrophysiology and, as such, they have been difficult to classify. Despite these differences, interneurons share some common characteristics that distinguish them from pyramidal neurons. These 'short-axon neurons' have predominately aspiny dendrites and restrict their projections locally within the neocortex. Interneurons use the inhibitory γ-amino-butyric acid (GABA) as their main neurotransmitter, but they also express a complement of calcium binding proteins (such as parvalbumin, calbindin, calretinin) and/or neuropeptides (somatostatin, vasoactive intestinal peptide and neuropeptide-Y (Parnavelas et al., 1989; Ramón y Cajal, 1909, 1911; Cauli et al., 1997; Kawaguchi & Kubota, 1997; The Petilla Interneuron Nomenclature Group, 2008).

Differences in morphology and biochemical properties between pyramidal neurons and interneurons reflect their distinct roles: whilst pyramidal neurons provide the major excitatory synaptic input in the cortex and relay information over long distances to and from subcortical and cortical targets, interneurons locally modulate neural activity and provide the major inhibitory synaptic input within the cortex. A balance in the excitatory and inhibitory synaptic input is crucial to cortical functioning, and disturbances in this balance underlie various neurological conditions in humans such as schizophrenia, autism, and epilepsy (Lewis et al., 2005; Cobos et al., 2005; Di Cristo et al., 2007).

How all of the diverse neuronal subtypes are generated and how they 'find' their appropriate areal and laminar positions, and are integrated to form highly specific and functional neural circuits, are questions that are currently subject to

extensive investigations in neurobiology. An understanding of how the neocortex develops is thus not only of great theoretical importance, but is also clinically very relevant.

1.2 CORTICOGENESIS

1.2.1 Neurulation

Early fate mapping and induction studies have shown that the entire vertebrate CNS derives from the neurectoderm, an early specified germ layer which flattens into a sheet known as the neural plate during early embryogenesis (Reviewed in Rubenstein et al., 1998). The neural plate undergoes extensive morphogenetic movements and upfolds at its lateral edges to fuse along the dorsal midline and form the neural tube. In humans, the neural tube first fuses twenty-two days post ovulation (Carnegie Stage 10) (Meyer, 2007) and this occurs at approximately embryonic day (E) 9.5 in the developing mouse (Juriloff et al., 1991).

The neural tube initially comprises a single-celled layer of dividing neuroepithelial cells. Continuous proliferation of the neuroepithelium results in the formation of three vesicles at its anterior end, and it is the anterior-most vesicle, the prosencephalon, which will give rise to the future forebrain. The prosencephalic vesicle expands further, evaginating bilaterally by the second half of gestation to form the future telencephalic hemispheres, with the lumen comprising the developing lateral ventricles. It is the dorsal neuroepithelial surface of the telencephalon that will give rise to most of the neurons and glia of

the cerebral cortex and hippocampus (the dorsal and medial pallium, respectively), with the ventral neuroepithelium generating the basal ganglia, amygdala, and the olfactory bulb (the subpallium). Exceptions to this are populations of cortical interneurons (see Section 1.3) and the amygdaloid complex which is formed from both pallial and subpallial derivates. Whereas neuronal populations within the basolateral amygdaloid complex express the pallial marker Emx-1, regions of the medial and central amygdale express subpallial markers. Thus the basolateral amygdaloid complex is thought to derive from pallial regions near the pallial and subpallial boundary (Puelles et al., 2000; Puelles, 2001). More recently a caudal amygdaloid stream of neurons has been identified which migrates from the dorsal pallium in the caudal cortex to populate the amygdaloid nuclei of the lateral olfactory tract (Remedios et al., 2007).

How a morphologically homogenous single neuroepithelial layer gives rise to all of the diverse cortical neuronal subtypes (neurogenesis), and how these subsequently migrate to their appropriate laminar and areal positions to form the six-layered neocortex is a process known as corticogenesis.

1.2.2 Neurogenesis

Whilst there are species specific differences in cortical development, the main sequence of events is largely conserved across mammals and this has been well elucidated in the embryonic rodent forebrain, which will be the focus of this study. Corticogenesis proceeds in a temporal-spatial gradient of maturation starting anteriorly, with middle and posterior regions of the cortex lagging by up

to two days in the embryonic rodent (Raedler and Raedler, 1978). Early histological and proliferation studies using radioactive [^{3}H]Thymidine, which is incorporated into dividing cells, have shown that cell proliferation was restricted to compartments near the lateral ventricles. These observations importantly suggested that post-mitotic neurons migrated away from these domains to form the superficial developing cortical layers (Rakić et al., 1974). It is now well established that the development of the cortex is reflected by the progressive expansion and stratification of the cortical wall, with the main phase of neurogenesis (E10.5-E17.5) preceding gliogenesis (E17.5-postnatal life).

1.2.2.1 Neuroepithelial stem cells and radial glial cells

The dorsal neuroepithelial lining of the lateral ventricles thus initially comprises a single primary germinal layer. These highly proliferating neuroepithelial cells span the depth of the developing cortical wall, with their apical processes contacting the ventricular surface, and their long extending basal processes forming a 'plump triangular end foot' immediately beneath the pial membrane (Raedler and Raedler 1978). This region is also named the ventricular zone (VZ) due to its close proximity to the developing lateral ventricles (Bystron et al., 2008). Close microscopic examination of the VZ reveals that the positioning of the nuclei of the proliferating neuroepithelial cells are located at varying distances from the ventricular wall, thus giving this an appearance of a 'pseudostratified layer'.

It is now known that these cells undergo interkinetic nuclear migration, with their nuclei moving away from and towards the ventricular surface as they

progress through the cell cycle (Misson et al., 1988; Takahashi et al., 1996a). Thus, when a neuroepithelial cell undergoes DNA synthesis (S-phase), its nucleus is positioned at the basal surface of the VZ, and then moves through the apical process during G1 phase to become positioned adjacent to the ventricular surface during mitosis (M-phase). This then cycles back through the apical process during G2 phase to once again reach the outer margin of the VZ. These neuroepithelial 'stem cells' give rise to multipotent and more restricted intermediate neural progenitors throughout development, thereby generating most of the neurons and glia of the cerebral cortex (Malatesta et al., 2000, 2003; Noctor et al., 2001, 2002; Hartfuss et al., 2001; Miyata et al., 2001;).

Whilst little is known of the mechanisms which regulate the transition of neuroepithelial cells to multipotent neural progenitors, a predominant neural progenitor identified within the VZ is the radial glial cell (RGC) (Hartfuss et al., 2001; Miyata et al., 2001; Malatesta et al., 2000; Noctor et al., 2001, 2002). Neuroepithelial cells lose their epithelial characteristics and form multipotent RGC progenitors prior to the onset of neurogenesis. Similar to their neuroepithelial predecessors, RGCs are highly polarised cells and span the depth of the cortical wall, with their apical processes apposed to the ventricle, and their long extending basal process forming a lining below the pial membrane. These exhibit interkinetic nuclear migration, and undergo mitosis at the apical surface of the VZ. Their basal processes further provide a major migratory substrate during development (Miyata et al., 2001; Tamamaki et al., 2001; Noctor et al., 2001, 2004). Whereas various multipotent progenitors are suggested to exist within the primate VZ (see below), the RGC is posited to be

the predominant apical multipotent progenitor within the rodent (Noctor et al., 2008) VZ. Interestingly, an additional short neural precursor was more recently reported in the rodent VZ (Gal et al., 2006).

1.2.2.2 Intermediate progenitors

In addition to apically dividing multipotent progenitors (neuroepithelial, short neural precursor cells and RGCs), a major group of progenitors within the primate and rodent cortex are the intermediate progenitors. These progenitors were first observed by the study of Smart and others in 1973, which identified mitotic figures positioned in basal regions of the developing germinal compartments and intermediate zone of the embryonic mouse cortex. More recent time lapse imaging studies have confirmed that intermediate progenitors are derived from RGCs (Haubensak et al., 2004; Noctor et al., 2004; Miyata et al., 2004; Attardo et al., 2008), and undergo mitosis within basal positions of the developing germinal compartments (Smart et al., 1973; Haubensak et al., 2004; Noctor et al., 2004; Miyata et al., 2004; Carney et al., 2007; Noctor et al., 2008; Attardo et al., 2008; Kowalczyk et al., 2009). Intermediate progenitors differ from RGCs in their mode of division (Attardo et al., 2008, see below) and further exhibit a more restricted neurogenic potential, are of a multipolar morphology, and do not exhibit interkinetic nuclear migration. As neurogenesis proceeds, intermediate progenitors accumulate within the basal VZ and contribute to the development of a secondary germinal subventricular zone (SVZ), which forms during mid and late stages of neurogenesis in the rodent (E13.5-E17.5) (Smart et al., 1973; Takahashi et al., 1995; Haubensak et al., 2004; Miyata et al., 2004; Noctor et al., 2004; Kowalczyk et al., 2009).

1.2.2.3 Progenitor cell division

Progenitors adopt two main modes of cell division during cortical development. These divide symmetrically to generate two identical daughter cells or asymmetrically to give rise to two non-identical neurons (Mione et al., 1997; Noctor et al., 2002, 2004). During early stages of development, both neuroepithelial cells and RGCs divide symmetrically, thus expanding the progenitor pool. RGCs subsequently switch to an asymmetric mode of cell division and give rise to a proliferating 'mother cell' which remains in the VZ and inherits the radial glial fibre, and a post-mitotic daughter neuron which migrates away from the VZ along the parental glial fibre (Miyata et al., 2001; Tamamaki et al., 2001; Noctor et al., 2001, 2004) to form a compact layer of neurons, known as the developing cortical plate (CP). The CP will comprise future layers II to VI of the adult neocortex.

This switch in cell division marks the onset of neurogenesis (E10.5 in the mouse) (Bystron et al., 2008) and the proportion of asymmetrical divisions increases as neurogenesis proceeds (Takahashi et al., 1996b). RGCs subsequently divide asymmetrically to give rise to intermediate progenitors. Intermediate progenitors adopt a predominantly symmetric mode of division and generate two post-mitotic daughter neurons, or divide undergo self-renewing divisions to give rise to a pair of intermediate progenitors, thereby amplifying the progenitor pool (Attardo et al., 2008). Thus cortical neurons are generated either, directly, by the asymmetric division of neuroepithelial and RGCs at the apical surface of the VZ, or, indirectly, through intermediate progenitors which

divide symmetrically in abventricular positions within the VZ, SVZ and IZ. The significance of this two step mode of neurogenesis has been suggested to amplify the total neuronal output from a given RGC progenitor unit (Haubensak et al., 2004; Miyata et al., 2004; Noctor et al., 2004; Cheung et al., 2007; Hevner et al., 2008).

1.2.2.4 Significance of intermediate basal progenitors

While the roles of intermediate progenitors remain to be fully elucidated, several models have been put forth to explain their significance in cortical development and evolution (Reviewed in Pontious et al., 2008). The first model is consistent with the observation that intermediate progenitors migrate to form the SVZ layer at a time when upper layer (II-IV) neurons are generated (E13.5-E17.5 in the mouse) (Takahashi et al., 1995; Noctor et al., 2004, 2008; Haubensak et al. 2004; Miyata et al., 2004; Attardo et al., 2008). This model is based on the observations that expression of upper layer molecular markers within the SVZ (Svet1, Satb2, Cux1 and Cux2), coincide with, or shortly preceed, the generation of upper layer neurons (II-IV) (Takahashi et al., 1995, 1999; Tarabykin et al., 2001; Zimmer et al., 2004; Nieto et al., 2004; Reviewed in Hevner et al., 2008). This is further supported by studies carried out in transgenic mice deficient in the Pax6 transcription factor (expressed by RGCs) which show an early depletion of intermediate progenitors, and a reduction in Tbr2 cells (markers of intermediate progenitors); this results in a coincident reduction in upper layer neurons (Englund et al., 2005; Quinn et al., 2007) These studies suggested that intermediate progenitors comprise a separate lineage of progenitors, restricted to give rise to neurons of an upper laminar (II-IV) fate (Tarabykin et al., 2001;

Zimmer et al., 2004; Wu et al., 2005).

Recent time-lapse imaging studies have challenged the suggestion that intermediate progenitors exclusively give rise to upper layer cortical neurons. These studies show intermediate progenitors positioned within the basal VZ from the onset of neurogenesis, suggesting that they have a more protracted role during neurogenesis (Smart et al., 1973; Haubensak et al., 2004; Attardo et al., 2008; Reviewed in Hevner et al., 2008; Kowalczyk et al., 2009). Indeed, intermediate progenitors have a limited proliferative activity, of one to three mitotic cycles, and this is consistently maintained across species suggesting they transiently amplify neuronal output throughout neurogenesis, and do not establish separate lineages within the SVZ (Haubensak et al., 2004; Miyata et al., 2004; Noctor et al., 2004; Wu et al., 2005; Attardo et al., 2008; Pontious et al., 2008). Time lapse imaging studies combined with genetic tracing of specific progenitor lineages have indeed shown that most of the neurons of a lower laminar fate are generated by abventricular intermediate progenitors within the VZ from the onset of neurogenesis (E10.5 in the mouse); thus suggesting that intermediate progenitors (and not RGCs directly) give rise to the majority of projection neurons of both a lower and upper layer fates (Kowalczyk et al., 2009).

The observation that gyrencephalic mammals, with expanded cortical surface areas and disproportionately thicker supragranular layers, have a thickened SVZ led to the suggestion that intermediate progenitors may account for increases in neuronal output required in the expansion in cortical surface area, lamination

and thickness during development and evolution (Smart et al., 2002; Molnár et al., 2006; Bystron et al., 2008). Comparative studies across mammalian species has indeed shown a correlation between the expansion of the SVZ (comprising populations of intermediate progenitors) and an increased complexity of the supragranular layers of the cortex, as well as an increased cortical surface area in 'higher' mammals (Smart et al., 2002; Molnár et al., 2006). Indeed, the primate SVZ is more elaborate and easily distinguished at an earlier stage of corticogenesis than in the rodent; and is further compartmentalised into molecularly and histologically distinct domains by invading fibre tracts (Smart et al., 2002).

Interestingly, whereas the internal SVZ (closest to the VZ) contains rounded and non-epithelial-like progenitors which are molecularly (Tbr2) analogous to basal progenitors within the rodent cortex; the outer SVZ comprises cells which maintain a strict apical-basal polarity and molecularly (Pax6) resemble multipotent apical progenitors within the primate and rodent VZ (Smart et al., 2002; Fish et al., 2008). It has therefore been suggested that the distinct molecular compartments may provide additional progenitor niches, which may account for the increased neuronal complexity (numbers and diversity of neurons) observed in the primate supragranular layers (Cheung et al., 2007). Smart and colleagues (2002) indeed suggested that progenitors within the outer SVZ of the primate cortex may comprise apical progenitors which retain their apical-basal polarity but have lost their interkinetic nuclear migratory behaviour, and attachment to the apical VZ. It is interesting to note that this may be analogous to the short neural precursors identified in rodents (Gal et al.,

2006).Thus a duplication of an additional VZ-like domain (i.e. the OSVZ) may have arisen during primate evolution, and accounted for the increase in neuronal numbers and diversity in primates and humans. The elaborate SVZ in primates is suggested to reflect an increased diversity and number of the intermediate progenitor cell populations. Whether this accounts for the expanded cortical surface area during primate and human evolution remains to be confirmed. The SVZ in humans indeed is a much more heterogenous region, comprising glial as well as interneuron progenitors within the outer SVZ.

A third role for intermediate progenitors was postulated by Hevner et al. (2008). Hevner suggests that intermediate progenitors transiently amplify the neuronal output from a given radial glial unit throughout neurogenesis, and that intermediate progenitors have a functional role in determining cortical thickness in distinct cortical areas (and not cortical surface area). This is based on the observation that intermediate progenitors give rise to neurons of all cortical layers (Kowalczyk et al., 2009), and maintains that the number of RG units are the primary determinants of the tangential expansion of the developing cortex (Rakić, 2000). This model further suggests that intermediate progenitors confer a flexible system by which extrinsic signals may locally modulate the transient amplification/proliferation of intermediate progenitors, thereby enabling differences in cortical cytoarchitecture to be generated in distinct areas, from an initial radial unit template (Hevner et al., 2008, 2009). Proliferation studies within the primate cortex have shown that area 17 within the visual cortex exhibited greater proliferative activity than an adjacent cortical area 18, consistent with the local modulation of cell-cycle dynamics and proliferation of

progenitors within the local germinal epithelium. This further was correlated with an increased tangential expansion of area 17, thus suggesting that changes in the proliferative activity of intermediate progenitors can locally influence the cortical expansion of specific cortical areas (Lukaszewicz et al., 2005, 2006). Local modulation of proliferative activity within specific areas could be achieved by extrinsic cues, such as secreted mitogens from incoming thalamocortical afferents (Dehay et al., 1995, 2001). The positioning of the invading fibres within the SVZ may play a similar role in this germinal region (Smart et al., 2002).

In addition to basal intermediate progenitors within developing germinal domains, scattered extraventricular progenitors have been observed throughout neurogenesis in both the primate and rodent cortex (Carney et al., 2007, see below). The last decade has thus shown neurogenesis to be a much more complex process than previously believed, with post mitotic neurons derived from spatially distinct and diverse multipotent and intermediate progenitors.

1.2.3 Histological observations

The cortical wall thus initially comprises a single-celled proliferating VZ, rich in multipotent neuroepithelial and RGC progenitors (Fig. 1.1A). This bi-stratifies shortly after neurogenesis has commenced (~E10.5 in the mouse), with a polymorphous layer of differentiated neurons and neuropil forming above the VZ (~E11.5m-12.5m) (Fig. 1.1B-C). This primordial plexiform layer (Marín-Padilla 1978), now commonly named the preplate layer (PPL) (Bystron et al., 2008), comprises a highly heterogeneous and mostly transient population of

post-mitotic neurons (Fig. 1.1B-C) (Parnavelas and Edmunds, 1983; Edmunds and Parnavelas, 1982; Derer and Derer, 1990; Meyer et al., 1998). Some proliferating cells are also observed in basal regions of the VZ at this stage (Smart et al., 1973), and these intermediate progenitors contribute to a second superficial germinal domain, the SVZ (~E13.5 in the mouse) (Fig. 1.1B-C; see arrow in Fig. 1.2A) (Tarabykin et al., 2001; Zimmer et al., 2004; Nieto et al., 2004; Reviewed in Hevner et al., 2008). Whilst this is especially conspicuous in primates (as illustrated in Fig 1.1C), the SVZ is more clearly defined at a later stage in the developing rodent cortex (~E15.5m) (Fig. 1.2B). Early projections from the PPL extend towards the subpallium, forming an additional intermediate zone (IZ) above the proliferating domains (McConnell et al., 1989; Molnár et al., 1998; De Carlos and O'Leary 1992; Morante-Oria et al., 2003) (Fig. 1.1D).

1.2.3.1 Preplate splitting

As neurogenesis proceeds, continuous proliferation of progenitors within the VZ causes the cortical wall to stratify further, with a compact layer of neurons coalescing within the PPL (Fig. 1.1D-E). These correspond to the CP neurons which will form future layer VI of the mature neocortex, and these are first observed within the lateral regions of the developing cortex at embryonic day 13.5 in the mouse (see CP in Fig. 1.2A). Subsequent rounds of division result in the thickening of the CP, comprising layers II to V of the mature cortex (Fig. 1.1E, 1.2B).

It was Marín-Padilla who first suggested that the developing CP splits the PPL tangentially (Marín-Padilla 1978). The use of radioactive [^{3}H]-Thymidine,

which is incorporated into dividing cells, later confirmed that the PPL is tangentially split into an overlying marginal zone (MZ) (Bystron et al., 2008) and an underlying subplate (SP) layer by later born cohorts of neurons (Luskin and Shatz, 1985a; Raedler and Raedler 1978;). This results in the asymmetrical distribution of a pioneering population of neurons, the Cajal-Retzius (CR) cells, to the upper MZ layer where these reside throughout embryonic development (Edmunds and Parnavelas, 1982; Reviewed in Marín-Padilla, 1998).

1.2.3.2 Formation of the cortical plate

The developing CP comprises layers II to VI of the adult neocortex, and will contain assemblies of constituent projection neurons and interneurons. Thymidine labelling studies in the cat (Luskin and Shatz 1985b) and primate (Rakić et al., 1974) have shown that layers II to VI of the CP are in fact generated in an 'inside out' pattern, whereby later born neurons migrate past their predecessors to settle in more superficial positions, and it has subsequently been shown that the laminar fate of cortical neurons is temporally determined within the germinal neuroepithelium prior to their last mitotic division (McConnell and Kaznowski, 1991). While early thymidine labelling studies in the mouse similarly suggested that neurogenesis proceeds in an inverted gradient of development (Angevine and Sidman 1961), subsequent work has shown that there is considerable overlap in the generation of neurons of distinct laminar fates, with neurons of distinct laminar fates generated during the same period of neurogenesis (Takahashi et al., 1999; Hevner et al., 2003b). Thus while higher mammals, with protracted periods of neurogenesis, exhibit a strict temporal correlation of projection neurons birth date and their laminar fate, this is less

well correlated within the developing rodent cortex.

As the CP thickens, the SVZ expands and the VZ simultaneously retracts (Fig. 1.1C-E). The SVZ comprises intermediate progenitors that will give rise to upper layers of the developing CP (Frantz and McConnell, 1996; Tarabykin et al., 2001;Zimmer et al., 2004). CP neurons further extend projections away from the pia and towards the ventral forebrain, which results in the thickening of the intermediate zone (IZ) (Fig.1.1 E). The IZ is thus more easily distinguishable as the CP thickens, and reciprocal thalamocortical afferent projections also enter this layer. Thus, the IZ will comprise the future corticofugal and thalamocortical white matter tracts in the adult cortex. The main phase of neurogenesis is completed prenatally (E17.5 in the mouse), prior to the main phase of gliogenesis which extends into postnatal life (Privat et al., 1975).

The CP thus develops within a framework of the transient populations of pioneering MZ and SP neurons (Edmunds and Parnavelas, 1982; Marín-Padilla, 1998; Meyer et al., 1998), which have been suggested to have a role in orchestrating its development (Reviewed in Supèr et al., 1998). As mentioned previously, the CP is generated in a largely inverted sequence, and it has subsequently been shown that the laminar fate of cortical neurons is temporally determined within the germinal neuroepithelium, prior to their last mitotic division (McConnell and Kaznowski, 1991). In addition, several studies have suggested that CP neurons of an upper layer fate are generated by intermediate progenitors within the sub-ventricular germinal domains however this remains to be confirmed (Frantz and McConnell, 1996; Zimmer et al., 2004), and has

been challenged by recent imaging studies in the embryonic mouse which has shown that intermediate progenitors are in fact present from the onset of neurogenesis in basal regions of the mouse VZ (E10.5) and give rise to neurons of both an upper layer and lower layer fate (Reviewed in Hevner et al., 2008; Kowalczyk et al., 2009). Intermediate progenitor subtypes are distinct in their molecular characteristics, morphology and positioning within the cortical VZ and SVZ, and while their significance remains to be elucidated, these have been suggested to be the main neurogenic progenitors during development (Kowalczyk et al., 2009). Thus the specific intermediate progenitor subtypes within the VZ or SVZ should be taken into consideration when investigating the specification of the laminar fate of projection neurons.

Cajal-Retzius which are positioned within the upper MZ have also been shown to have a role in regulating the laminar patterning of the developing CP (Caviness and Sidman, 1973; Supèr et al., 2000) through their secretion of the extra-cellular matrix molecule reelin (D'Arcangelo et al., 1995; Ogawa et al., 1995). As mentioned previously, few of these pioneering neurons survive postnatally, resulting in the cell sparse layer I of the mature neocortex (Edmunds and Parnavelas, 1982; Derer and Derer, 1990; Meyer et al., 1998). The SP similarly comprises a transient layer of cells and is suggested to have an important role in guiding the development of reciprocal connections between the cortex and the thalamus (Ghosh et al., 1990**;** Molnár et al., 1998). Whilst most SP neurons do not survive postnatally in rodents, a few upper SP interstitial neurons remain to form layer VIb in higher mammals however the extent of cell death within this region remains controversial (Kostovic & Rakic et al., 1990;

reviewed in Allendoerfer and Shatz 1994).

More recent studies have shown that neurons are in fact continuously added to the MZ and SP layers throughout corticogenesis in the primate and rodent, which suggests that these neurons comprise a dynamic population of cells, and thus PPL splitting and corticogenesis may be a much more complex process than previously believed (Smart et al., 2002; Meyer, 2007; Costa et al., 2007; Carney et al., 2007). Additional proliferating cells outside of the VZ and SVZ have important implications in our understanding of corticogenesis. Interestingly, these are observed from preplate stages of development and maintained throughout cortico-neurogenesis, and were further observed to similar extents within both the developing rodent and human cortex. While some extraventricular proliferating cells were found to express microglial markers, the identification and fates remain to be fully elucidated. While these comprise a relatively small population, this raises interesting questions as to their significance during corticogenesis, as well as highlighting the extent of different progenitor niches observed during embryonic development (arrowhead in Fig 1.2A) (Carney et al., 2007; Costa et al., 2007; Meyer, 2007).

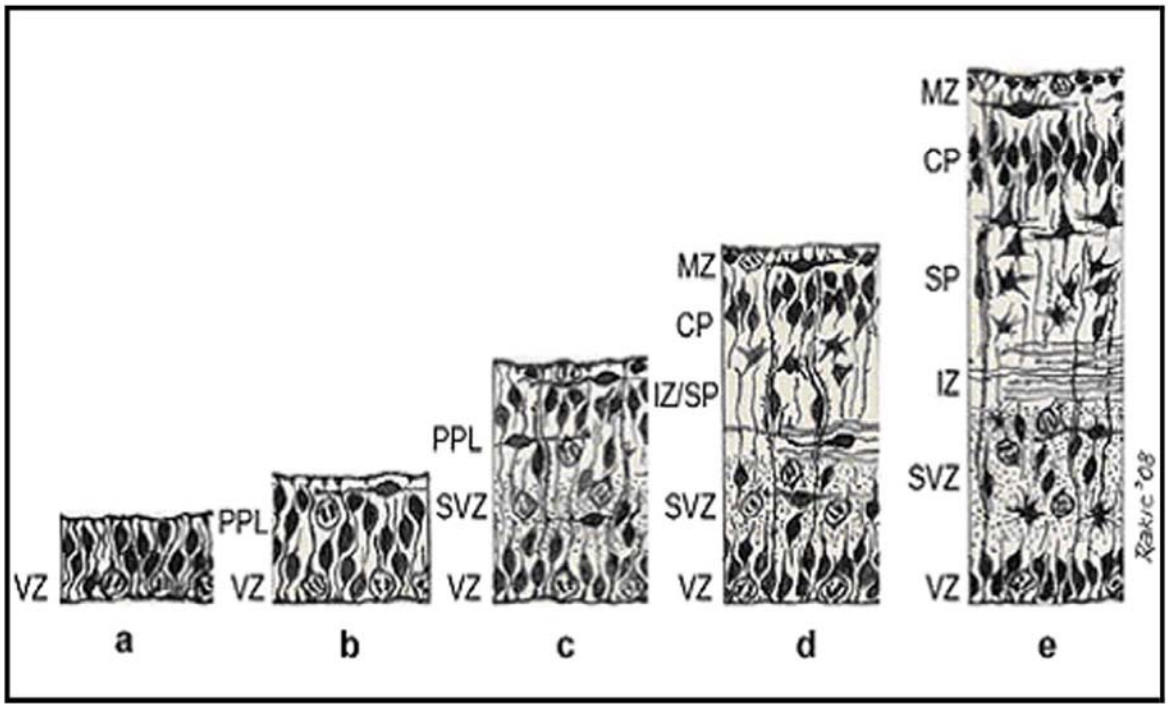

Fig. 1.1 Stages of human neocortical development. Schematic taken from Bystron et al. (2008) illustrating the progressive stratification and expansion of the cortical wall during human neocortical development. (a) (embryonic day (E)30 in human (h), ~E10.5 in the mouse (m)) The cortical enlage initially comprises a single layer of neural progenitors, the ventricular zone (VZ). (b) (E31-32h, ~E11.5-12.5m) Post-mitotic neurons migrate from subpallial and pallial sources and accumulate to form the superficial preplate layer (PPL). (c) (E45h, see note below) As neurogenesis proceedes a secondary germinal region forms, the subventricular zone (SVZ). These are the major sources of pyramidal neurons which migrate radially to form the developing cortical plate (CP). (d) (~E13.5m)The first wave of cortical plate neurons causes the preplate to split into a marginal zone (MZ) and subplate (SP) layer. (e) (gestational week 14, ~E15.5m) The cortical plate progressively expands as neurogenesis proceeds. (d,e) PPL and CP neurons extend axonal projections away from the pial membrane and contribute to the intermediate zone (IZ). Tangentially oriented neurons correspond to migrating subpallial sources of neurons, including cortical interneurons derived from the ganglionic eminences. While human sources of cortical interneurons are derived from both pallial and subpallial sources, in the rodent, cortical interneurons are exclusively derived from the ganglionic eminences. Note mitotic figures in basal regions of the VZ. While basal progenitors are observed at E13.5 in the rodent cortex, the SVZ is only clearly visible at a later stage ~E15.5m.

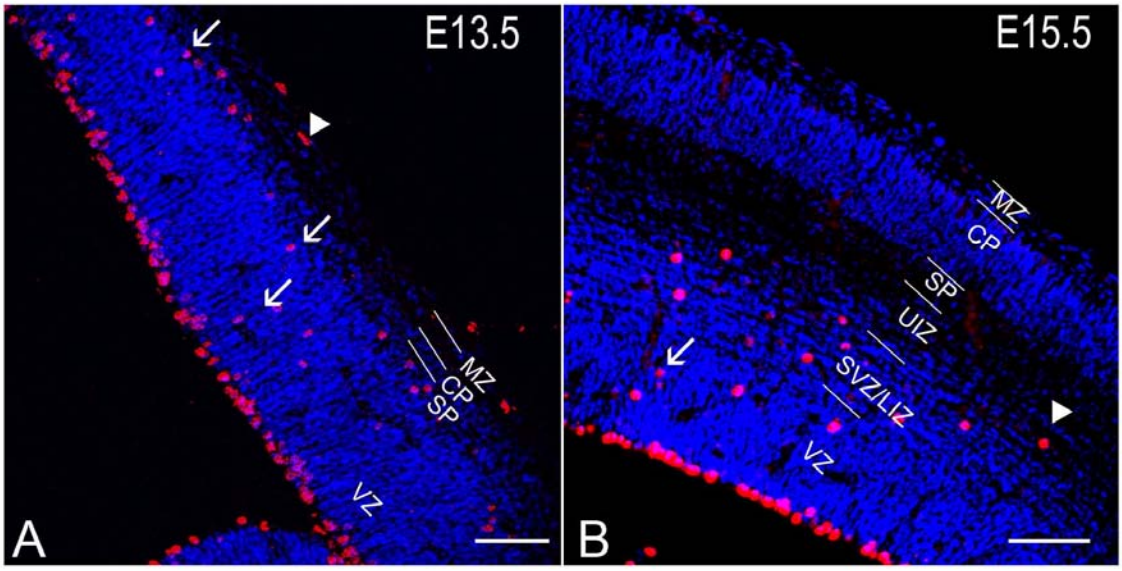

Fig. 1.2 Abventricular and extraventricular cell mitoses in the embryonic mouse cortex. Photomicrographs of coronal sections taken through the embryonic wild type mouse cortex at E13.5 (A) and E15.5 (B), processed for the proliferating marker phospho-histone 3 (PHis-3) and counter-stained with the nuclear marker DAPI. Mitotic PHis-3 immunopositive cells are predominantly localised at the apical surface of the ventricular zone (VZ) during early (A) and mid stages of neurogenesis (B), comprising proliferating multipotent neuroepithelial and radial glial cell progenitors. Some immunolabelled mitotic figures are also observed in basal positions of the VZ (arrows in A&B). These comprise intermediate progenitor cells, some of which subsequently form the second superficial germinal subventricular zone (SVZ). The SVZ is better distinguished during later stages of development in the developing mouse cortex (E15.5-E17.5), as exemplified by panel B. Some mitotic figures are also observed outside of these main germinal compartments, including within the superficial MZ and IZ layers (arrowheads in A&B); the identity of these cells remains to be fully elucidated. (MZ, marginal zone; CP, cortical plate; SP, subplate; UIZ, upper intermediate zone; SVZ/LIZ, subventricular zone/lower intermediate zone; VZ, ventricular zone). Scale bar is 100μm.

These early histological and proliferation studies have led to several important observations which underlie corticogenesis: i) neurons are not generated *in situ,* but by multipotent and intermediate progenitors within germinal regions near the lateral ventricles, and, thus, post-mitotic neurons must migrate away from these proliferative regions to form the superficially developing cortical layers; ii) apical, basal and extraventricular cell proliferation occurs throughout development, highlighting the importance in identifying distinct progenitor subtypes and potential neuronal subtypes generated and iii) the time of generation of CP neurons is correlated with their final laminar fate in the developing cortex (Angevine and Sidman, 1961; Bery and Rogers, 1965; Smart et al., 1973; Rakić et al., 1974). Thus recent imaging and genetic studies in the last decade have revolutionised prior concepts of corticogenesis and highlighted the complexity of this developmental process (Carney et al., 2007; Reviewed in Noctor et al., 2008 & Hevner et al., 2008).

1.3 PYRAMIDAL AND NON-PYRAMIDAL NEURONS ARE DERIVED FROM SEPARATE LINEAGES

It is now well established that cortical projection (pyramidal) neurons are generated by RGCs and intermediate progenitors within the neocortical VZ and SVZ (Tamamaki et al., 2001; Noctor et al., 2001, 2004, 2008; Kowalczyk et al., 2009). Whereas projection neurons are generated within the cortical VZ/SVZ and follow a predominantly radial and gliophillic trajectory to the CP, interneurons are derived from the ventral forebrain (Tamamaki et al., 1997; Anderson et al., 1997a, b, 2001; Lavdas et al., 1999; Sussel et al., 1999;

Wichterle et al., 1999, 2001). These cells migrate tangentially from the subpallium to populate the developing CP. Although tangentially dispersed GABAergic cells in the cortex had been previously observed (Reid et al., 1995), it was the introduction of recombinant retroviruses that first shed light on the separate origins of interneurons and pyramidal neurons.

Retroviral studies enabled individual proliferating cells to be labelled and, as the retroviral genome is integrated into the dividing host cell, the progeny of infected neurons could be fully traced without the label being diluted over subsequent rounds of cell division (Luskin et al., 1988; Price and Thurlow, 1988; Cepko et al., 1990; Walsh & Cepko, 1992). Initial retroviral lineage studies in the embryonic rodent showed clusters of cells within the neocortex which were often radially arranged in adjacent cortical layers, and these were proposed to be of the same lineage due to their close spatial proximity and homogenous pyramidal-like morphologies (Luskin et al., 1988; Price and Thurlow, 1988; Walsh & Cepko, 1992; Luskin et al., 1993).

Subsequent studies, indeed, confirmed these clones comprised glutamatergic pyramidal neurons (Mione et al., 1994). In addition to these clusters of labelled cells, smaller two-cell clones and single dispersed labelled cells were observed within the cortex (Luskin et al., 1988; Price and Thurlow, 1988; Walsh & Cepko, 1992). These were predominantly of a non-pyramidal morphology and were later confirmed to be GABAergic interneurons (Mione et al., 1994). Poignantly, when retroviral analysis was combined with BrdU labelling, it was shown that the single non-pyramidal cells were faintly labelled with BrdU,

suggesting that these were part of larger clones. Given that there is little apoptosis within the cortex during embryonic stages of development, it was thought unlikely that these had migrated radially from the VZ after their terminal mitotic division and that their clonal relatives had subsequently apoptosed (Mione et al., 1994; Thomaidou et al., 1997). It was, therefore, suggested that these had dispersed tangentially within the cortex. Lineage studies further strongly suggested that two separate lineages existed for pyramidal and non-pyramidal neurons within the cortical primordium, and that their neurotransmitter phenotype was strongly associated with their patterns of dispersal (Mione et al., 1994). Thus, whilst pyramidal neurons were predominately found to comprise large, radially oriented clusters, small clusters of cells were predominantly of a non-pyramidal phenotype and were tangentially dispersed throughout the cortex (Parnavelas et al., 1991; Walsh and Cepko, 1992; Mione et al., 1997).

Based on these findings, it was postulated that either progenitors of the non-pyramidal lineage widely dispersed within the VZ of the cortex (Fishell et al., 1993; Reid et al., 1995) or that post-mitotic neurons migrated tangentially within the cortex (Mione et al., 1997). The latter proposal was consistent with the direct observation of tangentially migrating neurons within the embryonic ferret cortex (O'Rourke et al., 1995). The observation that neurons could disperse tangentially within the cortex was of great importance as this showed that neurons, predominantly of a GABAergic phenotype, could mix extensively across ontogenetic boundaries and, therefore, did not follow a strict radial trajectory from the VZ (Herrup et al., 1994; Rakić et al., 1974, 1995).

Whilst these studies began to elucidate the extensive tangential movement of neurons within the embryonic cortex, it was still believed that these derived from distinct progenitors within the cortical VZ (Fishell et al., 1993). It was the observation of non-pyramidal cells expressing the subpallial specific transcription factor, distal-less homeobox 2 (Dlx2), which first suggested that non-pyramidal cells may have a ventral origin, and thus were not derived from progenitors within the cortical primordium (Porteus et al., 1994).

1.4 SUBPALLIAL ORIGINS OF GABAERGIC INTERNEURONS

Dlx1/2 are homeobox transcription factors expressed within the subpallial ganglionic eminences (GE) during early gestation (Bulfone et al., 1993; Puelles et al., 2000), and have a crucial role in regulating neuronal differentiation in these regions (Anderson et al., 1997b, Eisenstat et al., 1999; Cobos et al., 2007). The GEs comprise three evaginations: the lateral (LGE), medial (MGE) and caudal ganglionic eminences (CGE) which will give rise to the striatum, pallidum and amygdala respectively. In addition to subpallial neural cells, these also give rise to populations of cortical, hippocampal and olfactory bulb GABAergic interneurons. Indeed, whereas the cortical SVZ is a major source of interneurons in humans (Letinic et al., 2002; Rakić and Zecevic, 2003), it is believed that cortical interneurons in the developing rodent are almost exclusively derived from the ventral forebrain (Anderson et al., 1997a, 2001; Witchterle et al., 2001).

Although the observation of Dlx cells within the cortex suggested that these cells originated within the ventral forebrain, it was the direct observation of tangentially migrating cells in tracing studies in slice cultures which confirmed that cells from the LGE could traverse the cortico-striatal boundary and migrate through the PPL layer of the cortex during early stages of development (De Carlos et al., 1996). More detailed *in vitro* and *in vivo* cell tracing studies subsequently confirmed that tangentially migrating LGE-derived cells were in fact migrating neurons (expressing early neuronal markers MAP2 and NeuN) (Tamamaki et al., 1997), and these were GABA- and calbindin immunopositive interneurons (Anderson et al., 1997a).

Whilst the LGE was initially believed to be the predominant source of cortical interneurons, later *in vitro* cell tracing experiments confirmed that the MGE also contributes to this population of tangentially migrating cells (Lavdas et al., 1999). This was in accordance with studies which had shown that MGE derived cells exhibited a much more robust migratory behaviour than LGE cells (Wichterle et al., 1999), suggesting these had a greater propensity to migrate. Genetic studies in transgenic mice deficient in Nkx2.1, a homeobox gene involved in the regionalisation of the MGE, were consistent with this observation. These mutant animals showed a prominent (50%) reduction in GABAergic interneurons, as well as a near complete absence of calbindin positive cells (99% reduction) within the cortex (Sussel et al., 1999).

While these tracing studies showed that the MGE as well as the LGE gave rise to cortical interneurons, the relative contribution of each source was complicated

by the observation that interneurons derived from the MGE migrated through the LGE *en route* to the cortex (Anderson et al., 1997; Lavdas et al. 1999; Sussel et al., 1999; Wichterle et al., 2001). To discern this, subsequent transplantation studies in which early LGE or MGE donor tissue was labelled with BrdU prior to being isochronically (of the same age) or homotypically (of the same regional identity) transplanted into wild type host slice cultures were carried out. This study suggested that the MGE is the predominant source of interneurons throughout neurogenesis, with the LGE only contributing to a later born population (Anderson et al., 2001). *In utero* fate mapping studies directly confirmed the MGE to predominately give rise to cortical interneurons *in vivo* (Wichterle et al., 2001) and to contribute to the two major classes of parvalbumin and somatostatin positive interneurons in the mature neocortex. The LGE was only found to contribute to olfactory bulb interneurons during early stages of corticogenesis (E13.5). However, both transplantation and genetic studies (Anderson et al., 1997a, 2001) have confirmed that the LGE gives rise to interneurons that migrate along the SVZ/LIZ during later stages of development, contributing to a population of cortical interneurons as well as to olfactory bulb precursors. Genetic studies in transgenic mice which lacked both Dlx1/2 subpallial specific transcription factors were consistent with this; they showed a more drastic reduction (75% decrease) in GABA immunopositive cells within the cortex than when only the MGE is deficient in Nkx2.1 mice (Anderson et al., 1997a; Sussel et al., 1999). Thus, it is widely accepted that in addition to giving rise to interneurons of the hippocampus and olfactory bulb, the LGE also contributes to a later population of cortical interneurons (Anderson et al., 1997a, 2001; Pleasure et al., 2000).

More recently, additional subpallial sources of interneurons have been identified, consistent with the observation that the entire population of interneurons is not abolished in $Dlx1^{-/-}$; $Dlx2^{-/-}$ mutant mice. The CGE has been shown to contribute to the calretinin population of cortical interneurons which predominantly populate the caudal regions of the mature cortex (Nery et al., 2002; Yozu et al., 2005). Analysis of $Vax1^{-/-}$ transgenic mice, in which the septum fails to develop, has also suggested that the septum contributes to a substantial (30-40%) population of GABAergic neurons in the adult neocortex (Taglialatela et al., 2004).

1.5 ORIGINS OF CORTICAL INTERNEURON SUBTYPES

The observation that the MGE gives rise to most of the somatostatin-, parvalbumin- and neuropeptide Y- expressing populations of cortical interneurons, and the CGE primarily gives rise to the calretinin- expressing population (Wichterle et al., 2001; Nery et al., 2002; Xu et al., 2004; Butt et al., 2005), suggested that interneuron subtypes may be generated in spatially distinct progenitor domains. Regional variations in gene patterning within the GEs may further molecularly specify progenitor domains within these regions. Recent studies have confirmed that the GEs can be further subdivided on molecular grounds into distinct progenitor subdomains as delineated by the expression of transcription factors (Fogarty et al., 2007). This suggests that spatially distinct progenitor pools within the neuroepithelium may specify distinct interneuron fates (Fogarty et al., 2007). In addition, the interneuron subgroups generated

have also been shown to be temporally specified (Butt et al., 2005). Furthermore, whereas most cortical interneurons migrate dorsally from the MGE and LGE to the cortex, CGE-derived interneurons follow a posterior ventral-dorsal route (Nery et al., 2002; Yozu et al., 2005), suggesting different migratory behaviours may be determined intrinsically by their early phenotypic specification within the GEs. Indeed, *in vivo* heterotopic transplant studies have suggested that the distinct migratory fates of MGE- and CGE-derived interneurons are determined as early as E13.5 within the germinal neuroepithelium and prior to their migration (Nery et al., 2002). This raises a central question in developmental neurobiology: to what extent does the birth date and specific interneuron phenotype dictate its migratory behaviour, and to what extent do interneurons acquire their specific phenotypes while *en route* to the cortex through changing environmental cues? Indeed, given the complexity of their migratory routes and the vast heterogeneity of these cells, it is likely to involve a combination of factors.

1.6 TANGENTIAL MIGRATION

Cortical interneurons migrate along highly directed and temporally regulated tangential routes from their origins in the GEs to the developing cortex (Fig. 1.3). The MGE gives rise to early born interneurons (E11.5-E12.5 in the mouse) which migrate superficially to the developing striatum, and follow a superficial route within the cortex at the level of the PPL layer (E12.5) (Fig 1.3A) (Lavdas et al., 1999; Métin et al., 2006). A day later, and throughout the peak of tangential migration, interneurons follow a deeper route to the striatum and

migrate at the level of the IZ within the cortex (Fig 1.3B). The PPL stream of migrating cells is split into a MZ and SP stream by the developing CP, which begins to form in lateral regions of the embryonic cortex (E13.5) and, thus, three tangential streams are evident at this time (Fig.1.3C) (Métin et al., 2006).

At the peak of tangential migration (~E14.5 in the mouse), interneurons generated in the MGE continue to follow a deep route from the GEs to the striatum. However, these shift to a lower position within the cortex: at the boundary of the lower IZ and the SVZ (De Diego et al., 1994; De Carlos et al., 1996; Anderson et al., 1997a; Wichterle et al., 2001). At later stages of development (E15.5-E17.5) (Fig 1.3C), the LGE contributes to a major source of cortical interneurons, as well as to interneurons which populate the olfactory bulb and hippocampus (Pleasure et al., 2000; Anderson et al., 2001). These later-born interneurons migrate along deep tangential paths from the subpallial SVZ of the MGE and LGE to enter the lower IZ/SVZ within the cortex (Pleasure et al., 2000; Wichterle et al., 2001).

Thus, interneurons follow complex tangential routes and migrate over long distances to reach the developing cortex. Once they reach the cortex, they must adopt a radial trajectory and descend from their superficial MZ streams or ascend from the lower SP or LIZ/SVZ streams to enter the developing CP (Fig. 1.3D) (Nadarajah et al., 2002; Ang et al., 2003; Hevner et al., 2004; Tanaka et al., 2003, 2006).

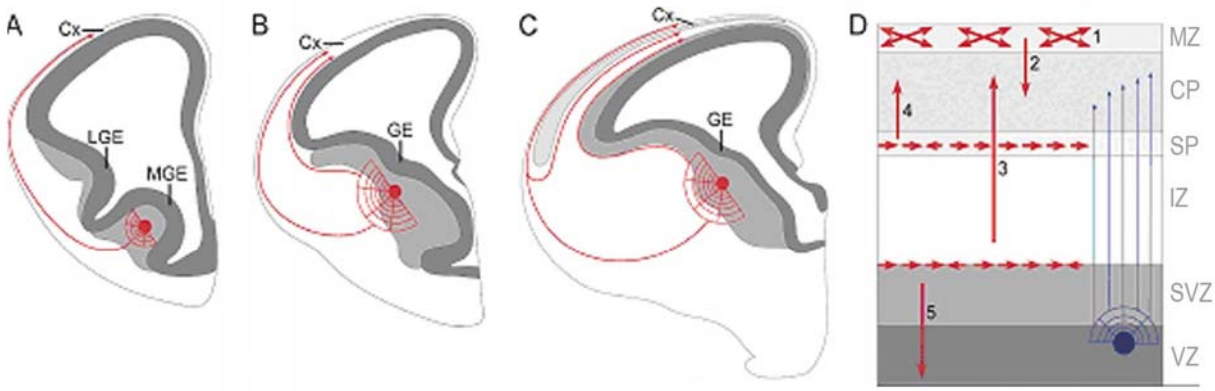

Fig. 1.3 Interneuron migration in the developing mouse forebrain. (A-C) Schematic illustration showing the migratory paths followed by interneurons (red) from the GEs to the developing cortex in the embryonic mouse forebrain during (A) early (E12.5), (B) mid (E13.5-E15.5) and (C) late (E15.5-E17.5) phases of migration. (D) Schematic illustrating the complex intra-cortical migratory routes followed by interneurons (red) during mid stages of migration (E13.5-E15.5). Interneurons (red) ascend (3,4 in D) or descend (2 in D) from their tangential migratory streams to entering the developing CP. Some interneurons further exhibit ventricle directed migration (5 in D) before ascending to enter the CP. The relatively simple radial trajectories followed by pyramidal neurons from their origins within the cortical VZ are delineated in blue. (Cx, cortex; LGE, lateral ganglionic eminence; MGE, medial ganglionic eminence; CGE, caudal ganglionic eminence; MZ, marginal zone; CP, cortical plate; SP, subplate; IZ, intermediate zone; SVZ, subventricular zone; VZ, ventricular zone). (Schematics were taken from Métin et al., 2006).

1.6.1 Intra-cortical migration of interneurons

Time-lapse imaging studies *in vivo* (Ang et al., 2003) as well as direct imaging of flat mount preparations and slice cultures *in vitro* (Nadarajah et al., 2002; Polleux et al., 2002; Ang et al., 2003; Tanaka et al., 2003, 2006; Hevner et al., 2004) have elucidated the intra-cortical migratory paths of interneurons. These studies have shown that interneuron migration within the cortex is much more complex than previously believed. Cortical interneurons ascend from their migratory streams within the LIZ/SVZ in both radial and non-radial trajectories to reach the MZ. These then migrate in multiple directions and extensively disperse throughout the MZ layer along the lateral-medial and rostral-caudal cortex, before re-descending to enter the CP (Fig.1.3D) (Polleux et al., 2002; Ang et al., 2003; Tanaka et al., 2003, 2006; Hevner et al., 2004). Similar multi-directional and extensive migratory behaviours have also been observed within the VZ, suggesting that interneurons disperse widely across the cortex *in vivo*. It has been postulated that this may enable the appropriate mixing of interneuron subtypes within the cortex (Tanaka et al., 2006). These neurons have additionally been shown to exhibit 'ventricle-directed migration', whereby interneurons actively descend from all migratory streams to enter the cortical VZ (Nadarajah et al., 2002) where these pause before re-ascending towards the developing cortical plate CP in a radial or oblique trajectory.

Cortical interneurons have been shown to follow a similar 'inside- out' sequence of development as their pyramidal counterparts (Ang et al., 2003; Valcanis and Tan, 2003; Hevner et al., 2004). Exceptions may be provided by the calretinin

subpopulation (Rymar and Sadikot, 2007) as well as by GABAergic neurons within the caudal cortex (Yozu et al., 2005). Thus, despite originating from spatially distinct progenitor domains, the development of cortical interneurons and pyramidal neurons appears to be largely synchronised. How these processes are coordinated remains to be clarified, however studies suggest that the laminar fate of populations of interneurons may be temporally specified prior to their last mitotic division, as has been shown for projection neurons (McConnell & Kanowzki 1991). However, it appears that interneurons have a more 'plastic' developmental potential, in that a proportion of both early and later born cells have been shown to respecify their laminar fate in a different aged host (Valcanis & Tan 2003; Pla et al., 2006). This is unlike late cortical progenitors that are restricted to generate neurons of an upper layer fate (Frantz & McConnell 1996). It has been proposed that the ventricle directed migration of interneurons may enable these to seek positional information within the VZ, thereby synchronising their development with their pyramidal counterparts (Nadarajah et al., 2002). A more recent study has suggested that interneurons may interact with their pyramidal counterparts within the SVZ/LIZ (Tiveron et al., 2006) as well as with projection neurons within the CP (Pla et al., 2006).

Whilst the complex migratory routes of cortical interneurons are well documented, the mechanisms by which interneurons are guided along their sub-pallial to pallial and intra-cortical routes to reach their appropriate positions within the developing CP, as well as the full significance of these trajectories, still remains to be elucidated. Given the complexity of these processes, this is likely to involve a combination of various intrinsic and extrinsic factors.

1.7 MOLECULAR AND CELLULAR MECHANISMS REGULATING INTERNEURON MIGRATION

1.7.1 Substrates

Unlike the mostly gliophillic radial migration of pyramidal neurons, cortical interneurons migrate through varying cellular (radial glial, axonal, and neuronal) environments and follow tortuous migratory paths over very long distances to reach the cortex. The substrates along which these cells migrate remain to be elucidated.

Interneurons predominantly migrate along trajectories which are orthogonal to radial glial processes, and whilst it has been suggested that they may make 'glancing contacts' with these processes within the cortical SVZ (O'Rourke et al., 1995, 1997), the tangential migration of interneurons is believed to be mostly independent of glial guidance. More recent live-imaging studies have suggested that interneurons may use RGC basal processes when they switch to a radial mode of migration to descend into the CP from the MZ (Ang et al., 2003; Tanaka et al., 2003, 2006; Hevner et al., 2004; Pla et al., 2006), but this remains to be confirmed. Furthermore, they may be guided by pioneering Cajal-Retzius cells that are located in more superficial positions within the MZ throughout their migration as well as by projection neurons within the cortex (Pla et al., 2006; Triveron et al., 2006). Such interaction has been suggested by the imaging studies of Ang and others (2003).

Some studies have also proposed that cortical interneurons use efferent corticofugal fibres in their tangential migration from the subpallium to the cortex (Métin and Godement 1996; Denaxa et al., 2001; Morante-Oria et al., 2003; McManus et al., 2004). This was suggested by the observation that interneurons are often closely associated with efferent fibres within the MZ and IZ layers of the cortex. Pioneering PPL neurons extend projections towards the subpallium (E11.5-E13.5), and pause within the GEs where these have been reported to be closely associated with neuronal-like cells, at a time when early cohorts of cortical interneurons migrate towards the cortico-striatal boundary (Métin and Godement 1996; Morante-Oria et al., 2003).

In addition, transient pioneering (E11.5-E12.5) reciprocal projections have been reported to extend to the cortical wall from the LGE, and these fibres were also found to be closely associated with calbindin immunopositive cells (Métin and Godement, 1996), suggesting that interneurons may use these reciprocal LGE afferent projections to migrate to the cortex. Both corticofugal axons and early projections from the PPL/MZ have been shown to express the cell adhesion molecule TAG-1, and *in vitro* studies suggest this is an important molecular substrate used by interneurons in their migration during development (Denaxa et al., 2001; Morante-Oria et al., 2003; McManus et al., 2004). Slice culture experiments in which TAG-1 function in pioneering and corticofugal fibre systems was blocked resulted in impaired tangential migration of cortical interneurons from the GE to the cortex *in vitro* (Denaxa et al., 2001; Morante-Oria et al., 2003). However, such an association has not been supported by the work of others, given that most interneurons were observed to migrate in the

lower IZ, below the axon-rich zone (Tanaka et al., 2003). More recently, the removal of TAG-1 in transgenic mice did not impair interneuron tangential migration, suggesting that TAG-1, alone, does not mediate their migration *in vivo* (Denaxa et al., 2005). It remains to be clarified whether interneurons may use other molecules expressed by these axonal tracts in their migration.

1.8 MOLECULAR SIGNALLING SYSTEMS AND INTERNEURON MIGRATION

As well as requiring a permissive substrate for their migration, interneurons orientate themselves away from the GEs and ventral forebrain to initiate their migration dorsally towards the cortex. Investigations into the molecular mechanisms that guide interneurons along their paths have identified an extensive number of molecules to be involved. These include early patterning molecules which set up the dorsal-ventral (BMP's, shh) axis of the developing forebrain through their regulation of transcription factors (Yung et al., 2002; Xu et al., 2005; Gulacsi and Anderson 2006). Transcription factors, in turn, regionally pattern and specify interneuron progenitor domains (Nkx2.1, Pax6 and Gsh2) (Sussel et al., 1999), as well as regulate the differentiation and migration (Dlx1, Dlx2, Lhx6) of cortical interneurons (Anderson et al., 1997a; Alifragis et al., 2004; Cobos et al., 2007; Liodinis et al., 2007). Dlx1/2 homeodomain proteins, for example, have recently been shown to inhibit the premature morphological differentiation of subpallial interneurons, thereby enabling these to adopt a bipolar morphology and migrate to the developing

cortex (Cobos et al., 2007). Dlx1/2 and, more recently Nkx2.1, have additionally been shown to directly regulate the expression of the neuropilin receptors, which have an important role in directing interneurons to the cortex (see below) (Le et al., 2007; Nobrega-Pereira et al., 2008).

1.8.1 Motogenic cues

Motogenic factors which initiate cell motility, such as the hepatocyte growth factor/scatter factor (HGF/SF) and growth factors such as the neurotrophins (Neurotrophin-4), have an important role in promoting interneuron migration to the cortex (Brunstrom et al., 1997; Powell et al., 2001). In addition to initiating cell motility, guidance cues that impart directionality to cell migration are crucial in guiding cortical interneurons along their migratory routes. Directional information may be provided by diffusible molecules, which act as attractive or repulsive cues (chemotropic), or set up diffusible gradients which interneurons migrate along (chemotaxis). These may also be membrane bound mediating directional guidance by direct cellular contact, thereby rendering a substrate molecularly permissive or non-permissive (Flames et al., 2004). As discussed previously, these substrates may be of a glial (O'Rourke et al., 1995, 1997; Hevner et al., 2004; Ang et al., 2003), axonal (Denaxa et al., 2001) or neuronal (Pla et al., 2006; Triveron et al., 2006) nature.

1.8.2 Directional guidance cues

Slice culture studies have suggested that the dorsal migration of cortical interneurons from the ventral forebrain is directed by the combined activity of diffusible repulsive cues within the basomedial forebrain (the VZ of the GEs,

preoptic area and septum) and chemoattractive activity within the cortex (Zhu et al., 1999; Witchterle et al., 2003; Marín et al., 2003; Britto et al., 2006; Flames et al., 2004). Gradients of chemorepulsive and chemoattractive cues are further observed across the lateral-medial extent of the developing cortex, and these appear to be temporally regulated. Thus, whilst the hippocampal (medial) cortex has been shown to inhibit the migration of cortical interneurons at E12.5, these regions are permissive and promote their migration a day later, suggesting these may regulate the dorso-medial migration of interneurons within the cortex (Britto et al., 2006).

1.8.3 Chemotropic molecules

Several major families of chemotropic molecules, acting through their appropriate receptor(s), have been shown to regulate interneuron migration during development, and these include: the class III semaphorins-neuropilins, neuregulins-ErbB, eprhins-ephrins and the slit-robo proteins. The role each of these groups play in the migration of interneurons will be discussed separately (see below).

1.8.3.1 The semaphorins-neuropilins

The class III semaphorins, typified by Sema3A and Sema3F, are diffusible molecules with chemorepulsive activity, and are strongly expressed within the developing striatum which remains an exclusion zone for cortical interneurons, throughout the period of tangential migration (E12-E16). The ectopic placement of semaphorin-expressing cells within the cortex has been shown to impede

interneuron migration in slice culture experiments (Marín et al., 2001a) and, indeed, cortical interneurons have been shown to express the neuropilin1 (Np1) and neuropilin2 (Np2) receptors, mediating semaphorin chemorepulsive activity. Np1/2+ expressing cortical interneurons have also been shown to be repelled by the semaphorin-expressing striatal neurons, and are channelled around this region. Thus, semaphorins create an exclusion zone within the striatum and this is suggested to sort cortical interneurons from striatal interneurons, as well as channelling and streaming cortical interneurons along their superficial and deep migratory routes towards the cortex (Marín et al., 2001a).

1.8.3.2 Neuregulins –ErbB receptors

Whilst semaphorins create a non-permissive cellular environment for cortical interneurons, neuregulins conversely specify a permissive corridor through which these migrate (Flames et al., 2004). Neuregulin-1 (Nrg1) proteins exist as both membrane-bound (class I and II) and diffusible (class III) isoforms and are expressed within the developing subpallium and cortex, respectively. These mediate short-range and long-range chemoattractive activity through their cognate tyrosine kinase ErbB receptors during development (Flames et al., 2004). The ErbB4 receptor is specifically expressed by a population of MGE-derived cortical interneurons as these migrate tangentially to the cortex (Yau et al., 2003). The non-secreted form of Neuregulin-1-CRD (cysteine rich domain) is expressed in a narrow region within the striatum which does not express the chemorepulsive semaphorin molecules, and thus comprises a permissive corridor through which ErbB4 expressing cortical interneurons migrate to the cortex (Flames et al., 2004). This acts in concert with the secreted form of

Neuregulin-1 which is expressed in a lateral-medial gradient within the cortical SVZ, and is chemoattractive to ErbB4 expressing cortical interneurons, at a time when these enter the LIZ/SVZ within the cortex (Flames et al., 2004).

1.8.3.3 Ephrins – Ephrin receptors

The ephrin molecules are also dynamically expressed within the developing forebrain during interneuron migration. Specifically, ephrinA5 is localised within the germinal VZ of the medial and lateral GEs, at a time when interneurons migrate dorsally through the SVZ of the LGE to reach the developing cortex (E14-E16) (Zimmer et al., 2008). This same study confirmed that cortical interneurons express the ephrinA4 receptor and are repelled by ephrinA5 directly in *in-vitro* stripe assays. It has further been suggested that ephrinA5 may prevent interneurons from migrating into the VZ of the GEs, thereby directing these dorsally towards the cortex (Zimmer et al., 2008).

As well as molecules that repel interneurons away from their germinal domains in the GEs and from the striatum, interneurons are also inhibited from migrating towards the basomedial forebrain and thus, are directed dorsally towards the cortex. The Slit family of proteins are key candidate molecules which have been suggested to mediate this role.

1.8.3.4 Slit-Roundabout (Robo)

Slit proteins were first isolated in Drosophila in a screen for mutations affecting the pattern of the larval cuticle (Nüsslein-Volhard et al., 1984) and these mutants were found to have defects in the formation of the CNS. Removal of Slit resulted in longitudinal and commissural axons converging and

coalescing at the Drosophila CNS midline, and Slit was subsequently shown to encode a large secreted protein (~190kDa) (Rothberg et al., 1988, 1990).

Whilst Slit was originally proposed to regulate the patterning and specification of midline cells (Rothberg et at., 1990), it was subsequently identified to be a midline chemorepellent (Kidd et al., 1999). Slit chemorepulsion in Drosophila was shown to prevent the aberrant crossing of ipsilateral projections and to ensure contralateral commissural axons did not re-cross the midline, respectively (Battye et al., 1999; Kidd et al., 1999). This repulsion is mediated by members of the Roundabout (Robo) receptor family, which are expressed in commissural axons (Kidd et al., 1998a,b).

Robo was similarly identified in a Drosophila genetic screen for mutants with midline axon guidance defects. These mutants exhibited aberrant crossing and re-crossing of their ipsilateral and commissural axons at their midline (hence the name, roundabout) (Seeger et al., 1993; Kidd et al., 1998a, b). Ironically, Robo was identified to mediate Slit chemorepulsion in a 'roundabout' way, through the simultaneous identification of the *commissural* (*comm*) mutant. As their name suggests, commissural mutants lacked the formation of virtually all commissures and exhibited a complementary axon-guidance defect to Slit in that these failed to cross the midline (Seeger et al., 1993; Tear et al., 1996; Kidd et al., 1998a,b).

Comm is expressed by midline glia and is transiently expressed on commissural axons growing towards the midline, and has been shown to

regulate Robo expression (Tear et al., 1996; Georgiou & Tear 2002; Kidd et al., 1998b). *Comm* appears to function by removing Robo from the membrane, in a DNedd4 ubiquitin ligase dependent manner (Myat et al., 2002), as commissural axons approach the midline. This results in Robo-mediated Slit chemorepulsion, thus enabling axons to cross this region. *Comm* is only transiently expressed and, once axons have crossed the midline, Robo is upregulated. This sensitises axons to Slit chemorepulsion and prevents them from recrossing the midline (Kidd et al., 1998b; Georgiou & Tear 2002, 2003; Keleman et al., 2002, 2005).

The observation that commissural axons in Robo mutants still retained some sensitivity to Slit chemorepulsion at the midline suggested that there were other Robo receptors mediating this chemorepulsive response. Two other members of the Drosophila Robo family, *robo2* and *robo3*, were subsequently identified to be expressed within commissural axons (Simpson et al., 2002; Rajagopalan et al., 2002a). More recently, it has been shown that the specific combination of Robo receptors expressed by commissural axons alters their sensitivity to mildline Slit and thus, specifies their medio-lateral positioning once they cross the midline (Simpson et al., 2000a,b; Rajagopalan et al., 2002).

Both Slit and Robo genes are highly conserved throughout evolution from Drosophila to humans, hinting at the important role these molecules play. Slits share conserved structural domains, including four leucine rich (LRR) repeat regions, nine (seven in Drosophila) EGF-like repeats, a laminin-G domain, and a cysteine-rich C terminal motif (Fig.1.4A) (Rothberg et al., 1990; Itoh et al., 1998). To date, three Slit mammalian homologues (Slit1, Slit2, Slit3) have been

cloned, and these are all expressed within the developing forebrain (Brose et al., 1999; Holmes et al., 1998; Yuan et al., 1999a).

Robo is a novel member of the immunoglobulin (Ig) Supèr family of cell adhesion molecules, which are also conserved throughout evolution from *Drosophila* to humans (Kidd et al., 1998a; Lee et al., 2001; Sundaresan et al., 1998a,b). Robo molecules contain five Ig domains (two are only present in Robo4), three type III fibronectin motifs, a transmembrane segment, and a cytoplasmic tail containing four conserved signalling motifs (CC0-CC3; Robo3 lacks the CC1 domain) that are thought to interact with downstream signalling molecules (Fig. 1.4B) (Bashaw et al., 2000; Yang et al., 2006; Li et al., 2006).

To date, four family members have been identified in vertebrates: Robo1/Dutt1, Robo2, Robo3 (also known as Rig1) and Robo4 (also known as magic roundabout) (Kidd et al., 1998a; Yuan et al., 1999a; Huminiecki et al., 2002). Robo1 and Robo2 are expressed in many tissues and organs during development and in adult life, but show strongest expression in the developing nervous system. Robo3 expression seems limited to the developing CNS (Camurri et al., 2004), while Robo4 is specifically found in endothelial cells (Park et al., 2003). All four Robos have been shown to bind to Slit proteins (Park et al., 2003; Liu et al., 2004; Camurri et al., 2005; Mambetisaeva et al., 2005). For Robo1, at least, this binding activity has been delineated to reside within Ig domains 1 and 2 (Liu et al. 2004), which are also the most highly conserved parts, highlighting the importance of these domains in Robo function (Kidd et al., 1998a). Recently, these two Ig domains of Robo have been shown

to interact with the leucine-rich regions in Slit proteins (Howitt et al., 2004; Morlot et al., 2007).

Like other cell adhesion molecules, human Robo1, Robo2 and Robo3 have recently been shown to mediate homophilic adhesion, functioning as both a ligand on one cell and a receptor on another, as well as interacting as heterophilic ligands (Hivert et al., 2002; Liu et al., 2004; Camurri et al., 2005). The significance of such homophilic and heterophilic interactions in terms of Robo function is unknown at present, but for other family members such as NCAM, L1 and the netrin receptor DCC, these interactions have been shown to be important in promoting neurite outgrowth (reviewed in Walsh and Doherty, 1997).

1.8.3.4.1 Slit-Robo and axon guidance

A role for Slit/Robo in axon guidance in vertebrates was shown in studies where Slit directly repelled motor, olfactory and hippocampal axons *in vitro* (Nguyen Ba-Charvet et al., 1999; Brose et al., 1999; Li et al., 1999). Analysis of Slit2 and Slit1;Slit2 double mutants subsequently confirmed that Slit plays a role in regulating the dorsal-ventral positioning of thalamocortical and corticothalamic axons in the embryonic forebrain (Bagri et al., 2002), as well as in the developing visual system *in vivo* (Plump et al., 2002; Thompson et al., 2006a,b). More recently, Slit has been shown to act through the Robo1 and Robo2 receptors in regulating axon guidance in the corticofugal, thalamocortical, and corticocortical callosal axons (Andrews et al., 2006; López-Bendito et al., 2007), as well as in the developing visual system (Plachez et al.,

2008).

1.8.3.4.2 Robo3

In addition to Robo1 and Robo2, a more distant member of the Robo family, Robo3/Rig-1, is also expressed within the developing CNS (Yuan et al., 1999a; Camurri et al., 2004). Rig-1 or Robo3 was first identified as a nervous system-specific gene following a differential display screen carried out in the retinoblastoma-deficient mutant mouse (Yuan et al., 1999a). Robo3 has similarly been shown to regulate axon guidance at the vertebrate midline, specifically, within the embryonic spinal cord (Sabatier et al., 2004) and in the hindbrain (Marillat et al., 2004; DiMeglio et al., 2008).

Robo3 is strongly localised in pre-crossing commissural axons in the mouse spinal cord, and this is down regulated after axons cross the midline. Robo3 mutants have a strong phenotype which resembles the Drosophila commissureless mutant (*d-comm)*, in which commissural neurons fail to project across the midline. It has, therefore, been suggested that Robo3 may play a similar regulatory role to d-comm in that Robo3 inhibits Robo1-mediated chemorepulsion, thereby enabling commissural axons to enter the Slit-rich midline. This is particularly pertinent, since a comm-like homologue has not been identified in vertebrates to date.

However, two mechanisms have been proposed by which Robo3 is thought to desensitize Robo1 on precrossing axons. The first model proposes that precrossing axons express a low level of Robo1, and a high level of Robo3, and

suggests that Robo3 acts as a competitive receptor for Slit, thus "mopping-up" Slit, and preventing Robo1-Slit mediated repulsion and thereby enabling axons to cross the midline (Sabatier et al., 2004). Since the extracellular domain of Robo3 has been shown to bind heterophilically to Robo1 *in vitro*, the second model proposes that Robo3 binds directly to Robo1 on pre-crossing axons, and prevents it from binding Slit (Camurri et al., 2005).

Interestingly, the human condition of horizontal gaze palsy and progressive scoliosis, which is associated with a failure of corticospinal and dorso column-medial lemniscus tracts to cross the midline, has been associated with homozygous mutations in the extracellular domain of Robo3/Rig1. (Jen et al., 2004). This condition is similar to Robo3$^{-/-}$ mouse mutants (discussed above, in that major axonal pathways fail to cross the midline within the hindbrain (Marillat et al., 2004), and further suggests that the mutated Robo3/Rig1 receptor's ability to bind Slit may be affected in these patients. Thus, Robo3 may similarly have a conserved role in regulating Slit-chemorepulsion at the midline in humans. .

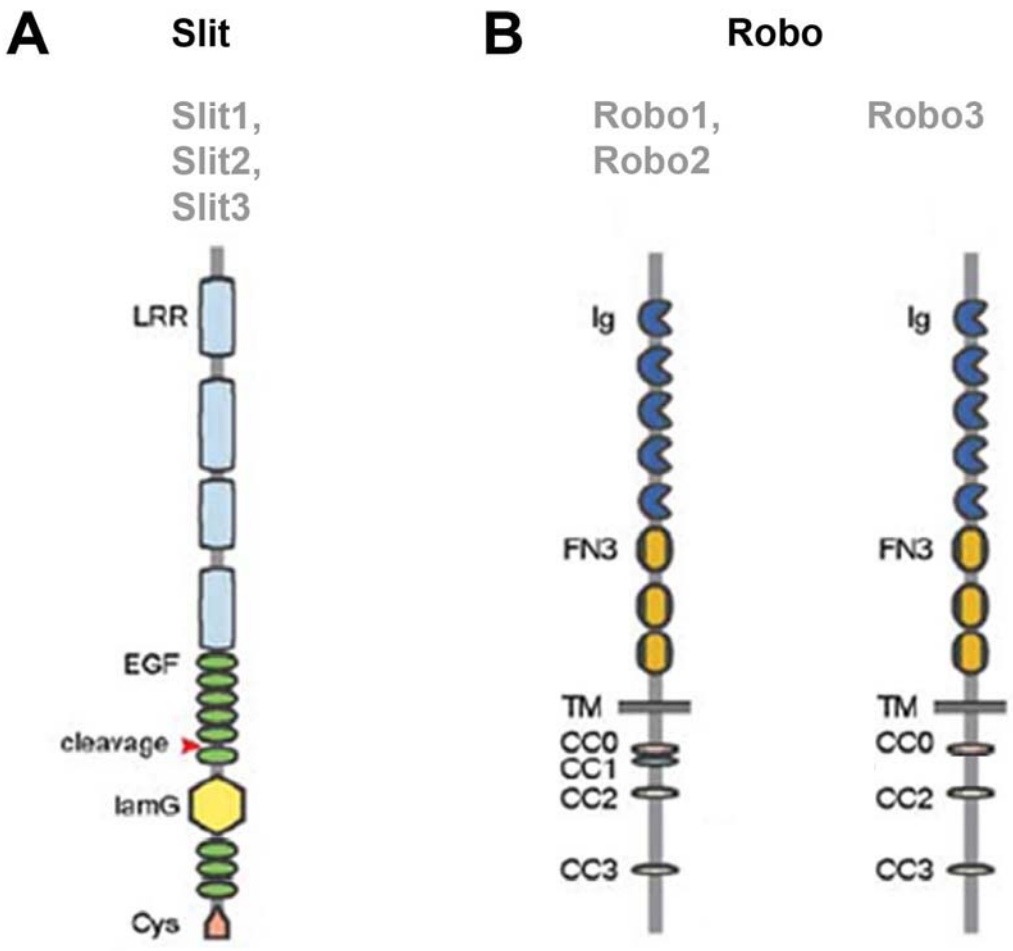

Fig. 1.4 Conserved structural domains in vertebrate Slit ligands and their cognate Robo receptors. (A) Schematic illustrating conserved motifs in the vertebrate Slit family (Slit1, Slit2, Slit3). Slit family members contain four tandem leucine-rich repeats (LRR), nine epidermal growth factor repeats (EGF), a laminin G (lamG) domain and a C-terminal cysteine knot (Cys). A conserved proteolytic cleavage site is localised between the fifth and sixth EGF repeats (red arrow). (B) Schematic of conserved motifs in the vertebrate Robo family (Robo1, Robo2, Robo3) of receptors. All vertebrate Robos share five conserved immunoglobulin domains (IgG), three fibronectin type-III motifs, a single transmembrane domain and conserved cytoplasmic motifs (CC0-3). Robo1 and Robo2 are highly homologous, sharing four conserved intracellular cytoplasmic motifs (CC0-CC3). Robo3 is more distantly related, lacking the second intracellular motif (CC1). (LRR, leucine-rich repeat; EGE, epidermal growth factor; lamG, laminin G, Cys, cystein knot; Ig, immunoglobulin; FN3, fibronectin type III repeats; TM, transmembrane; CC0-3, cytoplasmicconserved motifs 0-3). (Schematics were adapted from Wong *et al.*, 2002.)

1.8.3.4.3 Robo/Slit expression

Slits are highly expressed in the subpallial GE germinal regions (Slit1,Slit2) at a time when interneurons are being generated, and are also strongly expressed within the basomedial forebrain throughout their migration to the developing cortex (Fig. 1.5) (Yuan et al., 1999b, Marillat et al., 2002). Given the chemorepulsive role of Slits in axon guidance, and the observation that the basomedial forebrain is inhibitory to cortical interneurons *in vivo* (Marín et al., 2003a), it has been suggested that Slits may be candidate molecules which repel cortical interneurons away from the GE, septum and preoptic area (POA), and direct them dorsally towards the developing cortex (Zhu et al., 1999, Hu et al., 1999, Wu et al., 1999, Sang et al., 2002). Furthermore, the expression of Slit is complementary to both Robo1 and Robo2 mRNA which are localised within the germinal and differentiating fields of the GEs throughout the period of generation and migration of interneurons (E15.5-E19.5 in the rat) (Fig. 1.5A,B) (Marillat et al., 2002; Bagri et al., 2002; Whitford et al., 2002) (Fig.1.5).

In addition to Slit expression within the subpallium, a Slit gradient is also present along the tangential migratory routes taken by interneurons within the cortex. Specifically, during early stages of interneuron migration, Slit is expressed within the VZ (Slit1), MZ (Slit3) and CP (Slit1), and is mostly complementary to Robo expression within the early MZ/PPL (Robo1) and IZ (Robo2) (Fig.1.5A').

During later stages of development (E15.5-E17.5), Slit is down regulated within the MZ, but it continues to be expressed within the developing CP (Slit1) and

VZ (Slit1) (Yuan et al., 1999b; Bagri et al., 2002; Whitford et al., 2002). This overlaps with Robo within the CP (Robo1, Robo2), and is complementary to Robo within the IZ (Robo2) (Fig. 1.5B'). Thus, the expression of Slit/Robo throughout the period of generation and tangential migration of interneurons from the GEs to the developing cortex (E13.5-E17.5) (Yuan et al., 1999b; Bagri et al., 2002; Whitford et al., 2002; Marillat et al., 2002) is consistent with these molecules having a role in regulating their migration within the subpallium as well as along their tangential migratory routes within the cortex.

1.8.3.4.4 Slit and interneurons

Evidence that Slits directly repel migrating neurons has come from co-culture explant and slice culture studies carried out in the embryonic (Zhu et al., 1999; Hu et al., 1999; Sang et al., 2002) and postnatal (Wu et al., 1999) rodent forebrain. Explants taken from the embryonic septum or the GE-VZ (E15.5-E17.5 in the rat) were found to directly repel migrating GABAergic neurons from LGE-SVZ explants (Zhu et al., 1999). This endogenous diffusible chemorepulsive activity was shown to be mimicked by Slit (mouse Slit1) and was consistent with Slit expression within these regions *in vivo* (Slit1 in the VZ of the GEs, and Slit1, Slit2 in the septum). Furthermore, ectopic placement of Slit expressing cells at the cortico-striatal boundary was found to inhibit the tangential migration of GABAergic interneurons into the cortex in slice culture experiments (Zhu et al., 1999). Co-culture experiments in which Slit activity of the LGE-VZ was blocked using extra-cellular Robo (Ig) domains, which lack their intracellular portion and, therefore, act as active Slit competitors, further abolished the chemorepulsive effect *in vitro* (Zhu et al., 1999).

While this suggested that endogenous Slit activity was present within the VZ and septum, it was the isolation and purification of endogenous Slit from the septum that provided direct confirmation of this (Hu et al., 1999). Most of these studies were carried out when the LGE was posited to be the major source of interneurons *in vivo* (De Carlos et al., 1996; Anderson et al., 1997a; Tamamaki et al., 1997). A subsequent co-culture experiment similarly showed Slit to directly repel GABAergic interneurons from MGE explants and to inhibit their process elongation, consistent with Slit repelling interneurons and their processes *in vitro* (Sang et al., 2002). Interestingly, whilst MGE-derived interneurons were repelled away from the Slit source, GABAergic interneurons which were closest to the Slit source were not repelled, suggesting that the concentration of Slit protein gradients is important.

Poignantly, slits have been shown to direct olfactory bulb precursors from the LGE-SVZ along their rostral migratory streams *in vivo* (Nguyen Ba-Charvet et al., 2004). This study, using explants of the LGE-VZ and septum taken from Slit1;Slit2 double mutant mice, conclusively demonstrated that the combined activity of Slit1 and Slit2 proteins is required to repel olfactory interneuron precursors away from the septum *in vitro*. Analysis of mutant mice showed that removal of Slit1 and Slit2 resulted in the ectopic caudal misplacement of olfactory bulb neuronal precursors, confirming that both Slit1 and Slit2 regulate the positioning of the rostral migratory stream *in vivo* within the postnatal forebrain (Nguyen-Ba-Charvet et al., 2004).

A similar role for Slit in repelling cortical interneurons away from the GEs

and ventral forebrain and guiding them towards the dorsal cortex *in vivo* has also been suggested (Zhu et al., 1999; Andrews et al., 2006). The role of Slit in interneuron migration was investigated *in vivo*, using transgenic mice that were deficient for both Slit1 and Slit2 proteins ($Slit1^{-/-}$; $Slit2^{-/-}$) (Marín et al., 2003a). Surprisingly, cell tracing studies carried out in slice cultures prepared from Slit1; Slit2 double mutant mice showed no defects in the tangential migration of interneurons from the GE to the cortex. Moreover, there were no differences in the number or distribution of GABAergic interneurons (GABA+, Lhx6+, Dlx2+) within the cortex and hippocampus of Slit mutants *in vivo*.

Whilst removal of Slit1 and Slit2 did not appear to affect the dorsal migration of interneurons to the cortex *in vivo*, ectopic neuropeptide-Y and cholinergic neurons were observed to aberrantly accumulate and cross the midline in Slit double mutant mice, suggesting that Slit regulates the subpallial migration of neurons and defines their positioning near the ventral midline (Marín et al., 2003a). Whilst this *in vivo* study suggested that Slit1/2 do not direct interneurons along their dorsal trajectories to the cortex, this did not exclude the possibility of other unidentified Slits which may have compensated for the loss of Slit1 and Slit2 activity within the subpallium. However, a more recent study carried out in our laboratory, circumvented these possibilities by investigating Robo1-mediated signalling directly, using transgenic mice that were deficient for the Robo1 receptor (Andrews et al., 2006). This circumvented the possibility of redundant Slit functions within the basal ganglia or other ligands which may also signal through the Robo receptors, thereby compensating for the loss of Slit1 and Slit2 proteins.

1.8.3.4.5 Robo1 and cortical interneurons

Analysis of Robo1 deficient transgenic mice (Robo1$^{-/-}$) showed that removal of the Robo1 receptor resulted in an influx of calbindin immunopositive cells within the endogenously chemo-repulsive striatum (Fig.1.6), as well as in an approximately 50% increase in calbindin immunopositive interneurons within the embryonic cortex (E12.5) (Fig. 1.7A-C) (Andrews et al., 2006). The significant increase in the number of cortical interneurons within the cortex was also observed at later embryonic stages (E15.5-E18.5) and persisted into adulthood (Andrews et al., 2008) (Fig. 1.7D-F). Interestingly, this increase was only observed within the rostral-middle, but not in the caudal cortex (Andrews et al., 2006). Thus, contrary to the observations in Slit1; Slit2 double mutant mice, our analysis of Robo1 mutants suggested that the Robo1 receptor plays a role in preventing interneurons from migrating into the chemo-repulsive striatum, as well as regulating the number of cortical interneurons that enter the developing cortex (Fig. 1.8).

In addition to defects in interneuron migration, removal of the Robo1 receptor resulted in the early-arrival of thalamocortical and corticofugal tracts within the cortex and thalamus, respectively, in these mutant animals (Andrews et al., 2006). This is interesting as interneurons have been proposed to use the corticofugal fibre system in their tangential migration (Denaxa et al., 2001), raising the possibility that the increase in interneurons within the cortex may be explained by their premature migration along these tracts. Moreover, both Robo1 and Robo2 have been shown to bind homophilically and heterophilically

through their first extra-cellular Ig domains and to promote neurite outgrowth *in vitro* (Hivert et al., 2002; Liu et al., 2004). Given that Robo1 is also expressed by the thalamocortical and corticofugal axonal tracts, it has been suggested that Robo1-expressing interneurons may migrate along these fibres as mediated through homophilic and heterophilic Robo-Robo interactions (Andrews et al., 2006).

Whereas Robo1 mutants show an early arrival of the thalamocortical tracts and corticofugal fibres at their appropriate targets, Slit1; Slit2 double mutants have very few thalamocortical fibres reaching the cortex as these are misrouted within the diencephalon (Bagri et al., 2002; Andrews et al., 2006). The differences observed in axonal and interneuron defects in Robo and Slit mutants could be accounted for by the existence of other unidentified Slit isoforms, by differences in Slit or Robo mediated signalling, or by the existence of other ligands or receptor partners.

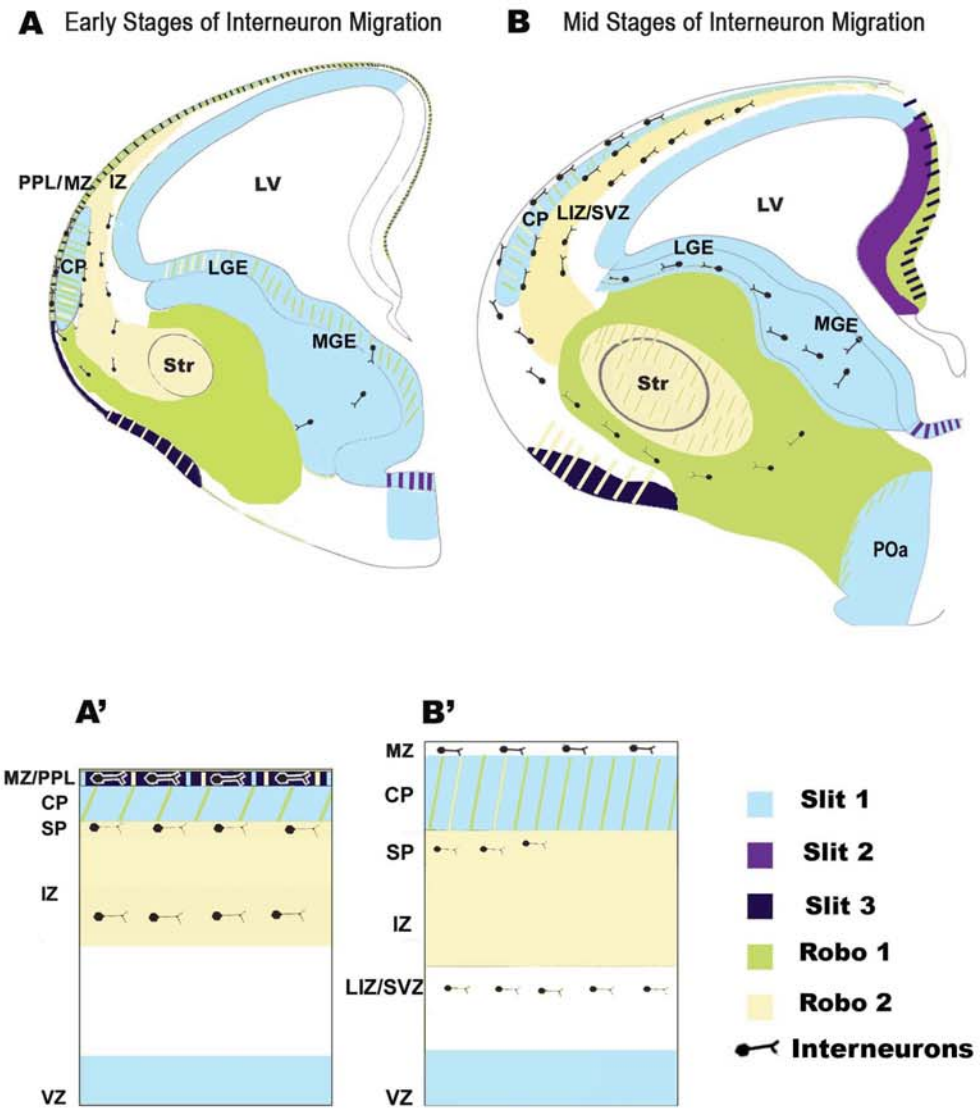

Fig. 1.5 Localisation of robo and slit mRNA in the developing rodent cortex. Schematic illustrating the localisation of robo 1 (green) and robo 2 (yellow) expression in relation to slit 1 (blue) slit 2 (purple) and slit 3 (dark blue) within the developing rodent forebrain (A,B) and cortex (A',B') during early (A, A') and mid stages of interneuron migration (B,B'). Hatched areas correspond to regions where robo and slit expression overlap. Slit 3 is strongly and transiently expressed within the developing preplate (PPL) and marginal zone (MZ) during early phases of migration (A,A', dark blue). Slit 1 is localised within the cortical plate (CP) and ventricular zone (VZ) (blue), and is mostly complementary to Robo2 expression within the developing intermediate zone (IZ) and subplate (SP) during early stages of interneuron migration (yellow). Robo1 is strongly expressed throughout the developing CP (green), and overlaps with Slit 1 (blue) in this region during early and mid stages of interneuron migration. (LV, lateral ventricle; MZ, marginal zone; CP, cortical plate; SP, subplate; IZ, intermediate zone; LIZ/SVZ, lower intermediate zone/subventricular zone; VZ, ventricular zone; Str, striatum; LGE, lateral ganglionic eminence; MGE medial ganglionic eminence; CGE, caudal ganglionic eminence; POa, preoptic area). (This figure is based on *in-situ* hybridization studies by Yuan *et al. (*1999) Marillat *et al.* (2002), Bagri *et al.* (2002) and Whitford *et al.* (2002)).

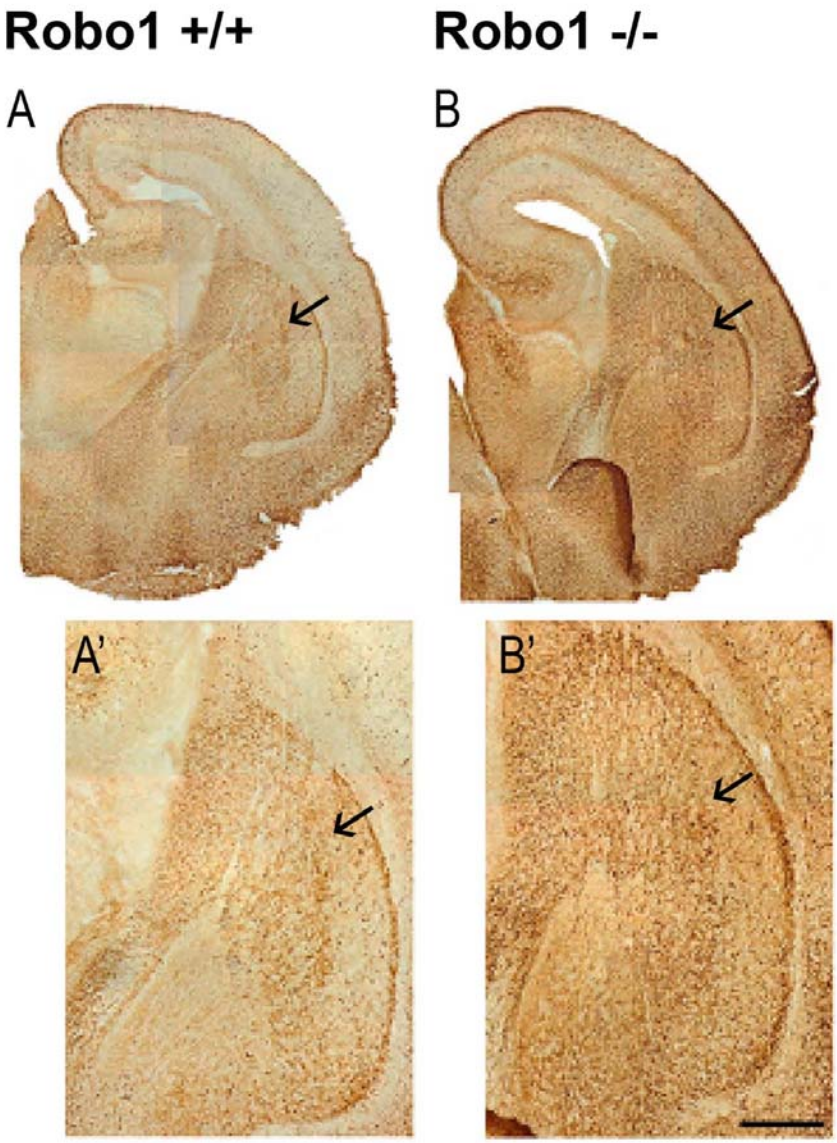

Fig. 1.6 An increase in (calbindin immunolabelled) interneurons is observed wtihin the striatum of Robo1 mutant embryonic mice. Photomicrographs show coronal sections through the embryonic mouse forebrain taken from Robo1 mutant (B,B') and wild type (A,A') animals, immunohistochemically processed for calbindin proteins. Comparative analysis of the localisation of calbindin immunopositive interneurons suggests that there is an increase in calbindin immunopositive cells within the striatum of Robo1 mutants (arrows B, B') relative to wild type animals (arrows A, A') at E18.5. Higher magnification of equivalent regions of the striatum are shown in A' and B' for these animals. Scale bar is 200 μm in A',B' and 400 μm in A,B. (Photomicrographs were taken from Andrews et al., 2006).

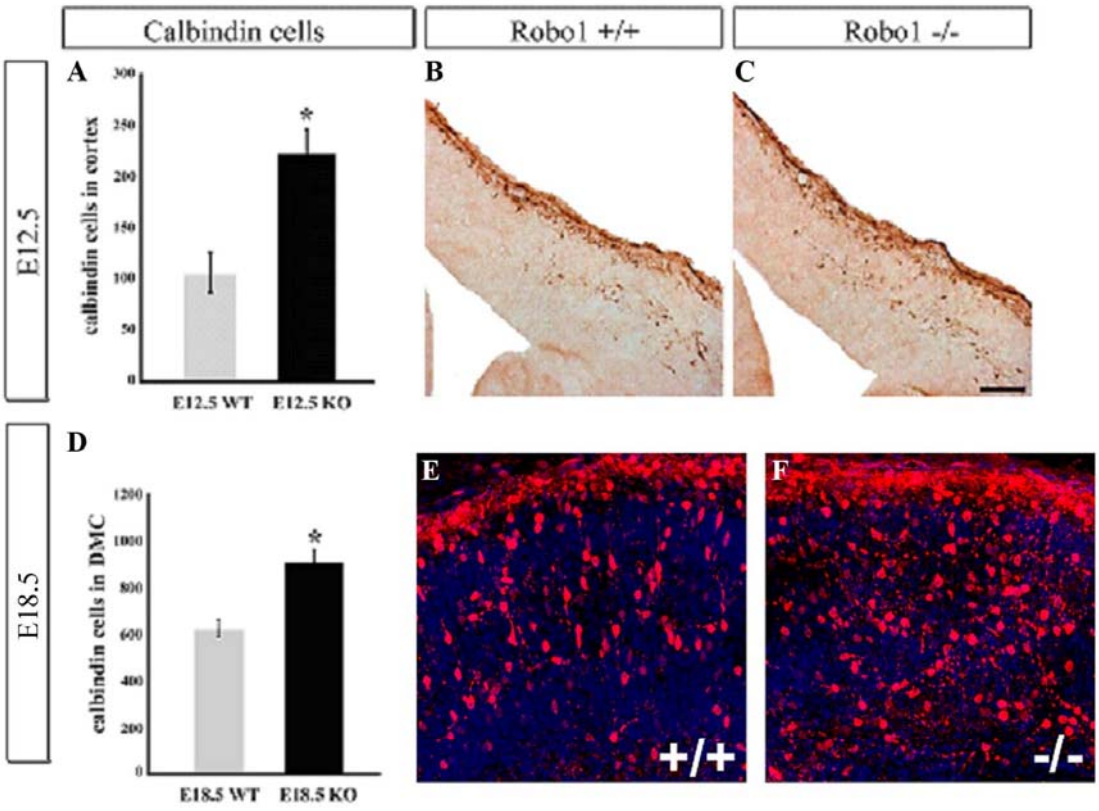

Fig. 1.7 Robo1 regulates the total numbers of (calbindin immunopositive) cortical interneurons during development. Photomicrographs of coronal sections taken from Robo1 mutant (C,F) and Robo1 wildtype (B,E) animals, immunohistochemically processed for calbindin proteins at E12.5 (B,C) and at E18.5 (E,F). Graphical representation of the total numbers of calbindin cells at E12.5 (A) and at E18.5 (D) shows a significant increase in calbindin labelled cells within the cortex of Robo1 mutants (black bars in A,D) relative to wild type animals (grey bars in A,D). (These figures are taken from Andrews et al., 2006, 2008).

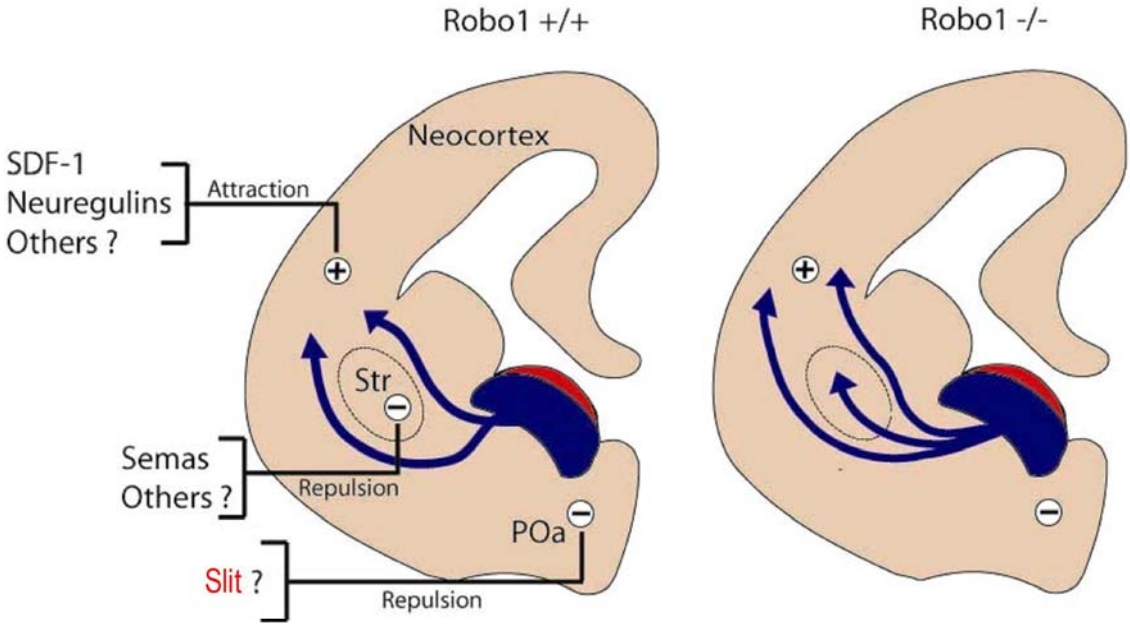

Fig. 1.8 Interneuron migration defects in Robo1 mutant animals. Schematic showing the influx of calbindin immunopositive interneurons (blue) within the chemo-repulsive (-) striatum in Robo1$^{-/-}$ mutant animals, relative to Robo1$^{+/+}$wild type littermates. Identified chemo-repulsive cues within the striatum, such as the semaphorins (Semas), repel cortical interneurons from this region and stream these cells towards the cortex. Chemo-attratcive cues (+) within the cortex such as the secreted chemokine SDF-1 and the Neuregulin family of proteins attract interneurons towards the cortex. Slit proteins are candidate chemorepulsive cues suggested to regulate the ventral-dorsal migration of interneurons. (This figure was taken from Andrews et al., 2007.)

1.9 AIMS: TO INVESTIGATE THE PUTATIVE ROLES OF THE ROBO2 AND ROBO3 RECEPTORS IN INTERNEURON DEVELOPMENT

Given the important role of Robo1 in interneuron development and the fact that Robo2 and Robo3 appear to be expressed within the developing forebrain, a putative role for the other members of the Robo family in the development of cortical interneurons was investigated. A detailed investigation into expression patterns of all three Robo receptors was therefore carried out within the embryonic forebrain using a panel of Robo-specific antibodies. The question whether interneurons express the other two Robo receptors, as has been shown for Robo1, was investigated immunohistochemically in co-localisation experiments using Robo antibodies and interneuron specific markers. The results of these experiments, presented in Chapter 3, demonstrated that both Robo2 and Robo3 co-localise with interneuron markers during different stages of development. This led to the investigation of the putative role of the Robo2 and Robo3 receptors in regulating interneuron numbers and their positions within the developing cortex, as well as ascertaining their potential role in determining the morphology of migrating interneurons during development. These studies were carried out *in vivo* in Robo2 and Robo3 single mutant mice (data presented in Chapters 4 and 5 respectively). Given that interneurons were found to express all three Robo receptors during development, there was a possibility that these may be functionally redundant and compensate for each other's putative roles in regulating these processes. An analysis of the role of Robo in interneuron development was, therefore, further investigated in Robo1;Robo2;Robo3 triple mutant animals; these results are presented in

In addition, all three Robos were observed to be robustly expressed within the early developing PPL at a developmental time point when Cajal-Retzius cells are generated, and in regions through which these cells migrate. Given the importance of Cajal-Retzius cells in cortical development, and the localisation of Robo proteins at the sites of origin and along the migratory routes taken by these cells, the possibility that Cajal-Retzius cells express these receptors was studied, and the putative role Robo may have in regulating the numbers of Cajal-Retzius cells in the developing cortex further examined *in vivo*. These results are presented in Chapter 6.

CHAPTER 2: MATERIALS AND METHODS

2.1 MATERIALS

2.1.1 Animals

Wild type animals were C57/bl6J mice obtained from Charles River Ltd. Robo1$^{-/-}$ (Dulox), Robo2$^{-/-}$ and Robo3$^{-/-}$ transgenic mice were generated as described previously (Andrews et al., 2008; Lu et al., 2007; Sabatier et al., 2004; respectively). Single Robo3 mutant and triple Robo1;Robo2;Robo3 mutant mice were bred and maintained in the laboratory of Dr. Alain Chédotal (Paris). GAD67-GFP (Δneo) mice (Tamamaki et al., 2003) were also used in this study, and all mouse strains were maintained in a C57/bl6J background. The day the vaginal plug was found was considered as embryonic day (E) 0.5.

2.1.2 Antibodies

Table 2.1 Panel of antibodies employed in immunohistochemical investigations

ANTIBODY	SOURCE	DILUTION	REFERENCE
Rabbit anti-Robo1	Prof F. Murakami	1:5000	Andrews et al., 2006
Rabbit anti-Robo2	Prof F. Murakami	1:5000	Andrews et al., 2008
Rabbit anti-Robo3	Prof F. Murakami	1:1000	
Goat anti-Robo1	R&D Systems	1:100	Andrews et al., 2008
Goat anti-Robo2	R&D Systems	1:100	Andrews et al., 2008

Rabbit anti-calbindin	Swant	1:3000	Andrews et al., 2006
Mouse anti-reelin (G10)	Prof. A.Goffinet	1:500	Tissir and Goffinet, 2003
Biotinylated goat anti-rabbit IgG	Vector Laboratories	1:200	
Rabbit anti-mouse 488	Alexa, Invitrogen Corp, UK	1:200	
Rabbit anti-mouse 568	Alexa, Invitrogen Corp, UK	1:200	
Mouse anti-rabbit 488	Alexa, Invitrogen Corp, UK	1:200	
Mouse anti-rabbit 568	Alexa, Invitrogen Corp, UK	1:200	
Donkey anti-goat 488	Alexa, Invitrogen Corp, UK	1:200	
Donkey anti-goat-568	Alexa, Invitrogen Corp, UK	1:200	

2.2 METHODS

2.2.1 Immunohistochemistry

Embryonic brains (E11.5-18.5) were fixed by immersion in 4% paraformaldehyde (PFA) in phosphate buffer (PB) at 4^0C overnight. Brains were subsequently cryoprotected in 30% sucrose in PB, embedded in a mixture of 15% sucrose/50%Tissue-Tek OCT (Sakura Finetek Europe, Zoeterwoude, The Netherlands), and sectioned in the coronal plane at 20 µm using a cryostat (Bright Instruments, Huntingdon, UK). Endogenous peroxidise activity was quenched by incubation with 0.3% Hydrogen Peroxide () for 40 minutes. Sections were washed in PB, blocked in a solution of 5% normal goat serum (S-1000, Vector Laboratories, Burlingame, CA) (v/v) and 0.5% triton X-100 (v/v) (Sigma, UK) in PB at 37^0C for 2 hours. They were then incubated in primary

antibodies for 4 hours at room temperature followed by 48 hours at 4^0C. Following incubations in primary antibodies, sections were washed in PB, and incubated in biotinylated anti-species for 2 hours. Sections were washed in PB and calbindin antibody staining was processed using the Avidin-Biotinylated immuno-peroxidase enzyme Complex (Vector Laboratories) and visualised with the 3, 3'-Di-amino-benzidine substrate (Sigma, UK). All Robo antibody staining was amplified using a Tyramide Amplification System (TSA; Perkin Elmer, Boston, MA) according to manufacturer's instructions. Sections were washed and counterstained with Methyl Green (1:50) (Vector Laboratories) or 4'-6-Diamidino-2-Phenyllindole (DAPI, 1:20,000; D-9542, Sigma) in phosphate buffered saline (PBS). Images were collected using a Leica light microscope (DM5000B) or a Leica (SP2) confocal microscope (Leica Microsystems, UK). Sequential images were reconstructed using Metamorph imaging software (Universal Imaging Corporation, West Chester, PA).

2.2.2 Quantification of reelin-positive cells

Counts of reelin-positive cells were made from sections using the x20 objective of a Leica (DM5000B) microscope. These cells were counted in the PPL and MZ layers of the cortex throughout its rostral-caudal extent (minimum of 6 sections per level, per animal, per condition). The cortex was further subdivided along its dorso-medial axis, and counts were taken from the neocortical and hippocampal cortices. In all counts, the experimenter did not know the condition of each animal.

2.2.3 Quantification of calbindin-positive cells

Calbindin-positive cell counts were made from images collected with a Leica (DM5000B) microscope. Counts were made in coronal strips (200-400 μm wide) spanning the thickness of the dorsal neocortex throughout its rostral-caudal extent at E12.5-18.5 (minimum of 6 sections from each of 3 animals for each condition). In all counts, the experimenter did not know the condition of the animals. Each coronal strip was divided into 5 or 6 bins arranged parallel to the pial surface that these corresponded to the different layers of the developing cortex (VZ/SVZ, IZ, SP, CP, MZ), from bin1 (VZ/SVZ) to bin 5 (CP) or bin 6 (MZ/PPL). The extent of each layer was determined by Nissl or methyl green counter-staining, which are cytoplasmic neuronal markers.

2.2.4 Morphological analysis of calbindin-positive cells

Approximately 30-50 calbindin-positive neurons were drawn at a primary magnification of x400 using a drawing tube attached to a Zeiss photomicroscope. Interneurons were taken from the IZ and PPL at E13.5; and from the SP and SVZ/LIZ layers of the developing cortex for each animal at E15.5, E18.5. Morphometric parameters analysed included total process length, number of processes and number of branch points (Appendix Figure 1). Measurements were made using image analysis software (ImageJ; NIH, version 1.3) with custom made programming macros. Means and standard error of the mean (SEM) were calculated and the differences were tested using a Student's t test or a one-way Anova test. Significance was set at a P value of <0.05.

2.2.5 Axonal tracing with carbocyanine dyes

Embryonic brains were fixed overnight in 4% PFA. To expose the dorsal thalamus, a coronal cut was made at the caudal edge of the diencephalon. Single crystals of DiI (1, 1- dioctadecyl –3, 3, 3',3'-tetramethylindocarbocyanine perchlorate; Molecular Probes), and of DiA (4-(4-(dihexadecylamino)styryl)-N-methylpyridium iodide; Molecular Probes), were placed using a fine tungsten wire into the dorsal thalamus or dorsal cortex under a dissecting microscope. Any residual crystal powder was gently removed using 1xPBS, to ensure only a single crystal remained in place. Brains were incubated in 4% PFA at room temperature for 3 weeks. These were then embedded in 4% agarose and 100 μm coronal sections were cut using the vibroslice (Leica VT1000S). Tissue was counterstained with DAPI (1:20,000; D-9542, Sigma). Sections were coverslipped in CITI-Fluor (LandD, London Ltd.) and analysed with a fluorescence microscope (Leica DM5000B) or a laser scanning confocal microscope (Leica SP2). Sequential images were reconstructed using Metamorph imaging software.

CHAPTER 3: ROBO EXPRESSION IN THE DEVELOPING MOUSE FOREBRAIN

3.1 INTRODUCTION

Robo/Slit signaling has been proposed to be a key cellular and molecular mechanism underlying the guidance and migration of interneurons from their origins within the subpallial GEs to their final positioning within the cortex (Zhu et al., 1999; Hu et al., 1999, Andrews et al., 2006). In order to elucidate the potential role of Robo/Slit signaling in regulating interneuron migration, a systematic investigation into the expression patterns of all three Robo receptors was carried out in relation to the interneuron marker calbindin (Anderson et al., 1997a, 2001) throughout the period of interneuron migration. This was further compared with established patterns of Slit expression during early, mid- and later phases of tangential migration.

The expression of Robo/Slit genes has previously been investigated, predominantly by *in situ* hybridisation, and these studies have shown that *robo (robo1 and robo2)* and *slit (slit1, slit2, slit3)* genes are dynamically expressed in complementary patterns during cortical development (Yuan et al., 1999b; Bagri et al., 2002; Whitford et al., 2002; Marillat et al., 2002). The lack of adequate Slit antibodies has prevented the visualisation of Slit protein gradients. However, transgenic mice that express a fluorescent marker protein in *Slit1* and *Slit2* loci have made it possible to visualise Slit-expressing cells, thus confirming the results from previous *in situ* hybridisation studies (Bagri et al.,

2002). Robo localisation is therefore discussed in relation to these established patterns of Slit expression.

Whilst the localisation of *robo1* and *robo2* is well established within the rodent forebrain (Whitford et al., 2002; Bagri et al., 2002; Marillat et al., 2002), the expression patterns of *robo3* has been investigated primarily within the spinal cord and hindbrain, and these studies only paid cursory attention to the developing forebrain (Yuan et al., 1999a; Camurri et al., 2004; Sabatier et al., 2004; Mambetisaeva et al., 2005). These *in situ* hybridisation studies showed that Robo3 was transiently expressed within the early developing CNS, corresponding to PPL stages of cortical development (E11.5-E12.5) (Yuan et al., 1999a; Camurri et al., 2004; Sabatier et al., 2004).

The expression patterns of all three Robo receptor proteins was, therefore, investigated in detail within the developing mouse forebrain using immunohistochemistry during both PPL (E11.5-E13.5) and CP (E15.5, E17.5) stages of development. Recently, Robo-specific antibodies have become available which are raised to the extracellular domains of Robo1, Robo2 and Robo3 proteins (Sabatier et al., 2004; Andrews et al 2008) and thus, enable specific Robo protein patterns to be investigated using immunohistochemistry (see Methods Table 2.1). All expression studies were carried out in C57/bl6J wild type strain of mice. A comparable study in the rat did not reveal any differences between the observed staining patterns (data not shown), and thus these expression studies are representative of Robo expression within the developing rodent forebrain.

3.1.1 Specificity of Robo antibodies

The specificity of the polyclonal rabbit (Fig. 3.1) and goat (data not shown) Robo antibodies was tested on mouse cortical tissue taken from Robo1 (Fig. 3.1A-B), Robo2 (Fig. 3.1C-D) and Robo3 (Fig. 3.1E-F) single knockout transgenic mice. These confirm that the localisation of Robo proteins was specific for each antibody (Fig. 3.1). Furthermore, when the primary antibody was omitted in the immunohistochemical processing, no staining was detected (data not shown), confirming that the observed staining is specific to each Robo protein and not a result of non-specific background staining. While antibodies were not tested using a Wetern Blot analysis here, previous studies by Long et al. (2004) (Robo1, Robo2) and Sabatier et al. (2004) (Robo3) have shown these antibodies (also sourced by F Murakami) to be specific.

The patterns of expression obtained using either polyclonal rabbit or goat Robo antibodies were further assessed to determine whether these were comparable and to determine if they were consistent with previous *in situ* hybridisation studies (Fig. 3.2) (see Discussion section 3.6). These showed that Robo antibodies raised in both goat and rabbit were comparable.

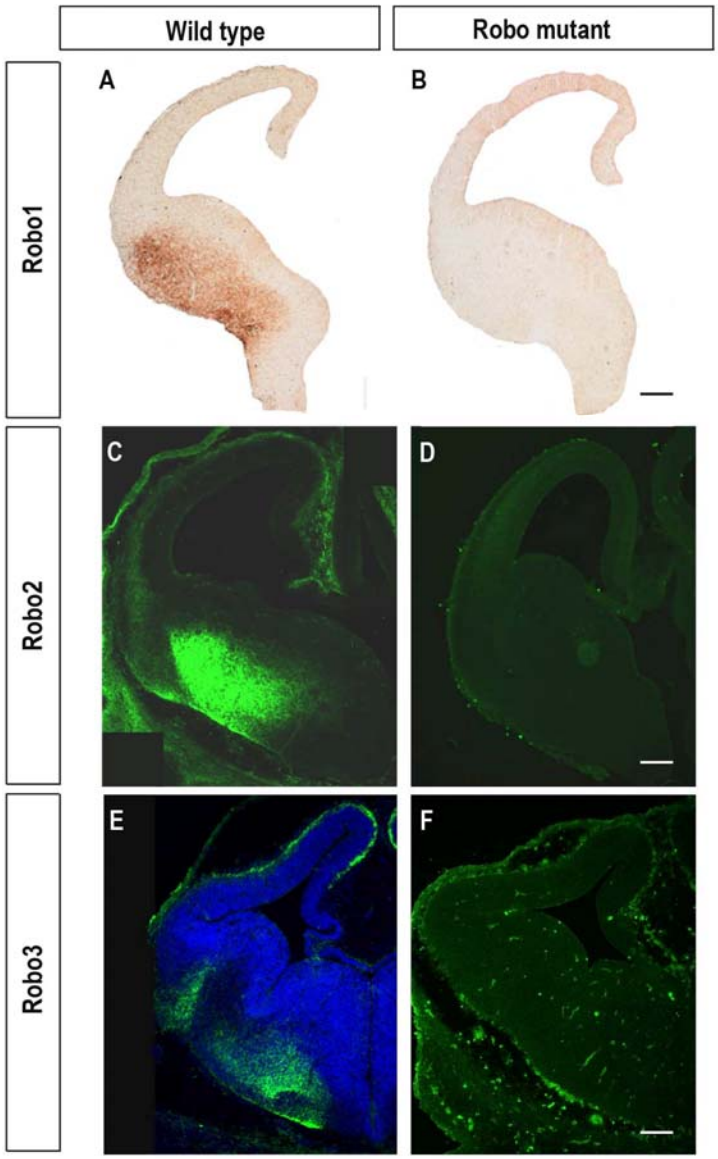

Fig. 3.1 Specificity of Robo antibodies. Panels B,D,F, show coronal sections through the forebrain of Robo1 (B), Robo2 (D) and Robo3 (F) mutant animals, immunohistochemically processed for Robo1, Robo2 and Robo3 proteins respectively, using Robo-specific antibodies. An absence of staining is observed when immunohistochemistry is performed on forebrain sections taken from Robo deficient mutants (B,D,F), in contrast to robust localisation of Robo proteins visualised in sections taken from wild type animals (A,C,E). Non-specific staining of blood vessles was sometimes observed in sections, as shown in panel F. The absence of staining in forebrain tissue taken from Robo deficient mice confirms Robo antibodies to be specific. Scale bar in B is 200 μm and corresponds to A,B; in D is 400 μm and corresponds C,D; and in F is 300 μm and corresponds to E,F. (Panels A&B were taken from Andrews et al. 2006).

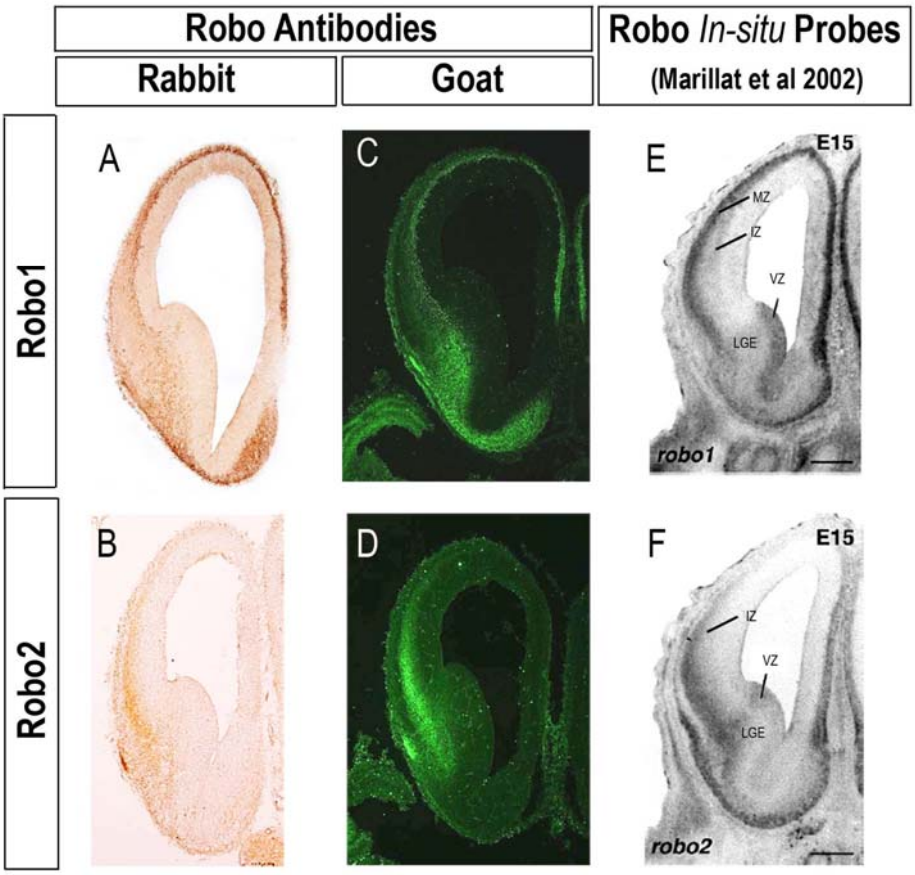

Fig. 3.2 Comparison of Robo protein and Robo mRNA expression profiles in the developing rodent cortex. Coronal sections taken from the E13.5 wild type mouse forebrain were immunohistochemically processed for Robo1 (A,C) and Robo2 (B,D) proteins using rabbit (A,B) and goat (C,D) antibodies. Identical patterns of Robo protein expression were observed by immunohistochemistry when using either rabbit (A,B) or goat (C,D) antibodies. A comparison of Robo protein localisation with Robo1 mRNA (E) and Robo2 mRNA (F) profiles was analysed at a comparable age in the developing rat forebrain (E15.5r) (E,F). Robo2 protein (B,D) and mRNA (F) expression coincide within the differentiating LGE and within the intermediate zone (IZ) of the developing cortex. Robo2 mRNA, however, is also expressed within anterior regions of the germinal LGE-VZ (F), a region devoid of Robo2 protein (B,D). Robo1 protein (A,C) and mRNA (E) are consistently expressed within the differentiating field of the LGE and within the MZ of the cortex (A,C). However, Robo1 protein is also clearly expressed wtihin the cortical IZ, where Robo1 mRNA is not localised at this time. In addition, Robo1 mRNA is observed throughout the germinal VZ of the GEs in the ventral forebrain (E), discrepant from the absence of Robo1 protein in this region (A,C). Scale bar in E-F is 200 μm, and corresponds to all images. (VZ, ventricular zone; LGE, lateral ganglionic eminence; IZ, intermediate zone; MZ, marginal zone). (*In-situ* figures are taken from the study of Marillat *et al*. 2002).

3.2 RESULTS: ROBO EXPRESSION IN THE DEVELOPING FOREBRAIN

3.2.1 Robo expression during preplate stages of development

A comparative analysis of the expression profiles of all three Robo proteins was investigated using immunohistochemistry at E11.5-E13.5. Given that a detailed analysis of the Robo3 receptor had not been previously carried out, the expression patterns for this receptor was investigated in greater detail.

At E11.5, Robo2 and Robo3 were robustly expressed within the PPL throughout the rostral-caudal extent of the cortex (Fig. 3.3B, E, H and 3.3C, F, I, respecitvely), and staining was of a cellular nature. This was especially prominent for the Robo3 receptor which was expressed in a distinctive later-medial gradient (Fig. 3.3C); Robo1 was only weakly expressed within the PPL at this time (3.3D), and was more laterally restricted within this region. In the subpallium, all three Robo receptors showed distinct, but overlapping, patterns of expression within the medial septum (Fig. 3.3A-C) as well as throughout the LGE (Fig. 3.3A-F) and CGE (Fig. 3.3G-I). Stream-like staining extended ventrolaterally from the medial septum towards the LGE (arrows in 3.3A-C). Robo1 and Robo3 proteins also overlapped within the developing preoptic area where these were distinctly expressed (Fig. 3.3G, I). Whilst Robo1 and Robo3 receptors were broadly expressed in overlapping patterns within the MGE, Robo2 expression was restricted to a narrow stream of cells in the dorsal-most region of this structure (Fig. 3.3E). Stream-like patterns of Robo protein were also observed to extend dorsally from the MGE and LGE towards the cortico-

striatal boundary in rostral and middle levels of the forebrain (arrowheads in Fig. 3.3D-F), and from the CGE within caudal regions (arrowheads Fig. 3.3G-I). Expression emanating from the GEs was contiguous with Robo protein localised within the PPL and this was especially distinctive of Robo3 protein (arrowheads in Fig. 3.4). Closer examination of sections processed for the Robo3 receptor protein revealed distinctly labelled cells that exhibited morphologies characteristic of migrating neurons (Fig. 3.5D). This stream of migrating cells extended dorso-medially from the level of the cortico-striatal boundary and, in rostral and middle regions, it reached the prospective cingulated cortex (Fig. 3.5A); in more caudal regions, it extended to the cortical hem (Fig. 3.5B).

A day later (E12.5), Robo1 and Robo3 were clearly localised within the PPL in a reverse gradient of expression, with the protein most strongly expressed within the cortical hem of the dorso-medial cortex and diminishing in a medio-lateral gradient (Fig. 3.5 E-G). This was especially distinctive of Robo3 protein, and closer analysis showed this to comprise a stream of Robo3 immunopositive cells (Fig. 3.5H). Robo2 was only weakly expressed in this layer (Fig. 3.6E). All three Robo proteins were localised in the GE at this stage (Fig. 3.6D-F). Specifically, Robo1 and Robo3 showed similar patterns of expression both within the MGE and LGE, and overlapped in regions where Robo1 protein was most robustly localised within the LGE (arrowheads, Fig. 3.6D, F). Interestingly, Robo2 expression appeared to be complementary to that of Robo3 within the subpallium, whilst overlapping with that of Robo1 in the LGE. All three Robos were also strongly localised within the CGE at this stage (data not shown).

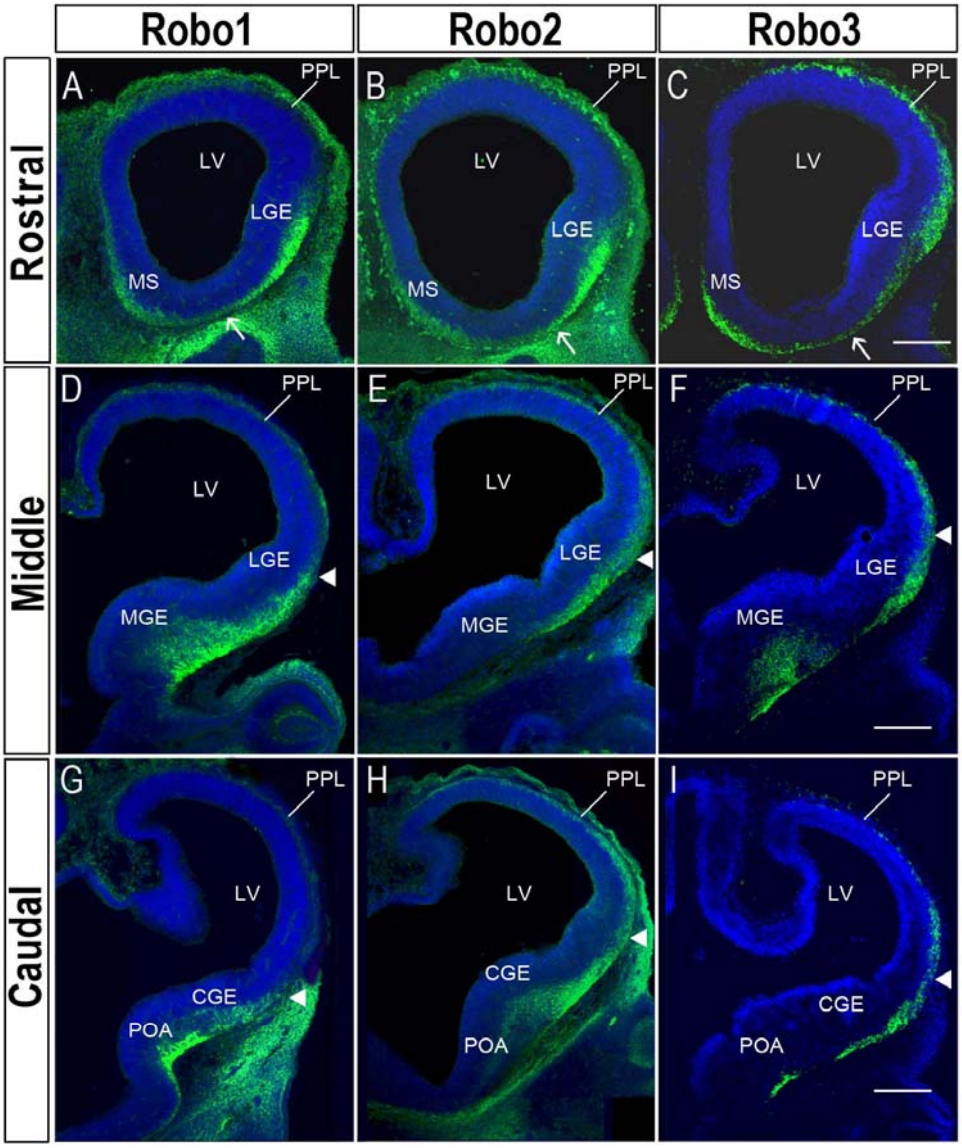

Fig. 3.3 Expression of Robo receptors in the murine forebrain during preplate stages of development. Comparative analysis of Robo1 (A,D,G), Robo2 (B,E,H) and Robo3 (C,F,I) proteins at rostral, middle and caudal levels of the embryonic mouse forebrain at E11.5. Note stream-like staining as it extends from the differentiating LGE (D-F) and CGE (G-I) towards the cortex (arrowheads). A stream of Robo protein also extends ventrolaterally from the MS to the LGE (arrows in A-C). Scale bar is 200 μm in C,F,I and applies to all panels. (LV, lateral ventricle; PPL, preplate; LGE, lateral ganglionic eminence; MGE, medial ganglionic eminence; CGE, caudal ganglionic eminence; POA, preoptic area; MS, medial septum).

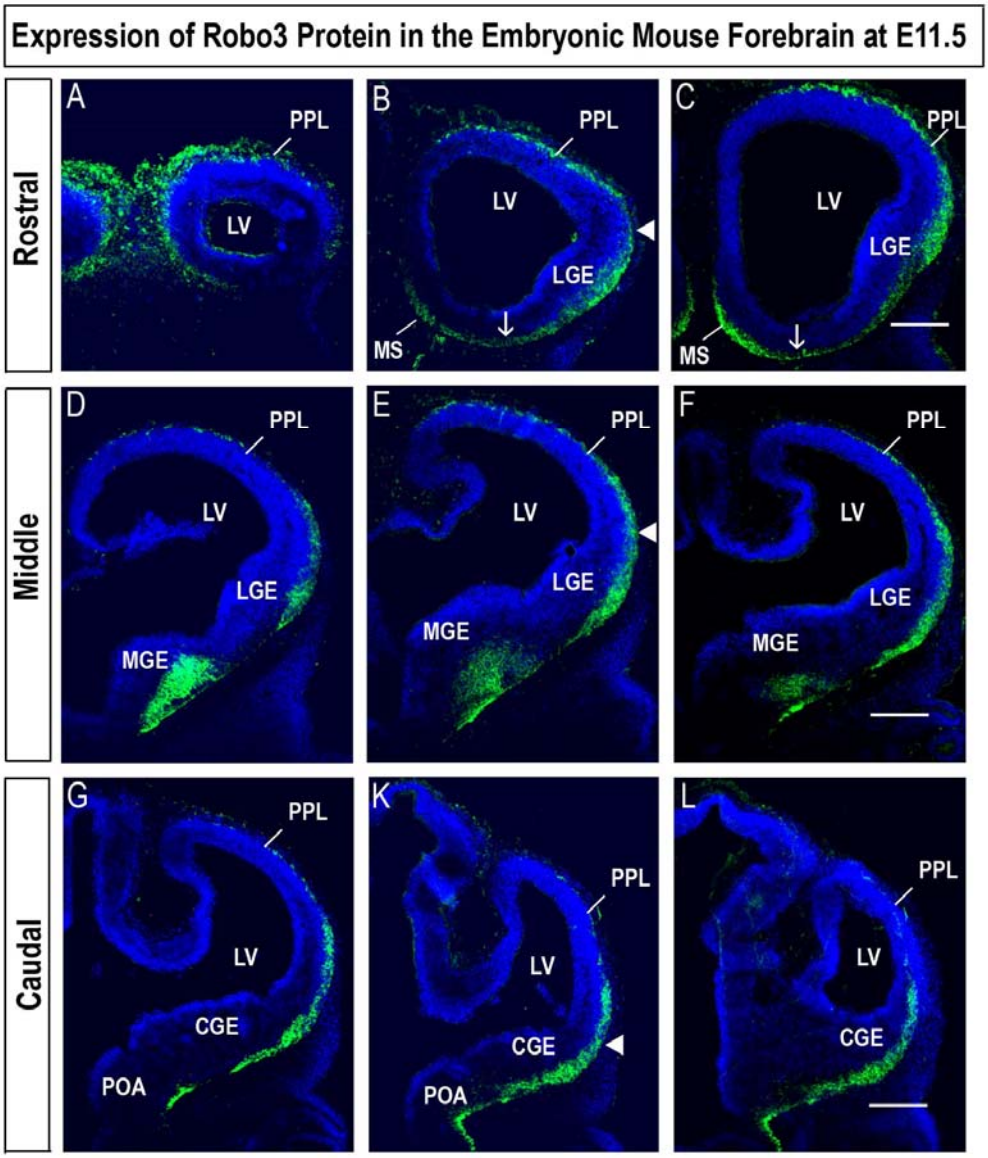

Fig 3.4 Robo3 expression in the embryonic mouse forebrain at E11.5. Expression of Robo3 proteins at rostral (A-C), middle (D-F) and caudal (G-L) levels of the embryonic mouse forebrain. Robo3 protein is localised within the GEs from which a stream of protein extends dorsolaterally towards the PPL (arrowheads). Stream-like staining is also observed within the MS which extends ventrolaterally to the LGE (arrows, B,C). Scale bar in C,F,L is 200 μm, and corresponds to all images. (LV, lateral ventricle; PPL, preplate; LGE, lateral ganglionic eminence; MGE, medial ganglionic eminence; CGE, caudal ganglionic eminence; POA, preoptic area; MS, medial septum).

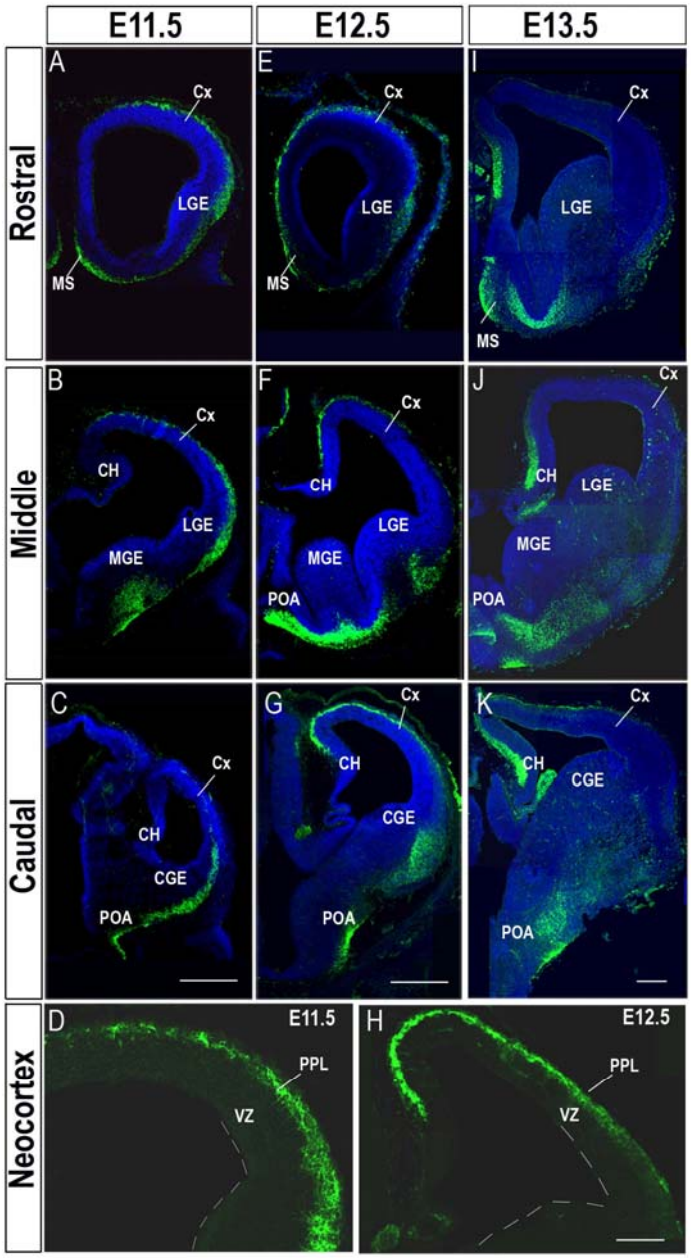

Fig. 3.5 Expression of the Robo3 receptor in the embryonic murine forebrain during preplate stages of development (E11.5-E13.5). Immunohistochemical localisation of the Robo3 receptor at rostral (A,E,I), middle (B,F,J) and caudal (C,G,K) levels of the embryonic mouse forebrain at E11.5-E13.5. Scale bar in C,G,K is 200 μm, and applies to panels of equivalent ages. Higher magnification images taken through middle levels of the cortex at E12.5 (H) shows a reversal in the lateromedial gradient of Robo3 expression observed at E11.5 (D). Scale bar is 200 μm in H, and applies to D. (Cx, cortex; PPL, preplate; CH cortical hem; VZ, ventricular zone; LGE, lateral ganglionic eminence; MGE, medial ganglionic eminence; CGE, caudal ganglionic eminence; POA, preoptic area).

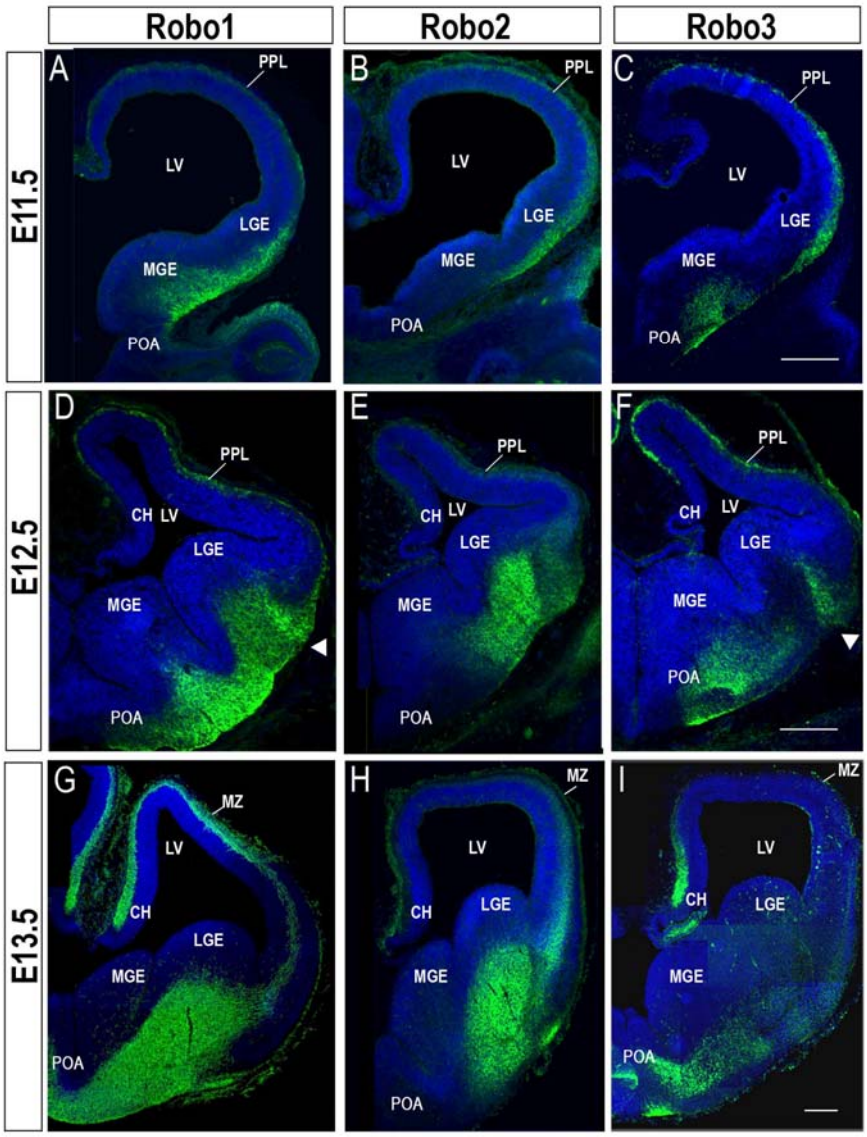

Figure 3.6 Comparative analysis of Robo expression during preplate stages of development. Localisation of Robo1 (A,D,G), Robo2 (B,E,H) and Robo3 (C,F,I) receptors in coronal sections taken from middle levels of the embryonic mouse forebrain at E11.5-E13.5. Robo1 and Robo3 overlap within the developing ganglionic eminences (GEs) and cortex, with Robo3 expression within the lateral ganglionic eminence (LGE) corresponding to regions where Robo1 is most robustly localised (arrowheads in D,F). Robo2 is predominately restricted to the developing LGE within the ventral forebrain, during these early stages of development. Scale bar in C,F,I is 200 μm, and applies to panels of equivalent ages. (CH, cortical hem; LV, lateral ventricle; MZ, marginal zone; PPL, preplate; LGE, lateral ganglionic eminence; MGE, medial ganglionic eminence; CGE, caudal ganglionic eminence; POA, preoptic area).

Analysis at E13.5 showed that while Robo3 expression was mostly down regulated within the cortex and ventral forebrain (Fig. 3.6I), consistent with previous observations (Camurri et al., 2004), Robo1 and Robo2 continued to be strongly expressed within the embryonic forebrain (Fig. 3.6 G&H, respectively). Robo1 and Robo2 were expressed in mostly complementary patterns within the ventral forebrain at this stage. While Robo2 protein was predominantly restricted to the differentiating LGE, Robo1 continued to be broadly expressed throughout the differentiating GEs. Robo3 expression was now restricted to ventral regions of the MGE, where dispersed Robo3 immunopositive cellular-like staining was observed (Fig. 3.6G and I). Both Robo1 and Robo3 were also robustly localised within the preoptic area and septum (Fig.3.6 G & I) at this time.

All three receptors were expressed within the developing cortex at E13.5. Robo1 and Robo3 receptors were strongly expressed within the cortical hem, and this extended in a decreasing mediolateral gradient throughout the PPL/MZ of the cortex (Fig. 3.6G-I). Robo2 showed a more restricted expression within medial regions of the cortical hem, with diffuse staining observed within the PPL/MZ (Fig. 3.6H). This receptor showed strongest expression within the IZ, where this overlapped with Robo1 (Fig.3.6G & I), consistent with previous reports (Marillat et al., 2002; Andrews et al., 2008). Taken together, these observations show that all three Robo receptors are expressed at the early stages of forebrain development (E11.5-13.5), with Robo1 and Robo3 overlapping to a high degree both within the subpallium and developing cortex, suggesting that Robo3 may play similar roles to the other two receptors, and that it may be expressed by the same cell types.

3.2.2 Robo expression during cortical plate stages of development

While Robo3 was largely down regulated within the forebrain during CP stages of development (E15.5, E17.5), consistent with previous observations (Camurri et al., 2004), both Robo1 and Robo2 continued to be robustly expressed throughout its rostral-caudal extent.

Analysis at E15.5 showed that Robo1 expression was strongly maintained throughout the differentiating GEs (3.7A-C), septum (Fig. 3.7A) and preoptic area (Fig.3.7B) in the ventral forebrain. Robo2 expression persisted within the differentiating LGE (Fig. 3.7D-E), however, it was now more broadly expressed within the subpallium and extended ventromedially to dorsal regions of the differentiating MGE (Fig. 3.7E), where it overlapped with Robo1. Thus, while Robo1 and Robo2 continued to be expressed in largely complementary patterns within the ventral forebrain, they overlapped to a greater degree within the GEs.

Both Robos were expressed throughout the rostral-caudal extent of the developing cortex at E15.5, and were distinctly localised within the IZ (Fig. 3.7G-L). Although Robo1 and Robo2 overlapped to some degree within this layer, they exhibited differing patterns of expression. Robo1 protein expression was observed within the lower IZ and further extended to the SVZ (Fig. 3.7G-I). Robo2 expression was superficial to Robo1, and was localised within the upper IZ (Fig. 3.7J-L). Closer analysis showed that Robo1 staining was of a punctate nature and that this was interspersed in dense fibrous-like staining within these layers (see arrows in Fig. 3.7G and H). Robo2 staining was more diffuse than Robo1 but some cellular-like staining was similarly visible within the IZ (arrow

in Fig 3.7 L). Both Robos were also observed at low levels within the developing CP, MZ and SP layers at this time (Fig. 3.7G-L; see also arrowhead in 3.7E).

In addition, both Robo1 and Robo2 receptors were evident within some developing fiber systems in the forebrain at E15.5. Robo2 was distinctly expressed within the lateral olfactory tract (Fig. 3.7D), where Robo1 was also noted at low levels (Fig. 3.7A). Distinctive fibrous-like staining for both Robo1 and Robo2 was also observed within the developing internal capsule (Fig. 3.7C and F). Whereas Robo1 positive fibers were observed at all levels of the internal capsule (Fig. 3.7A-C), this was particularly evident for Robo2 in caudal levels of the forebrain (3.7F). Salient fibrous-like Robo1 staining was also observed within the dorsal thalamus. In addition, marked Robo1 expression was observed in fiber tracts traversing through the cortical IZ and these extended dorsomedially to the cingulated cortex at rostral levels of the forebrain, where fibers of the anterior commisure and fornix were distinctly labeled (Fig. 3.7A). The hippocampal commissural tract was also strongly Robo1 immunopositive (Fig. 3.7 B, C) in more caudal levels of the forebrain. Robo2 expression was diffuse within the IZ, however some fibers within the subplate were labeled (arrowhead in 3.7E). Interestingly, while Robo3 expression was down regulated within the forebrain at this stage, striking fibrous-like staining was observed within the fornix in rostral levels of the forebrain (Fig. 3.8A).

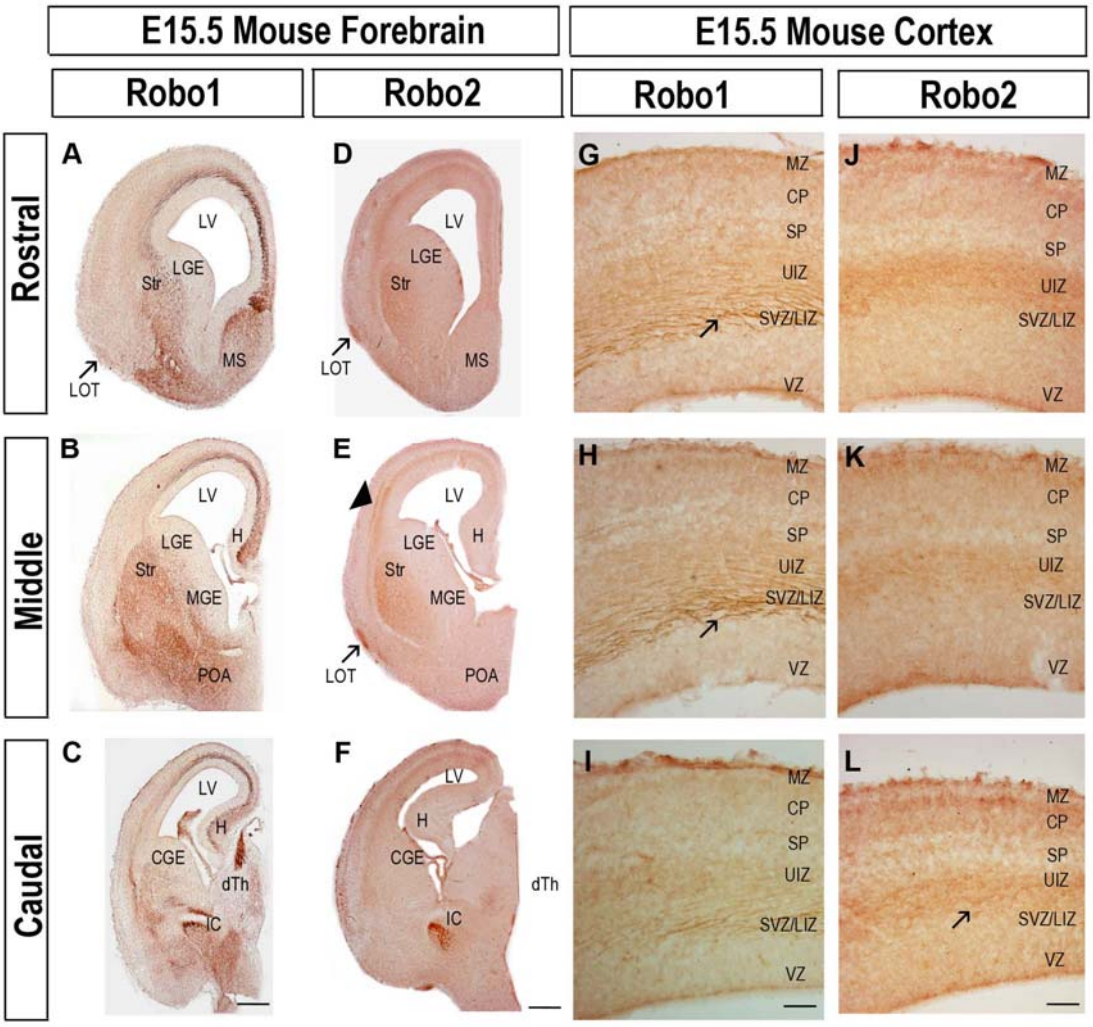

Fig. 3.7 Expression of Robo1 and Robo2 in the embryonic mouse forebrain at E15.5. Immunohistochemical localisation of Robo1 (A-C) and Robo2 (D-F) receptors at rostral (A,D), middle (B,E) and caudal (C,F) levels of the embryonic mouse forebrain. Higher magnification images taken through corresponding levels of the cortex are shown in G-L. Robo1 (G-I) and Robo2 (J-L) are strongly expressed within the cortical IZ and upper SVZ, where staining of a punctate and fibrous-like nature is observed (arrows in G,H,L). Scale bar is 300 μm in C,F and corresponds to A-F; Scale bar in I,L is 75 μm and corresponds to G-L. (H, hippocampus; LV, lateral ventricle; LGE, lateral ganglionic eminence; MGE, medial ganglionic eminence; CGE, caudal ganglionic eminence; MS, medial septum; Str, striatum; POA, preoptic area; LOT, lateral olfactory tract; dTh, dorsal thalamus).

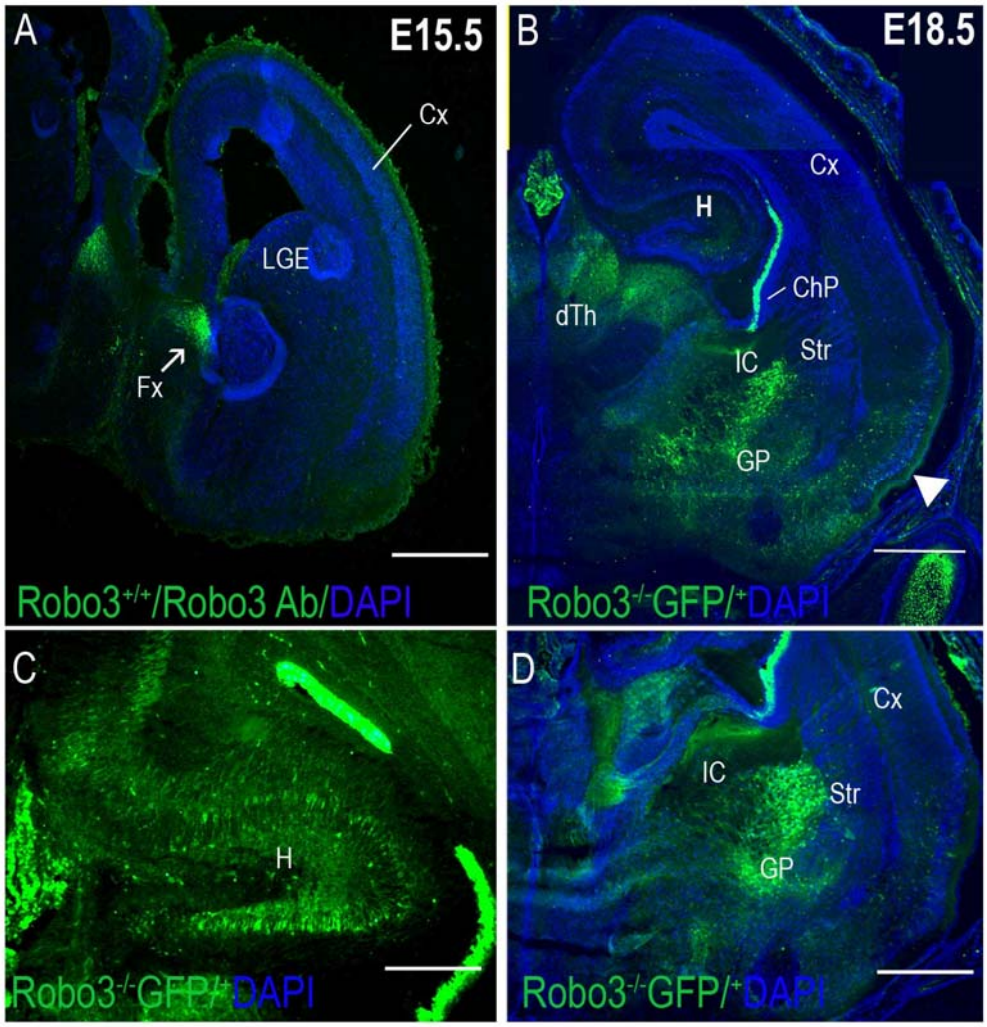

Fig. 3.8 Robo3 expression in the embryonic mouse forebrain during cortical plate stages of development. Robo3 localisation using immunohistochemistry shows distinctly labelled fibres of the fornix in rostral levels of the embryonic wild type mouse forebrain at E15.5 (A). Coronal section taken from a transgenic Robo3 mutant mouse forebrain at E18.5, in which Robo3 was tagged with GFP, (Robo3$^{-/-GFP+/+}$) is shown in panel B. GFP positive cellular-like staining is distinctly observed within the hippocampus (H) and in the differentiating basal ganglia at this stage, and is further illustrated by higher magnification photomicrographs in panels C,D. Diffuse staining is also observed in the dTh, and within the rhinencephalon (arrowhead in B). Scale bar in A is 500 μm; in B is 850 μm; and in C-D is 600 μm. (Cx, neocortex; H, hippocampus; Fx, fornix; LGE, lateral ganglionic eminence; ChP, choroid plexus; IC, internal capsule; Str, striatum; GP, globus pallidus; dTh, dorsal thalamus).

At E17.5, Robo1 and Robo2 were noticeably down regulated in the differentiating basal ganglia, however, these receptors continued to be expressed in a more restricted pattern within dispersed cells in the differentiating LGE (striatum) and MGE (pallidum) at this time (Fig. 3.9). Robo2 was expressed at low levels within the striatum and within the nucleus accumbens in rostral levels of the forebrain (Fig. 3.9D), where Robo1 protein also persisted (Fig. 3.9A). In addition, Robo1 was expressed throughout the germinal SVZ of the LGE and MGE. Staining was of a punctate and fibrous-like nature, comprising some fibers of the developing internal capsule in this region (Fig. 3.9A-C), and this extended towards the cortico-striatal boundary (arrowheads in 3.9A, B). Similarly, diffuse Robo2 staining within the GEs appeared to be contiguous with staining within the cortex (arrowhead in Fig. 3.9D, E). While Robo1 was down regulated, low levels of this receptor was still expressed within the septum (Fig. 3.9A) and preoptic area (Fig. 3.9B) at this time.

Robo1 and Robo2 expression was sustained throughout the rostral-caudal extent of the developing cortex at E17.5 (Fig. 3.9G-L). Both receptors were distinctly localised within the LIZ/SVZ, and were diffusely expressed throughout the developing CP. Robo1 staining was of a fibrous-like nature with punctate staining clearly interspersed within the fibers (arrows in Fig. 3.9 G,H), and this extended dorso-medially to the cingulated (Fig. 3.9A) and hippocampal (Fig. 3.9B) cortex. Robo2 staining within the IZ was mostly diffuse; however, some cellular like staining was visible throughout the rostral-caudal extent of the IZ (arrows Fig. 3.9K). It too, extended dorso-medially to the cingulated cortex at rostral levels, and to the hippocampal cortex at middle and caudal levels of the forebrain (Fig. 3.9D-F).

In addition, both Robo1 and Robo2 were expressed within the developing corpus callosum (data not shown) and within fiber tracts in the lower IZ within the cortex (Fig. 3.7A, D). This was especially distinctive of Robo1 (A-C), which was also expressed by the anterior and hippocampal commisure in middle levels of the forebrain (Fig. 3.9B). While Robo1 was strongly maintained throughout the internal capsule, Robo2 was only diffusely expressed in these regions (3.9 D-F). Fibers of the developing lateral olfactory tract continued to express both Robo1 and Robo2 (Fig. 3.9A, D) receptors at this time, and the optic tract was also strongly Robo2 immunopositive (Fig. 3.9F).

The immunohistochemical investigation of the expression patterns of the Robo3 receptor at E17.5, suggested that Robo3 was down regulated throughout the cortex and ventral forebrain, with no clear staining visible in these regions (data not shown). Another way of investigating putative Robo3 expression *in vivo* was to use *Robo* transgenic mice in which the green fluorescent protein (GFP) reporter gene had been inserted into the loci encoding the *Robo3* gene. Thus, coronal sections taken from both Robo3 heterozygote and Robo3 mutant E18.5 mice were analysed for GFP. GFP staining was not evident within the cortex of heterozygote mice. Given that only a single copy of the GFP-encoding allele is present, GFP fluorescence was further enhanced using a GFP-specific antibody. This similarly did not show any marked staining within the embryonic cortex (data not shown) of Robo3 heterozygotes. Thus, these studies showed that Robo3 was down regulated within the cortex at this time, consistent with previous observations (Camurri et al., 2004).

Interestingly, analysis of Robo3$^{-/-}$;GFP+ mutant mice showed discrete populations of cells which were strongly labeled with GFP both within the cortex and basal telencephalon (Fig. 3.8B-D). Populations of Robo3$^{-/-}$/GFP+ cells were observed within the hippocampal cortex (Fig. 3.8C), the differentiating field of the striatum at caudal levels of the forebrain (Fig. 3.8D), as well as in some dispersed cells within the developing rhinencepahlon (arrow in Fig. 3.8B). Diffuse GFP+ staining was also observed within the dorsal thalamus (Fig.3.8B). The accumulation of Robo3$^{-/-}$;GFP+ cells within the differentiating striatum within basal telencephalon was striking and, interestingly, this was only observed at caudal levels of the forebrain. The histological boundary between the lateral and medial GEs is, morphologically, less easily distinguished during later stages of development. Furthermore, it has been shown that the striatum and globus pallidus comprise populations of neurons derived from distinct sources (Sussel et al., 1999; Marín et al., 2001b; López-Bendito et al., 2008). Indeed striatal cortical interneurons migrate from their origins within the MGE to populate the striatum during early stages of development (Marín et al., 2001b). Given the expression of Robo3 within the MGE during early stages of neurogenesis, it is tempting to speculate that striatal interneurons may also express the Robo3 receptor. The molecular characterization of these cells using LGE (Gsh1,2, Islet, Ebf1, Meis 2) (López-Bendito et al., 2008) and MGE (Nkx2.1, Lhx6) (Sussel et al., 1999) regional markers will help characterize the origins and identity of these Robo3$^{-/-}$/GFP+ cells within the basal telencephalon.

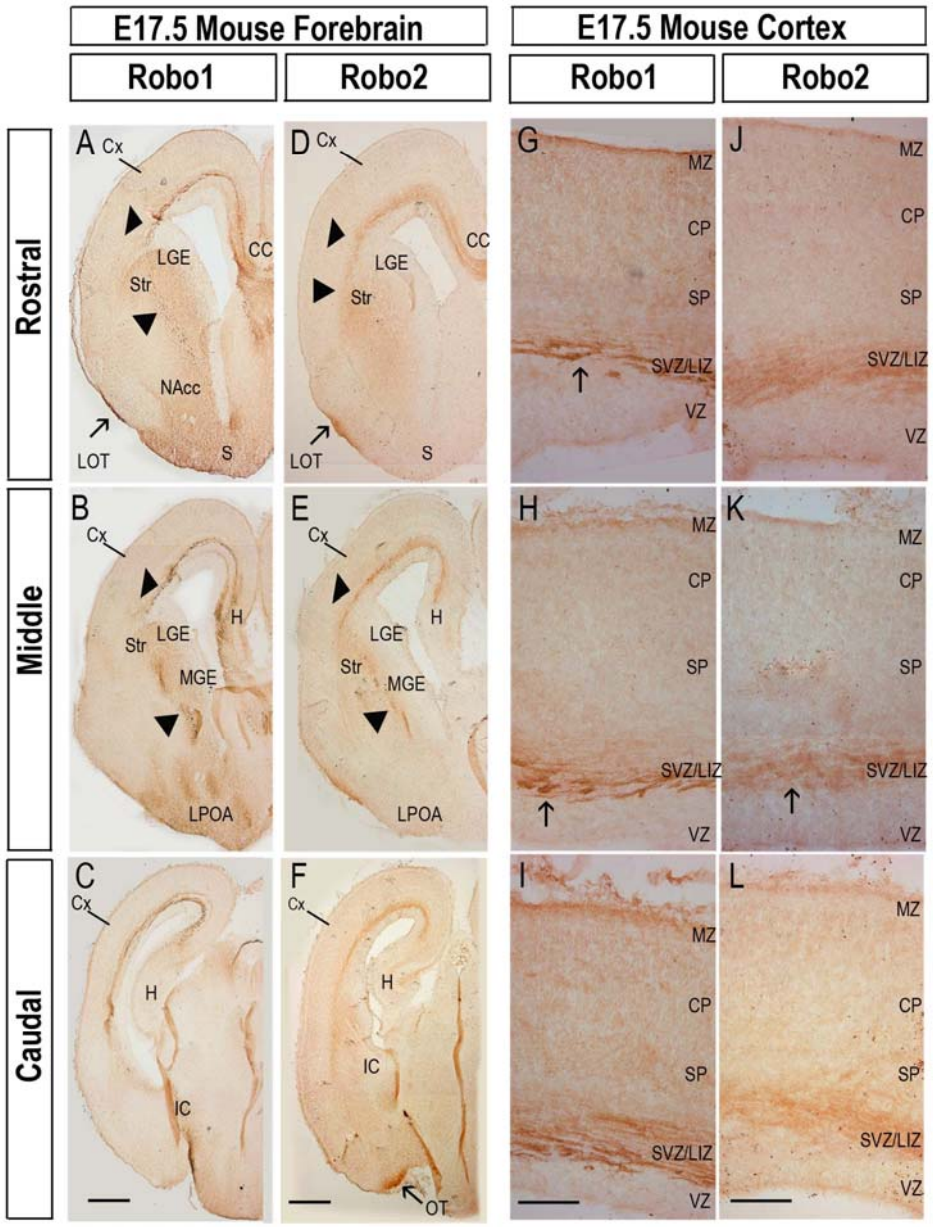

Fig. 3.9 Robo1 and Robo2 expression in the embryonic mouse forebrain at E17.5. Immunohistochemical localisation of Robo1 (A-C, G-I) and Robo2 (D-F, J-L) receptors at rostral, middle and caudal levels of the embryonic mouse forebrain (A-F) and neocortex (G-L) at E17.5. Robo protein is strongly localised within the SVZ/LIZ of the cortex, where staining of a punctate and fibrous-like nature is visible (arrows in G,H,K). Scale bar in C,F is 500 μm, and corresponds to A-F. Scale bar in I,L is 200 μm and applies to images G-L. (H, hippocampus; Cx, cortex; CC, corpus callosum; LGE, lateral ganglionic eminence; MGE medial ganglionic eminence; CGE caudal ganglionic eminence; Str, striatum; LPOA, lateral preoptic area; S, septum; IC, internal capsule; NAcc, nucleus accumbens; LOT lateral olfactory tract; OT, optic tract; MZ, marginal zone; CP, cortical plate; SP, subplate; SVZ/LIZ, subventricular zone/lower intermediate zone; VZ, ventricular zone).

While the Robo3-/-/GFP+ staining did not reflect the endogenous expression of Robo3 *in vivo,* this tentatively suggested that populations of cells may express the Robo3 receptor during later stages of development. Nonetheless, immunohistochemical studies in wild type animals and analysis of GFP+ staining in Robo3$^{+/-}$ heterozygote and Robo3$^{-/-}$ homozygote null mutant animals confirmed the absence of Robo3 protein within the neocortex during later stages of corticogenesis (E18.5).

3.4 DO INTERNEURONS EXPRESS ROBO PROTEINS?

Given the robust expression of all three Robos within the GEs, a major source of interneurons, as well as the distinctive cellular-like localisation of Robo protein in regions through which these cells migrate, suggested that interneurons may express all three Robo receptors during development. The expression patterns of Robo were thus compared with the interneuron marker calbindin (Anderson et al., 1997a, 2001) during all stages of interneuron migration. As Robo3 is mostly down regulated within the cortex by E13.5, only Robo1 and Robo2 receptors were investigated in relation to calbindin during later stages of development (E15.5-17.5).

3.4.1 Robo and calbindin during preplate stages of development

Robo1 and Robo3 expression patterns strongly correlated with that of calbindin within the differentiating basal ganglia and cortex at E13.5 (Fig. 3.10). Calbindin was distinctly expressed in the differentiating GEs and extended dorso-laterally from the differentiating LGE and CGE towards the cortex. This corresponded to the superficial route followed by early cohorts of migrating

interneurons to the cortex (Lavdas et al., 1999; Anderson et al., 1997a, 2001; Marín et al., 2003b; Métine et al., 2006) (see arrows in Fig. 3.10D,H). Robo1 and Robo3 overlapped with calbindin expression within the differentiating MGE (Fig. 3.1E,G,H), and this was complementary to Robo2 expression which was mostly restricted to the differentiating LGE at this time (Fig. 3.10F).

Calbindin was strongly expressed in the IZ and PPL at E13.5 (Fig. 3.11D,H,L), corresponding to the tangential migratory routes interneurons follow within the cortex at this stage. All three Robos overlapped with calbindin within the developing PPL (Fig. 3.11), with Robo1 and Robo2, but not Robo3, also overlapping within the IZ (exemplified by Fig. 3.11E,F,G, respectively).

Given that all three Robo proteins corresponded to areas where calbindin was expressed within the early developing forebrain, this suggested that interneurons may express these receptors during development. Double labeling experiments were, therefore, carried out for Robo and calbindin proteins. These showed that Robo1 (Fig. 3.12A), but not Robo2 (Fig. 3.12D), co-localised with calbindin within the IZ at E13.5 (Fig. 3.12C,F respectively). Some double labeled Robo1 and calbindin positive cells were also observed within the MZ at this time (see arrowhead in Fig. 3.12C).

As both Robo3 and calbindin antibodies were polyclonal antibodies raised in rabbit, double labeling experiments could not be carried out in this manner for Robo3. To circumvent this problem, coronal slices were taken from GAD67-GFP mice at a developmental time point when Robo3 was robustly expressed within the MGE, corresponding to early stages of interneuron neurogenesis

(E11.5), and these were labeled with Robo3 antibody (Fig. 3.13). In these transgenic mice, GFP has been inserted into the GAD67 loci, which codes for an enzyme in the GABA synthesizing pathway. Hence, any MGE cells, which fluoresce green, are considered to be GABAergic interneurons (Tamamaki et al., 2003). Labeling studies showed co-localisation of Robo3 receptor protein with GFP positive cells within the early MGE and in a stream extending dorsally towards the cortex (Fig 3.13A-C), confirming that early cohorts of interneurons also express the Robo3 receptor *in vivo*.

The co-localisation of the Robo3 receptor with interneuron markers was further confirmed in dissociated MGE cultures taken from E13.5 GAD67-GFP mice. These were immunohistochemically processed for the Robo3 receptor. These experiments showed that Robo3 protein was expressed within the cell soma and throughout the processes of GAD67-GFP positive cells, further confirming that early born interneurons express the Robo3 receptor (Fig 3.13D-F).

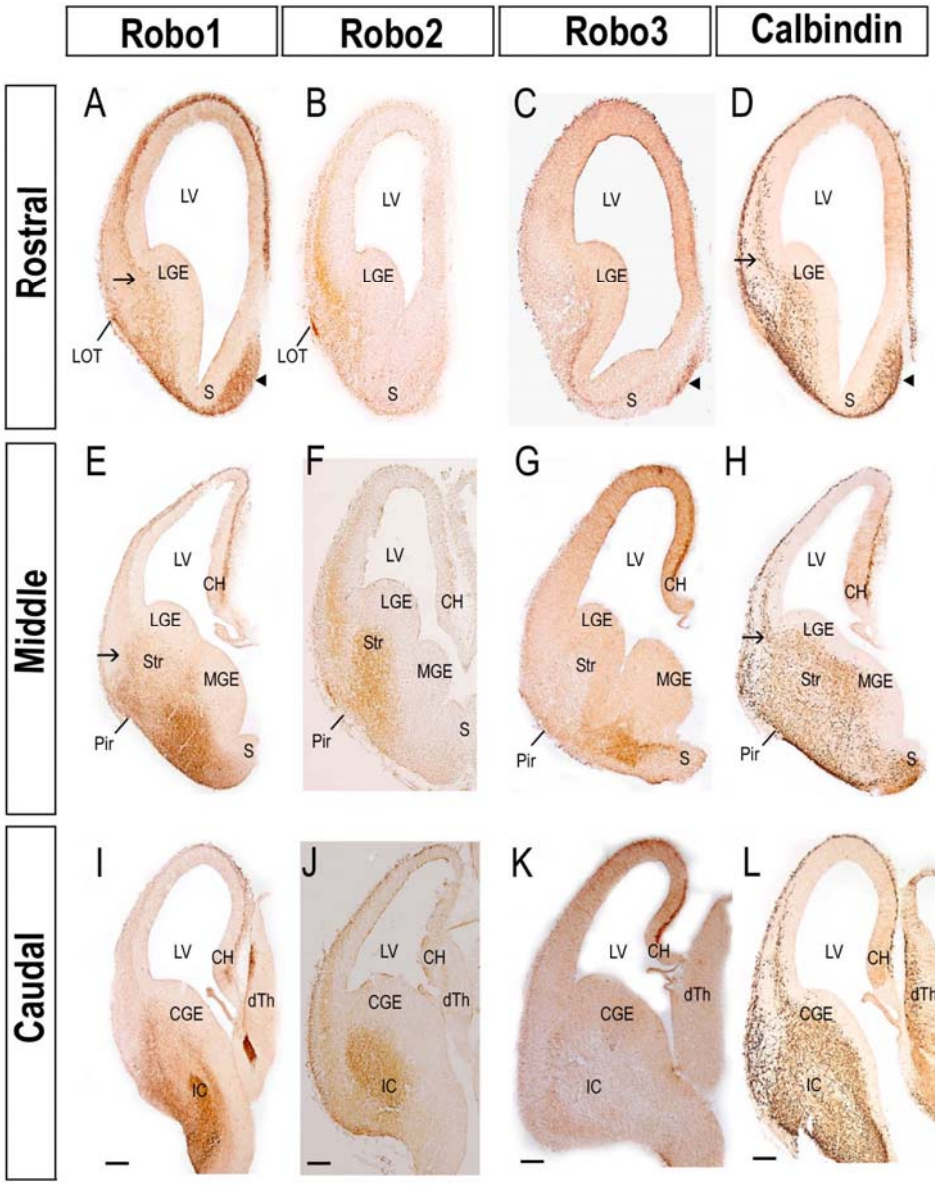

Fig. 3.10 Comparative analysis of Robo expression and the interneuron marker calbindin in the developing mouse forebrain at E13.5. Localisation of Robo1 (A,E,I), Robo2 (B,F,J), Robo3 (C,G,K) and calbindin (D,H,L) proteins at rostral (A-D), middle (E-H) and caudal (I-L) levels of the embryonic mouse forebrain. Robo1 and calbindin expression overlap within the ventral forebrain. Stream-like Robo1 and calbindin staining extends dorsolaterally from the LGE (arrows in A,D) and MGE (arrows in E,H) towards the cortex. Scale bar in I,J,K,L is 200 μm and corresponds to all images. (CH, cortical hem; LV, lateral ventricle; LGE, lateral ganglionic eminence; MGE, medial ganglionic eminence; CGE, caudal ganglionic eminence; Str, striatum; S, septum; LOT, lateral olfactory tract; IC, internal capsule; dTh, dorsal thalamus; Pir, piriform cortex).

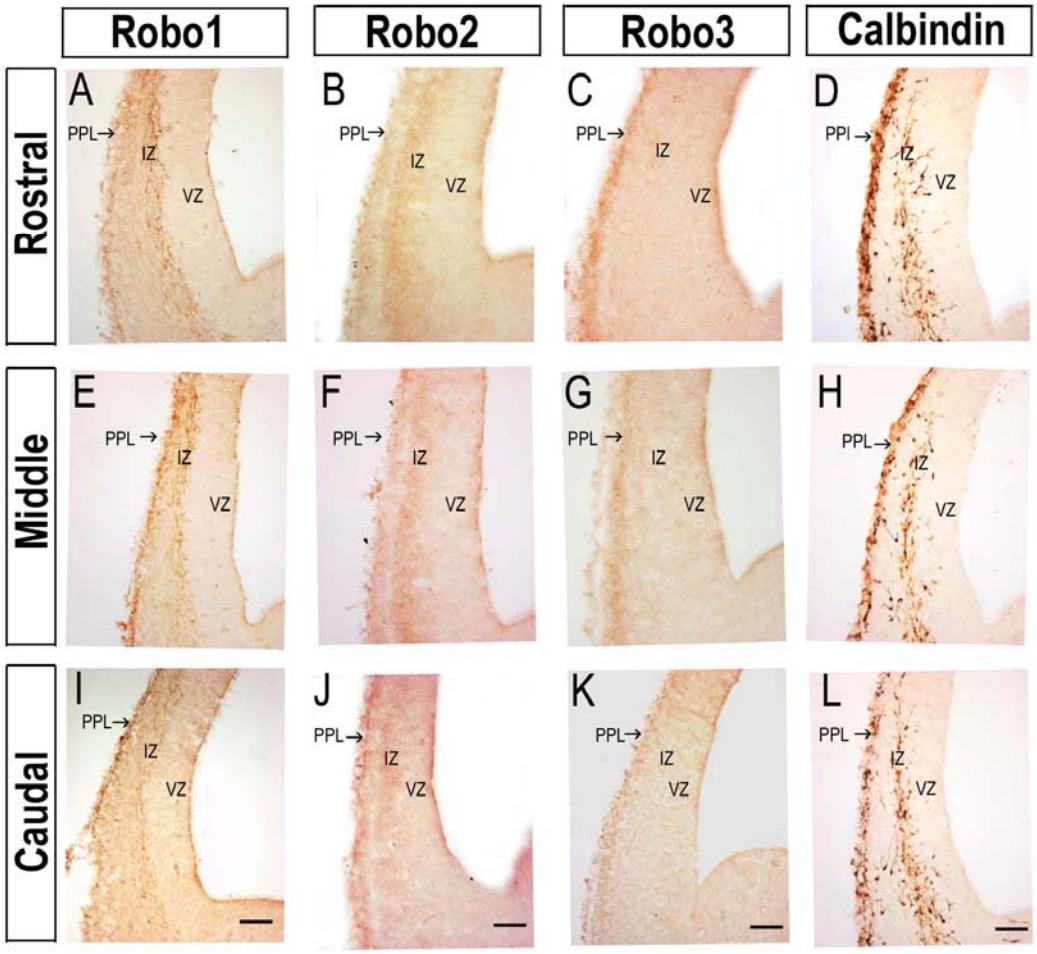

Fig. 3.11 Comparative analysis of Robo and calbindin expression in the developing mouse cortex at E13.5. Localisation of Robo1 (A,E,I), Robo2 (B,F,J), Robo3 (C,G,K) and calbindin (D,H,L) proteins in rostral, middle and caudal levels of the developing cortex using immunohistochemistry. All three Robo receptors are expressed within the developing preplate layer (PPL) of the cortex, where calbindin immunopositive interneurons are distinctly localised. Robo1 and Robo2 also overlap with calbindin expression within the intermediate zone (IZ). Scale bar in I-L is 100 μm and corresponds to all images. (PPL, preplate; IZ, intermediate zone; VZ, ventricular zone).

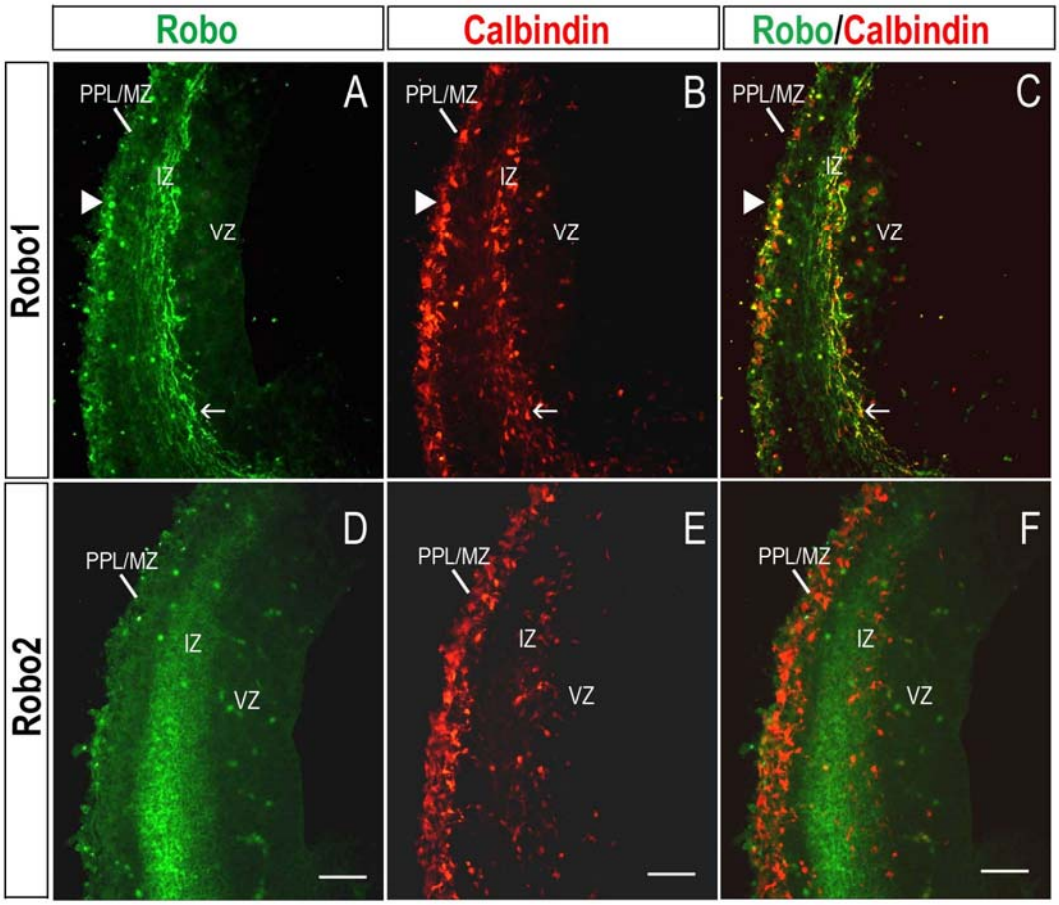

Fig. 3.12 Colocalisation of Robo with calbindin immunopositive cortical interneurons at E13.5. Coronal sections through the E13.5 mouse cortex, immunohistochemically processed for the Robo1 (A) and Robo2 (D) (green) receptors, and double labelled with calbindin (red). Robo1 co-localises with calbindin immunopositive cells (yellow), within the IZ (arrow in C) and PPL (arrowhead in C), confirming cortical interneurons express the Robo1, but not the Robo2 receptor at E13.5. Scale bar in D-F is 100 μm and corresponds to all panels. (PPL/MZ, preplate/marginal zone; IZ, intermediate zone; VZ, ventricular zone).

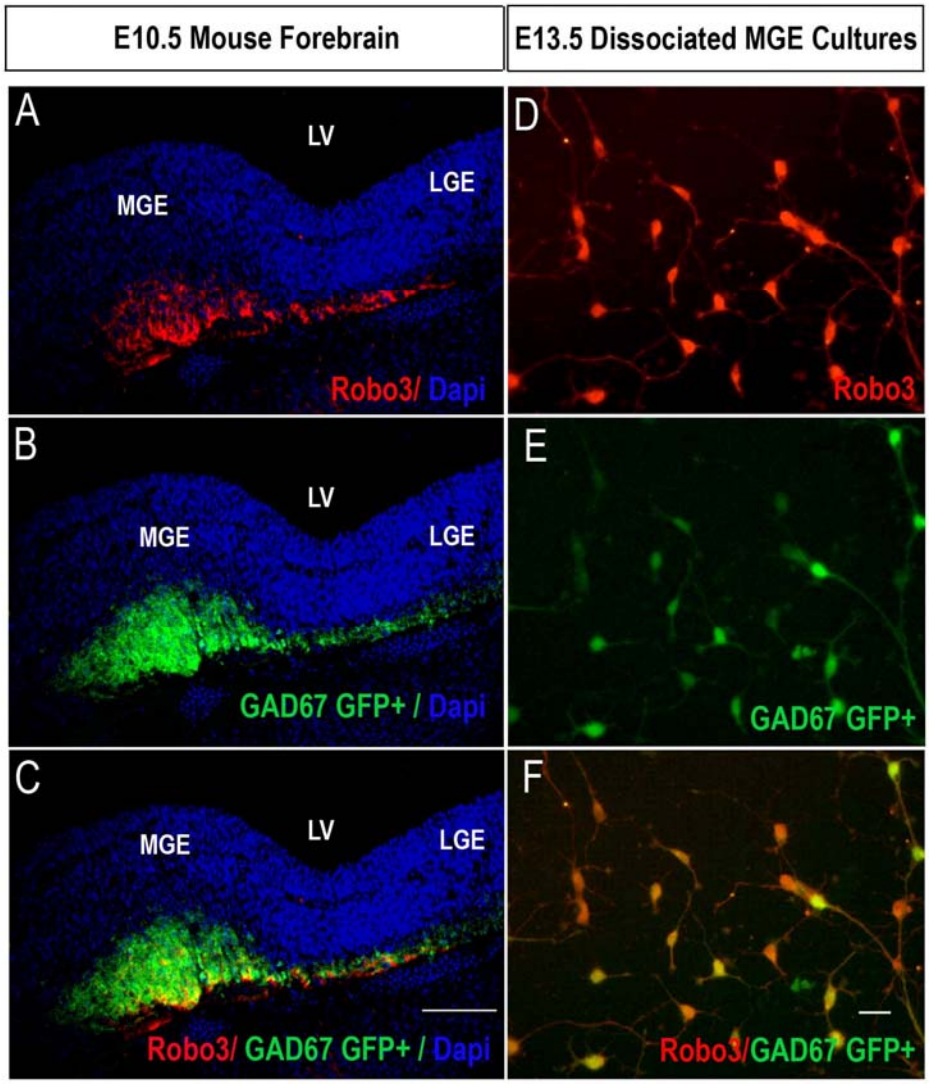

Fig. 3.13 Colocalisation of Robo3 with the interneuron marker GAD67. Panel B shows a coronal section through the ventral forebrain of an E10.5 transgenic mouse, in which the GAD67 coding locus has been tagged with a green fluorescent protein (GAD67-GFP+). GAD67 (shown in green in panels B,C) is strongly localised within the differentiating MGE. Immunohistochemical processing for Robo3 (shown in red in panels A,C) shows this receptor is expressed in a similar pattern to GAD67 (compare panels A with B), and further colocalises with GAD67 in a stream of cells extending from the MGE towards the cortico-striatal boundary (shown in yellow in panel C). Dissociated MGE cultures prepared from GAD67-GFP+ transgenic mice (green cells in panels E,F), were double labelled with Robo3 (red cells, panel D,F). A number of dissociated GAD67-GFP+ MGE neurons co-express Robo3, as shown by some yellow cells in panel F. Scale bar in C is 100 μm and corresponds to A-C; in D is 30 μm and corresponds to D-F. (LV, lateral ventricle; LGE, lateral ganglionic eminence; MGE, medial ganglionic eminence).

3.4.2 Robo and calbindin during cortical plate stages of development

The previous expression studies showed that Robo3 was mostly down regulated within the embryonic mouse forebrain (Fig.3.8) during later stages of development. However, both Robo1 and Robo2 were expressed more broadly within the differentiating LGE and MGE, and comparison with calbindin expression, showed that all three proteins were expressed in these regions. Streams of Robo protein were observed to extend dorsally from the SVZ of the LGE and CGE towards the cortex. This was particularly evident for Robo1 (arrowheads in Fig. 3.14A,D), and further mirrored calbindin expression (arrowheads in Fig. 3.14C,F) within this region. This corresponded to the deep migratory route interneurons follow to the cortex at this time (Marín et al., 2003b, Métin et al., 2006). Once interneurons reach the cortex, they migrate along the level of the developing LIZ/SVZ (Marín et al., 2003b; Métin et al., 2006) (Fig. 3.15G-I). Robo1 and Robo2 were strongly expressed within these layers of the developing cortex at this time, where they overlapped with calbindin expression. In addition, diffuse Robo1 (3.15A-C) and Robo2 (3.15D-F) expression was also maintained within the developing CP, where calbindin staining (3.15G-I) was also visualised.

Given that both Robo1 and Robo2 proteins overlapped with calbindin positive cells within the GEs and cortex at E15.5, this strongly suggested that interneurons express both receptors. Double labeling experiments for Robo1 and calbindin revealed that these proteins co-localised extensively in interneurons throughout all layers of the cortex at E15.5 (Fig. 3.16A-C). Double labeled Robo1/calbindin cells (shown in yellow) were observed within the SP (Fig. 3.16B) and lowe IZ/SVZ (Fig. 3.16C) migratory streams and appeared to be migrating into the developing CP and

VZ, respectively. Robo2 was robustly expressed within the upper IZ and SP (3.16D,F), and double labeled Robo2/calbindin interneurons could similarly be seen throughout all cortical layers, including within the CP (3.16E). Double labeled Robo2/calbindin (yellow) cells were also observed with their processes directed towards the VZ (3.16F), suggesting that they were migrating towards this zone. Thus, Robo1 and Robo2 expressing (calbindin positive) interneurons could be seen with their leading processes directed towards the VZ (arrows in Fig. 3.16C,F), i.e. suggestive of these neurons exhibiting ventricle directed migration, as well as in cells ascending into the CP (Fig. 3.16B,E respectively). Quantitative analysis of the proportion of calbindin cells that expressed either Robo1 or Robo2 receptors at E15.5 showed that the vast majority of the calbindin population of interneurons (~90%) expressed either Robo1 or Robo2 receptors. This was observed in all cortical layers, except for within the VZ where ~70-80% of interneurons expressed either receptor (Fig. 3.16G). The quantification of Robo expressing interneurons was carried out by Dr. William Andrews.

Analysis of Robo1 (Fig. 3.1B,C) and Robo2 (Fig. 3.1E,F) proteins with calbindin at E17.5 similarly showed that both proteins overlapped with calbindin (Fig. 3.17H,I) within the LIZ and upper SVZ. Robo1, and to a lesser extent Robo2, also overlapped with calbindin within the germinal SVZ of the GEs in the ventral forebrain (Fig. 3.17A,D,G, respectively). This was consistent with interneurons continuing to express Robo1 and Robo2 receptors as they migrate from the ventral forebrain and along their deep tangential migratory route within the cortex during later stages of development (Marín et al., 2003b). While staining within the developing CP was of a diffuse nature for both Robo1 and Robo2 proteins, these are regions in which calbindin proteins were also localised (Fig.3.17B-I).

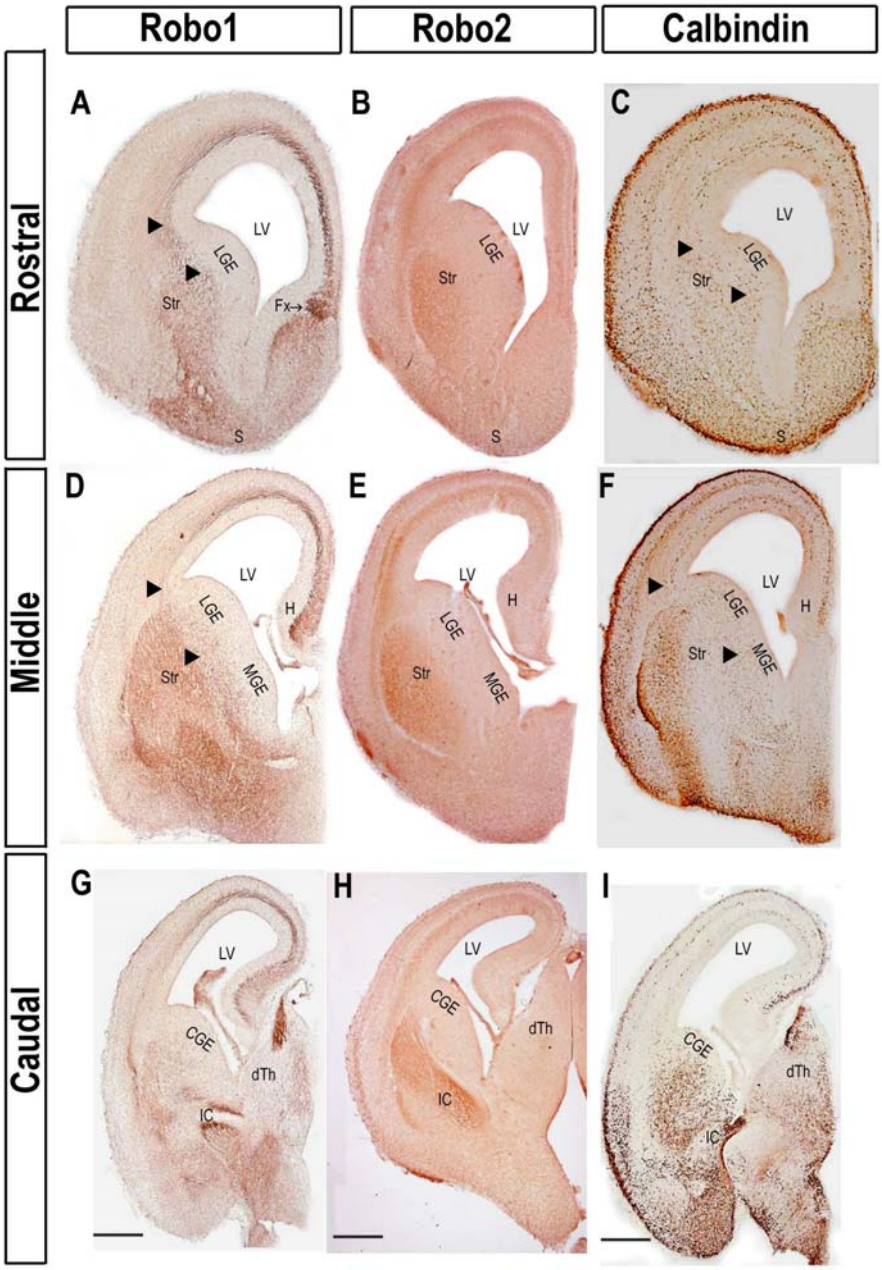

Fig. 3.14 Comparative analysis of Robo and calbindin expression in the developing mouse forebrain at E15.5. Localisation of Robo1 (A,D,G), Robo2 (B,E,H) and calbindin (C,F,I) immunopositive cortical interneurons in the embryonic mouse forebrain at E15.5, using immunohistochemistry. Robo1 (A,D) and Robo2 (B,E) are robustly expressed within the differentiating LGE and MGE and overlap with calbindin expression in these regions (E,F). Robo2 (B,E) is more anteriorly restricted within the MGE. Distinctive Robo1 and calbindin expression is observed in the germinal SVZ of the LGE and MGE, with stream-like staining extending dorsolaterally towards the cortex (arrowheads in A,C,D,F). Scale bar in G-I is 500 μm and corresponds to all images. (H, hippocampus; LV, lateral ventricle; LGE, lateral ganglionic eminence; MGE, medial ganglionic eminence; CGE, caudal ganglionic eminence; Str, striatum; S, septum; Fx, fornix; IC, internal capsule; dTh, dorsal thalamus).

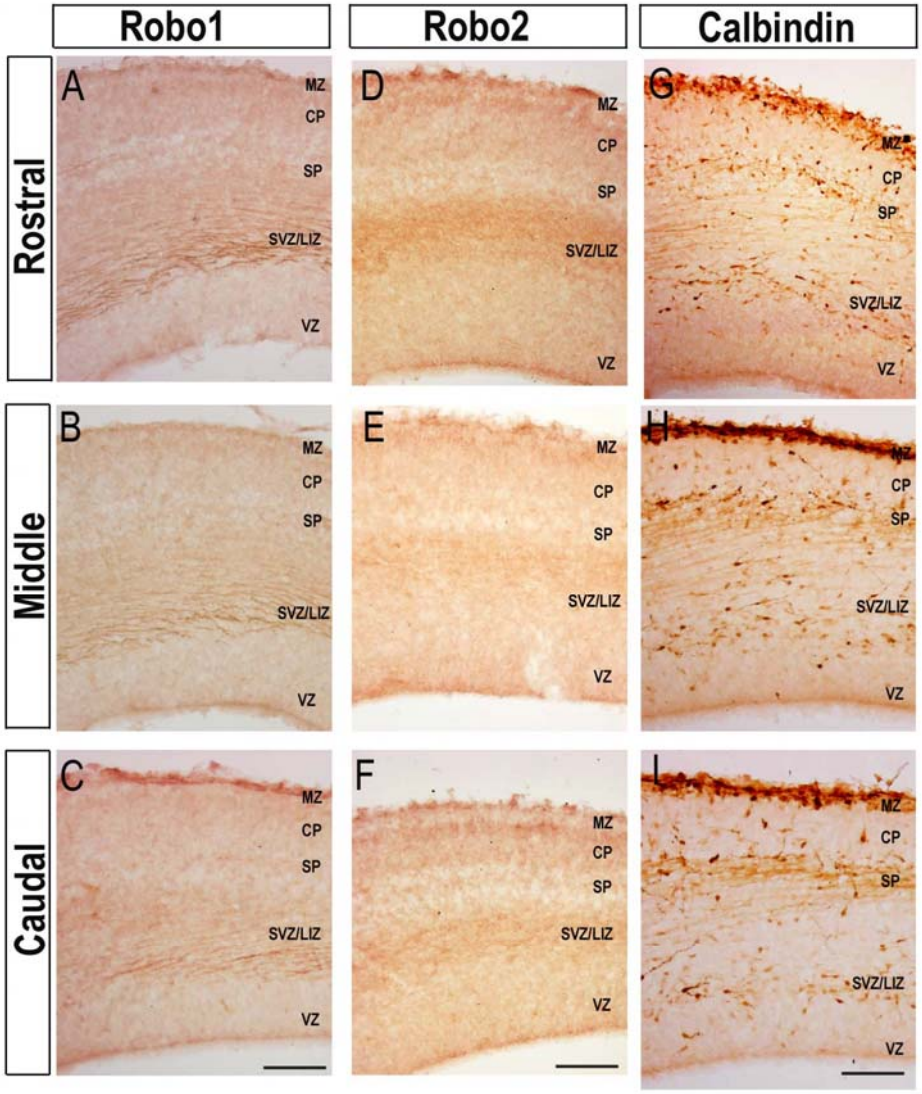

Fig. 3.15 Comparative analysis of Robo expression with the interneuron marker calbindin in the embryonic mouse cortex at E15.5. Immunohistochemical localisation of Robo1 (A-C), Robo2 (D-F) and calbindin (G-I) proteins throughout the rostral-caudal extent of the developing cortex. Robo1 and Robo2 are strongly expressed within the lower intermediate zone (LIZ), with Robo1 expression extending to the upper subventricular zone (SVZ); these are regions where a stream of calbindin immunopositive interneurons are distinctly localised. Diffuse Robo1 and Robo2 expression is also observed throughout the rostral-caudal extent of the developing cortical plate (CP) where some calbindin immunopositive interneurons are observed at this time (G-I). (Scale bar in C,F,I is 150 μm and corresponds to all images. (MZ, marginal zone; CP, cortical plate; SP, subplate; SVZ/LIZ, subventricular zone/lower intermediate zone; VZ, ventricular zone).

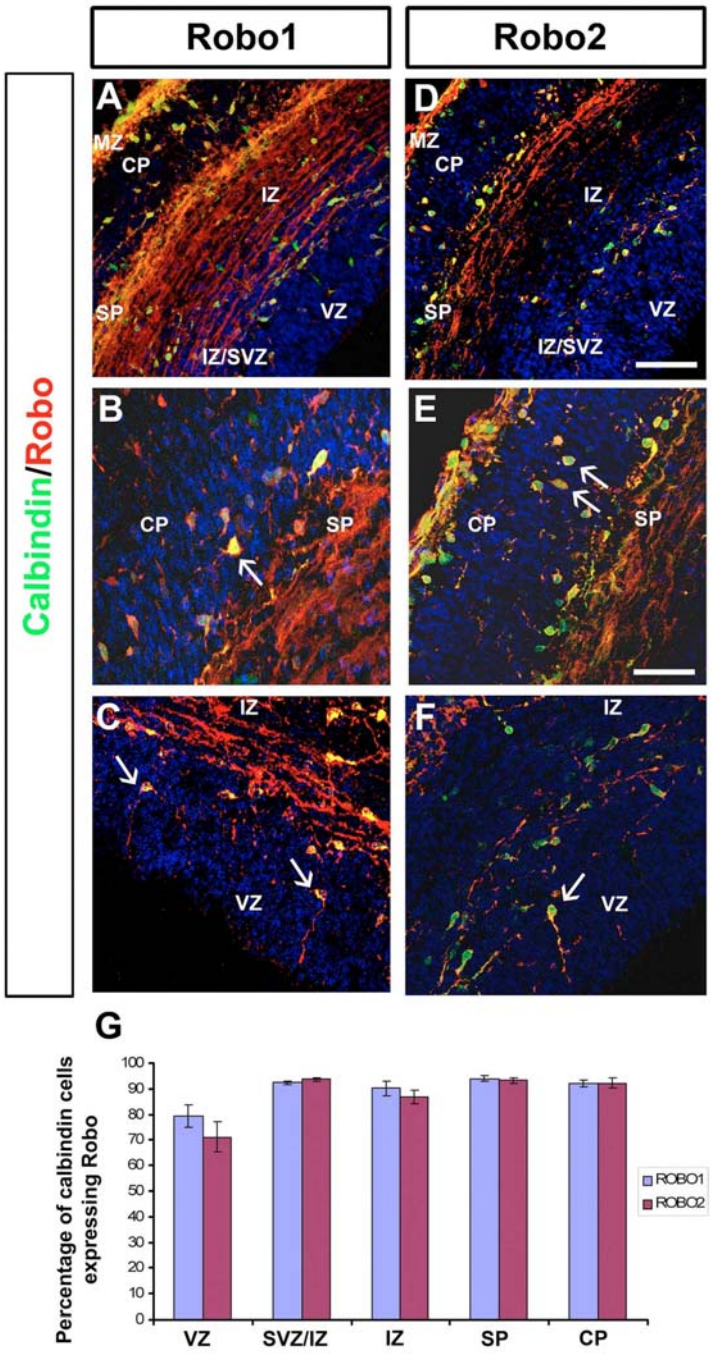

Fig. 3.16 Populations of calbindin immunopositive interneurons express Robo1 and Robo2 receptors during cortical plate stages of development. Colocalisation of Robo1 (A-C) (red) and Robo2 (D-F) (red) proteins with calbindin (green) in the developing murine cortex at E15.5. Double labelled Robo1/calbindin and Robo2/calbindin cells (yellow, arrows) can be seen throughout all cortical layers. Graphical representation (G) of the percentage of calbindin immunopositive cells that express either Robo1 or Robo2 at this stage of development. Scale bar in D is 100 μm and applies to A,D; and in E is 50 μm and corresponds to B-F. (VZ, ventricular zone; SVZ/IZ, subventricular zone/lower intermediate zone; IZ, intermediate zone; SP, subplate; CP, cortical plate; MZ, marginal zone).

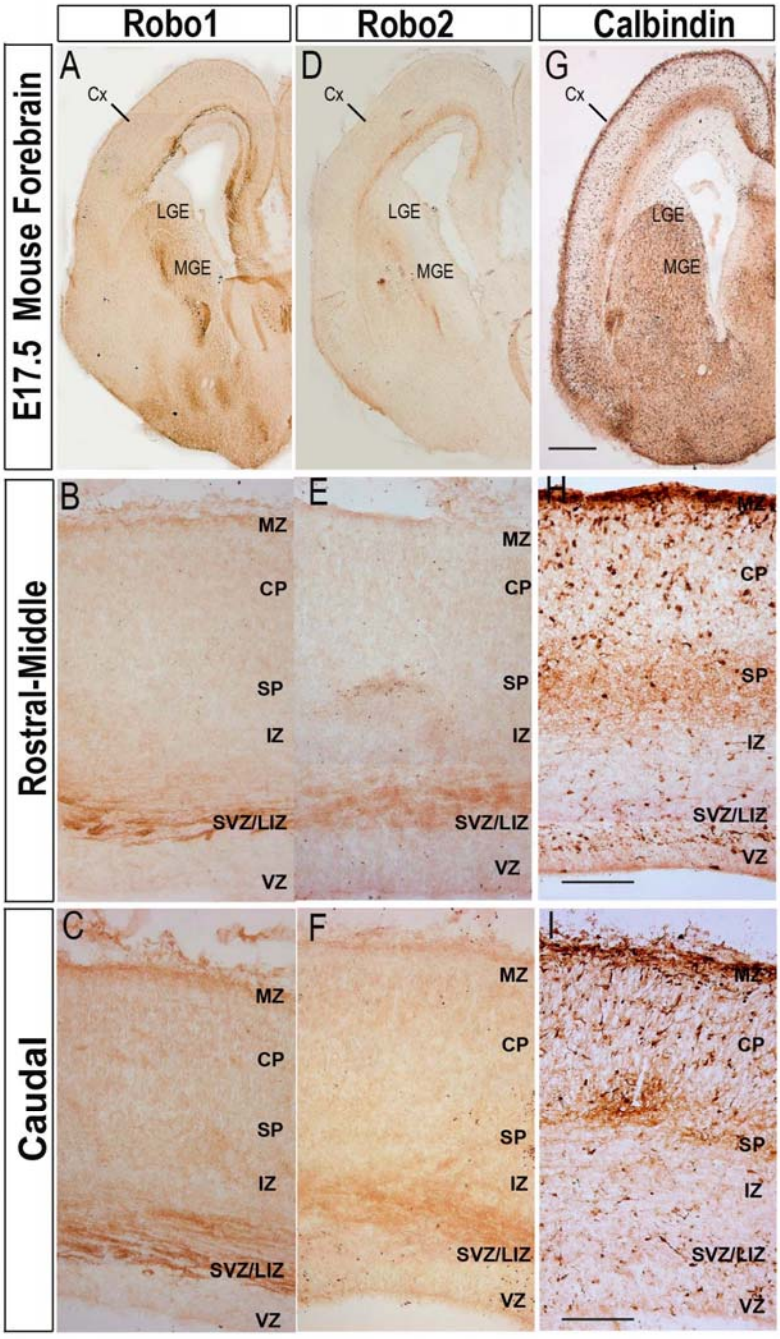

Fig. 3.17 Comparative analysis of Robo expression with calbindin in the developing mouse forebrain at E17.5. Immunohistochemical localisation of Robo1 (A-C), Robo2 (D-F) and calbindin (G-I) proteins throughout the rostral-caudal extent of the embryonic mouse cortex at E17.5. Robo1(A-C) and Robo2 (D-F) are distinctly expressed within the lower intermediate zone and upper subventricular zone (SVZ/LIZ) where calbindin immunopositive cells are observed at this time. Scale bar in H,I is 200 μm and corresponds to B,C,E,F,H,I. Scale bar in G is 300 μm and corresponds to A,D,G. (Cx, cortex; LGE, lateral ganglionic eminence; MGE, medial ganglionic eminence; MZ, marginal zone; CP, cortical plate; SP, subplate; IZ, intermediate zone; SVZ/LIZ, subventricular zone/lower intermediate zone; VZ, ventricular zone).

3.5 DISCREPANCIES BETWEEN IMMUNOHISTOCHEMICAL STUDIES AND *IN SITU* HYBRIDISATION STUDIES

While the immunohistochemical studies shown here confirmed that all three Robos were expressed within the ventral forebrain and cortex during embryonic development, some discrepancies were found with previous studies. While Robo1 protein was clearly localised in the developing IZ of the cortex at all ages investigated (Fig. 3.18A,C), Robo1 mRNA had not been previously detected within this region. Former *in situ* hybridisation studies in the embryonic mouse (Yuan et al., 1999b; Bagri et al., 2002) and rat (Whitford et al., 2002; Marillat et al., 2002) forebrain, at corresponding developmental time points (see arrows in Fig. 3.18C,D), showed Robo1 mRNA to be localised exclusively within the developing CP. As *in situ* hybridisation detects *robo* mRNA which is located within the soma of cells, this could be explained by the presence of Robo1 protein in axonal fiber tracts which course through this region during development (E13.5) (Métin and Godement et al., 1996; López-Bendito and Molnár, 2003; Morante-Oria et al., 2003; Molnár et al., 1998). Indeed, Robo1 and Robo2 receptors have been shown to be important in regulating the development of these major corticofugal and thalamocortical tracts (Andrews et al., 2006; López-Bendito et al., 2008), consistent with these observations. However, we show here that while Robo1 staining is indeed fibrous-like, consistent with the expression of this receptor in developing corticofugal and thalamocortical tracts, staining of a punctate nature was also clearly visible within this region (Fig. 3.15 & 3.17). The co-expression of calbindin and Robo1 within this zone further confirmed the cellular localisation of Robo1 protein in

interneurons at E13.5 (Fig. 3.12A-C) as well as at E15.5 (Fig. 3.17A-C) (Andrews et al., 2006, 2008). Thus, the absence of mRNA within this region could be explained by differences in the specificity between the two assays used.

A second discrepancy was observed within the germinal VZ of the LGE and MGE (Fig. 3.18A-B) during early stages of development. *In situ* studies at an equivalent developmental stage in the rat (E15.5) (Marillat et al., 2002) has shown Robo mRNA to be present in the germinal regions of the GEs during early stages of development (E15 in the rat; E13 in the mouse). These investigations showed Robo1 mRNA to be localised within the VZ of both the LGE and MGE (Fig. 3.18B), and Robo2 mRNA to be restricted to anterior regions of the LGE (Fig. 3.18F) (Marillat et al., 2002). These regions appeared to be devoid of Robo protein at an equivalent stage in the mouse (Fig. 3.18A,E). However, on closer examination Robo1 protein was distinctly localised within the VZ of both the MGE and LGE (Fig. 3.18I-J) and Robo2 expression was restricted to the VZ of the LGE at this time point (Fig. 3.18K and L), consistent with the *in situ* hybridization observations. Robo3 protein was also diffusely expressed within the germinal MGE at E13.5 (data not shown). Punctate Robo staining was clearly visible in the fringes of the SVZ of the GEs at E13.5 and this was maintained at later stages for Robo1 and Robo2, but not Robo3 proteins (E15.5). This suggests that interneuron progenitors express Robo1 and Robo2 proteins within the germinal VZ and SVZ of the GEs at a time when interneurons are generated and continue to express Robo receptors as they migrate to the cortex.

A third discrepancy was regarding the expression of Robo3. Robo3 mRNA has previously been shown to be expressed during early development, with its peak expression between E11- E12, after which it is down regulated in the developing mouse forebrain (Camurri et al., 2004). Whilst Robo3 protein was mostly down regulated by E13.5, consistent with previous observations, Robo3 was surprisingly still expressed, albeit at low levels, within restricted regions in the basal forebrain throughout CP stages of development. Specifically, this was maintained within fibers of the fornix at E15.5 (Fig. 3.8A). Our analysis of Robo3$^{-/-}$ GFP mutant mice suggests, tentatively, that Robo3 may be expressed as late as E18.5 within discrete cell populations in the hippocampus, rhinencephalon and differentiating striatum (Fig. 3.8B-D). Previous *in situ* hybridisation studies mainly focused on hindbrain and spinal cord regions of the embryonic mouse, and were not carried out after E13.5 in the mouse due to down regulation of gene expression based on reverse transcription PCRs. Thus, I suggest here that Robo3 expression may be maintained by discrete populations of cells during later stages of development, implying that this receptor has a role in the development of these cells. Ascertaining the identity of these cells will require the molecular characterization and careful tracing of the origins of this population.

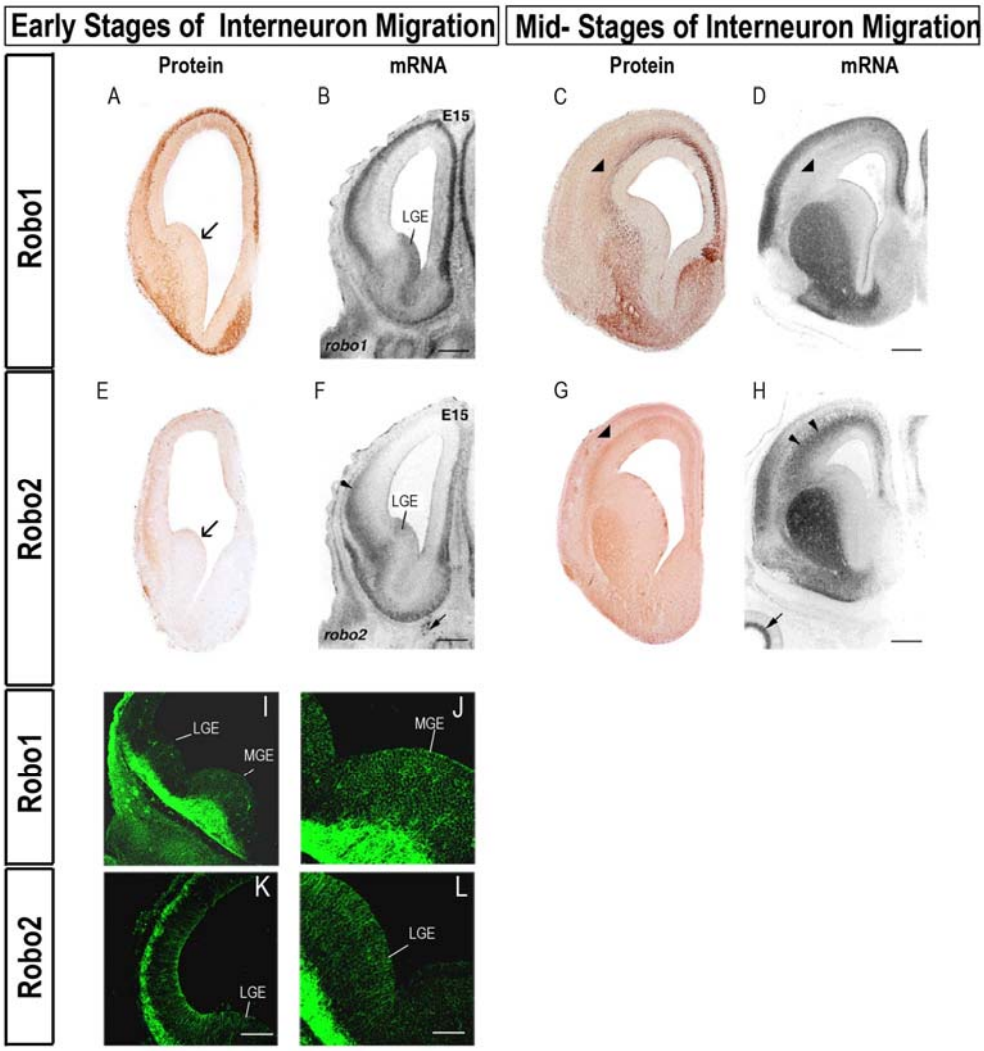

Fig. 3.18 Comparative analysis of Robo protein and Robo mRNA in the developing rodent forebrain. Localisation of Robo1 (A,C,I,J) and Robo2 (E,G,K,L) protein, and robo1 (B,D) and robo2 (F,H) mRNA in the developing rodent forebrain. Coronal sections taken from the embryonic mouse forebrain during early (E13.5m) (A,E) and mid stages (E15.5m) (C,G) of development were processed for Robo1 (A,C) and Robo2 (E,G) proteins using immunohistochemistry. In-situ images in panels B,F,D,H show the localisation of robo1 (B,D) and robo2 (F,H) mRNA in the developing rat forebrain at comparable stages (E15.5r; B,F and E17.5r; D,H) of development. While Robo2 protein expression within the IZ is consistent with the localisation of Robo2 mRNA in this region (arrowheads in G and H, respectively), Robo1 protein, but not Robo1 mRNA is observed in the IZ (arrowheads in C and D, respectively) during mid stages of development. Note Robo1 (B) and Robo2 (F) mRNA are clearly localised within the VZ of the lateral ganglionic eminence (see LGE in B,F) during early stages of development. While Robo protein is restricted to the differentiating fields of the GEs, and not to the VZ (see arrows in A,E) at this stage, both Robo1 (I,J) and Robo2 protein (K,L) are robustly expressed within the VZ of the ganglionic eminences (GEs) at E11.5. Higher images of the MGE-VZ and LGE-VZ are shown in J and L, respectively. Scale bar in B,D,F,H is 200 μm and applies to A-H; in K is 100 μm and applies to I,K; and in L is 50 μm and applies to J,L. (LGE, lateral ganglionic eminence; MGE, medial ganglionic eminence; IZ, intermediate zone). (In-situ images were taken from the study of Marillat et al. 2002).

3.6 DISCUSSION

3.6.1 Early born interneurons express Robo 1 and Robo3 receptors

The detailed immunohistochemical expression studies carried out here has shown that all three Robo receptors are expressed in the early developing basal ganglia and cortex at E11.5-E13.5 in the embryonic mouse forebrain (Fig. 3.3-3.6). This is a time when early populations of interneurons are generated within the MGE (E11.5-E13.5) and predominantly migrate along a superficial route around the differentiating striatum (E12.5-E13.5) to the cortex (Lavdas et al., 1999; Anderson et al., 2001; Marín et al., 2003a; Métin et al., 2006). Within the cortex, early born interneurons migrate through the MZ/PPL and IZ. Both Robo1 and Robo3 receptors were strongly expressed within the MGE during these early stages of development (Fig. 3.10), as well as throughout the MZ/PPL layer within the cortex, consistent with early populations of interneurons expressing these receptors (Fig. 3.11). While Robo2 was transiently expressed within the dorsal MGE at E11.5, it was later restricted to the differentiating LGE (E12.5-E13.5). Robo2 expression was, interestingly, complementary to Robo1 and Robo3 within the MGE, however overlapped with Robo1 expression within the IZ in the cortex (Fig. 3.10- 3.11).

Double labeling experiments confirmed that the calbindin population of interneurons expressed the Robo1, but not the Robo2 receptor, during these early stages of development (Fig. 3.12). Robo3 was similarly shown to colocalise with GAD67-GFP within a stream of interneurons which extended from the MGE towards the cortex (Fig. 3.13). Thus, these studies suggest that

early born interneurons express Robo1 and Robo3, but not Robo2, receptors as these leave the MGE and migrate dorsally towards the cortex (Fig. 3.20A, A').

Furthermore, Robo expression was complementary to established patterns of Slit within the germinal VZ/SVZ of the GEs (Slit1), as well as within the endogenously chemorepulsive ventral forebrain (preoptic area (Slit1) and septum (Slit1; Slit2) (Bagri et al., 2002; Marillat et al., 2002) (Fig. 3.20A). This was consistent with Slits repelling Robo1 and Robo3 expressing interneurons away from the GEs and towards the cortex (Zhu et al., 1999; Andrews et al., 2006, 2008). Both Robo1 and Robo3 protein expression also overlapped with Slit, which is expressed within the developing preplate/MZ (Slit1,3) (Fig. 3.19) and VZ (Slit1) at this time (Fig. 3.20A'). These Slit-rich regions within the cortex could putatively prevent interneurons from entering the cortex prematurely and further may have a role in creating exclusion zones within the cortex, thereby maintaining the medio-lateral positioning of the migratory streams (Zhu et al., 1999; Andrews et al., 2006) of interneurons.

These expression studies are therefore consistent with a role of Robo1/Slit and Robo3/Slit signaling in controlling the development of early born interneurons.

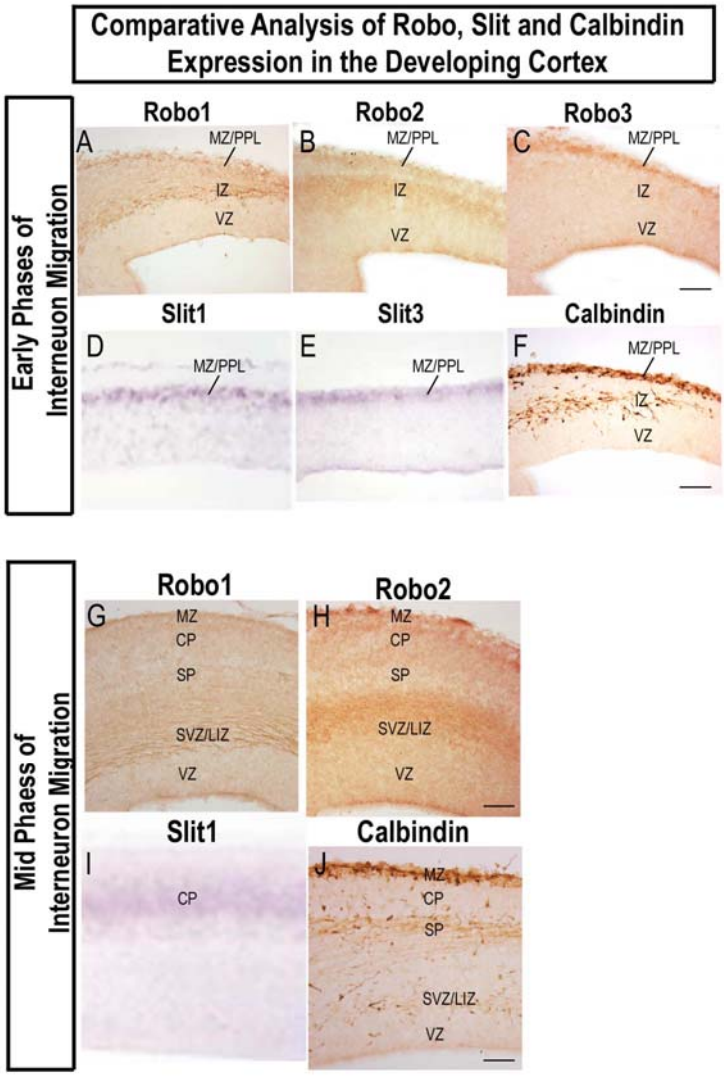

Fig. 3.19 Analysis of Robo and calbindin expression in relation to slit in the developing rodent cortex. Localisation of Robo receptors (A-C, G,H) and calbindin (F,J) immunopositive interneurons in the developing mouse cortex, in relation to slit mRNA in the rat forebrain (D,E,I) at a comparable age during early (E13.5 in the mouse, E15.5 in the rat) and mid (E15.5 in the mouse, E17.5 in the rat) stages of interneuron migration. All three Robos (A-C) and calbindin (F) overlap with slit (D,E) expression within the superficial preplate layer (PPL) and marginal zone (MZ) of the cortex during early stages of development, suggesting that a population of robo-expressing interneurons migrate through a slit rich region at this time. Slit is restricted within the developing cortical plate (CP) during mid stages of interneuron migration (I). This is mostly complementary to Robo1 (G) and Robo2 (H) expression within the MZ, subplate (SP) and subventricular zone and lower intermediate zone (SVZ/LIZ), where a stream of calbindin immunopositive interneurons are localised (F). This is consistent with robo-expressing interneurons predominately avoiding slit-rich regions during mid stages of their migration. Scale bar in C,F is 100 μm and applies to A,B,C,F; and in H,J is 100 μm and corresponds to G,H,J. (MZ, marginal zone; PPL, preplate; CP, cortical plate; SP, subplate; SVZ/LIZ, subventricular zone/lower intermediate zone; VZ,ventricular zone). (The in-situ images presented here were taken from Whitford et al. 2002).

3.6.2 Later born interneurons express Robo1 and Robo2 receptors

While Robo3 was down regulated during later stages of corticogenesis, Robo1 and Robo2 receptors continued to be robustly expressed within the basal ganglia and cortex (E15.5-E17.5) (Fig. 3.17, 3.19). Both Robo1 and Robo2 receptors overlapped within mantle regions of the differentiating LGE and to a lesser extent in the differentiating MGE. Punctate Robo1 staining was clearly visible in the SVZ of the GEs, and this expanded dorsally to the corticostriatal boundary and mirrored calbindin expression within these regions. This was consistent with the stream of interneurons which migrate deep to the differentiating striatum at this time, and further complemented Slit expression within the germinal VZ and SVZ of the GEs and at the ventral midline of the forebrain (Marillat et al., 2002; Bagri et al., 2002) (Fig. 3.20B). Thus, Robo1, Robo2 and Slit expression patterns are consistent with their role in directing later born interneurons within the subpallium.

Once later born interneurons arrive at the cortico-striatal boundary, they migrate predominately along the lower IZ/SVZ as well as along the SP and MZ (Fig. 3.19J). Robo1 was observed throughout the lower IZ/SVZ and SP layers (Fig. 3.19G), and this overlapped with Robo2 to a degree, within the IZ (Fig. 3.19H) (Yuan et al., 1999b; Marillat et al, 2002). Double labeling studies confirmed that interneurons express both Robo1 and Robo2 receptors throughout their tangential migration within the subpallium (data not shown) as well as within all tangential routes within the cortex (Fig. 3.16). Robo expression further complemented Slit expression within the basal ganglia (Fig.

3.20B) and developing cortex (Fig.3.19), strongly suggesting that Robo1/Slit and Robo 2/Slit signaling may have a role in regulating the migration of interneurons from their subpallial origins to the cortex during mid and later stages of development (E15.5-E17.5), as well as potentially regulating their final positioning within the CP (Fig. 3.20B').

3.7 SUMMARY

The detailed Robo expression studies carried out here throughout the whole period of corticogenesis have shown that all three Robo receptors are expressed within sources of interneurons within the GEs, as well as within regions through which these migrate in the cortex. Furthermore, early populations of interneurons were confirmed to express the Robo1 and Robo3 (but not Robo2) receptors, with later born cohorts of migrating interneurons expressing Robo1 and Robo2 (but not Robo3) receptors during corticogenesis. These expression studies thus suggest that all three Robos may have a role in regulating the ventral-dorsal migration of interneurons from the GEs to the cortex, as well as regulating their tangential trajectories and final positions within the cortex.

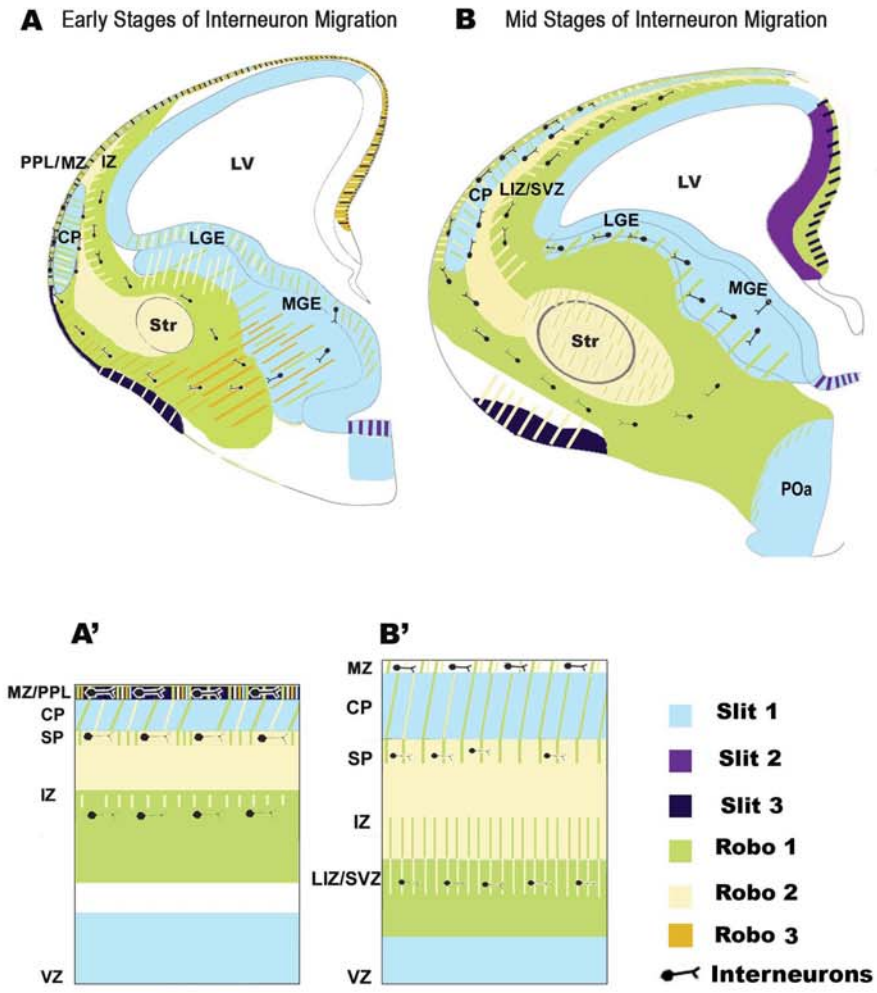

Fig. 3.20 Robo and Slit expression in the developing rodent cortex during early and mid phases of interneuron migration. Schematic illustrating the immunohistochemical localisation of robo 1 (green), robo 2 (yellow) and robo 3 (orange) receptors in relation to slit 1 (blue), slit 2 (purple) and slit 3 (dark blue) mRNA expression within the developing forebrain (A,B) and cortex (A',B'), during early (A,A') and mid stages of interneuron migration (B,B'). Hatched areas correspond to regions where robo and slit expression overlap. Slit1 is robustly expressed within the VZ of the ganglionic eminences (GE) throughout interneuron migration, and is largely complementary to Robo expression within the developing GEs. Robo3 (orange) is transiently expressed within the developing MGE and during early stages of development (A), and overlaps with robo1 within this region. All three robo receptors are localised within the preplate (PPL) and marginal zone (MZ) of the cortex (A') during early stages of tangential migration, where slit 3 mRNA is robustly localised at this time (dark blue). Slit 1 expression is maintained within the developing cortical plate (CP) and cortical ventricular zone (VZ) (blue) throughout interneuron migration. and is complementary to Robo1 and Robo2 expression within the developing intermediate zone (IZ), and lower intermediate zone/subventricular zone (LIZ/SVZ) during early (A) and mid (B) stages of interneuron migration, respectively. Robo1 and Robo2 receptors are also strongly expressed throughout the developing CP (green), where they overlap with Slit 1 mRNA throughout interneuron migration. (LV, lateral ventricle; MZ, marginal zone; CP, cortical plate; SP, subplate; IZ, intermediate zone; LIZ/SVZ, lower intermediate zone/subventricular zone; VZ, ventricular zone; Str, striatum; LGE, lateral ganglionic eminence; MGE medial ganglionic eminence; CGE, caudal ganglionic eminence; POa, preoptic area). (This figure is based on *in-situ* hybridization studies by Yuan *et al. (*1999) Marillat *et al.* (2002), Bagri *et al.* (2002) and Whitford *et al.* (2002)).

CHAPTER 4: THE ROLE OF ROBO2 IN THE DEVELOPMENT OF CORTICAL INTERNEURONS

4.1 INTRODUCTION

Recent work has shown that Robo1 plays a major role in guiding interneurons around chemorepulsive regions within the striatum, as well as in regulating the total number of interneurons that enter the developing cortex (Andrews et al., 2006; 2008). In addition, Robo1-Slit interactions have been shown to regulate the morphology of migrating interneurons during cortical development (Andrews et al., 2008). Given that the majority of the calbindin positive population of interneurons (~90%) also express the Robo2 receptor during peak phases of tangential migration (E15.5) (Fig. 3.16), and that Robo2 expression is complementary to that of Slit within the ventral forebrain and cortex, this suggested that Robo2 may have a role in regulating interneuron numbers and their migratory morphologies during development.

The potential role of Robo2 in interneuron migration was therefore investigated in Robo2 transgenic mice. A quantitative analysis of the total numbers of interneurons was quantified at two levels in the developing neocortex in order to enable gradients of interneurons along the dorso-medial axis of the cortex to be assessed. The first sample was taken in the dorsal cortex, and a second sample was taken half way along the lateral-medial extent of the

neocortex (see Fig. 4.1A, C); these regions were thus called the 'dorsal' and 'dorso-lateral' neocortex, respectively. Analysis was carried out at a developmental time point corresponding to just after peak phases of interneuron migration (E15.5) when the vast majority of the calbindin population of interneurons (~90%) expressed the Robo2 receptor (Fig.3.16). As interneurons follow distinct and developmentally regulated tangential migratory paths within the cortex, the number of labelled cells within each cortical zone was further assessed for any changes in their positioning. As discussed previously, defects in Robo1 null mutant mice were not found within the caudal (occipital) cortex and so potential defects in interneuron number and positioning was separately investigated in rostral-middle (Fig. 4.1A,B and 4.2) and caudal (Fig. 4.1C,D & 4.3) cortical regions in Robo2 null mutant mice.

4.2 RESULTS: ROBO2 AND CORTICAL INTERNEURONS

4.2.1 Robo2 and cortical interneurons

The total number of interneurons within the developing cortex was investigated during peak (E15.5) phases of tangential migration. Coronal sections were taken throughout the rostral-caudal extent of Robo2 mutant and wild type littermate forebrains and were immunohistochemically processed for the interneuron marker calbindin (Anderson et al., 1997a, 2001) (Fig. 4.1A, C). The total number of calbindin positive cells was counted in 200 μm wide strips in two regions within the developing neocortex (Fig. 4.1A, C). This was quantified within rostral-middle (Fig. 4.1A, B) and caudal regions (4.1C, D) of the forebrain.

Analysis of Robo2 deficient cortices at E15.5 ($Robo2^{-/-}$ n=4; $Robo2^{+/+}$ n=3) showed that there were no significant differences in the total numbers of calbindin positive cells in dorso-lateral ($Robo2^{-/-}$ 81.9±6.01; $Robo2^{+/+}$ 75.3±5.17; Student's t-test $p<0.415$) or within dorsal regions of the neocortex ($Robo2^{-/-}$ 35.8±1.86; $Robo2^{+/+}$ 36.9±1.88) (Fig. 4.1B) at rostral-middle levels of the forebrain, when compared with control wild type littermates. Similarly, counts made within caudal levels of the forebrain showed comparable numbers of calbindin positive cells in both dorso-lateral ($Robo2^{-/-}$ 52.9±2.99; $Robo2^{+/+}$ 54.5±3.21) and dorsal regions of the neocortex ($Robo2^{-/-}$ 43.9±1.95; $Robo2^{+/+}$ 45.0±2.41) in Robo2 mutants and wild type littermate animals (Fig. 4.1D).

In order to investigate whether Robo2 has a possible role in regulating the positioning of interneurons along their tangential migratory routes within the cortex, the total number of calbindin positive interneurons was quantified within each cortical layer. This was investigated by dividing cortical strips into five bins along the ventricle to pial axis which corresponded to cortical zones as delineated by Nissl staining (Fig. 4.2C). Cortical strips of a minimum width of 200 μm were thus counted, with bin 1 corresponding to the ventricular zone (VZ), and bin 5 corresponding to the developing CP and MZ (Fig. 4.2C).

When the distribution of calbindin cells was assessed within the different zones of the cortex ($Robo2^{-/-}$ n=4; $Robo2^{+/+}$ n=3), this showed that there was a significant (23%) increase in calbindin cells specifically within the CP and MZ layers in the rostral-middle cortex in Robo2 mutant animals, relative to wild

type mice (Fig. 4.2A) ($Robo2^{-/-}$ 31.3±1.86; $Robo2^{+/+}$ 24.6±2.02; $p<0.02$). Interestingly, analysis at a second point along the neocortex, in more dorsal regions, showed that there were no changes in the distribution of calbindin cells within the cortex of these animals (Fig 4.2B).

When the distribution of calbindin cells was similarly investigated within the caudal cortex, the total numbers of calbindin cells within each layer was comparable between Robo2 mutant and Robo2 wild type littermates within all layers of the neocortex, in both dorsal-lateral (Fig. 4.3A) and dorsal regions (Fig. 4.3B). Thus, Robo2 does not appear to play a major role in regulating the total number or positioning of interneurons within the cortex at E15.5.

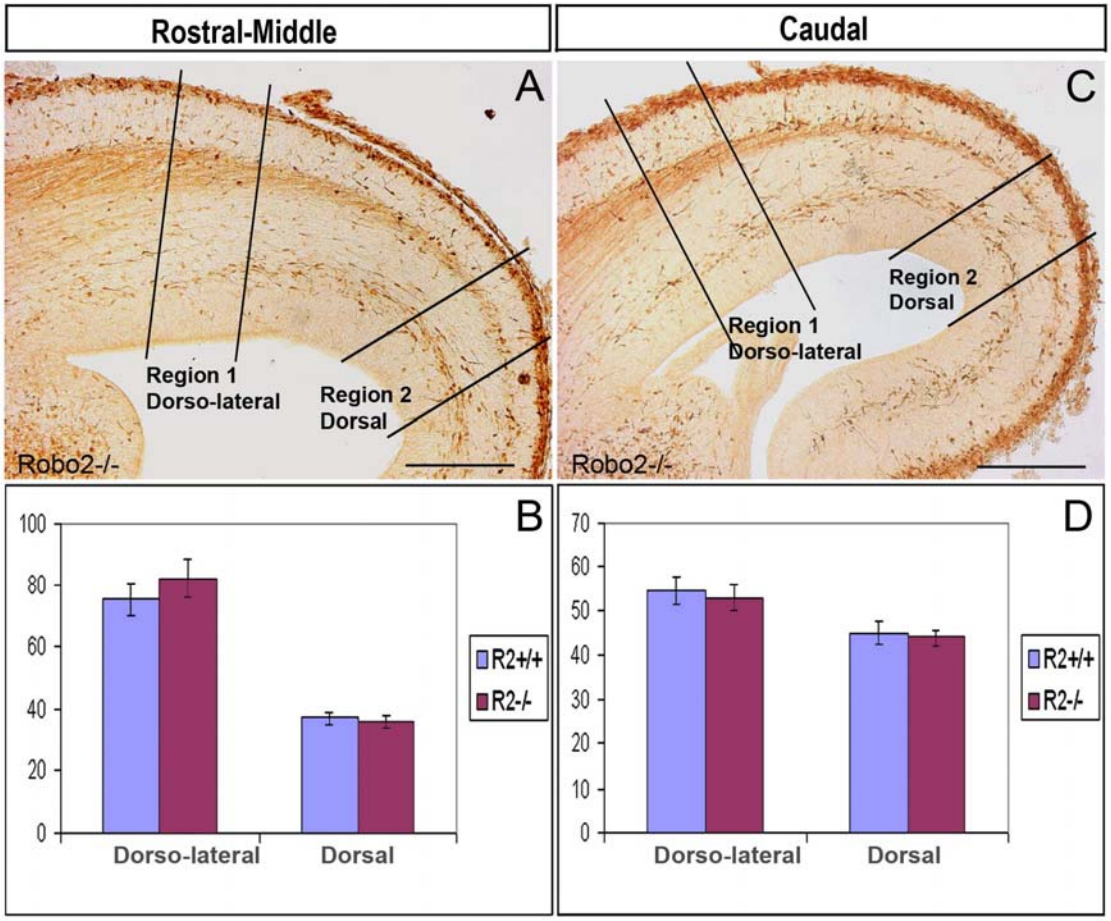

Fig. 4.1 Total numbers of (calbindin immunopositive) interneurons within the developing cortex of Robo2 mutant animals at E15.5. Panels A,C show coronal sections taken from rostral-middle (A) and caudal (C) levels of the Robo2 mutant cortex, and immunohistochemically processed for calbindin proteins. Counts were made in strips vertical to the pial surface in two regions along the dorso-lateral cortex. Quantitative analysis of the total numbers of calbindin immunopositive cells within the rostral-middle (A,B) and caudal (C,D) cortex showed no significant differences in interneuron numbers in Robo2$^{-/-}$ mutant relative to wild type animals at E15.5. Scale bar: is 200 μm.

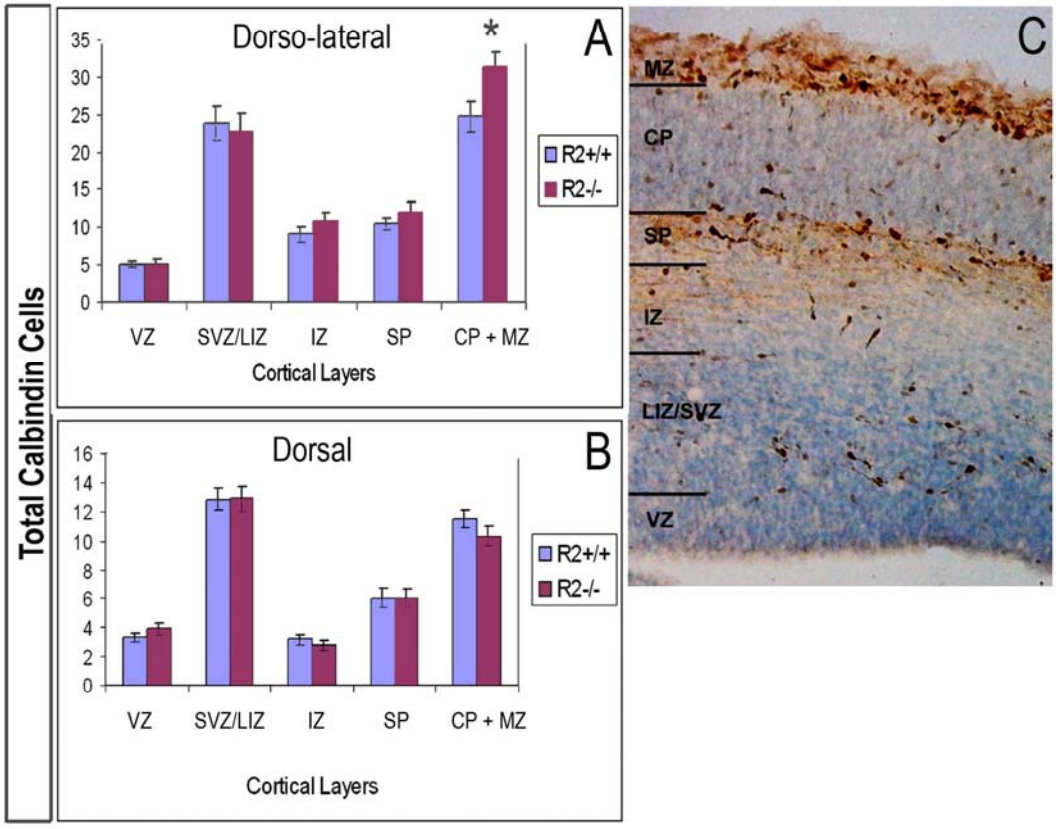

Fig. 4.2 Distribution of interneurons in rostral-middle levels of the Robo2 mutant cortex at E15.5. Photomicrograph showing a coronal section through the Robo2 mutant cortex immunohistochemically processed for the interneuron marker calbindin and counterstained with DAPI (C). Graphical representation of the distribution of calbindin immunopositive cells within all layers of the developing embryonic mouse cortex in wild type and Robo2 mutant animals. Counts were made in dorso-lateral (A) and dorsal (B) regions of the neocortex. A significant (20%) increase in calbindin immunopositive interneurons was observed within the cortical plate and marginal zone in dorso-lateral regions of the cortex in Robo2 mutants relative to wild type littermates at E15.5 (R2-/- 31.3±1.86; Robo2+/+ 24.6±2.02) ($p \leq 0.02$). Scale bar: 100 μm. (VZ, ventricular zone; LIZ/SVZ, lower intermediate zone/subventricular zone; IZ, intermediate zone; SP, subplate; CP, cortical plate; MZ, marginal zone).

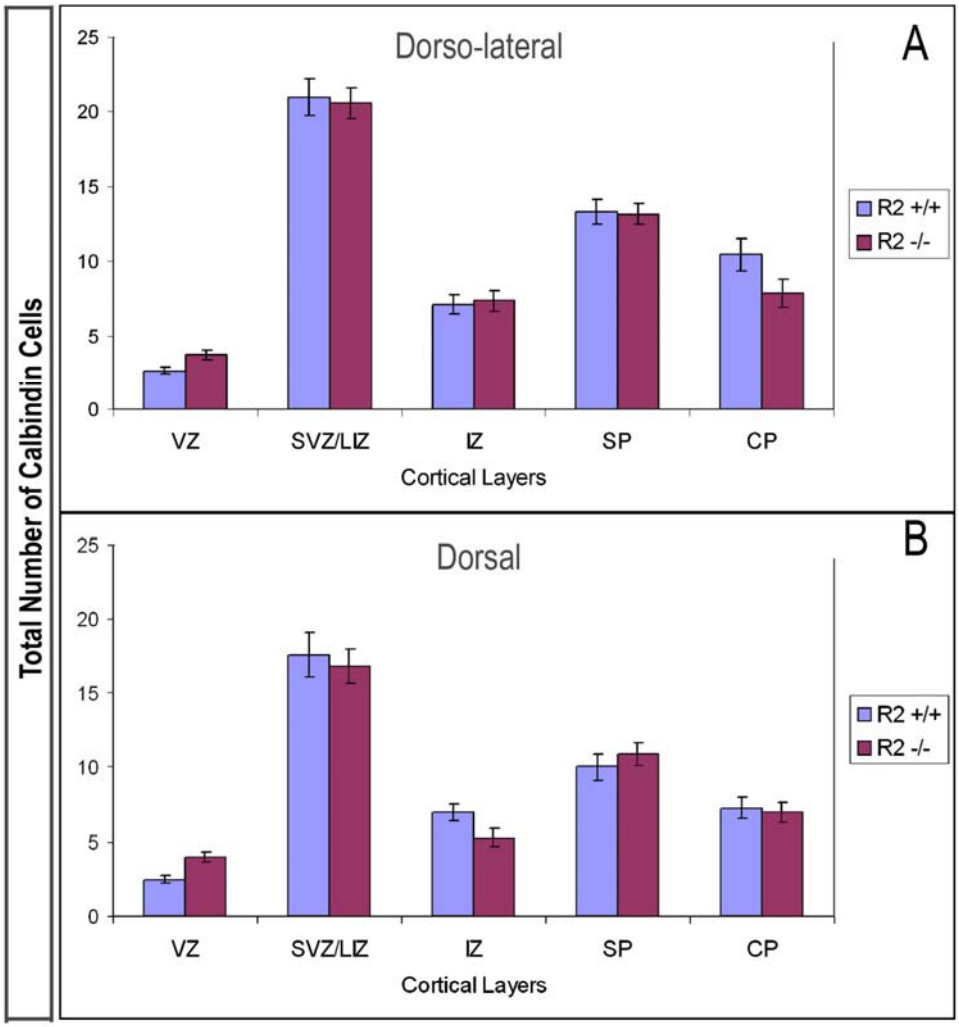

Fig. 4.3 Distribution of (calbindin immunopositive) interneurons within the caudal cortex of Robo2 mutant mice at E15.5. Graphical representation of the total numbers of calbindin immunopositive cells in dorso-lateral (A) and dorsal regions (B) of the developing caudal cortex. Counts were made in all layers of the developing caudal cortex. (VZ, ventricular zone; SVZ/LIZ, subventricular zone/lower intermediate zone; IZ, intermediate zone; SP, subplate; CP, cortical plate).

The small increase in calbindin cells in dorso-lateral, but not within dorsal regions of the neocortex was interesting as this could potentially reflect changes in the rate of migration of interneurons along their dorso-lateral trajectories. Analysis of the total number of calbindin immunopositive cells in Robo2 deficient and Robo2 wild type littermates was, therefore, similarly studied during late stages of interneuron migration (E17.5) within the developing forebrain ($Robo2^{-/-}$ n=3; $Robo2^{+/+}$ n=3). Coronal sections taken throughout the rostral-caudal extent of Robo2 deficient and wild type mice were stained with calbindin (Fig.4.4A), and counts were made in 400 μm wide cortical strips. The distribution of calbindin cells within each cortical zone was further analysed, with bin1 corresponding to the VZ and bin 6 to the MZ, as delineated by methyl-green counter-staining (Fig. 4.4A).

Analysis at E17.5, showed that there were no significant differences in the total numbers of calbindin immunopositive cells in Robo2 mutant relative to Robo2 wild type littermates in either rostral-middle ($Robo2^{-/-}$ 174.1±6.9; $Robo2^{+/+}$ 182.1±8.1; $p<0.51$) or caudal areas ($Robo2^{-/-}$ 150.1±9.2; $Robo2^{+/+}$ 144.3±11.3; $p<0.90$) of the E17.5 embryonic cortex (Fig. 4.4B). When the number of calbindin cells was quantified within each cortical zone, no significant differences were found between Robo2 mutant and Robo2 wild type littermate animals within either the rostral-middle (Fig 4.4C) or caudal (Fig4.4D) cortex.

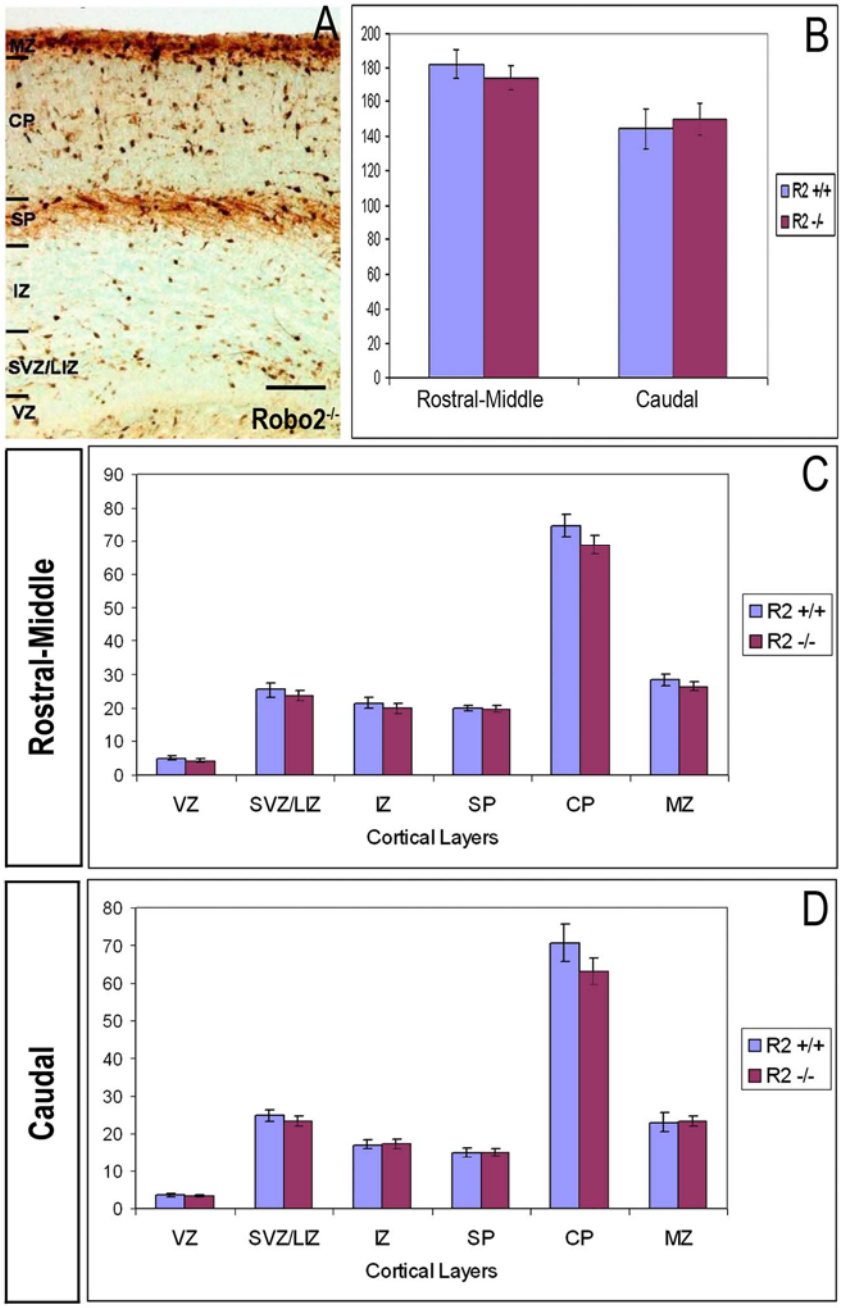

Fig. 4.4 Analysis of the total numbers and distribution of (calbindin immunopositive) cortical interneurons in Robo2 mutant animals at E17.5. Panel A shows a coronal section through the cortex of a Robo2$^{-/-}$ deficient mouse forebrain, immunohistochemically processed for calbindin proteins and counterstained with methyl green. Graphical representation of counts made in rostral-middle (B,C) and caudal regions of the cortex (B,D). Scale bar: 100 μm. (VZ, ventricular zone; SVZ/LIZ, subventricular zone/lower intermediate zone; IZ, intermediate zone; SP, subplate; CP, cortical plate; MZ, marginal zone).

4.2.2 Results: Robo2 and cortical interneuron morphology

Robo and Slit have previously been shown to regulate the elongation and branching of neuronal processes within the developing CNS (Murray and Whittington, 1999; Wang et al., 1999; Ozdinler and Erzurumlu, 2002; Ma and Tessier-Lavigne, 2007). Slit has also been shown to directly regulate neurite elongation and branching of GABAergic neurons *in vitro* in dissociated cultures and GE explants (Zhu et al., 1999; Sang et al., 2002, 2003). More recently, a study in our laboratory has confirmed that removal of Robo1 or both Slit1/Slit2 has a marked effect on the morphology of migrating interneurons *in vivo,* thus confirming that these molecules play a major role in controlling interneuron morphology during development (Andrews et al., 2008).

Similar to Robo1, Robo2 protein is also localised throughout the length of neurite processes of interneurons *in vivo* (Fig.3.16F), suggesting this receptor may have a similar role to Robo1. The putative role of Robo2 in regulating the morphological differentiation of migrating interneurons was therefore investigated *in vivo* using transgenic mice that lacked the Robo2 receptor. Coronal sections were taken from the cortices of Robo2 deficient and control littermate mice ($Robo2^{-/-}$ n=5; $Robo2^{+/+}$ n=4) and these were immunohistochemically processed for calbindin. Morphometric parameters analysed included the total neurite length, number of neurite processes, and number of branch points of interneurons (see Methods 2.25 and Appendix Fig. 1). This was investigated primarily within two major migratory streams that traverse through the SVZ/LIZ and SP regions of the developing cortex at E15.5.

Removal of the Robo2 receptor had no effect on the number of neurite processes (Fig. 4.5C, D) or branch points (Fig. 4.5E, F) of interneurons within either the SVZ/LIZ or SP layers of the cortex at E15.5. The total length of neurite processes, however, was significantly longer in interneurons from the SVZ/LIZ of the rostral-middle cortex (SVZ/LIZ $Robo2^{-/-}$ 87.2 ± 4.7μm; $Robo2^{+/+}$ 69.2 ± 4.0μm; $p<0.004$) (Fig. 4.5A). Interestingly, this was not observed for interneurons in the SP (SP $Robo2^{-/-}$ 69.6 ± 4.3μm; $Robo2^{+/+}$ 70.0 ± 4.98μm; $p<0.94$) (Fig. 4.5A). Similar analysis in the caudal cortex revealed no significant differences in process length of interneurons migrating within either the SVZ/LIZ (SVZ/LIZ $Robo2^{-/-}$ 89.8 ± 5.3μm; $Robo2^{+/+}$ 82.6 ± 5.2 μm; $p <0.33$) or SP ($Robo2^{-/-}$ 69.1 ± 4.9μm; $Robo2^{+/+}$ 67.6 ± 4.0μm; $p< 0.82$) layer (Fig. 4.5B).

These results suggest that while Robo2 does not appear to have an affect on the branching or number of interneuron processes, this receptor may be involved in maintaining and/or inhibiting the process elongation of a population of cortical interneurons that migrate through the SVZ/LIZ of the cortex. This is consistent with the expression of Robo2 in this layer of the cortex during mid-stages of interneuron migration (Fig. 3.16D-F).

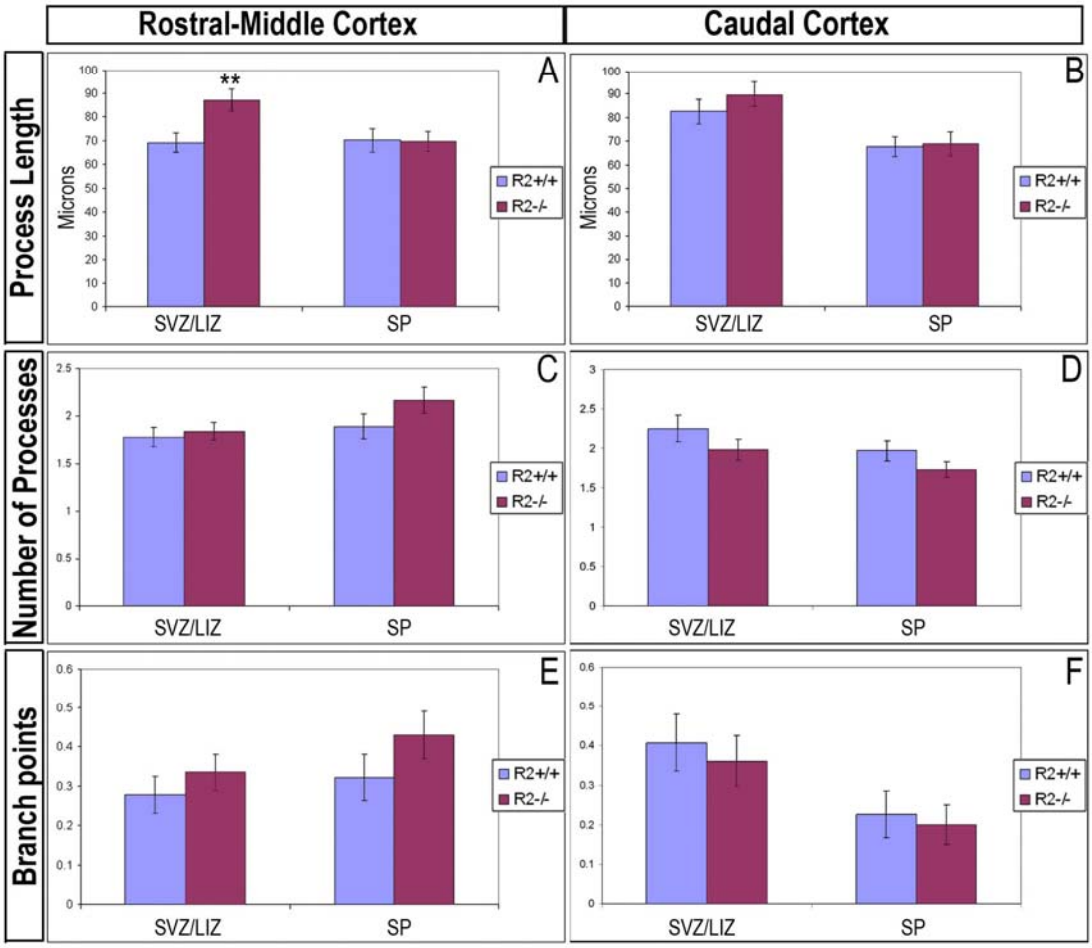

Fig. 4.5 Morphological analysis of migrating interneurons in the Robo2 deficient cortex. Calbindin immunopositive interneurons were taken from the subventricular zone/lower intermediate zone (SVZ/LIZ) and subplate (SP) layer of the E15.5 Robo2 deficient and wild type cortex, and analysed for their total process length (A,B), number of processes (C,D) and branch points (E,F). This was investigated at rostral-middle (A,C,E) and caudal levels (B,D,F) of the developing cortex. Interneurons from rostral-middle levels of the Robo2 deficient cortex, that specifically migrated within the SVZ/LIZ, exhibited significantly longer processes when compared with cortical interneurons analysed from wild type littermates ($R2^{-/-}$ n=5; $R2^{+/+}$ n=4)($R2^{-/-}$ 87.2 ± 4.7μm; $R2^{+/+}$ 69.2 ± 4.0μm; ** p<0.004).

4.3 RESULTS: ROBO2, THALAMOCORTICAL AND CORTICOFUGAL TRACTS

The observation that both Robo1 and Robo2 are expressed within the early PPL (E11.5) (Fig.3.3 -3.6) and IZ of the developing cortex, at a time when pioneering axons from PPL and corticofugal neurons start to project ventrally through the IZ to reach the internal capsule (E14.5-E15.5) (Fig.4.6A-D) (Métin and Godement, 1996; López-Bendito & Molnár, 2003; Morante-Oria et al., 2003), suggested that corticofugal projections may express both Robo1 and Robo2 receptors during development.

To confirm this, double labelling immunohistochemical studies for Robo and the neuronal adhesion molecule TAG1, specifically expressed by corticofugal fibres as these traverse through the cortical IZ (Denaxa et al., 2001; Jones et al., 2002), was carried out. Both Robo1 (Fig. 4.7B) and Robo2 (Fig. 4.7E) proteins were found to partially co-localise with TAG1 in a subset of fibres within the upper IZ (shown in yellow in 4.7C & F, respectively), suggesting that some corticofugal projections express Robo1 and Robo2 receptors during development. In addition, both Robo1 and Robo2 were expressed within the dorsal thalamus and throughout the developing internal capsule at a time when thalamocortical axons turn dorsally to enter the internal capsule at the diencephalic and telencephalic boundary (E13.5-E14.5) (Fig.4.6 A,B) and course along a rostral-dorsal trajectory to enter the developing cortex (E15.5-E17.5) (Fig. 4.6C,D) (Molnár et al., 1998, 2003). This suggested that

thalamocortical fibre tracts may also express both Robo1 and Robo2 receptors during development.

Pertinently, Robo1 has previously been shown to play a role in regulating the development of these fibre tracts *in vivo,* with removal of this receptor resulting in the early arrival of both thalamocortical and corticofugal axons at their respective targets within the cortex and thalamus (Andrews et al., 2006). The potential role that Robo2 may have in regulating the formation of these fibre tracts was therefore investigated. This study was carried out in collaboration with Dr Sonja Rakić, who carried out the DiI and DiA crystal placements.

The thalamocortical and corticofugal tracts were labelled by placing crystals of fluorescent carbocyanine lipophilic dyes (1,1-dioctodecyl-3,3,3',3'-tetralmethylindocarbocyanine (DiI) or 4-(4-(dihexadecylamino)styryl)-N-methylpyridium iodide (DiA) dyes) within the thalamus and cortex, respectively. The highly lipophilic nature of these dyes results in their diffusion throughout the axonal membrane of a single labelled cell, thus enabling single projections and fibres to be traced. To investigate the formation of thalamocortical tracts in Robo2 deficient mice, a single crystal of DiI was placed in the dorsal thalamus of embryonic mice at E16.5 ($R2^{-/-}$ n=2; $R2^{+/+}$ n=2), corresponding to a time when thalamocortical axons have traversed through the internal capsule and extended dorsally to enter the IZ and accumulate within the SP layer within the developing cortex. Analysis of Robo2 mutants showed no major defects in the trajectories of the thalamocortical fibres when compared with their wild type littermates (compare Fig. 4.8A-D with 4.8E-H). However,

in some sections taken from a single Robo2 mutant animal, ectopically placed fibres were observed which appeared to project ventrally from the dorsal thalamus towards the hypopthalamus (data not shown). In addition, some axonal fibres appeared to deviate from the internal capsule and to project ventrally within the basal forebrain (Robo2$^{-/-}$, n=1) arrow in Fig. 4.8E and F). Thalamic dye injections also revealed occasional retrogradely labelled cells within lateral regions of the CP in Robo2 mutants (n=1) (arrows in Fig. 4.8I-K). While carbocyanine dye placements made within the cortex (R2$^{-/-}$, n=2) resulted in diffuse labelling, labelled fibres were observed within the dorsal thalamus consistent with the arrival and correct targeting of these projections within these regions (data not shown). Thus, unlike Robo1, Robo2 does not appear to have a major role in regulating the development of these major forebrain tracts and is consistent with more recent studies carried out by López-Bendito and others (2007).

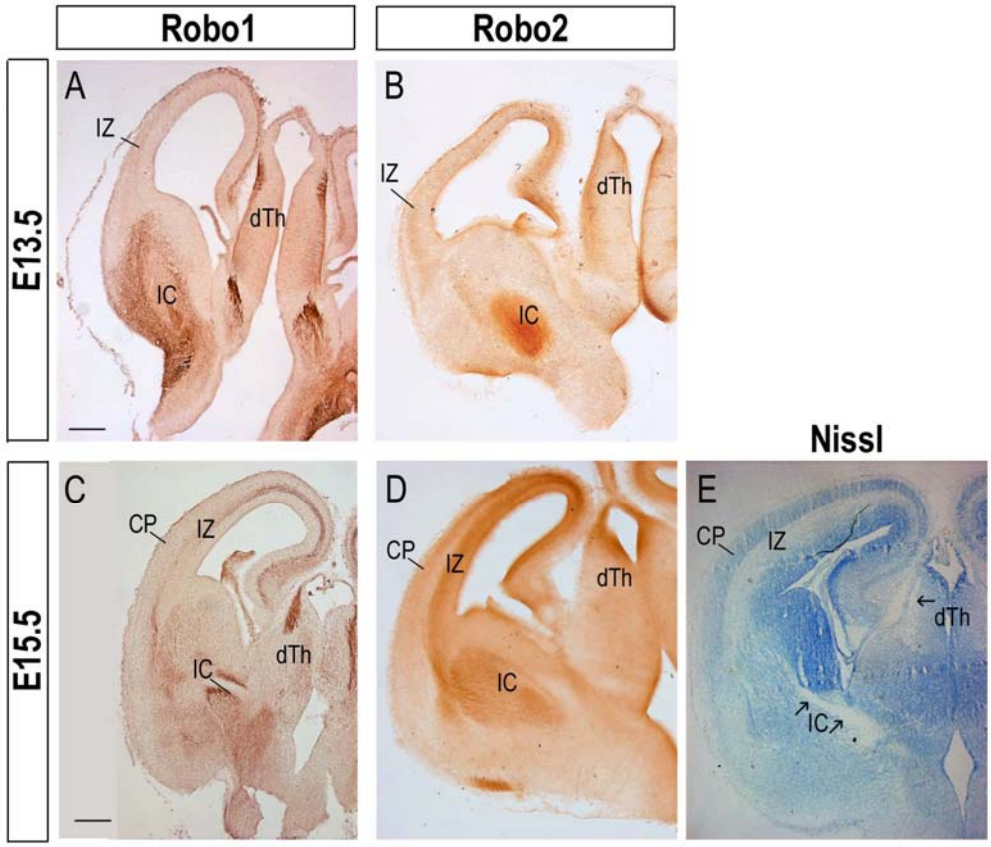

Fig. 4.6 Robo expression in the developing corticofugal and thalamocortical fiber tracts in the embryonic mouse forebrain. Panels show the immunohistochemical localisation of Robo1 (A,C) and Robo2 (B,D) receptors in the embryonic mouse forebrain at E13.5 (A,B) and E15.5 (C,D), in sections taken from caudal levels of the forebrain. Robo1 (A) and Robo2 (B) are expressed within the differentiating dorsal thalamus and in fibres wtihin the developing internal capsule (IC) at E13.5, consistent with thalamocortical axons extending through these regions at this time. Robo1 and Robo2 localisation within the preplate and IZ of the cortex at E13.5 is consistent with pioneering preplate axons and corticofugal neurons projecting ventrally through the IZ towards the IC at this time. Both Robo1 and Robo2 continue to be expressed wtihin the CP and in fibres throughout the IZ and IC at E15.5. Note distinctive Robo1 immunopositive fibres within the differentiating dorsal thalamus at E15.5; diffuse Robo2 staining is also observed in the dorsal thalamus. Panel E illustrates a comparable section at E15.5, stained with the nuclear marker Nissl. Some of the tracts associated with the dorsal thalamus (arrows) are free of stain. Scale bar in A is 200μm and applies to A,B; in C is 400μm and corresponds to C-E. (IZ, intermediate zone; CP, cortical plate; IC, internal capsule; dTh, dorsal thalamus).

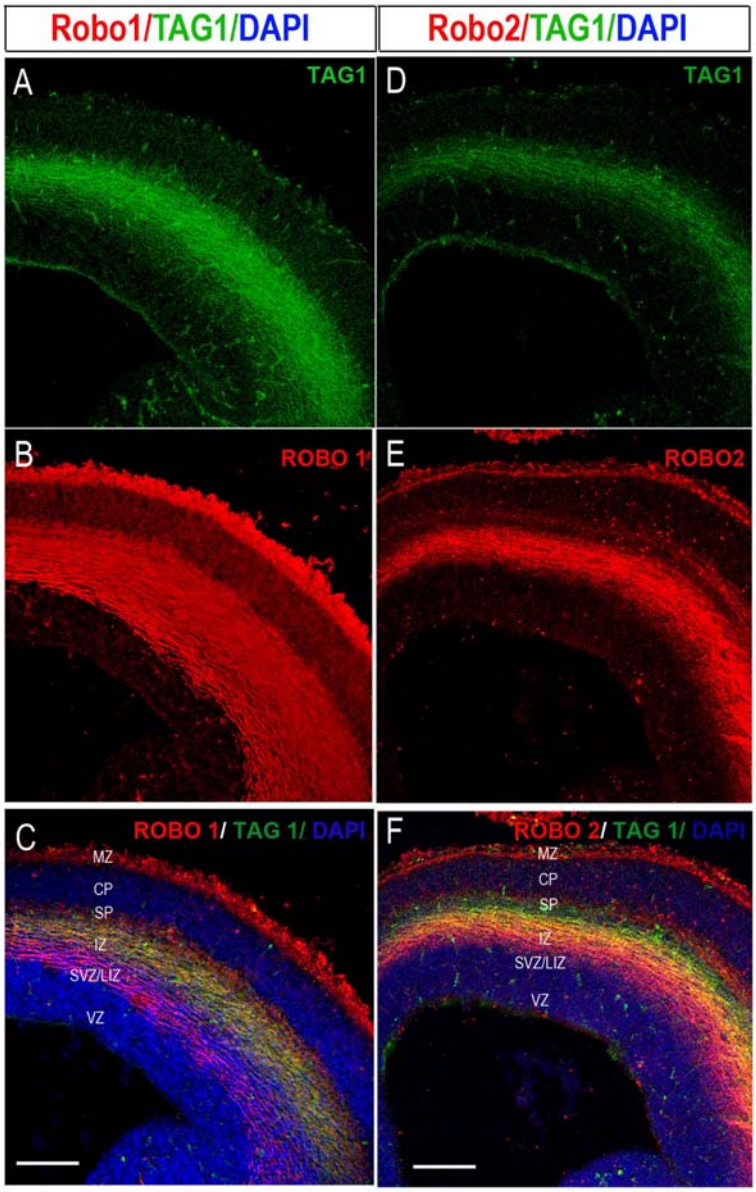

Fig. 4.7 Expression of Robo1 and Robo2 receptors by subsets of TAG1 immunopositive corticofugal fibres. Panels show coronal sections taken through the cortex of E15.5 mice immunohistochemically processed for Robo1 (B) (red) or Robo2 (E) (red) receptors, and double labelled with the neuronal cell adhesion molecule TAG1 (A,D) (green). Sections were counterstained with DAPI (blue). Partial co-localisation of Robo1 and Robo2 receptors (red) with TAG1 (red) is observed in some fibres within the cortical IZ, shown in yellow in panels C and F, respectively. Scale bar in C,F is 100 μm and applies to all panels. (MZ, marginal zone; CP, cortical plate; SP, subplate; IZ, intermediate zone; SVZ/LIZ, sub-ventricular zone/lower intermediate zone; VZ, ventricular zone).

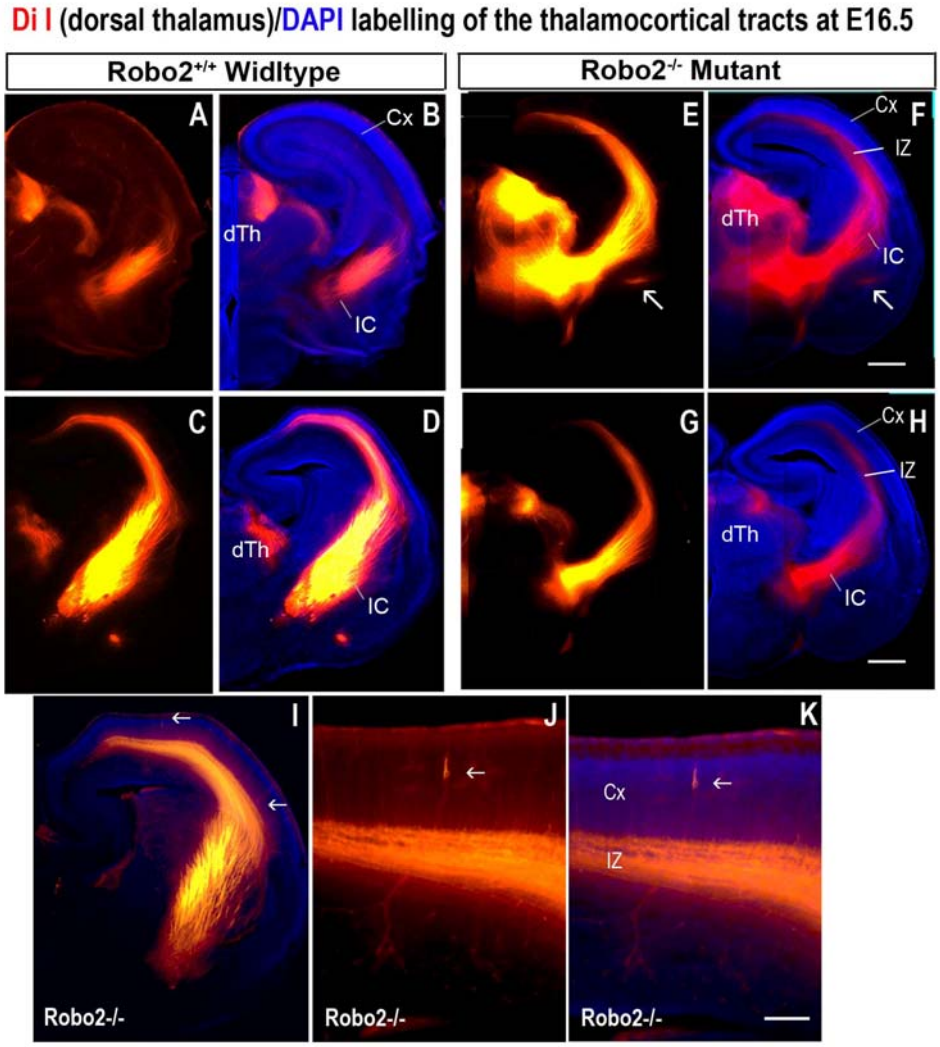

Fig. 4.8 Analysis of the developing thalamocortical axonal tracts in the Robo2$^{-/-}$ deficient forebrain. Crystals of DiI were placed into the dorsal thalamus of Robo2$^{+/+}$ wild type (n=2) (A-D) and Robo2$^{-/-}$ mutant animals (E-K) (n=2) at E16.5. Thalamocortical axons course through the internal capsule (IC) to reach the developing intermediate zone (IZ) of the cortex of Robo2 mutant animals (E-H), similar to wild type littermates (A-D). Labelled fibres (see arrow in E,F) were sometimes seen to deviate from the IZ and project to basal regions of the ventral forebrain in Robo2 mutant animals (n=1), suggesting these may be misrouted. Some retrogradely labelled cells were also sometimes observed in lateral regions of the Robo2 mutant cortex (Fig. J-K) (n=1). Scale bar in F,H is 450 μm and corresponds to A-I; and in K is 200 μm and applies to J,K. (Cx, cortex; IZ, intermediate zone; IC, internal capsule; dTh, dorsal thalamus).

4.4 DISCUSSION: ROBO2 AND CORTICAL INTERNEURONS

The putative role of Robo2 in regulating cortical interneuron numbers, and their ventral-dorsal migration was investigated *in vivo* in Robo2 deficient mice. Given that Robo2 is restricted to the differentiating striatum and does not co-localise with interneuron markers within the cortex during early phases of cortical development (E13.5), this was investigated during mid stages of tangential migration (E15.5) when the vast majority of (90%) the calbindin population of interneurons express this receptor.

The total number of calbindin cells was investigated at two different points along the neocortex in Robo2 deficient mice, which would enable any changes in the dorso-lateral migration of interneurons in the cortex to be studied. Previously, Robo1 has been shown to play a role in regulating interneuron numbers within rostral-middle, but not within caudal regions of the cortex (Andrews et al., 2006). Putative changes in interneuron numbers was therefore separately investigated within the rostral-middle and caudal cortex. These studies revealed that there was a comparable number of calbindin cells throughout the rostral-caudal extent of the neocortex in Robo2 mutant and Robo2 wild type littermates at this time. Similarly, there were no changes in the total number of calbindin cells when investigated during later stages (E17.5) of tangential migration, a time when most interneurons have reached the developing cortex (Anderson et al., 2001; Marín et al., 2003b; Métin et al., 2006).

Once interneurons arrive in the developing cortex, they migrate along specific and highly directed tangential paths (Lavdas et al., 1999; López-Bendito et al., 2008) before entering and assuming their correct positions within the developing CP (Polleux et al., 2002; Ang et al., 2003; Tanaka et al., 2003, 2006; Hevner et al., 2004). Thus, the total number of calbindin cells was investigated within each cortical layer, as any changes in the distribution of these cells may reflect changes in their trajectories within the cortex. Moreover, this could potentially reflect a defect in their final positioning within the CP. Analysis during mid phases of interneuron migration (E15.5) showed that there was a significant (23%) increase in calbindin cells within the CP and MZ layers in Robo2 mutant mice when compared with wild type animals, suggesting there was a change in the positioning of migrating interneurons at this time. However, this was only restricted to dorso-lateral regions of the neocortex. While we initially speculated that this may reflect a delay in the migration of interneurons along their dorso-medial trajectories, analysis at a later stage of interneuron migration (E17.5) showed no changes in the total numbers of calbindin positive cells within Robo2 deficient mice compared to wild type animals. Thus it would appear that, unlike Robo1, Robo2 does not have a major role in regulating interneuron numbers and is not required in the ventral to dorsal migration of interneurons from the GEs to the cortex. Analysis of the distribution of calbindin cells was also comparable within the Robo2 deficient and wild type cortex, suggesting that Robo2 is not required in maintaining the correct positioning of migrating interneurons or in specifying their tangential streams within the cortex.

The putative role of Robo2 in regulating the morphology of migrating interneurons was also investigated, as Robo1-Sli1/2 signalling has been shown to have an important role in regulating these processes both *in vitro* (Sang et al., 2002) and *in vivo* (Andrews et al., 2008). Like Robo1, Robo2 is similarly expressed throughout the length of processes of migrating interneurons, consistent with a role in regulating their morphology. This was investigated *in vivo* during mid-phases of tangential migration, and elucidated that removal of Robo2 resulted in significantly longer neuronal processes in interneurons within Robo2 deficient cortices, when compared with wild type controls. This was specifically observed in interneurons migrating through the LIZ/SVZ, where Robo2 is strongly expressed at this time, suggesting that Robo2 has a role in inhibiting or maintaining the process elongation of this population of interneurons.

Thus, it appears that, unlike Robo1, Robo2 does not have a prominent role in modulating the morphology of migrating interneurons *in vivo,* but is involved in controlling the process length of a population of interneurons that specifically migrate through the SVZ/LIZ. Given that Robo2 is strongly expressed by the vast majority of interneurons during mid phases of tangential migration, it was surprising that removal of this receptor did not have a prominent effect on their development, as has been previously shown for Robo1 (Andrews et al., 2006, 2008). However, as Robo1 is also expressed by approximately 90% of (calbindin positive) interneurons, it is possible that Robo1 may compensate for the loss of Robo2, thus rendering this receptor functionally redundant. A comparison of Robo1;Robo2 double mutants with single Robo1 and Robo2

mutants would help elucidate the contribution of Robo2 in regulating these processes *in vivo*.

4.5 DISCUSSION: ROBO2 AND THALAMOCORTICAL AND CORTICOFUGAL AXON TRACTS

In addition to the expression of Robo2 in populations of migrating interneurons, this receptor was localised within the dorsal thalamus and in fibres within the developing internal capsule at a time when thalamocortical projections are being formed (E13.5-E15.5). Furthermore, Robo2 protein expression was visualised within the developing CP and IZ of the early cortex (E13.5), corresponding to a time when corticofugal projections extend towards the cortico-striatal boundary and enter the internal capsule (E15.5) (Molnár et al., 2003), suggesting that thalamocortical and corticofugal tracts express this receptor. To confirm this, double labelling studies were carried out using Robo and the neuronal adhesion molecule, TAG1, which is specifically expressed by corticofugal axons within the cortical IZ (Denaxa et al., 2001; Jones et al., 2002; López-Bendito & Molnár, 2003). These showed a partial colocalisation of Robo1 and Robo2 proteins with TAG1 expression which was restricted to subsets of fibres within the UIZ (yellow in Fig. 4.7C & F, respectively), consistent with corticofugal fibres traversing through this region at this time. Some fibres coursing within the subplate layer of the cortex were immunopositive for Robo1 (red in 4.7B,C) and Robo2 (red in 4.7E,F), but did not coincide with TAG1 expression in this region; similarly, subsets of Robo2 immunolabeled fibres within the upper IZ did not colocalise with TAG1

expression in this region (red in 4.7F). These could represent thalamocortical axons which first enter the cortex at this time and accumulate within the subplate layer, prior to entering the developing cortical plate (Molnár et al., 2003). In addition, some immunolabeled Robo1 fibre tracts are observed at deeper levels of the LIZ and SVZ (Fig. 4.7C) which did not colocalise with TAG1 expression (see below).

Thus, these double immunolabeling studies confirmed that some corticofugal fibres express both the Robo1 and Robo2 at a time in development when these axonal tracts extend towards, and enter the developing internal capsule, consistent with these receptors having a putative role in the development of the corticofugal tracts.

Analysis of Slit mutants as well as Slit knock-down experiments have previously shown that these proteins have a crucial role in regulating the development of corticofugal and thalamocortical projections *in vivo* (Bagri et al., 2002; Shu et al., 2003). Similarly, analysis of Robo1 mutants has demonstrated that removal of Robo1 resulted in the premature arrival of thalamocortical fibres within the cortex, as well as reciprocal corticofugal fibres entering the internal capsule earlier than in wild type animals (Andrews et al., 2006). This is particularly interesting as interneurons have been suggested to migrate along corticofugal tracts during development (Denaxa et al., 2001). Given that interneurons express all three Robo receptors, and that these bind homophilically and heterophilically *in vitro* (Liu et al., 2004; Camurri et al., 2005), it is tempting to speculate that interactions between Robo-expressing

interneurons and Robo-expressing fibre tracts, may mediate their migration along these axonal substrates.

The putative role of Robo2 in the development of the thalamocortical and corticofugal fibre tracts was studied by placing single crystals of carbocyanine dyes within the dorsal-lateral cortex or dorsal thalamus, respectively. This was carried out at a time when reciprocal connections have been made between the cortex and dorsal thalamus ($R2^{-/-}$, n=2; $R2^{+/+}$ n=2) (E16.5). Removal of the Robo2 receptor did not result in any major defects within either the corticofugal or thalamocortical fibre tracts, with these being correctly targeted within the dorsal thalamus and cortex, respectively. Injections made within the dorsal thalamus resulted in a few retrogradely labelled cells within lateral regions of the cortex in some sections, further confirming the correct targeting of some corticofugal projections within the dorsal thalamus.

Some subtle defects were observed within the developing thalamocortical tract in a single Robo2 mutant animal however. Injections within the dorsal thalamus revealed subsets of fibres which were ectopically misplaced within the ventral hypothalamus (data not shown). In addition, labelled fibres appeared to deviate from the internal capsule, and project within the basal forebrain (arrow in Fig. 4.8E). It is possible that these displaced fibres could represent misrouted retinal ganglion cell (RGC) axons. A recent study by Plachez et al., (2008) has shown that Robo2 has a major role in regulating the development of the optic tract, from it's origin within the retina, and throughout its growth over the diencephalon to reach the superior colliculus. This study reported that some

RGC fibres deviate from the optic tract to erroneously enter the internal capsule within the diencephalon in Robo2 mutant animals (Plachez et al., 2008). DiI labelling within the dorsal thalamus in the study of Plachez and others (2008) further showed retinal ganglion cell projections which were labelled at the level of the internal capsule, and projected ventrolaterally within the amygdala, similar to the defects observed in this study. A more extensive analysis is required to elucidate the origin of these minor defects observed within the developing internal capsule of a single Robo2 mutant animal. Simultaneous labelling of the dorsal thalamus and optic tract, by injecting Robo2 mutant eyes with carbocyanine dyes would help discern whether deviations within the internal capsule originate from the putative misrouting of subsets of thalamocortical fibres in the Robo2 mutant animals, or by the aberrant entry of retinal ganglion cell projections within the internal capsule.

The minor alterations observed in the thalamocortical tracts of a single Robo2 mutant here, was consistent with the findings of López-Bendito and others (2007) which showed that removal of Robo2 resulted in only subtle defects within the developing thalamocortical and corticofugal tracts. These studies similarly showed that while most thalamocortical projections normally traversed along the internal capsule to reach the developing cortex, subsets of fibres were sometimes shown to mis-project to the hypothalamus. In addition, while most corticofugal fibres were shown to reach the dorsal thalamus, consistent with our observations, fibres were also sometimes reported to aberrantly cross the ventral midline at the level of the anterior commisure. Furthermore, corticofugal axons within the dorsal thalamus were found to be

abnormally defasciculated and ventrally displaced in Robo2 mutants. It would appear that the Robo2 mutant mice analysed by López-Bendito and others (2007) display a more severe phenotype than our mice. Nonetheless, most projections from the thalamus and cortex were shown to develop normally as found in this study. Differences in the genetic backgrounds of these Robo2 mutants may explain the subtle differences observed between these strains of mice. Moreover, both Robo1 and Robo2 are strongly expressed within the thalamocortical and corticofugal fibres, and so these may be functionally redundant. Indeed, severe defects were observed in the Robo1;Robo2 double mutant mice in the same study carried out by López-Bendito and others (2007). This study showed that few thalamocortical axons reached the cortex, with most axons projecting ventrally within the hypothalamus. The rare projections which entered the internal capsule further deviated ventrolaterally within the caudal cortex, and some fibres aberrantly crossed the midline at more rostral levels of the cortex. Consistent with a loss of sensitivity at the midline, corticofugal axons prematurely crossed the midline at the level of the anterior commisure, with few projections coursing through the internal capsule to reach the dorsal thalamus. These defects were comparable with Slit1;Slit2 double mutants (Bagri et al., 2002) and thus it appears that the co-ordinated activity of both Robo1 and Robo2 receptors and their Slit1 and Slit2 ligands is required for the correct development and targeting of these fibres tracts *in vivo*.

Interestingly, deeply positioned fibrous-like Robo1 immunopositive staining was also observed at the level of the lower IZ and SVZ (red in 4.7B&C) in the expression studies carried out. These fibres did not colocalise with TAG1 staining. While this may in part be explained by the presence of Robo1-

expressing interneurons migrating through this region at this time (see Fig. 3.16C), the distinctive fibrous like nature of labelling in this region strongly suggests these also comprise axonal tracts. Immunolabeled Robo1 and Robo2 fibres were similarly observed at the level of the SVZ and lower IZ at E17.5 (Fig.3.17). These tracts are deeply positioned within the LIZ and SVZ, and further investigations would be required to determine the origins of these deeply positioned fibre tracts, given that thalamocortical and corticofugal fibres predominantly traverse through more superficial regions of the IZ in the cortex at these stages of development (De Carlos et al., 1992; Molnár et al., 2003 Price et al., 2006).

It is interesting to note that the developing SVZ within the primate cortex is divided into an internal and external region by invading fibre tracts (Smart et al., 2002). Poignantly, studies in the enucleated primate cortex have suggested that afferent thalamocortical fibres may modulate neurogenesis within the cortical VZ and SVZ (Dehay et al., 1993, 1996). More recently, thalamocortical afferents have also been shown to exert a mitogenic effect on progenitors within the murine cortical VZ, through their release of diffusible factors, in organotypic cultures *in vitro* (Dehay et al., 2001). This is interesting in view of the close location of Robo immunopositive fibre tracts to the cortical VZ/SVZ, and the possibility that they may regulate the proliferation of intermediate and multipotent progenitors within these regions. Further experiments in which small crystals of DiI are placed within the cortical SVZ, combined with proliferation studies, would enable the origin and significance of these fibres to be investigated.

4.6 Summary

The putative role of the Robo2 receptor in the development of cortical interneurons was investigated *in vivo,* using Robo2 transgenic mice deficient in this receptor. Analysis revealed that Robo2 mutant mice have similar numbers of calbindin positive interneurons within the cortex, and that their distribution is comparable with wild type littermates. This suggests that Robo2 does not have a major role in specifying cortical interneuron numbers, and is not required in their ventral-dorsal migration from the GEs to the cortex. Furthermore, we showed that Robo2 is expressed by corticofugal axons and is also expressed within the dorsal thalamus and internal capsule, at a time when these projections are formed. In light of these observations, the putative role of Robo2 in regulating these developing axonal systems was investigated within the forebrain of Robo2 mutant mice. Removal of Robo2 resulted in only minor alterations within the thalamocortical tract, suggesting that this receptor does not have a major role in the development of either the corticofugal or thalamocortical tracts. This is consistent with the study of López-Bendito et al. (2007) which reported severe defects in Robo1;Robo2 double mutant mice, highlighting that both Robo1 and Robo2 receptors are required to mediate the normal development of these processes *in vivo*.

CHAPTER 5: THE ROLE OF ROBO3 IN THE DEVELOPMENT OF CORTICAL INTERNEURONS

5.1 RESULTS: ROBO3 AND CORTICAL INTERNEURONS

The finding that an early population of interneurons expressed the Robo3 receptor raised the question whether this may have a role in the migration and morphological differentiation of interneurons during development. This was studied in the cortices of Robo3 deficient mice ($Robo3^{-/-}$) during early (E13.5) phases of tangential migration (Fig. 5.1C-D). While Robo3 is down regulated within the cortex by E15.5, it is possible that an early role of Robo3 may be manifested during later stages of development and so, this was further investigated at E18.5 (Fig. 5.1E-F).

Coronal sections from the cortex of mutant and heterozygote littermates were immunohistochemically processed for the interneuron marker calbindin (Anderson et al., 2001; Andrews et al., 2006) (Fig. 5.1A-B). Analysis of Robo3 deficient cortices (n=3 $Robo3^{-/-}$) during the early (E13.5) phase of tangential interneuron migration showed no significant changes in the total number of calbindin cells within rostral-middle ($Robo3^{-/-}$ 130.9±5.3; $Robo3^{+/-}$ 132.7±4.8) or caudal levels ($Robo3^{-/-}$ 119.4±3.1; $Robo3^{+/-}$ 104±10.4) of the cortex compared with Robo3 heterozygote littermates (n=3 $Robo3^{+/-}$) (Fig. 5.1C-D). When the distribution of calbindin positive cells was assessed within the different layers of the developing cortex, a significant 20% reduction in the number of cells was observed within the MZ of Robo3 deficient mice compared with heterozygote

littermates (Robo3$^{-/-}$ 42.9±1.8; Robo3$^{+/-}$ 54.5±1.8; $p<0.0001$) in rostral-middle levels and a marked 30% reduction in caudal levels of the cortex (Robo3$^{-/-}$ 27.3±3.4; Robo3$^{+/-}$ 39.7±1.7; $p<0.01$) (Fig. 5.1C-D) at E13.5. This decrease within the MZ of the Robo3 mutant cortex coincided with a small, but not significant, increase of cells in some of the other layers of these animals.

Analysis at a later phase of corticogenesis (E18.5) similarly revealed no differences in the number of calbindin cells in rostral-middle levels of the cortex (Robo3$^{-/-}$ n=3, 211.1±4.75; Robo3$^{+/-}$ n=3, 211.4±7.02) (Fig. 5.1E). However, a small but significant decrease (11%) was observed within the caudal cortex of mutant animals relative to heterozygote littermates (Robo3$^{-/-}$ 194.4± 4.0; Robo3$^{+/-}$ 218.5±5.5; $p<0.01$) which was distributed across most layers (Fig. 5.1F). Thus, Robo3 does not appear to have a major role in regulating the number of interneurons within the developing cortex, but it does appear to have a small effect on the distribution of interneurons specifically within the MZ.

5.2 ROBO3 AND INTERNEURON MORPHOLOGY

As shown previously, in addition to regulating interneuron numbers in the developing cortex, both Robo1 and Robo2 receptors play a role in regulating the morphology of migrating cortical interneurons (Fig 4.5; Andrews et al., 2008). Thus, studies were carried out in the laboratory by Dr. William Andrews, to determine whether Robo3 has a similar role in regulating process elongation of migrating interneurons during their tangential migration. The morphology of migrating (calbindin immunopositive) interneurons was assessed by measuring the total process length, the number of processes and the number of branch

points (see Appendix Fig.1) of migrating interneurons. This was investigated in Robo3 deficient transgenic mice during early (E13.5) (n=3 Robo3$^{-/-}$, n=3 Robo3$^{+/-}$) (Fig. 5.2) and late (E18.5) (n=3 Robo3$^{-/-}$, n=3 Robo3$^{+/-}$) stages (Fig. 5.3) of tangential migration within the rostral-middle cortex.

This analysis indicated that, at E13.5, interneurons in Robo3$^{-/-}$ cortices (n=422 neurons Robo3$^{-/-}$; n= 298 neurons Robo3$^{+/-}$) showed significantly greater process length (Robo3$^{-/-}$ 77.32±17.23 μm; Robo3$^{+/-}$ 43.56±1.14 μm) (Fig. 5.2A), and significantly more processes (Robo3$^{-/-}$, 1.77±0.04; Robo3$^{+/-}$, 1.60±0.04) (Fig. 5.2B) and branch points (Robo3$^{-/-}$, 0.40±0.03; Robo3$^{+/-}$ 0.29±0.03) (Fig. 5.2C) than interneurons taken from heterozygote littermates.

Interestingly, analysis at later stages of development (E18.5) showed there were no significant differences in interneuron morphology between Robo3 mutant and Robo3 heterozygote littermates (n= 322 Robo3$^{-/-}$; n= 295 Robo3$^{+/-}$) (Fig. 5.3). Interneurons exhibited comparable total process length (Robo3$^{-/-}$ 65.95±1.72 μm; Robo3$^{+/-}$ 62.33±1.67 μm) (Fig. 5.3A), number of processes (Robo3$^{-/-}$ 1.65±0.04; Robo3$^{+/-}$ 1.67±0.05) (Fig. 5.3B) and branch-points (Robo3$^{-/-}$ 0.34±0.03; Robo3$^{+/-}$ 0.32±0.03) (Fig. 5.3C) at this time. These observations are consistent with the down-regulation of Robo3 within the neocortex at this time point (Fig. 3.8). This data also suggests that Robo3 plays a role in regulating the morphology of migrating early born cortical interneurons.

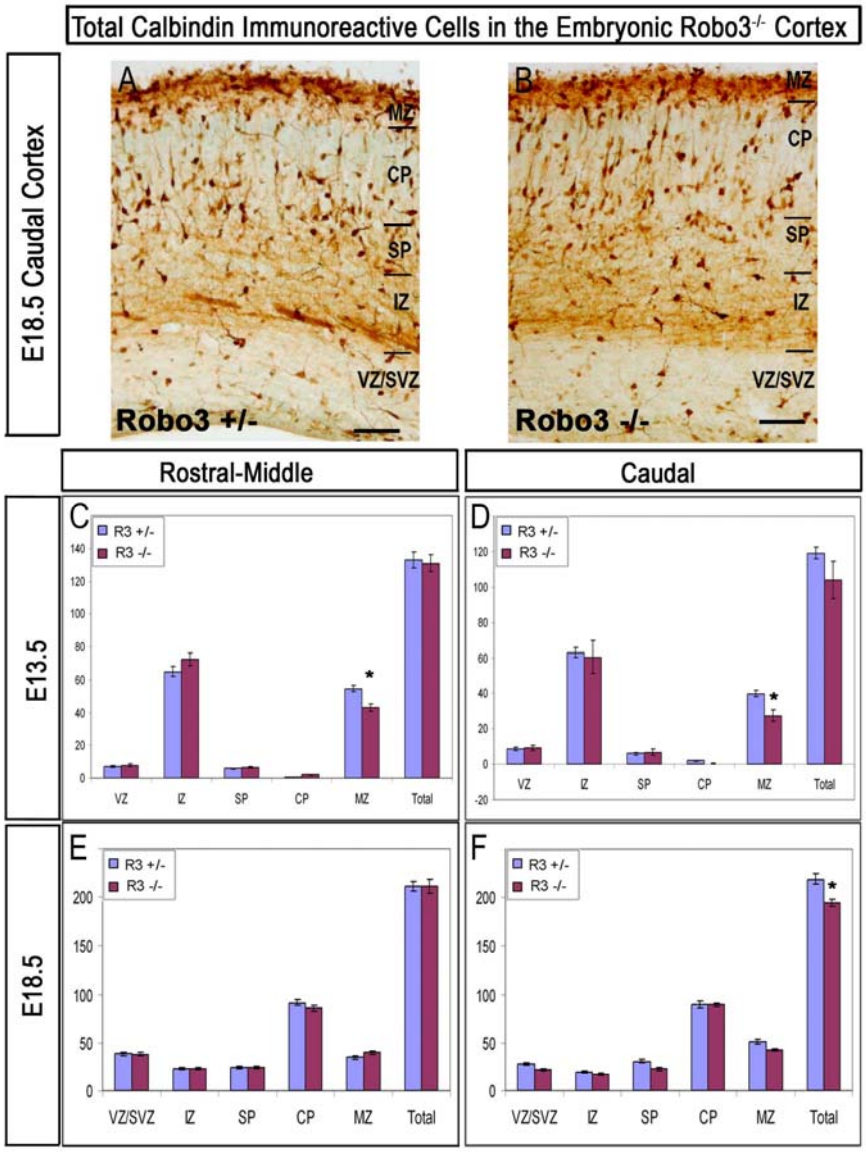

Fig. 5.1 Analysis of the number and distribution of calbindin immunoreactive interneurons in the developing Robo3 deficient mouse cortex. Photomicrographs of coronal sections through the caudal cortex of E18.5 Robo3$^{-/-}$ mutant (B) and Robo3 $^{+/-}$ heterozygote (A) mice, processed for calbindin proteins and counterstained with methyl green. Graphical representation of counts made in rostral-middle (C,E) and caudal (D,F) regions of the cortex at E13.5 (C,D) (n=3 Robo3$^{-/-}$, n=3 Robo3$^{+/-}$) and at E18.5 (E,F) (n=3 Robo3$^{-/-}$, n=3 Robo3$^{+/-}$). A significant decrease in calbindin immunopositive cells was observed within the MZ of Robo3$^{-/-}$ mutant animals at E13.5 in rostral-middle (C) (Robo3$^{-/-}$ 42.9±1.8; Robo3$^{+/-}$ 54.5±1.8; $p<0.0001$) and caudal levels of the cortex (Robo3$^{-/-}$ 27.3±3.4; Robo3$^{+/-}$ 39.7±1.7; $p<0.01$), when compared with heterozygote littermates. A small and significant decrease in the total number of calbindin immunoreactive interneurons was observed within the caudal, but not in rostral-middle levels of the cortex in Robo3 mutants relative to heterozygote littermates at E18.5 (E,F) (Robo3$^{-/-}$ 194.4±4.0; Robo3$^{+/-}$ 218.5±5.5; $p<0.01$). Scale bar: 150μm. (VZ, ventricular zone; SVZ, subventricular zone; IZ, intermediate zone; SP, subplate; CP, cortical plate; MZ, marginal zone).

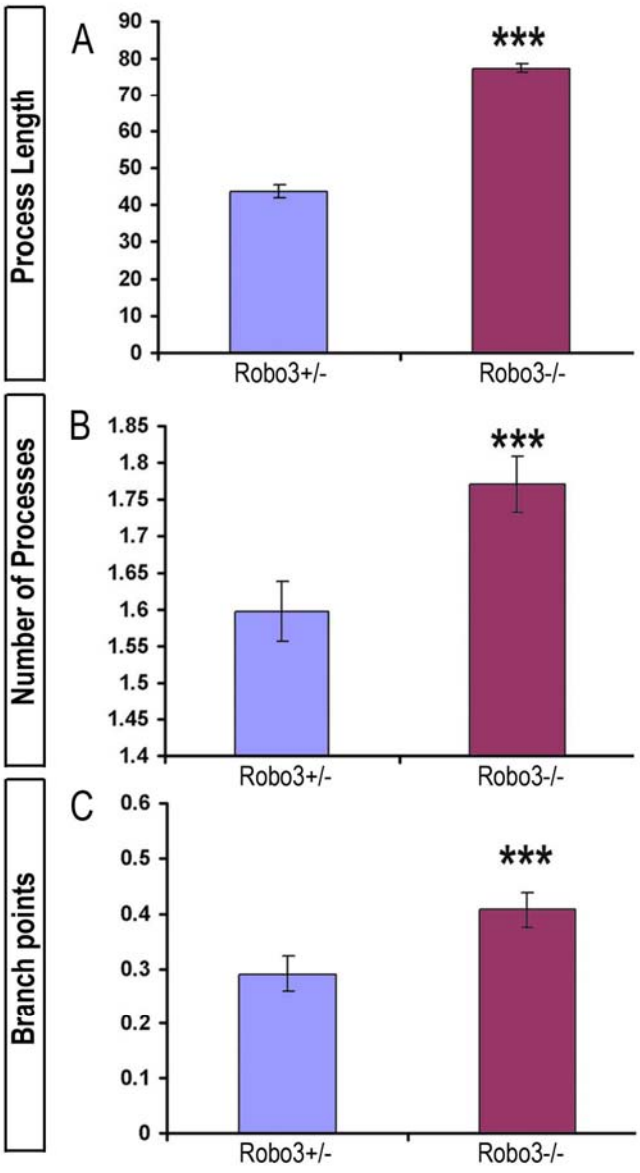

Fig. 5.2 Morphological analysis of migrating interneurons in the Robo3$^{-/-}$ deficient cortex at E13.5. Graphical representation showing total process length (A), number of processes (B) and branch points (C) of migrating interneurons in the cortex of Robo3$^{-/-}$ mutant (purple) and heterozygote (blue) littermate animals at E13.5. (n=3 Robo3$^{-/-}$, n=3 Robo3$^{+/-}$) Cortical interneurons taken from Robo3 deficient mice exhibited significantly greater process length (A) (Robo3$^{-/-}$ 65.95±1.72 μm; Robo3$^{+/-}$ 62.33±1.67 μm), increased number of processes (Robo3$^{-/-}$ 1.65±0.04; Robo3$^{+/-}$ 1.67±0.05) and branch points (Robo3$^{-/-}$ 0.34±0.03; Robo3$^{+/-}$ 0.32±0.03), when compared with heteroygote animals. (*** $p<0.0001$). (This analysis was carried out by Dr. W. Andrews).

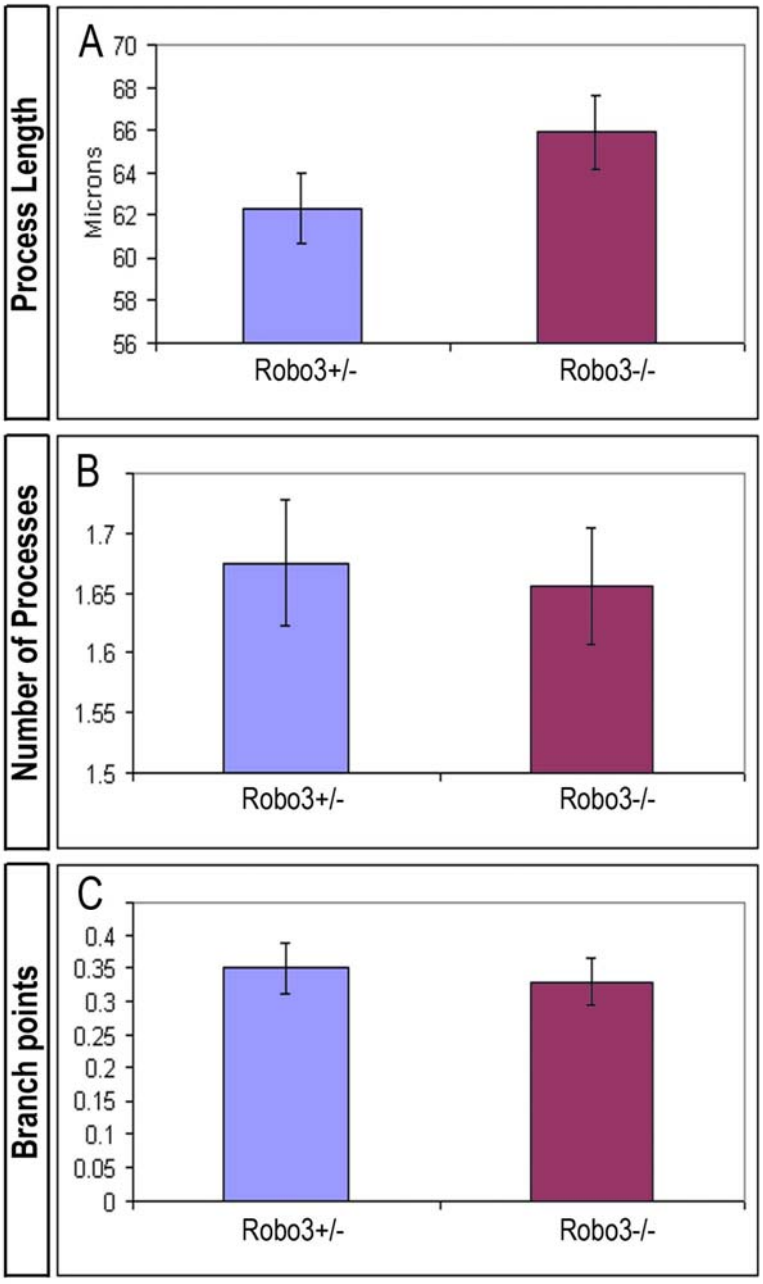

Fig. 5.3 Morphological analysis of migrating interneurons in the Robo3$^{-/-}$ deficient mouse cortex at E18.5. Graphical representation showing the total process length (A), number of processes (B) and branch points (C) of migrating interneurons in the cortex of Robo3$^{-/-}$ mutants (purple) relative to Robo3$^{+/-}$ heterozygote littermates (blue) at E18.5. (This analysis was carried out by Dr. W. Andrews).

5.3 ANALYSIS OF INTERNEURON DEVELOPMENT IN TRIPLE ROBO1$^{-/-}$ROBO2$^{-/-}$ROBO3$^{-/-}$ MUTANT MICE

5.3.1 Cortical interneuron numbers in triple Robo1;Robo2;Robo3 mutants

The previous immunohistochemical studies have shown that all three Robo receptors are expressed in overlapping patterns both within the ventral and dorsal telencephalon during early stages of development, prompting speculation that individual neurons in the GE and cortex express more than one receptor. Furthermore, the three receptors exert a differential effect on the number and positions of cortical interneurons *in vivo* (see Figures 4.2-4.3, 5.1; Andrews et al., 2006, 2008). In view of these observations, it is possible that silencing one of the receptors may induce a compensatory response from the others. For this reason, we wished to investigate the number and morphology of cortical interneurons in transgenic mice that lack all three Robo receptors. Coronal sections, taken from the cortex of triple Robo mutant (Robo1$^{-/-}$Robo2$^{-/-}$Robo3$^{-/-}$) mice, were immunohistochemically processed for calbindin. The total number and distribution of interneurons was assessed throughout the rostral-caudal extent of the developing cortex.

Analysis at the early stages of corticogenesis was difficult due to lack of appropriate control littermate animals. However, a decrease in the total number of calbindin cells was observed within the cortices of triple Robo mutant animals (n=2) (Fig. 5.4C) relative to animals which were heterozygote for both Robo1 and Robo2 receptors and fully deficient for the Robo3 receptor (n=1, Robo1$^{+/-}$Robo2$^{+/-}$Robo3$^{-/-}$) (Fig. 5.4A), or compound animals which were

deficient in both Robo1 and Robo2 receptors and heterozygote for the Robo3 receptors (n=2, $Robo1^{-/-}Robo2^{-/-}Robo3^{+/-}$) (Fig. 5.4B). Specifically, there was a significant 34% decrease in the total number of calbindin cells within the rostral-middle cortex in triple Robo mutants relative to either heterozygote littermates ($Robo1^{-/-}Robo2^{-/-}Robo3^{-/-}$, 93.5±9.14; $Robo1^{+/-}Robo2^{+/-}Robo3^{-/-}$, 141.4±4.54; $p<0.05$); or when compared with $Robo1^{-/-}Robo2^{-/-}Robo3^{+/-}$ compound animals ($Robo1^{-/-}Robo2^{-/-}Robo3^{-/-}$, 93.5±9.14; $Robo1^{+/-}Robo2^{+/-}Robo3^{-/-}$, 139.6±3.84; $p<0.05$) (Fig. 5.4D). Interestingly, a comparable 30% decrease in total calbindin cells was observed within caudal regions of the cortex of triple Robo mutant animals when compared with Robo heterozygote animals ($Robo1^{-/-}Robo2^{-/-}Robo3^{-/-}$, 106.3±5.34; $Robo1^{+/-}Robo2^{+/-}Robo3^{-/-}$, 150.5±6.78; $p<0.05$), but not with Robo compound mutants deficient in both Robo1 and Robo2 and heterozygote for the Robo3 receptor ($Robo1^{-/-}Robo2^{-/-}Robo3^{-/-}$, 106.3±5.34; $Robo1^{-/-}Robo2^{-/-}Robo3^{+/-}$, 109.7± 7.32) (Fig. 5.4D). Analysis of the distribution of calbindin cells showed there was a prominent reduction in these cells especially within the IZ and MZ/PPL layers of the cortices of Robo triple mutant animals (Fig. 5.4E, F & Table 5.1). These zones correspond to the positions of streams of migrating interneurons at this time.

Table 5.1

Calbindin counts in cortical layers of triple Robo1;Robo2;Robo3 mutant mice at E13.5

	Rostral-Middle		Caudal	
	IZ	MZ/PPL	IZ	MZ/PPL
$Robo1^{-/-}Robo2^{-/-}Robo3^{-/-}$	35.92±5.14	41.42±4.13	46.6±3.17	35.9±2.56
$Robo1^{-/-}Robo2^{-/-}Robo3^{+/-}$	63.27±2.49	51.68±2.16	49.1±3.64	39.6±3.72
$Robo1^{+/+}Robo2^{+/+}Robo3^{+/-}$	64.14±2.99	48.29±0.64	72.7±3.84	47.5±2.41

Cell counts at E18.5 were consistent with observations at E13.5. They showed that removal of all three Robo receptors resulted in a significant (approximately 38%) decrease in the number of calbindin cells within rostral-middle regions of the cortex compared to single Robo3 heterozygote littermates (n=1 $Robo1^{-/-}Robo2^{-/-}Robo3^{-/-}$, 167±8.63; n=1 $Robo1^{+/+}Robo2^{+/+}Robo3^{+/-}$, 285.5±28.4) (Fig. 5.5A), and to compound Robo mutants (n=1 $Robo1^{-/-}Robo2^{-/-}Robo3^{-/-}$, 167±8.63; n=1 $Robo1^{-/-}Robo2^{-/-}Robo3^{+/-}$, 270.6±7.79). A prominent 30% decrease in total cell number was similarly observed within caudal regions of the cortex in triple mutants relative to Robo3 heterozygote ($Robo1^{-/-}Robo2^{-/-}Robo3^{-/-}$, 184.5±9.88; $Robo1^{+/+}Robo2^{+/+}Robo3^{+/-}$, 260.2±33.1) and Robo compound littermates ($Robo1^{-/-}Robo2^{-/-}Robo3^{-/-}$, 184.5±9.88; $Robo1^{+/-}Robo2^{+/-}Robo3^{-/-}$, 261.2±14.74). Interestingly, this was less pronounced when triple Robo mutants were compared with single Robo3 knockouts ($Robo1^{-/-}Robo2^{-/-}Robo3^{-/-}$, 184.5±9.88; $Robo1^{+/+}Robo2^{+/+}Robo3^{-/-}$, 221.2±8.81) (Figure 5.5A) in caudal levels of the cortex. Analysis of the numbers of calbindin positive cells

within all cortical layers of Robo3 mutant animals, specifically within rostral-middle regions of the forebrain, showed a decrease in these cells throughout most layers; this was especially prominent within the germinal VZ/SVZ, the IZ and SP compared to Robo3 heterozygote littermates (Fig. 5.5B and Table 5.2). A comparable reduction in calbindin cells was also seen within the germinal VZ/SVZ and SP layers within the caudal cortex of Robo triple mutant animals compared to Robo3 heterozygote and compound littermates (Figure 5.5C and Table 5.2).

Table 5.2 Number of calbindin cells in the different cortical layers of Robo triple mutant at E18.5

Rostral-Middle	VZ/SVZ	IZ	SP	CP	MZ
$Robo1^{-/-}Robo2^{-/-}Robo3^{-/-}$	14.0±1.08	13.3±1.11	25.8±1.89	75.8±2.92	38.3±7.98
$Robo1^{+/-}Robo2^{+/-}Robo3^{-/-}$	38.29±3.58	27.3±1.73	47.3±5.68	97.6±4.32	60.1±3.97
$Robo1^{+/+}Robo2^{+/+}Robo3^{+/-}$	36.7±6.25	34.5±5.30	71.8±16.1	94±5.58	48.5±7.68
Caudal	VZ/SVZ	IZ	SP	CP	MZ
$Robo1^{-/-}Robo2^{-/-}Robo3^{-/-}$	9.5±0.85	13.4±1.24	35.3±4.89	82.0±4.16	44.4±3.33
$Robo1^{+/-}Robo2^{+/-}Robo3^{-/-}$	26.4±2.27	18.92.23	51.4±6.98	99.8±5.52	64.7±6.47
$Robo1^{+/+}Robo2^{+/+}Robo3^{-/-}$	24.4±1.74	13.8±1.71	33.2±1.46	93.5±5.98	56.2±3.21
$Robo1^{+/+}Robo2^{+/+}Robo3^{+/-}$	32.0±5.20	15.2±3.73	53.8±5.13	101.8±13.48	57.4±21.4

Thus, these preliminary data suggest that removal of all three Robo receptors resulted in a significant decrease in the total number of interneurons throughout all cortical layers along the rostral-caudal extent of the developing cortex.

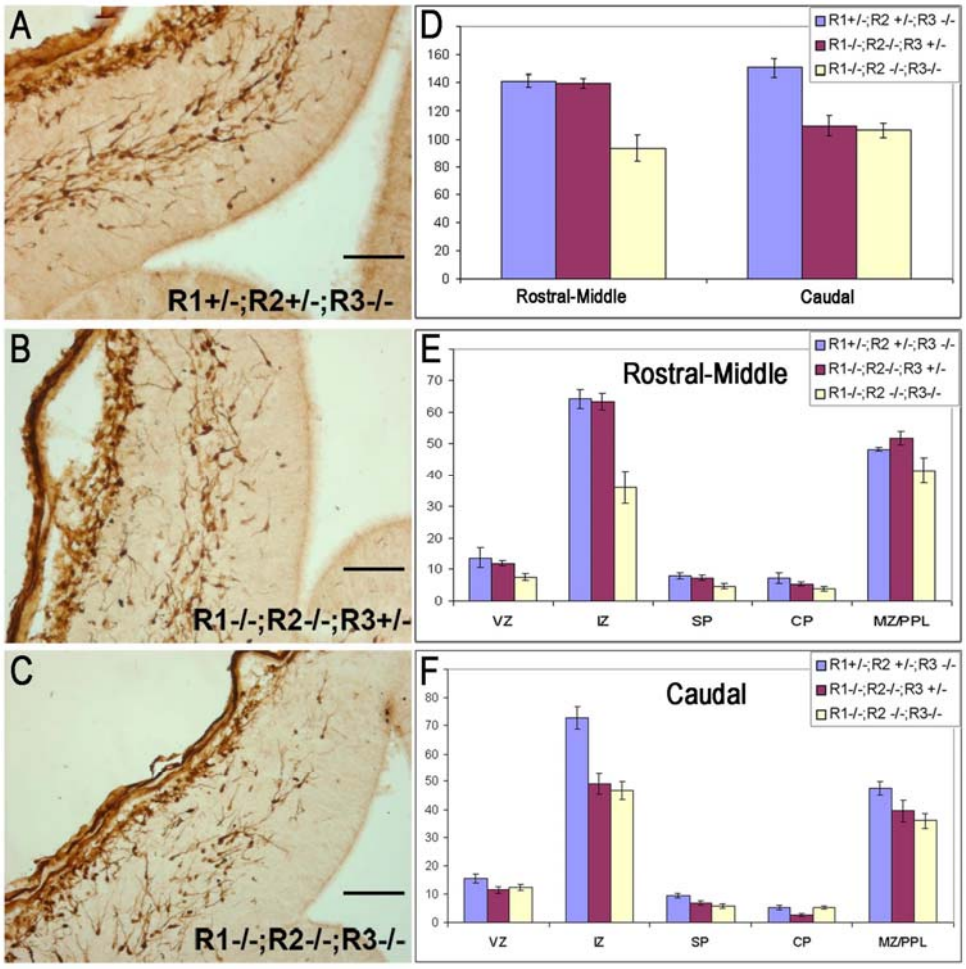

Fig. 5.4 Total numbers of the calbindin population of interneurons in the cortex of triple Robo mutant mice. Photomicrographs through the cortex of Robo triple mutant (n=2) (C), and Robo compound (A, Robo1$^{+/-}$Robo2$^{+/-}$Robo3$^{-/-}$ (n=1); B, Robo1$^{-/-}$Robo2$^{-/-}$Robo3$^{+/-}$(n=2)) mutant mice, immunohistochemically processed for calbindin proteins. Counts were made in all cortical layers within rostral-middle (E) and caudal (F) regions of the cortex. Graphical representation of the analysis of the total numbers (D) and distribution (E,F) of calbindin cells in the developing cortex of triple Robo (Robo1$^{-/-}$Robo2$^{-/-}$Robo3$^{-/-}$, yellow) and compound Robo (Robo1$^{-/-}$Robo2$^{-/-}$Robo3$^{+/-}$, purple),(Robo1$^{+/-}$Robo2$^{+/-}$Robo3$^{-/-}$, blue) mutant mice. Scale bar: 150 mm. (VZ, ventricular zone; IZ, intermediate zone; SP, subplate; CP, cortical plate; MZ/PPL, marginal zone/preplate).

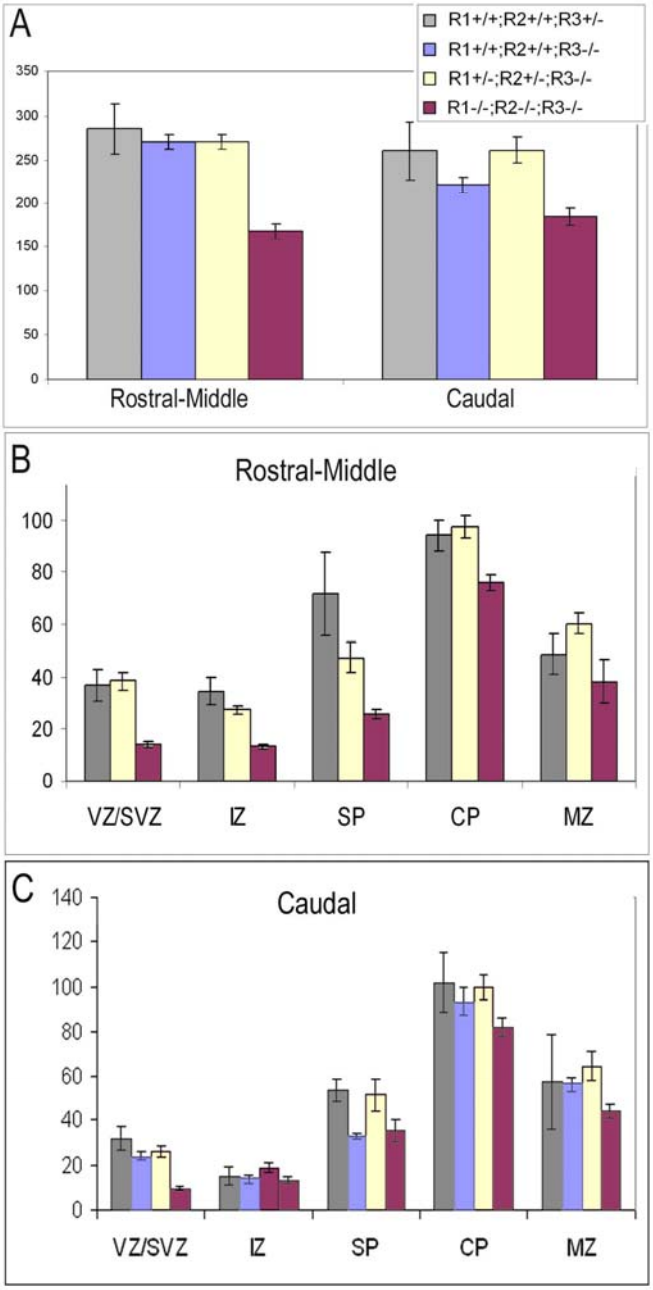

Fig.5.5 Analysis of the total numbers and distribution of calbindin immunoreactive interneurons in the cortex of triple Robo mutant mice at E18.5. Graphical representation of the total numbers of calbindin immunoreactive cells in triple Robo (n=1) (Robo1$^{-/-}$ Robo2$^{-/-}$Robo3$^{-/-}$, shown in purple) and compound Robo (n=1) (Robo$^{+/-}$Robo$^{+/-}$Robo$^{-/-}$, shown in yellow) mutant mice, relative to single Robo3$^{-/-}$ mutant (n=1) (shown in blue) and Robo3$^{+/-}$ heterozygote (n=1) littermates (shown in grey) at E18.5 (A). Counts were made in all cortical layers within rostral-middle (B) and caudal (C) regions of the cortex. (VZ/SVZ, ventricular zone/sub-ventricular zone; IZ, intermediate zone; SP, subplate; CP, cortical plate; MZ, marginal zone).

5.3.2 Morphology of interneurons in Robo triple mutant mice

Given that the morphology of migrating interneurons is altered in all three Robo mutants (Robo1$^{-/-}$, Robo2$^{-/-}$, Robo3$^{-/-}$) as well as in Slit1;Slit2 double mutant mice (data presented here and in Andrews et al., 2008), this raised the question of whether the morphology of migrating interneurons was affected in Robo triple mutant animals. (The morphological analysis was carried out by Dr William Andrews.)

Again, because of the absence of suitable control littermates, the morphometric data obtained from neurons taken from Robo triple animals was compared with data obtained from Robo3 heterozygote (n=3) and Robo3$^{-/-}$ single mutant (n=3) animals. This was investigated during early stages of interneuron migration (E13.5). A significant increase in total process length was observed in Robo triple mutants (n=2) compared to Robo3 heterozygotes (n=3) (Robo1$^{-/-}$Robo2$^{-/-}$Robo3$^{-/-}$ [161 neurons], 66.17±2.21; Robo1$^{+/+}$Robo2$^{+/+}$Robo3$^{+/-}$, 43.56±1.15 [298 neurons]), while no significant differences were observed between Robo triple and Robo3 mutants (n=3) (Robo1$^{-/-}$Robo2$^{-/-}$Robo3$^{-/-}$ [161 neurons], 66.17±2.21; Robo1$^{+/+}$Robo2$^{+/+}$Robo3$^{-/-}$, 60.4±1.36 [420 neurons]) (Figure 5.6D). No significant differences were observed in the number of neurite processes between Robo triple mutants and Robo3 heterozygotes (Robo1$^{-/-}$ Robo2$^{-/-}$Robo3$^{-/-}$ 1.65±0.06; Robo1$^{+/+}$Robo2$^{+/+}$Robo3$^{+/-}$, 1.60±0.04) (Fig. 5.6E). However, a significant increase in the number of neurite branch points was observed between Robo triple and Robo3 heterozygotes mutants (Robo1$^{-/-}$ Robo2$^{-/-}$Robo3$^{-/-}$ 0.45±0.06; Robo1$^{+/+}$Robo2$^{+/+}$Robo3$^{+/-}$, 0.29±0.03) (Fig. 5.6F).

Thus, while it appears that removal of all three Robo receptors appears to have an effect on interneuron morphology, we did not observe an additive effect to that seen in single mutants, suggesting that a complicated interplay exists between the different Robo receptors in controlling interneuron morphology.

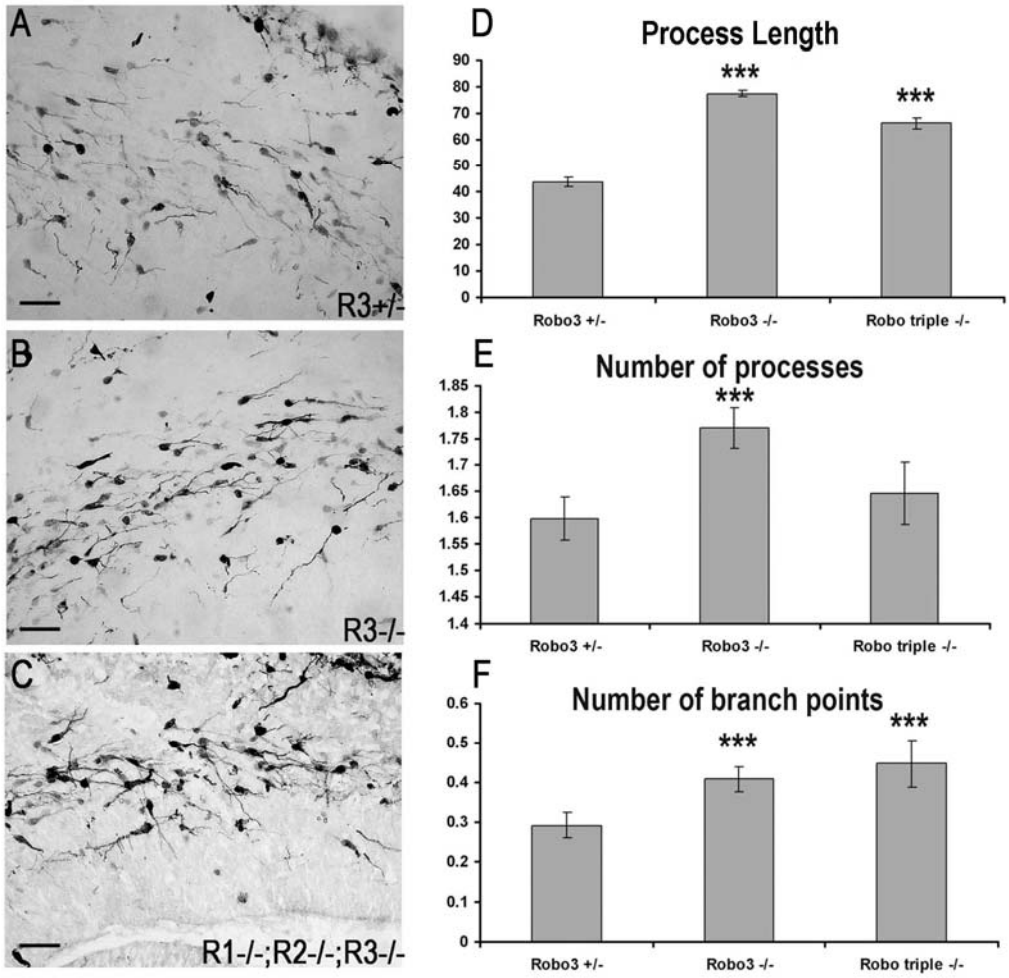

Fig.5.6 Morphological analysis of migrating interneurons within the cortex of Robo1,2,3 triple mutant animals. Coronal sections through the cortex of Robo3 heterozygote $^{+/-}$ (n=3) (A) , Robo3 mutant $^{-/-}$ (n=3) (B), and Robo1,2,3 triple mutant mice (n=2) (C) at E13.5, immunohistochemically processed for calbindin proteins. Graphical representation of the morphometric analysis of calbindin immunoreactive interneurons in the cortex of Robo3$^{+/-}$ heterozygote (n=3), Robo3$^{-/-}$ mutant (n=3) and Robo1$^{-/-}$;Robo2$^{-/-}$;Robo3$^{-/-}$ triple mutant animals (n=2). Parameters measured included total process length (D), number of processes (E) and number of branch points (F). Scale bar is 50 μm. (This morphometric analysis was carried out by Dr. W. Andrews).

5.4 DISCUSSION: ANALYSIS OF INTERNEURON DEVELOPMENT IN ROBO3$^{-/-}$ MUTANT MICE

5.4.1 Robo3 and cortical interneuron numbers

The expression studies carried out previously confirmed that early populations of interneurons express the Robo3 receptor *in vivo,* and thus prompted the investigation into the putative role of this receptor in interneuron development. Analysis of Robo3 mutant and Robo3 heterozygote animals showed comparable numbers of the calbindin-expressing population of interneurons during early (E13.5) stages of tangential migration, with a small, but significant (11%), decrease in interneurons observed specifically within the caudal cortex during late stages of interneuron migration (E18.5). Thus Robo3 does not appear to have a major role in regulating cortical interneuron numbers during early development.

However, removal of Robo3 did result in a significant decrease in the number of interneurons migrating in the superficial PPL/MZ layers of the cortex. This is interesting in view of the fact that Slit1- and Slit3 mRNA are strongly expressed within the MZ of the early cortex (Bagri et al., 2002; Marillat et al., 2002; Whitford et al., 2002), suggesting that removal of Robo3, but not the other two Robo receptors, alters the sensitivity of interneurons to chemorepulsion within this region. Such a role for Robo3 is plausible, as it has been shown to modulate the responsiveness of Robo1 to Slit chemorepulsion in vertebrate midline axon guidance systems (Jen et al., 2004; Sabatier et al., 2004). Thus, the analysis of interneuron number and distribution in Robo3

mutants indicates that unlike Robo1, but similar to Robo2, Robo3 does not have a role in regulating interneuron numbers within the developing cortex. However, Robo3 does appear to have a role in regulating the positioning of a population of interneurons that migrate through the early developing cortex. This did not persist at later stages, suggesting that Robo3 plays only a minor role in regulating cortical interneuron distribution during development.

5.4.2 Robo3 and interneuron morphology

Previous studies have shown that Robo1 (Andrews et al., 2008) and Robo2 (data presented here), have a role in regulating the morphology of migrating interneurons during development. Given that early cohorts of interneurons express the Robo3 receptor, the putative role of Robo3 in regulating the morphology of migrating interneurons was investigated. The morphological analysis of Robo3 mutants, carried out by Dr. Andrews, showed that Robo3 plays a prominent role in regulating the morphology of early born interneuron, with removal of this receptor resulting in significantly increased interneuron process length, process branching and number of processes. Similar to Robo1, Robo3 has a major role in regulating the morphologies of interneurons as these migrated tangentially within the cortex. This was not observed during later stages (E18.5) of development, consistent with the down-regulation of Robo3 within the neocortex at this time.

5.5 DISCUSSION: ANALYSIS OF INTERNEURON DEVELOPMENT IN TRIPLE ROBO1$^{-/-}$;ROBO2$^{-/-}$;ROBO3$^{-/-}$ MUTANT MICE

The finding that cortical interneurons express all three Robo receptors during development raises the possibility that these may express more than one Robo receptor and that these may compensate for their functions. In view of these findings, the effect of removing all three Robo receptors on interneuron development was investigated in triple Robo mutant mice. Interestingly, these studies showed a marked 30% decrease in the total number of (calbindin positive) interneurons within the cortices of triple mutants during early (E13.5) and late (E18.5) stages of interneuron migration, when compared with Robo compound mutants or single Robo3 heterozygote mice. This was observed throughout all layers of the developing cortex, suggesting that all three Robo receptors have a role in regulating cortical interneuron numbers during development. While Robo1 and Robo3 receptors alone have been shown to have a prominent effect on the morphology of migrating interneurons, we found that removal of all three Robo receptors had a more subtle effect on interneuron morphology, pointing to a complex interplay between these receptors. The isolation and identification of distinct Robo populations of interneurons will help distinguish the specific contribution of each receptor in regulating these processes.

5.6 Summary

The potential role of the Robo3 receptor was investigated using knock-in transgenic mice. Analysis showed that there was a small reduction in the total number of interneurons within the caudal cortex of Robo3 mutant animals, when compared with heterozygote littermates. A shift in the distribution of calbindin positive cells was observed throughout the rostral-caudal extent of Robo3 mutant cortex, suggesting that Robo3 may regulate the positioning of interneurons migrating within the superficial MZ layer during early stages of development (E13.5). A morphometric analysis of the calbindin population of interneurons showed that removal of the Robo3 receptor resulted in interneurons exhibiting significantly increased process length, branching and a greater number of processes, when analysed during early (E13.5) but not late (E18.5) stages of development. This suggests that Robo3 may regulate the positioning of and morphology of migrating interneurons during early stages of development. Given that all three Robos are expressed in overlapping patterns within the GE and cortex, it is possible that these may compensate for their respective functions. The effect of removing all three receptors was therefore investigated in Robo triple mutant mice. This showed a marked reduction in the total numbers of calbindin cells throughout the rostral-caudal extent of the cortices of triple mutant mice when compared with wild type littermates, suggesting that all three Robos may regulate cortical interneuron numbers during development.

CHAPTER 6: ROBO AND CAJAL-RETZIUS CELLS

6.1 INTRODUCTION

Cajal-Retzius (CR) cells are a morphologically conspicuous population of pioneering neurons, which are positioned in the upper MZ throughout embryonic development (Edmunds and Parnavelas, 1982; Frotscher, 1997; Marín-Padilla, 1998; Meyer et al., 1998). They were first identified by Retzius in the brains of human fetuses (6-8 months old) (1893, 1894), and characterised by their large cell soma, horizontal axon plexus and extensive radial processes which contact the pial membrane. Ramón y Cajal simultaneously confirmed the existence of analogous cells in the non-primate MZ (1890, 1891, 1929). While Cajal-Retzius cells comprise a highly heterogeneous population, the reelin-producing members make up a large portion of this group (Alcantara et al., 1998; Meyer et al., 1999).

Reelin is a large extra-cellular matrix protein that is thought to be essential for the establishment of normal lamination in the developing cortex (D'Arcangelo et al., 1995; Ogawa et al., 1995; Supèr et al., 2000). Analyses of the cortex of *reeler* mutant mice, which are deficient in this protein, show that the PPL fails to split with subsequently born CP neurons (layers II to VI) accumulating below the unsplit preplate, known as the 'superplate' (Caviness and Sidman 1973; D'Arcangelo et al., 1995; Ogawa et al., 1995; Supèr et al., 2000). Furthermore, the laminar positioning of neurons is largely inverted within the superplate.

Mice that lack the reelin receptors (VLDR, ApoE) or intracellular components of the reelin-pathway (Dab-1) show similar defects in the laminar organisation of the CP, suggesting that reelin regulates the radial migration of projection neurons to the developing CP.

Given that Cajal-Retzius cells comprise diverse and changing populations of cells (Parnavelas and Edmunds, 1983; Derer and Derer, 1990; Meyer et al., 1998, 1999), it is perhaps unsurprising that these cells are derived from multiple sources. The vast majority invade the MZ by tangential migration from both cortical (Meyer et al., 1998; Hevner et al., 2003a; Takiguchi-Hayashi et al., 2004; Siegenthaler and Miller, 2008) and extracortical sources (Lavdas et al., 1999; Shinozaki et al., 2002; Takiguchi-Hayashi et al., 2004; Bielle et al., 2005). Recent evidence suggests that the cortical hem is the main source of those of cortical origin (Takiguchi-Hayashi et al., 2004; Yoshida et al., 2006; García-Moreno et al., 2007; Siegenthaler and Miller, 2008).

6.2 RESULTS: DOES ROBO CO-LOCALISE WITH CAJAL-RETZIUS CELL MARKERS?

The robust and transient expression of all three Robo receptors throughout the PPL and MZ during early corticogenesis was of interest, as this corresponded to a time when Cajal-Retzius cells are generated (E10.5-E12.5 in the mouse) (Meyer at al., 1998; García-Moreno et al., 2007) and migrate tangentially to populate these zones. In particular, Robo1 and Robo3 proteins were strongly expressed within the cortical hem (Fig. 3.6D,G,F,I), a major

source of these neurons (Takiguchi-Hayashi et al., 2004; Yoshida et al., 2006; García-Moreno et al., 2007; Siegenthaler and Miller, 2008). The expression patterns of Robo during these early stages suggested that Cajal-Retzius cells may express these receptors. Furthermore, previous studies have localised Slit2 within the cortical hem (Nguyen Ba-Charvet et al., 1999) at a time when these neurons are generated (E10.5), and Slit3 expression within the superficial MZ (Whitford et al., 2002; Bagri et al., 2002; Marillat et al., 2002), which is consistent with Slit-Robo signalling playing a role in regulating their early development.

Double labelling experiments for Robo and reelin, a marker of Cajal-Retzius cells (Ogawa et al., 1995; Frotscher, 1997; Tissir and Goffinet, 2003), were therefore carried out to establish whether these cells express Robo receptors. These studies showed that most Robo-positive cells were located within the lower half of the PPL/MZ and below a single layer of strongly labeled reelin immunopositive cells (Figs. 6.1 & 6.2). A number of cells located in the most superficial aspect of the PPL/MZ contained both proteins, as exampled by Robo3 (Fig. 6.2), but co-localisation with reelin was observed more frequently within the deeper layers of the cortical hem (Fig. 6.1A'-C'). The receptors were also noted in subpallial regions that have been reported to give rise to a number of these distinctive cells: the MGE (Lavdas et al., 1999), the pallial-subpallial boundary, the preoptic area and medial septum (Bielle et al., 2005) (see Figs. 3.3, 3.6). The distinct expression of Robos within the MZ and in the germinal regions of Cajal-Retzius cells suggests that these receptor proteins play a role in their development and migration.

6.3 CAJAL-RETZIUS CELLS AND ROBO MUTANTS

The putative role of Robo receptors in the development of Cajal-Retzius cells was investigated using transgenic mice that lacked functional Robo1 ($Robo1^{-/-}$), Robo2 ($Robo2^{-/-}$) or Robo3 ($Robo3^{-/-}$) receptors. Analysis was carried out using reelin as a marker of Cajal-Retzius cells (Alcantara et al., 1998; Meyer et al., 1999), and by assessing the total numbers of reelin cells within the developing cortex of single mutant animals during early (PPL; E12.5, E13.5) and later stages of development (E17.5, E18.5). The number of reelin immunopositive cells, specifically within the hippocampal cortex and neocortex, was further analysed as this may reflect putative changes in the medio-lateral distribution of CR cells, which in turn, might indicate changes in the tangential migration of these neurons from the cortical hem. No significant differences were observed in the total number of reelin immunopositive cells in Robo1 mutant mice compared to wild type littermates ($Robo1^{+/+}$ n=3; $Robo1^{-/-}$ n=3) within the neocortex ($Robo1^{-/-}$ 61.26±2.34; $Robo1^{+/+}$ 59.5±1.90) or within the hippocampus ($Robo1^{-/-}$ 43.32 ±3.90; $Robo1^{+/+}$ 36.85±3.11) at E12.5 (Fig. 6.3A). Cell counts in Robo2 deficient mice ($Robo2^{+/+}$ n=3; $Robo2^{-/-}$ n=3) at the same stage of development (E12.5) showed no significant changes in the number of reelin immunopositive cells within the neocortex compared to wild type littermates ($Robo2^{-/-}$ 62.7±4.33; $Robo2^{+/+}$ 71.5±5.84) (Fig. 6.3B). However, a significant increase (38%) in reelin- containing cells was observed within the hippocampal cortex of Robo2 mutant animals compared to wild type littermates ($Robo2^{-/-}$ 47.2±3.2; $Robo2^{+/+}$ 34.0±1.97; $p<0.05$) (Fig. 6.3B).

Similar examination of Robo3 deficient cortices (n=3, $Robo3^{-/-}$) revealed no significant changes in the total number of reelin positive cells within the PPL of the developing neocortex ($Robo3^{+/-}$ 59.9±3.2; $Robo3^{-/-}$ 63±3.2) or in the hippocampus ($Robo3^{+/-}$ 41.1±2.07; $Robo3^{-/-}$ 46.5±2.8) compared with heterozygote littermates (n=3, $Robo3^{+/+}$) at E13.5 (Fig. 6.3C). Similar analysis at later stages of corticogenesis were consistent with this (E18.5; n= 3 $Robo3^{+/-}$; n= 3 $Robo3^{-/-}$), with comparable numbers of reelin cells within the neocortex ($Robo3^{+/-}$ 62.1±3.5; $Robo3^{-/-}$ 62.7±2.2), and hippocampus ($Robo3^{+/+}$ 51.3±3.8; $Robo3^{-/-}$ 53.7±2.7) of Robo3 mutant and Robo3 heterozygote animals. While removal of Robo receptors appeared to have no significant effect on the overall number of Cajal-Retzius cells within the developing cortex, a small increase in reelin cells was observed within the hippocampal cortex in all Robo single mutant mice. However, this was only statistically significant in the Robo2 deficient cortex. It would, therefore, appear that the Robo2 receptor may regulate the numbers of reelin cells and/or their distribution, specifically within the hippocampal cortex.

As discussed previously for interneurons, the overlapping patterns of Robo expression within the cortical hem and PPL raises the possibility that CR cells may express more than one Robo receptor during development, suggesting that removal of a single receptor may be compensated by the others. In order to circumvent possibilities of functional redundancy between Robo receptors, a similar investigation was carried out using Robo triple mutant animals that lack all three receptors at E13.5. A preliminary analysis showed that the total numbers of reelin cells were similar between Robo triple mutants and compound

Robo heterozygote or compound Robo double mutant littermates (n=2, $Robo1^{-/-}$ $Robo2^{-/-}Robo3^{-/-}$, 159.6±10.59; n=1, $Robo1^{-/-}Robo2^{-/-}Robo3^{+/-}$, 150.1±4.15; n=1, $Robo1^{+/-}Robo2^{+/-}Robo3^{-/-}$, 154.9±5.83). Analysis specifically within the hippocampal cortex however, showed that there was a 17% increase in reelin immunopositive cells in Robo triple mutant mice compared with compound Robo heterozygotes in this region ($Robo1^{-/-}Robo2^{-/-}Robo3^{-/-}$, 80.8±5.28; $Robo1^{+/-}Robo2^{+/-}Robo3^{-/-}$, 68.6±4.06). A similar 21% increase in reelin cells was observed when both Robo1 and Robo2 receptors were removed in compound double Robo mutant mice compared with compound Robo heterozygotes ($Robo1^{-/-}Robo2^{-/-}Robo3^{+/-}$, 83.0±4.55; $Robo1^{+/-}Robo2^{+/-}Robo3^{-/-}$, 68.6±4.06). Interestingly, a comparable 20% decrease in reelin cells was observed within the neocortex in compound Robo double mutants ($Robo1^{-/-}Robo2^{-/-}Robo3^{+/-}$, 67.1±2.60; $Robo1^{+/-}Robo2^{+/-}Robo3^{-/-}$, 82.3±6.52) when compared with Robo heterozygotes. However there were no changes in the number of reelin cells within the neocortex of triple mutant animals relative to heterozygote littermates at this time ($Robo1^{-/-}Robo2^{-/-}Robo3^{-/-}$, 78.8±6.75; $Robo1^{+/-}Robo2^{+/-}Robo3^{-/-}$, 86.3±6.51) (Fig. 6.4, Table 6.1).

While some differences in the number of reelin cells were observed between Robo triple mutant and Robo compound mutant littermates, I wanted to compare these observations with animals that more closely reflected the wild type condition. A comparative analysis was, therefore, made with single Robo3 mutants (n=3) and Robo3 heterozygote animals (n=3) at E13.5, as these were not only generated in the same genetic background as the triple mutants, but also came from the same source. While these experiments were inconclusive due to

the low number of animals available, the preliminary analysis suggested that compound and triple Robo mutant animals showed a marked 50% increase in the total number of reelin cells within the cortex relative to single Robo3 mutants (Fig. 6.4, Table 6.2).

Table 6.1 Comparative analysis of CR number in the cortex of Robo3$^{-/-}$ single and Robo triple mutant mice at E13.5

E13.5 Cortex	Neocortex	Hippocampus	Whole Cortex
(Robo3$^{+/-}$)	61.4±3.42	37.5±3.52	99.1±4.75
(Robo3$^{-/-}$)	64.1±2.83	37.8±3.55	101.6±5.56
(Robo1$^{+/-}$Robo2$^{+/-}$Robo3$^{-/-}$)	82.3±6.52	68.6±4.06	154.9±5.83
(Robo1$^{-/-}$Robo2$^{-/-}$Robo3$^{+/-}$)	67.1±2.60	83.0±4.55	150.2±4.15
(Robo1$^{-/-}$Robo2$^{-/-}$Robo3$^{-/-}$)	78.8±6.75	80.8±5.28	159.6±10.59

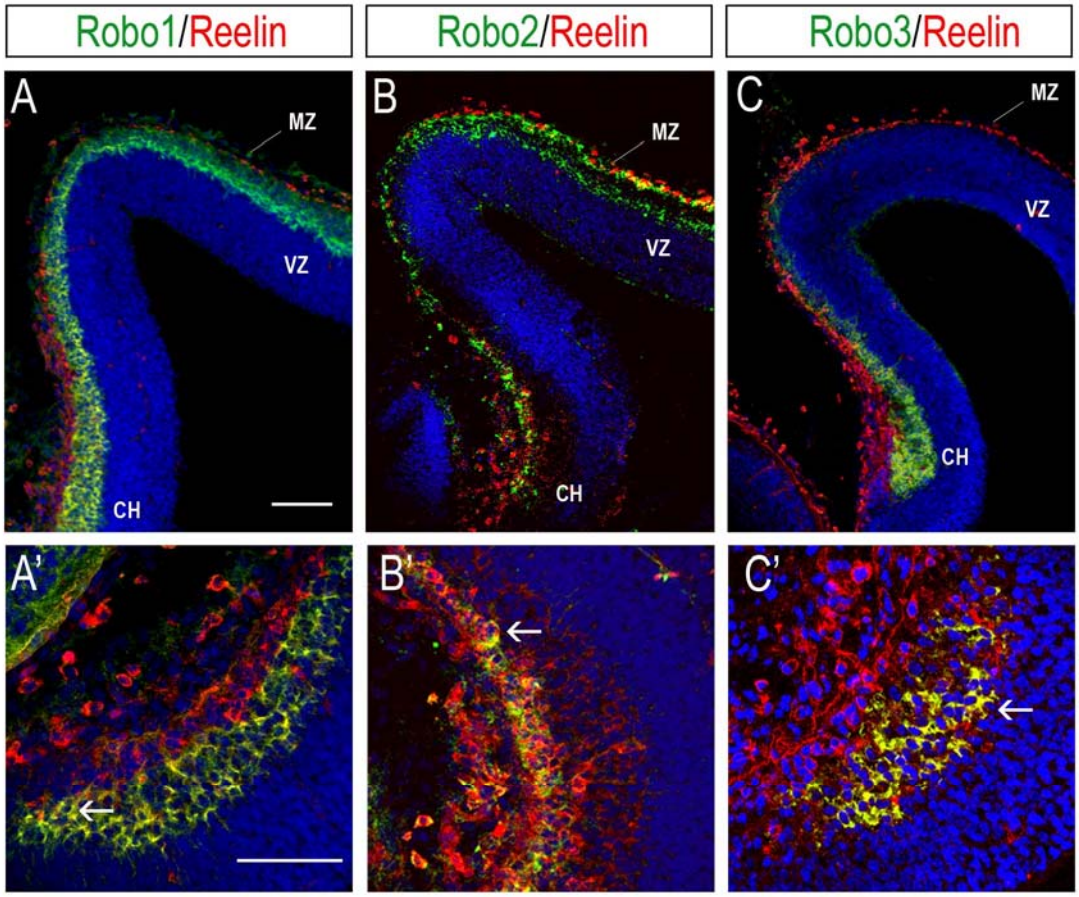

Fig. 6.1 Populations of (reelin immunoreactive) Cajal Retzius cells express Robo receptors during preplate stages of development. Colocalisation of Robo1 (A,A') Robo2 (B,B') and Robo3 (C,C') proteins (green) with a popluation of reelin immunoreactive cells (red) within the developing cortical hem (CH) at E12.5. A number of double labelled Robo1/reelin (A'), Robo2/reelin (B') and Robo3/reelin (C') cells (yellow) are indicated by arrows. Scale bar in A is 100 μm and corresponds to A-C; in A' is 150μm and corresponds to A'-C'. (CH, cortical hem; VZ, ventricular zone; MZ, marginal zone).

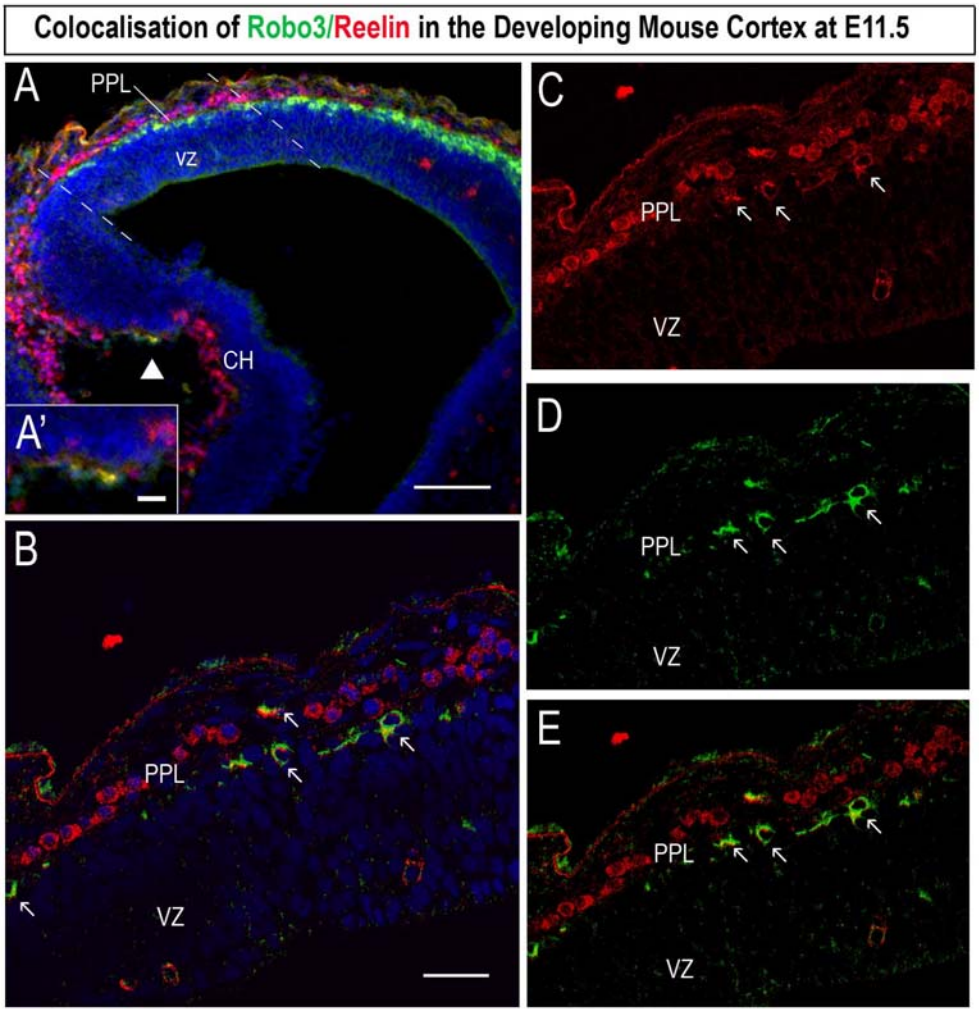

Fig. 6.2 Populations of Cajal Retzius cells express the Robo3 receptor during preplate stages of development. Colocalisation of Robo3 (green) and reelin (red) proteins in a population of Cajal-Retzius cells within the preplate of the E11.5 mouse cortex. Most double labelled Robo3/reelin cells (see arrows in B,E; yellow) are located below the layer of strongly immunoreactive reelin cells (A,C,E, red) within the lower half of the preplate (PPL). Robo3/reelin co-localise in some cells which appear to migrate away from the cortical hem (arrowhead in A, and at higher magnification in A'). Scale bar in A is 100 μm, in A' is 20 μm; and in B is 35 μm and corresponds to B-E. (CH, cortical hem; VZ, ventricular zone; PPL, preplate).

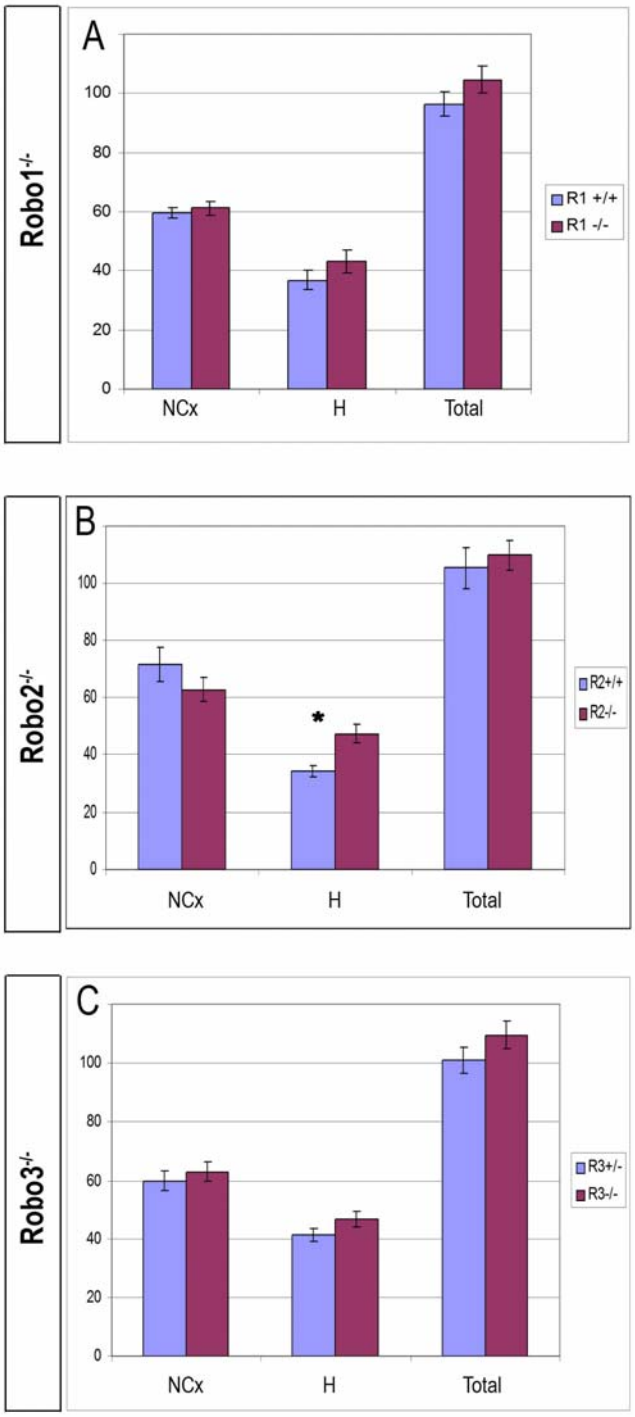

Fig. 6.3 Total numbers of (reelin immunoreactive) Cajal Retzius cells in the developing Robo deficient cortex. Analysis of the total numbers of reelin immunoreactive cells in the developing neocortex (NCx) and hippocampaus (H) of single Robo1$^{-/-}$ (A), Robo2$^{-/-}$ (B) and Robo3$^{-/-}$ (C) mutant animals relative to wild type and heterozygote mice during preplate stages of development (E12.5-E13.5). A significant (38%) increase in reelin immunopositive cells was observed in the hippocampal cortex of Robo2 mutants (n=3), relative to wild type littermates (n=3) (R2$^{-/-}$ 47.2±3.2; R2$^{+/+}$ 34.0±1.97; * $p<0.05$).

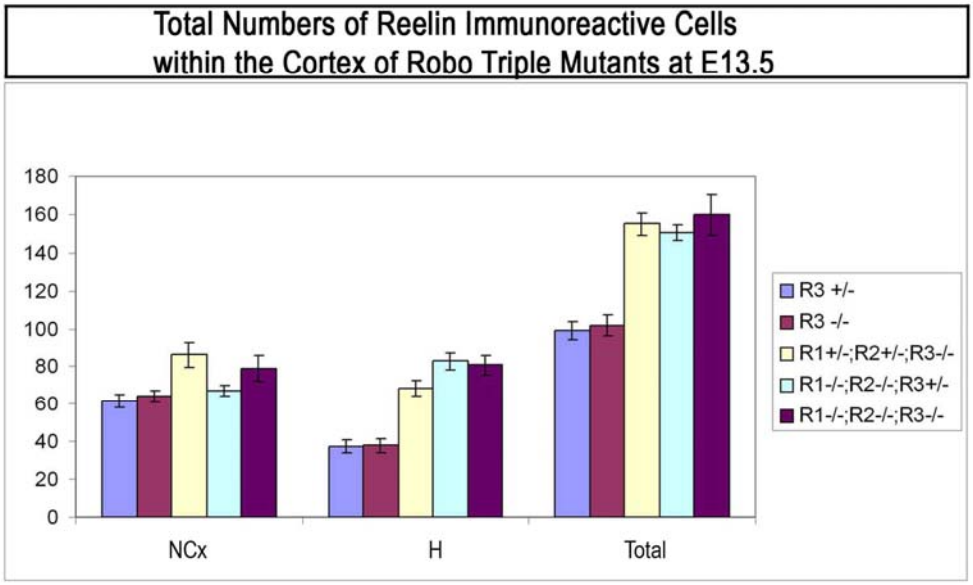

Fig. 6.4 Total numbers of reelin immunoreactive Cajal Retzius cells in the developing neocortex of Robo1,2,3 triple mutant animals. Graphical representation of the quantitative analysis of total reelin immunopositive cell counts within the neocortex (NCx) and hippocampus (H) of Robo triple mutant ($Robo1^{-/-}Robo2^{-/-}Robo3^{-/-}$) and Robo compound mutant ($Robo1^{+/-}Robo2^{+/-}Robo3^{-/-}$) ; ($Robo1^{-/-}Robo2^{-/-}Robo3^{+/-}$) animals, relative to $Robo3^{+/-}$ heterozygote (n=3) and $Robo3^{-/-}$ single mutant (n=3) animals at E13.5. Preliminary analysis shows a marked ≥ 50% increase in the total number of reelin immunoreactive cells within the cortex of Robo triple mutant (159.6±10.59, n=1) and Robo compound mutant ($Robo1^{-/-}Robo2^{-/-}Robo3^{+/-}$, 150.2±4.15, n=1), ($Robo1^{+/-}Robo2^{+/-}Robo3^{-/-}$, 154.9±5.83, n=1) animals, relative to single Robo3 mutant (101.6±5.56, n=3) or Robo3 heterozygote (99.1±4.75, n=3) mice.

6.4 DISCUSSION: ROBO AND CAJAL RETZIUS CELLS

Cajal-Retzius cells comprise a highly diverse and dynamic population of neurons in the MZ of the early developing cortex, with new neurons continuously added to the MZ while others apoptose having fulfilled their developmental role (Edmunds and Parnavelas, 1982; Frotscher, 1997; Marín-Padilla, 1998). The Reelin-producing members of the Cajal-Retzius family make up a large portion of this group (Alcantara et al., 1998; Meyer et al., 1999) and, given that the secreted protein is thought to be crucial for the establishment of normal lamination in the CP (D'Arcangelo et al., 1995; Ogawa et al., 1995; Supèr et al., 2000), there has been much interest in their origins and development.

In addition to regulating the migration of projection neurons during development, some studies have suggested that CR cells regulate the laminar positioning of cortical interneurons through the secretion of reelin (Hammond et al., 2006; Yabut et al., 2007). While this remains controversial (Hevner et al., 2004; Pla et al., 2006), studies have suggested that reelin regulates the final laminar positioning of populations of cortical interneurons (Hammond et al., 2006). A more recent study, carried out in *reeler* mutant mice, reported that in addition to interneurons failing to acquire their appropriate laminar positions within the cortex, they exhibited aberrant processes, suggesting that reelin may also have a role in regulating their morphological differentiation (Yabut et al., 2007). We, therefore, wished to investigate the development of CR cells as these

may have important implications in the laminar fate and morphological differentiation of cortical interneurons.

Recent work has shown that the vast majority of Cajal-Retzius cells invade the preplate by their tangential migration from cortical (Meyer et al., 1998; Takiguchi-Hayashi et al., 2004; Siegenthaler and Miller, 2008) and extracortical sources (Lavdas et al., 1999; Shinozaki et al., 2002; Takiguchi-Hayashi et al., 2004; Bielle et al., 2005). The cortical hem has been shown to be the main cortical source of these cells (Takiguchi-Hayashi et al., 2004; Yoshida et al., 2006; García-Moreno et al., 2007; Siegenthaler and Miller, 2008), with Cajal-Retzius cells migrating along highly directed caudal to rostral routes to populate the PPL. Furthermore, a strict medio-lateral positioning of these migratory tangential streams is strictly maintained.

The observation that Slit is expressed within the cortical hem and superficial MZ during early development (Whitford et al., 2002; Bagri et al., 2002; Marillat et al., 2002), together with our finding that groups of Cajal-Retzius cells express all three Robo receptors would suggest that Slit-Robo signalling plays a role in the development of this precocious neuronal population. This was particularly interesting as, to date, few directional guidance cues have been identified which regulate the tangential migration of CR cells during development. While the chemokine SDF-1 and its cognate cytokine CXCR4 receptor have been shown to regulate the tangential dispersion and positioning of (CXCR4+) Cajal-Retzius cells below the (SDF-1 secreting) pial membrane, SDF1 is expressed homogenously throughout these regions (Borrell & Marín, 2006). The molecules

and mechanisms which impart directionality to Cajal-Retzius cell migration are, therefore, still unknown. Interestingly, SDF1/CXCR4 has been shown to interact with Slit/Robo in developing axon-guidance systems in zebra-fish (Chalasani et al., 2007), raising the possibility that these two systems may be implicated in the migration of these cells.

While we found that a population of Cajal-Retzius cells express all three Robo receptors, silencing of a single Robo receptor had no effect on the number of reelin-positive cells within the developing cortex. Closer analysis however showed a small increase in reelin cells within the hippocampal cortex of single Robo mutants which was only significant in Robo2 mutant mice. Given that a population of Cajal-Retzius cells express all three Robo receptors, it is possible these may have compensated for the removal of a single receptor. Our preliminary analysis in Robo triple mutants tentatively suggests that removal of all three Robo receptors results in a marked increase in Cajal-Retzius cells within the cortex, and this is especially prominent within the hippocampal cortex. A more detailed analysis is required which specifically focuses on the Robo-expressing population of Cajal-Retzius cells. Proliferation studies within the cortical hem would help determine whether the observed increase in reelin cells within the hippocampal cortex is a result of increased proliferation within this region, or due to defects in the migration of these neurons from the early cortical hem which may result in the accumulation of these cells within the hippocampal cortex. Such a marked increase in reelin+ cells in the triple Robo mutants was surprising given that only a small population of reelin+ cells express Robo receptors. It should be mentioned that the exact origins of the

reelin cells counted here were not known, and thus could only be ascertained if combined with tracing studies carried out within the cortical hem. Thus one can not exclude the possibility that other extra-cortical sources may contribute to the observed increase in reelin+ cells within the PPL. Indeed, Robo3 in particular was robustly expressed within the medial septum, preoptic area and at the pallial/subpallial boundary which are known subpallial sources of the Dbx (developing brain, homeobox gene) expressing population of Cajal-Retzius cells (Bielle et al., 2005). A distinctive stream of neuronal-like cells was observed to migrate from the medial septum through the basomedial wall of the forebrain to the PPL, reminiscent of the migratory routes of Dbx positive CR cells (Fig. 6.5). It is, therefore, possible that Robo-expressing CR cells may comprise a heterogeneous population of pioneering neurons.

While a population of CR cells was identified which expressed the Robo3 receptor, most Robo3-positive cells were positioned below the reelin+ cells, within the lower regions of the PPL/MZ. This was interesting as the human MZ has been shown to be stratified into a superficial reelin containing layer and an underlying calretinin positive layer, corresponding to other pioneering neurons which are generated during early development (Meyer et al 1998, 2007). An analogous population of neurons has been identified in the rodent cortex (Meyer et al., 1998; Morante-Oria et al., 2003), some of which have been shown to derive from the LGE (Morante-Oria et al., 2003). This appears to be consistent with Robo3 expression within these regions. While the roles of these pioneering neurons remain to be identified, it has been shown that once they arrive within the PPL, they send early projections back to the striatum. These early projections

were associated with neuronal like cells in the ventral forebrain and it has been suggested that interneurons may use these projections to migrate to the cortex (Morante-Oria et al., 2003; Métin and Godement, 1996). The transient expression of Robo in these early populations of neurons suggests that Robo has an important role in their development. However, this remains to be elucidated.

6.5 SUMMARY

Robo1 and Robo3 are strongly expressed within the cortical hem, a major source of CR cells, and all three Robo receptors are localised within the PPL, a region through which these cells migrate during early stages of corticogenesis (E11.5-E12.5). We show that a population of Cajal-Retzius cells, which appear to be derived from the cortical hem, express all three Robo receptors during early PPL stages of development. This is complementary to Slit expression in this layer, suggesting Robo-Slit signalling may regulate their development. However, analysis of the number of reelin+ cells was unchanged in the neocortex of single Robo1, Robo2 and Robo3 mutants, with a small increase of reelin+ cells restricted to the hippocampal cortex of Robo2 mutants. Our preliminary analysis in triple Robo mutants showed these mutants have a marked increase in reelin+ cells within the cortex, suggesting Robo may regulate the development of these cells.

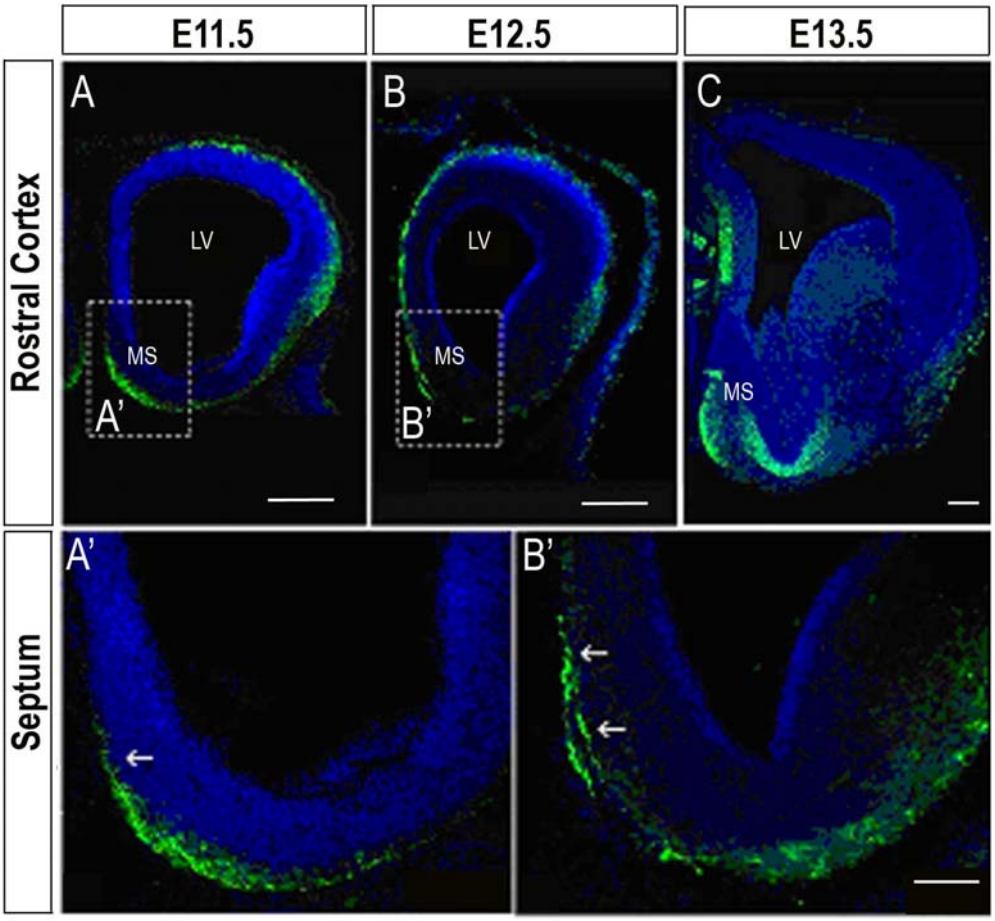

Fig. 6.5 Expression of Robo3 in subpallial sources of Cajal Retzius cells. Immunohistochemical localisation of the Robo3 receptor within the medial septum (MS) of the embryonic mouse forebrain during preplate stages of development (E11.5-E13.5) (A-C). Robo3 is strongly expressed within the medial septum (MS). Boxed areas in A, B are shown at a higher magnification (A',B'), elucidating the stream of Robo3 immunopositive cells which appear to migrate dorsally through the medial wall of the forebrain between E11.5 and E12.5 (arrows in A'- B', respectively). Scale bar in A-C is 200 μm; and in B' is 100 μm and applies to A',B'. (LV, lateral ventricle; MS, medial septum).

CHAPTER 7: GENERAL DISCUSSION AND FUTURE WORK

Cortical interneurons follow distinct and developmentally regulated migratory routes from their origins within the subpallial GEs to reach the developing cortex (Tamamaki et al., 1997; Anderson et al., 1997a, 2001; Lavdas et al., 1999; Wichterle et al, 2001). These cells are guided by intrinsic and extrinsic cues along their tortuous journey to the cortex, where they disperse in all layers and form functional circuits with their pyramidal counterparts. Much effort has recently been devoted to understanding the molecular mechanisms that regulate interneuron migration, as a deficiency of these cells in the cortex results in an imbalance of excitation and inhibition that underlies a number of neurological disorders (Powell et al., 2003; Cobos et al., 2005; Mallet et al., 2006; Di Cristo, 2007). These efforts have identified a number of molecules that regulate the tangential migration of these cells from the subpallium to the cortex, such as the semaphorins-neuropilins (Marín et al., 2001a), neuregulins-erbB receptors (Flames et al., 2004), ephrin-ephrin receptors (Zimmer et al., 2008) and slit-robo (Andrews et al., 2006, 2008), as well as molecules that direct interneurons to their appropriate laminar and areal positions within the cortex (Li et al., 2008; López-Bendito et al., 2008).

7.1 SLIT- ROBO EXPRESSION AND INTERNEURONS

Consistent with Robo/Slit regulating interneuron migration from the subpallium to the cortex, Slit (*Slit1, Slit2, Slit3*) and Robo (*Robo1, Robo2*) are expressed within the GEs and cortex throughout the period of generation and

tangential migration of interneurons in mostly complementary patterns (shown here in Chapter III, Marillat et al., 2002). The expression pattern of the more distantly related Robo3/Rig receptor had not been previously investigated in detail within the developing forebrain (Yuan et al., 1999b; Camurri et al., 2004), and so a detailed immunohistochemical analysis of all three Robo receptors was carried out in the developing forebrain. These studies showed that all three Robo receptors are expressed within the major sources of cortical interneurons and in regions through which these cells migrate. Furthermore, all three Robos colocalise with interneuron markers, confirming that populations of interneurons express these receptors during development.

Both Robo1 and Robo3 proteins were distinctly localised within the MGE (E11.5-E12.5) at a time when the first wave of interneurons are generated, and in the PPL/MZ (E11.5-E13.5) through which early interneurons migrate. Their expression was mostly complementary to Robo2 protein within the LGE, but Robo2 was also weakly expressed within the early PPL/MZ. While interneurons have previously been shown to express the Robo1 receptor (Andrews et al., 2006), an early population of these cells was also shown to express Robo3 by showing the presence of the receptor in GAD67-GFP positive cells both *in vivo* and *in vitro*.

During later phases of migration (E13.5-E15.5), interneurons follow a deep route to the non-permissive striatum, and primarily migrate at the level of the IZ/SVZ as well as within the MZ and SP layers (after the split of the PPL) (Anderson et al., 1997a, 2001; Tamamaki et al., 1997; Lavdas et al., 1999;

Wichterle et al., 2001). While Robo3 is down regulated, both Robo1 and Robo2 are expressed more broadly within the GEs where they overlap to a greater degree, and are also expressed in regions corresponding to the three tangential interneuron migratory streams within the cortex at this time. Consistent with this, double-labelling experiments confirmed that a major proportion (~90%) of the calbindin population of interneurons express either Robo1 or Robo2 receptors during mid phases of interneuron migration (E15.5) (see Fig. 3.16). The co-localisation of Robo1/calbindin and Robo2/calbindin was observed within cells in all cortical layers suggesting that, in addition to Robo/Slit playing a role in the ventral-dorsal migration of interneurons from the GEs, they may also regulate their intracortical migration and final positioning within the developing CP.

These expression studies also showed that early cohorts of interneurons primarily express the Robo1 and Robo3 receptors as they leave the MGE and that this is complementary to Slit expression within the germinal epithelium of the GEs (Slit1) as well as at the ventral midline (Slit1, Slit2) and preoptic area (Slit1, Slit2). Slit proteins are robustly expressed within these regions throughout interneuron migration and have been shown to directly repel GABAergic interneurons from GE explants *in vitro* (Zhu et al., 1999; Sang et al., 2002), consistent with a role of Slit repelling Robo-expressing cohorts of interneurons away from the ventral forebrain and towards the cortex.

A gradient of Slit proteins is also expressed along the migratory routes of interneurons within the cortex. Slit is transiently localised within the MZ (Slit3)

layer at a time when early cohorts of Robo1 and Robo3 expressing interneurons migrate through this region (Bagri et al., 2002; Marillat et al., 2002). Slit expression is subsequently maintained within the CP (Slit1) and VZ (Slit1) at later stages (Bagri et al., 2002; Marillat et al., 2002; Yuan et al., 1999b) and is complementary to subsequent cohorts of Robo1 and Robo2 expressing interneurons that migrate along their tangential routes within the IZ/SVZ, MZ and SP layers.

It has been suggested that Slit proteins in the cortex may prevent the premature entry of interneurons into the cortex (Andrews et al., 2006). This is consistent with slice culture experiments that show ectopic application of Slit at the cortico-striatal boundary inhibits interneuron migration into the cortex (Zhu et al., 1999). Slit proteins may also have a role in maintaining the positions of interneuron migratory streams by creating exclusion zones within the cortex and preventing migrating interneurons from entering the cortical plate or VZ. A study in which an *in utero* injection of Slit was made into the lateral ventricles of the forebrain reported that, while projection neurons were unaffected, interneurons were repelled from the ectopic Slit source when these were analysed during postnatal stages. This suggested that Slit may differentially affect GABAergic interneurons and cortical pyramidal neurons *in vivo* (Sang et al., 2002). While substantial *in vitro* evidence has suggested that Slit regulates the ventral to dorsal migration of GABAergic interneurons (Zhu et al., 1999; Wu et al., 1999; Sang et al., 2002), analysis of Slit1;Slit2 double mutant mice *in vivo* has conversely shown that the tangential migration of interneurons is unaltered in these animals (Marín et al., 2003a). Furthermore, the total number and

distribution of cortical interneurons in Slit mutants is comparable to wild type animals suggesting that Slit does not have a major role in regulating the migration, total numbers or final positioning of these cells in the developing cortex.

7.2 ROBO1 AND INTERNEURONS

Evidence from our own laboratory has shown that Robo1 has a major role in regulating the total numbers of interneurons that enter the cortex (Andrews et al., 2006, 2008). This receptor also plays a role in steering migrating cells around the striatum, and it has been suggested that the increase in interneurons may be a result of these cells taking a 'short-cut' through the striatum to reach the cortex. It is poignant to note that during early phases of interneuron migration, Robo2 expression is restricted to the differentiating LGE, while Robo1 and Robo3 are complementary to this and are expressed by migrating interneurons. Given that Robo receptors have been shown to bind homophilically and heterophilically through their extracellular Ig domains (Liu et al., 2004; Camurri et al., 2005), it is tempting to speculate that Robo2 may have a similar role to the semaphorin-producing striatal neurons. Specifically, Robo2 heterophilic signalling may lead to the repulsion and exclusion of early Robo1 or Robo3 expressing interneurons from the striatum, thereby preventing these cells from entering this region as they migrate towards the cortex. It would be interesting to investigate these possible interactions using in-vitro stripe assays

More recently, work in our laboratory by Dr. William Andrews has shown that Robo1 regulates interneuron proliferation, with removal of this receptor resulting in a significant ~30% increase in proliferation within the GEs (Andrews et al., 2008). Interestingly, a comparable increase was observed in Slit1;Slit2 double mutant mice in this study, consistent with Robo1-Slit1;Slit2 protein interactions regulating interneuron proliferation during development. Thus, Robo1-Slit signalling appears to regulate the generation of interneurons, with Robo1 regulating the migration of interneurons around the striatum as well as the total numbers of interneurons that enter the cortex during development.

7.3 ROBO2 AND ROBO3 AND CORTICAL INTERNEURON NUMBERS

Given that populations of interneurons express both Robo2 and Robo3 receptors during development, their putative roles in interneuron development was investigated to determine if these may have similar roles to Robo1 during development. This was investigated *in vivo*, in transgenic mice that lacked either the Robo2 or Robo3 receptors. Unfortunately, Robo2$^{-/-}$ mutant mice develop severe kidney and urinary defects and do not survive postnatally (Grieshammer et al., 2004; Lu et al., 2007). Similarly, Robo3$^{-/-}$ mutants exhibit severe midline crossing defects both within the peripheral and central nervous system (Sabatier et al., 2004; Marillat et al., 2004), and die prenatally. Therefore, the putative role of both receptors could only be investigated during embryonic stages of development. This was investigated just after peak stages of interneuron migration (E15.5) in Robo2 mutants, at a time when Robo2 is broadly expressed within the subpallium and when more than ~90% of cortical interneurons express the receptor. Analysis of the Robo2 mutants showed that

there were no changes in the total number of interneurons within the cortex at this time or during later stages of migration (E17.5).

Analysis of the total numbers and distribution of interneurons within each cortical layer showed there was a 23% increase in the number of interneurons, which was restricted to the cortical plate and marginal zone layers of Robo2 mutant animals at E15.5. This was interesting as Slit proteins are expressed within the developing cortical plate throughout development (Marillat et al., 2002; Bagri et al., 2002; Whitford et al., 2002), thus raising the possibility that Robo2 interneurons are no longer sensitive to Slit within this region and enter this region prematurely. However, analysis at a later stage showed that the total numbers and positioning of cortical interneurons was comparable between Robo2 mutant and wild type animals. Thus, Robo2 does not appear to play a major role in regulating interneuron numbers or their positions within the cortex during development.

A role for Robo2 in proliferation however, cannot be excluded as recent evidence presented by Dr. Oscar Marín at the Cortical Development Meeting in Crete, suggested that removal of both Robo1 and Robo2 receptors results in defects in the proliferation of cortical intermediate basal progenitors. Robo2 deficient (Tbr2+) progenitors were reported to be unable to exit the cell cycle, suggesting Robo-Slit may have a ubiquitous role in regulating cell proliferation in distinct neuronal cell types. It would be interesting to investigate the specific roles of each Robo receptor in the process of cell proliferation, and how these may interact to regulate cortical interneuron and Cajal-Retzius cell numbers

during development.

These studies have confirmed that an early population of interneurons also express the Robo3 receptor. Analysis of Robo3 mutant animals showed no changes in total interneuron numbers during early (E13.5) or later stages (E18.5) of migration. However, closer analysis showed that removal of this receptor resulted in a small, though significant, decrease in the number of interneurons within the MZ of the cortex. This is interesting in view of the fact that Slit1- and Slit3 mRNA are strongly expressed within this layer of the early cortex (Bagri et al., 2002; Marillat et al., 2002; Whitford et al., 2002), suggesting that removal of Robo3 alters the sensitivity of interneurons to chemorepulsion in this region. Such a role for Robo3 is plausible, as it has been shown to modulate the responsiveness of Robo1 to Slit chemorepulsion in vertebrate midline axon guidance systems (Jen et al., 2004; Sabatier et al., 2004). This possibility however remains to be investigated.

It is also plausible that Robo3 may regulate the proliferation of a specific population of interneurons that migrate through the MZ layer. Robo3 was initially identified as a gene that was upregulated in the retinoblastoma (Rb) mutant (Yuan et al., 1999a). Rb is a cell cycle regulatory protein which has a ubiquitous role in regulating cell proliferation, as well as controlling neuronal differentiation and apoptosis during development (Ferguson et al., 2002, 2005). It was subsequently found to directly repress Robo3 transcription, suggesting that Robo3 had a role in mediating the nervous-specific effects of Rb (Yuan et al., 1999a, 2002). Furthermore, it was shown that over-expression of Robo3 in

neuronal cell lines (Neuro2A) promoted their cell cycle entry into the S-phase of mitosis, consistent with the notion that this receptor has a role in cell proliferation. It is interesting that, while removal of Robo1 results in increased cell proliferation and an increase in total interneuron numbers within the cortex (Andrews et al., 2008), removal of the Robo3 receptor resulted in a reduction of interneurons within the MZ. Robo3 differs from the other Robo family members in that it lacks the CC1 intracellular motif, suggesting that this transduces distinct intracellular signalling events (Bashaw et al., 2000, 2001). Moreover, Robo3 has been shown to bind heterophilically and homophilically with the other Robo members (Camurri et al., 2005), and given that its transmembrane form can regulate cell proliferation in neuronal cell lines, it is tempting to speculate that Robo1-Robo3 or Robo2-Robo3 interactions regulate this process in interneuron progenitors. This is consistent with both Robo1 and Robo3 expression within the germinal regions of the MGE at this early stage of interneuron genesis.

A more accurate way of investigating a putative role for Robo3 in interneuron proliferation would be to restrict the analyses specifically to the Robo3-expressing population of interneurons which accounted for a relatively small proportion of the total number of calbindin-positive interneurons. Indeed, the Robo3 transgenic line used in this study was generated by Alain Chédotal's laboratory, using a gene knock-in strategy, in which a GFP reporter gene was inserted into the Robo3 loci. Proliferation studies within the MGE in Robo3 transgenic mice would enable any changes in the generation of populations of Robo3-GFP+ to be investigated. Time lapse-imaging studies, which specifically

trace the migratory behaviours of Robo3 GFP+ cells within the early cortex, would further clarify whether the aforementioned decrease in interneurons within the MZ is due to a change in the proliferation of populations of interneurons and/or due to a change in their migratory paths within the cortex.

It is also interesting that a small decrease in the total numbers of interneurons persists within the caudal cortex at a time when Robo3 is mostly down regulated within the embryonic forebrain. While Robo3 is down regulated within the neocortex, our GFP visualisation studies at E18.5 tentatively suggest that the receptor may be expressed within restricted populations of cells in the developing hippocampus at this time. It is well established that, as well as giving rise to cortical interneurons, the GEs also give rise to interneurons which migrate tangentially to populate the hippocampus during development (Wichterle et al., 1999; Pleasure et al., 2000). These cells are predominantly generated at E12.5 in the mouse, a time when Robo3 is robustly expressed in the GEs. However, the populations of interneurons first reach the hippocampus at ~E16.5, raising the speculation that the decrease in calbindin cells observed within the MZ may reflect changes in this population of cells during later stages of development (E18.5) (Pleasure et al., 2000). Alternatively, one could speculate that if Robo3 regulates the proliferation and/or differentiation of an early population of interneurons during early stages of development, this decrease could be reflected during later stages of interneuron migration, as interneurons do not acquire their final positions within the cortex until the first postnatal week (P0-P7) (Hevner et al., 2004). Furthermore, the observation of populations of Robo3 deficient cells within the differentiating striatum at E18.5

in the Robo3 GFP transgenic mouse forebrain, raises the interesting speculation that populations of striatal neurons may also express this receptor during development. The molecular characterisation of these cell popualations would help elucidate their origins and potential roles during development.

In light of the above investigations, I suggest that unlike Robo1, Robo2 and Robo3 receptors, alone, do not have a major role in regulating cortical interneuron numbers during development. While Robo2 and Robo3 had subtle changes in interneurons within the CP and MZ layers respectively, these did not appear to have a prominent role in regulating the positioning of interneurons during interneuron migration. These analyses are complicated by the finding that, similar to Robo2, nearly 90% of the calbindin population of interneurons also express the Robo1 receptor. Indeed, it is likely that interneurons may express a combination of Robo receptors, thus raising the possibility that these may compensate for their function. Dissecting out the specific contribution of each Robo receptor in regulating these processes will be invaluable in elucidating their respective roles in regulating interneuron proliferation and numbers during development.

7.4 ROBO2 AND ROBO3 AND INTERNEURON MORPHOLOGY

Slit and Robo continue to be expressed in layer-specific patterns within the rodent forebrain during developmental phases when neurons undergo extensive morphological differentiation, and elaborate their dendritic arbours and axonal branches. This is consistent with them playing a role in the morphological differentiation of interneurons once they have reached their appropriate areal

and laminar positions within the developing CP (Marillat et al., 2002; Whitford et al., 2002). While this could not be investigated postnatally, due to the non-viability of Robo2$^{-/-}$ and Robo3$^{-/-}$ mutants, the putative role of Slit-Robo in regulating the morphology of migrating interneurons during development was thus investigated. (The morphological analysis of cortical interneurons carried out in the Robo3 single mutants and triple Robo mutants was carried out by Dr. Andrews.)

Previous reports have shown Robo-Slit to positively regulate neuronal process elongation and branching in the developing CNS (Murray and Whittington, 1999; Wang et al., 1999; Ozdinler and Erzurumlu, 2002; Ma and Tessier-Lavigne, 2007). While this may seem counterintuitive to Slit's chemorepulsive role in axon guidance and cell migration, Slit (Slit2) has been shown to be proteolytically cleaved into a large amino (N)-terminal fragment and a smaller carboxyl (C)-terminal fragment, suggesting that they exert different functional activities *in vivo* (Brose et al., 1999; Wang et al., 1999). The N-terminal fragment (N-Slit), but not full length Slit2 for example, has been shown to positively regulate the branching and elongation of dorsal root ganglion cells' axon collaterals, and it was further suggested that full-length Slit2 may act as an antagonist to N-Slit2 (Wang et al., 1999). Moreover, the specific Slit-response is axon specific. Thus, while N-terminal Slit2 specifically promotes the branching and elongation of dorsal root ganglion cell axonal collaterals (Wang et al., 1999), N-Slit2 mediates the repulsion of olfactory bulb axons and olfactory interneuron precursors from the SVZ of the LGE (Chen et al., 2001). Thus, Slit appears to have a dual role in repelling axons and

positively regulating process branching and elongation *in vivo* (Wang et al., 1999; Ma and Tessier-Lavigne, 2007). Consistent with this, Slit (Slit2) has been shown to promote dendritic growth and branching of dissociated cortical cell cultures, while simultaneously promoting their axonal repulsion (Whitford et al., 2002). Importantly, this study showed that Slit was endogenously secreted by cortical neuronal cells, and further confirmed that the effects of Slit on branching and dendritic elongation were mediated through the Robo1 and Robo2 receptors. Primary cortical cell cultures were transfected with recombinant Robo receptors that lacked their intra-cellular signalling domains, thereby acting ilke dominant-negative receptors. Transfection of mixed neuronal cultures with these Robo-deficient receptors resulted in neurons with inhibited process branching and dendritic growth. Conversely, primary rat cortical cultures transfected with recombinant Robo receptors, in which intracellular Robo signalling could be stimulated, was found to promote dendritic growth and branching, confirming Robo-Slit interactions mediate these processes in mixed cortical cultures.

A more pertinent study investigated the effect of Slits specifically on interneurons, and showed that this molecule promoted interneuron process elongation and branching in MGE explants and dissociated MGE and cortical cell cultures (Sang et al., 2002; Sang and Tan, 2003). This study importantly found that the Slit response of early born and later born interneurons was different and, furthermore, that the branch-promoting activity of Slit was specific to GABAergic cells, but not their pyramidal counterparts in mixed cortical cultures (Sang et al., 2002).

Thus, when Slit was exposed to E13.5 MGE explants, corresponding to a time when early cohorts of interneurons migrate tangentially to the cortex *in vivo*, Slit was found to repel GABAergic interneurons and their processes away from the Slit source, consistent with the chemorepulsive role of Slit in cell migration and axon guidance. Similarly, when dissociated MGE or cortical cell cultures prepared from E13.5 brains were immediately exposed to slit, interneurons from both MGE and cortical cultures exhibited significantly shorter neurite lengths. However, when they were cultured for 5 days prior to Slit treatment (corresponding to ~ E18.5 cultures), interneurons exhibited significantly longer and more extensively branched processes. These studies suggested that, while Slit is repulsive to interneurons and inhibits neurite extension during interneuron migration, it also promotes interneuron branching and neurite elongation during later stages of development. Interneurons have been shown to migrate to their final positions within the CP weeks after they initially arrive in the cortex, extending into the postnatal period (Hevner et al., 2004), and thus Robo/Slit may promote their morphological differentiation once these are correctly positioned in the cortex (Whitford et al., 2002).

Recent work in our laboratory has shown that removal of the Robo1 receptor resulted in significantly increased process elongation and branching of interneurons within the cortices of Robo1 deficient mice when investigated during mid stages of interneuron migration (Andrews et al., 2008). These results were comparable to removal of both Slit1 and Slit2 proteins *in vivo* at this time (Andrews et al., 2008), thus suggesting that Robo1-Slit1,Slit2 protein

interactions inhibit the differentiation of interneurons during stages of development, when interneurons are still actively migrating to the cortex, and before they are correctly positioned within the cortical plate, consistent with observations by Sang et al. (2002). A similar investigation into the putative roles of Robo2 and Robo3 receptors in regulating the morphology of migrating interneurons was therefore studied *in vivo*. The morphological analysis carried out by Dr. Andrews showed an increase in all parameters (number of neurites, total neurite length and number of branch points) of labelled migrating interneurons in the Robo3 deficient mice during early (E13.5), but not later stages of development (E18.5). This was comparable to increases in process length and branching in Robo1 single mutants and Slit1;Slit2 double mutants (Andrews et al., 2008). Removal of the Robo2 receptor however, had a more subtle effect on interneuron morphology, with a significant increase in interneuron length but no changes in process branching. Interestingly, this was restricted to interneurons within the rostral-middle cortex as they specifically migrate through the SVZ/LIZ, where this receptor is strongly expressed at this time.

It was surprising that Robo2 did not appear to have a significant role in regulating interneuron numbers or their morphological differentiation during development, especially since more than 90% of calbindin-positive interneurons express this receptor during mid phases of their tangential migration. However, both Robo1 and Robo2 expression patterns overlap during these stages of development and it is possible that interneurons may express both receptors. Silencing Robo2 may have resulted in a compensatory response from the Robo1

receptor, which is similarly expressed by 90% of the calbindin population of interneurons. Indeed, early populations of interneurons express all three receptors, and so these may be functionally redundant. For this reason, the effect of removing all three Robo receptors on interneuron development was investigated.

Interestingly, while removal of Robo1 resulted in a marked increase in the numbers of cortical interneurons, removal of all three Robo receptors showed a marked (~30%) reduction in the total number of interneurons during early (E13.5) and late (E18.5) stages of migration. This decrease was observed throughout all layers of the developing cortex, and was especially prominent within the two major migratory streams at the levels of the LIZ/SVZ and SP regions, suggesting that all three Robo receptors have a role in regulating cortical interneuron numbers during development. However, the mechanisms which are responsible for this decrease remain to be elucidated.

While Robo1 and Robo3 receptors alone had a prominent effect on the morphology of migrating interneurons, removal of all three Robo receptors had a more subtle effect on interneuron morphology, as shown by the work of Dr. Andrews. This further points to a complex interplay between these receptors. Again, the isolation and identification of distinct Robo populations of interneurons will help distinguish the specific contribution of each receptor in regulating these processes.

Given that interneurons express all three Robo receptors and these are

expressed in distinct, though overlapping, patterns within the GEs and along their migratory paths, it is tempting to speculate that distinct populations of interneurons express different receptors or combinations of receptors which may specify their distinct interneuron phenotypes and their migratory fates. Recent work has shown that the GEs are subdivided into molecularly distinct progenitor domains, and has recently been delineated by combinations of transcription factors (Flames et al., 2007, Fogarty et al., 2007; Du et al., 2008). Given that Robo receptors are expressed in distinct and overlapping patterns within the VZ, it is tempting to speculate that distinct interneuron populations, which express different Robo receptors, may correspond to distinct interneuron subtypes and exhibit specific migratory fates. This highlights the importance of understanding the complex interplay between these receptors in regulating these pleiotropic events.

More recently, additional Robo splice variants have been identified (Yue et al., 2006; Camurri et al., 2005) which show different binding capacities to Slit *in vitro* (Camurri et al., 2005). This suggests that their variants may have different functional roles during development, adding to the complexity of Robo-Slit signalling system. Axon guidance systems have shown that, while the Robo3.1 isoform inhibits Slit-chemorepulsion of spinal cord commissures at the midline, the expression of Robo3.2 receptor is subsequently upregulated and mediates Slit-chemorepulsion as these cross the midline (Chen et al., 2008). Perhaps it is not surprising that Slit-Robo have such pleiotropic roles in interneuron development given the complexity of this system.

APPENDIX

Total Process length		Number of Processes		Number of Branch Points	
	1		1		0
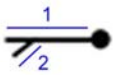	1+2		2		1
	1+2		2		0
	1+2+3		3		1
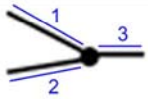	1+2+3	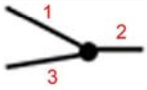	3		0
			5		2

Appendix Methods Fig 1.Characterisation of morphological parameters used in the analysis of the morphology of migrating interneurons. (Andrews et al., 2008).

REFERENCES

Abdel-Mannan O, Cheung AF, Molnár Z. Evolution of cortical neurogenesis (2008) Brain Res Bull. 75:398-404. Review.

Alcantara S, Ruiz M, D'Arcangelo G, Ezan F, de Lecea L, Curran T, Sotelo C, Soriano E (1998) Regional and cellular patterns of reelin mRNA expression in the forebrain of the developing and adult mouse. J Neurosci 18:7779-7799.

Alifragis P, Liapi A, Parnavelas JG (2004) Lhx6 regulates the migration of cortical interneurons from the ventral telencephalon but does not specify their GABA phenotype. J Neurosci 24:5643-8.

Allendoerfer KL, Shatz CJ (1994) The subplate, a transient neocortical structure: its role in the development of connections between thalamus and cortex. Annu Rev Neurosci. 17:185-218. Review.

Anderson SA, Eisenstat DD, Shi L, Rubenstein JL (1997a) Interneuron migration from basal forebrain to neocortex: dependence on Dlx genes. Science 278:474-476.

Anderson SA, Qiu M, Bulfone A, Eisenstat DD, Meneses J, Pedersen R, Rubenstein JL (1997b) Mutations of the homeobox genes Dlx-1 and Dlx-2 disrupt the striatal subventricular zone and differentiation of late born striatal neurons. Neuron 19:27-37.

Anderson SA, Marín O, Horn C, Jennings K, Rubenstein JL (2001) Distinct cortical migrations from the medial and lateral ganglionic eminences. Development 128:353-63.

Andrews W, Liapi A, Plachez C, Camurri L, Zhang J, Mori S, Murakami F, Parnavelas JG, Sundaresan V, Richards LJ (2006) Robo1 regulates the development of major axon tracts and interneuron migration in the forebrain. Development 133:2243-2252.

Andrews W, Barber M, Parnavelas JG (2007) Slit-Robo interactions during cortical development. J Anat 211:188-198.

Andrews W, Barber M, Hernández-Miranda LR, Xian J, Rakić S, Sundaresan V, Rabbitts TH, Pannell R, Rabbitts P, Thompson H, Erskine L, Murakami F, Parnavelas JG (2008) The role of Slit-Robo signalling in the generation, migration and morphological differentiation of cortical interneurons. Dev Biol 313:648-658.

Ang ES Jr, Haydar TF, Gluncic V, Rakić P (2003) Four-dimensional migratory coordinates of GABAergic interneurons in the developing mouse cortex. J Neurosci 23:5805–5815.

Angevine JB Jr, Sidman RL (1961) Autoradiographic study of cell migration during histogenesis of cerebral cortex in the mouse. Nature 192:766-8.

Attardo A, Calegari F, Haubensak W, Wilsch-Bräuninger M, Huttner WB (2008) Live imaging at the onset of cortical neurogenesis reveals differential appearance of the neuronal phenotype in apical versus basal progenitor progeny. PLoS ONE 3:e2388

Bagri A, Marín O, Plump AS, Mak J, Pleasure SJ, Rubenstein JL, Tessier-Lavigne M (2002) Slit proteins prevent midline crossing and determine the dorsoventral position of major axonal pathways in the mammalian forebrain. Neuron 33:233-248.

Bashaw GJ, Kidd T, Murray D, Pawson T, Goodman CS (2000) Repulsive axon guidance: Abelson and Enabled play opposing roles downstream of the roundabout receptor. 101:703-15.

Bashaw GJ, Hu H, Nobes CD, Goodman CS (2001) A novel Dbl family RhoGEF promotes Rho-dependent axon attraction to the central nervous system midline in Drosophila and overcomes Robo repulsion. J Cell Biol 155:1117-22.

Battye R, Stevens A, Jacobs JR (1999) Axon repulsion from the midline of the Drosophila CNS requires slit function. Development 126:2475-81.

Berry M, Rogers AW (1965) The migration of neuroblasts in the developing cerebral cortex. J Anat 99:691-709.

Bielle F, Griveau A, Narboux-Neme N, Vigneau S, Sigrist M, Arber S, Wassef M, Pierani A (2005) Multiple origins of Cajal-Retzius cells at the borders of the developing pallium. Nat Neurosci 8:1002-12.

Borrell V, Marín O (2006) Meninges control tangential migration of hem-derived Cajal-Retzius cells via CXCL12/CXCR4 signalling. Nat Neurosci 9:1284-1293.

Britto JM, Obata K, Yanagawa Y, Tan SS (2006) Migratory response of interneurons to different regions of the developing neocortex. Cereb Cortex;16 Suppl 1:i57-63.

Brodmann K (1909) Vergleichende Lokalisationslehre der Grosshirnrinde in ihren Prinzipien dargestellt auf Grund des Zellenbaues, Leipzig: J.A. Barth.

Brose K, Bland KS, Wang KH, Arnott D, Henzel W, Goodman CS, Tessier-Lavigne M, Kidd T (1999) Slit proteins bind Robo receptors and have an evolutionarily conserved role in repulsive axon guidance. Cell 96:795-806.

Brunstrom JE, Gray-Swain MR, Osborne PA, Pearlman AL (1997) Neuronal heterotopias in the developing cerebral cortex produced by neurotrophin-4. Neuron 18:505-17.

Bulfone A, Puelles L, Porteus MH, Frohman MA, Martin GR, Rubenstein JL (1993) Spatially restricted expression of Dlx-1, Dlx-2 (Tes-1), Gbx-2, and Wnt-3 in the embryonic day 12.5 mouse forebrain defines potential transverse and longitudinal segmental boundaries. J Neurosci 13:3155-72.

Bulfone A, Smiga SM, Shimamura K, Peterson A, Puelles L, Rubenstein JL (1995) T-brain-1: a homolog of Brachyury whose expression defines molecularly distinct domains within the cerebral cortex. Neuron 15:63-78.

Butt SJ, Fuccillo M, Nery S, Noctor S, Kriegstein A, Corbin JG, Fishell G (2005) The temporal and spatial origins of cortical interneurons predict their physiological subtype. Neuron 48:591–604.

Bystron I, Blakemore C, and Rakić P (2008) Development of the human cerebral cortex: Boulder Committee revisited. Nat Rev Neurosci 9:110-22. Review.

Camurri L, Mambetisaeva E, Sundaresan V (2004) Rig-1 a new member of Robo family genes exhibits distinct pattern of expression during mouse development. Gene Expr Patterns 4:99-103.

Camurri L, Mambetisaeva E, Davies D, Parnavelas J, Sundaresan V, Andrews W (2005) Evidence for the existence of two Robo3 isoforms with divergent biochemical properties. Mol Cell Neurosci 30:485-93.

Carney RS, Bystron I, López-Bendito G, Molnár Z (2007) Comparative analysis of extra-ventricular mitoses at early stages of cortical development in rat and human. Brain Struct Funct 212:37-54.

Cauli B, Audinat E, Lambolez B, Angulo MC, Ropert N, Tsuzuki K, Hestrin S, Rossier J (1997) Molecular and physiological diversity of cortical nonpyramidal cells. J Neurosci 17:3894-3906.

Caviness VS, Sidman RL (1973) Time of origin or corresponding cell classes in the cerebral cortex of normal and *reeler* mutant mice: an autoradiographic analysis. J Comp Neurol 148:141-151.
Cell 103:1033-45.

Cepko CL, Austin CP, Walsh C, Ryder EF, Halliday A, Fields-Berry S (1990) Studies of cortical development using retrovirus vectors. Cold Spring Harb Symp Quant Biol.55:265-78.

Chalasani SH, Sabol A, Xu H, Gyda MA, Rasband K, Granato M, Chien CB, Raper JA (2007) Stromal cell-derived factor-1 antagonizes slit/robo signaling in vivo. J Neurosci 27:973-80.

Chen JH, Wen L, Dupuis S, Wu JY, Rao Y (2001) The N-terminal leucine-rich regions in Slit are sufficient to repel olfactory bulb axons and subventricular zone neurons. J Neurosci 21:1548-56.

Chen Z, Gore BB, Long H, Ma L, Tessier-Lavigne M (2008) Alternative splicing of the Robo3 axon guidance receptor governs the midline switch from attraction to repulsion. Neuron 58:325-32

Cheung AF, Pollen AA, Tavare A, DeProto J, Molnár Z (2007) Comparative aspects of cortical neurogenesis in vertebrates. J Anat 211:164-76 Review.

Cobos I, Calcagnotto ME, Vilaythong AJ, Thwin MT, Noebels JL, Baraban SC, Rubenstein JL (2005) Mice lacking Dlx1 show subtype-specific loss of interneurons, reduced inhibition and epilepsy. Nat Neurosci 8:1059-1068.

Cobos I, Borello U, Rubenstein JL (2007) Dlx transcription factors promote migration through repression of axon and dendrite growth. Neuron 54:873-88.

Corbin JG, Nery S, Fishell G (2001) Telencephalic cells take a tangent: non-radial migration in the mammalian forebrain. Nat Neurosci 4:1177-1182.

Costa MR, Kessaris N, Richardson WD, Götz M, Hedin-Pereira C (2007) The marginal zone/layer I as a novel niche for neurogenesis and gliogenesis in developing cerebral cortex. J Neurosci 27:11376-88.

D'Arcangelo G, Miao CG, Chen S-C, Soares HD, Morgan JI, Curran T (1995) A protein related to extracellular matrix proteins deleted in the mouse mutant *reeler*. Nature 374:719-723.

De Carlos JA, O'Leary DD (1992) Growth and targeting of subplate axons and establishment of major cortical pathways. J Neurosci 12:1194-211.

De Carlos JA, López-Mascaraque L, Valverde F (1996) Dynamics of cell migration from the lateral ganglionic eminence in the rat. J Neurosci 16:6146-56.

De Diego I, Smith-Fernández A, Fairén A (1994) Cortical cells that migrate beyond area boundaries: characterization of an early neuronal population in the lower intermediate zone of prenatal rats. Eur J Neurosci 6:983-97.

Dehay C, Giroud P, Berland M, Smart I, Kennedy H (1993) Modulation of the cell cycle contributes to the parcellation of the primate visual cortex. Nature 366:464–466.

Dehay C, Giroud P, Berland M, Killackey HP, Kennedy H (1996) The contribution of thalamic input to the specification of cytoarchitectonic cortical fields in the primate: effects of bilateral enucleation in the fetal monkey on the boundaries and dimensions of striate and extrastriate cortex. J Comp Neurol 367:70–89.

Dehay C, Savatier P, Cortay V, Kennedy H (2001) Cell-cycle kinetics of neocortical precursors are influenced by embryonic thalamic axons. J Neurosci. 21:201-14.

Denaxa M, Chan CH, Schachner M, Parnavelas JG, Karagogeos D (2001) The adhesion molecule TAG-1 mediates the migration of cortical interneurons from the ganglionic eminence along the corticofugal fiber system. Development 128:4635-44.

Denaxa M, Kyriakopoulou K, Theodorakis K, Trichas G, Vidaki M, Takeda Y, Watanabe K, Karagogeos D (2005) The adhesion molecule TAG-1 is required for proper migration of the superficial migratory stream in the medulla but not of cortical interneurons. Dev Biol 288:87-99.

Derer P, Derer M (1990) Cajal-Retzius cell ontogenesis and death in mouse brain visualised with horseradish peroxidise and electron microscopy. Neuroscience 36:839-856.

Di Cristo G (2007) Development of cortical GABAergic circuits and its implications for neurodevelopmental disorders. Clin Genet 72:1-8. Review.

Di Meglio T, Nguyen-Ba-Charvet KT, Tessier-Lavigne M, Sotelo C, Chédotal A (2008) Molecular mechanisms controlling midline crossing by precerebellar neurons. J Neurosci 28:6285-6294.

Donoghue MJ, Rakic P (1999) Molecular gradients and compartments in the embryonic primate cerebral cortex. Cereb Cortex 9:586-600.

Du T, Xu Q, Ocbina PJ, Anderson SA (2008) NKX2.1 specifies cortical interneuron fate by activating Lhx6. Development 135:1559-67.

Edmunds SM, Parnavelas JG (1982) Retzius-Cajal cells: an ultrastructural study in the developing visual cortex of the rat. J Neurocytol 11:427-446

Eisenstat DD, Liu JK, Mione M, Zhong W, Yu G, Anderson SA, Ghattas I, Puelles L, Rubenstein JL (1999) DLX-1, DLX-2, and DLX-5 expression define distinct stages of basal forebrain differentiation. J Comp Neurol. 414:217-37.

Englund C, Fink A, Lau C, Pham D, Daza RA, Bulfone A, Kowalczyk T, Hevner RF (2005) Pax6, Tbr2, and Tbr1 are expressed sequentially by radial glia, intermediate progenitor cells, and postmitotic neurons in developing neocortex. J Neurosci 25:247-51.

Ferguson KL, Vanderluit JL, Hébert JM, McIntosh WC, Tibbo E, MacLaurin JG, Park DS, Wallace VA, Vooijs M, McConnell SK, Slack RS (2002) Telencephalon-specific Rb knockouts reveal enhanced neurogenesis, survival and abnormal cortical development. EMBO J 21:3337-46.

Ferguson KL, McClellan KA, Vanderluit JL, McIntosh WC, Schuurmans C, Polleux F, Slack RS (2005) A cell-autonomous requirement for the cell cycle regulatory protein, Rb, in neuronal migration. EMBO J 24:4381-91.

Fish JL, Dehay C, Kennedy H, Huttner WB (2008) Making bigger brains-the evolution of neural-progenitor-cell division. J Cell Sci. 121:2783-93. Review.

Fishell G, Mason CA, Hatten ME (1993) Dispersion of neural progenitors within the germinal zones of the forebrain. Nature 362:636-8.

Flames N, Long JE, Garratt AN, Fischer TM, Gassmann M, Birchmeier C, Lai C, Rubenstein JL, Marín O (2004) Short- and long-range attraction of cortical GABAergic interneurons by neuregulin-1. Neuron 44:251-261.

Flames N, Pla R, Gelman DM, Rubenstein JL, Puelles L, Marín O (2007) Delineation of multiple subpallial progenitor domains by the combinatorial expression of transcriptional codes. J Neurosci 27:9682-95.

Fogarty M, Grist M, Gelman D, Marín O, Pachnis V, Kessaris N (2007) Spatial genetic patterning of the embryonic neuroepithelium generates GABAergic interneuron diversity in the adult cortex. J Neurosci 27:10935-46.

Frantz GD, McConnell SK (1996) Restriction of late cerebral cortical progenitors to an upper-layer fate. Neuron 17:55-61.

Frotscher M (1997) Dual role of Cajal-Retzius cells and reelin in cortical development. Cell Tissue Res. 290:315-322.

Gal JS, Morozov YM, Ayoub AE, Chatterjee M, Rakić P, Haydar TF (2006) Molecular and morphological heterogeneity of neural precursors in the mouse neocortical proliferative zones. J Neurosci 26:1045-56.

García-Moreno F, López-Mascaraque L, De Carlos JA (2007) Origins and migratory routes of murine Cajal-Retzius cells. J Comp Neurol 500:419-432.

Georgiou M, Tear G (2002) Commissureless is required both in commissural neurones and midline cells for axon guidance across the midline. Development 129:2947-56

Georgiou M, Tear G (2003) The N-terminal and transmembrane domains of Commissureless are necessary for its function and trafficking within neurons. Mech Dev 120:1009-19.

Ghosh A, Antonini A, McConnell SK, Shatz CJ (1990) Requirement for subplate neurons in the formation of thalamocortical connections. Nature 347:179-81.

Grieshammer U, Le Ma, Plump AS, Wang F, Tessier-Lavigne M, Martin GR (2004) SLIT2-mediated ROBO2 signaling restricts kidney induction to a single site. Dev Cell 6:709-17.

Gulacsi A, Anderson SA (2006) Shh maintains Nkx2.1 in the MGE by a Gli3-independent mechanism. Cereb Cortex 16 Suppl 1:i89-95.

Hammond V, So E, Gunnersen J, Valcanis H, Kalloniatis M, Tan SS (2006) Layer positioning of late-born cortical interneurons is dependent on Reelin but not p35 signalling. J Neurosci 26:1646-1655.

Hartfuss E, Galli R, Heins N, Götz M (2001) Characterization of CNS precursor subtypes and radial glia. Dev Biol 229:15-30.

Haubensak W, Attardo A, Denk W, Huttner WB (2004) Neurons arise in the basal neuroepithelium of the early mammalian telencephalon: a major site of neurogenesis. Proc Natl Acad Sci U S A 101:3196-201.

Herrup K, Silver J (1994) Cortical development and topographic maps: patterns of cell dispersion in developing cerebral cortex. Curr Opin Neurobiol 4:108-11.

Hevner RF, Neogi T, Englund C, Daza RA, Fink A (2003a) Cajal-Retzius cells in the mouse: transcription factors, neurotransmitters, and birthdays suggest a pallial origin. Brain Res Dev Brain Res 141:39-53.

Hevner RF, Daza RA, Rubenstein JL, Stunnenberg H, Olavarria JF, Englund C (2003b) Beyond laminar fate: toward a molecular classification of cortical projection/pyramidal neurons. Dev Neurosci 25:139-51.

Hevner RF, Daza RA, Englund C, Kohtz J, Fink A (2004) Postnatal shifts of interneuron position in the neocortex of normal and *reeler* mice: evidence for inward radial migration. Neuroscience 124:605-618.

Hivert B, Liu Z, Chuang CY, Doherty P, Sundaresan V (2002) Robo1 and Robo2 are homophilic binding molecules that promote axonal growth. Mol Cell Neurosci. 21:534-45.

Hohenester E (2008) Structural insight into Slit-Robo signalling. Biochem Soc Trans 36:251-6. Review

Holmes GP, Negus K, Burridge L, Raman S, Algar E, Yamada T, Little MH (1998) Distinct but overlapping expression patterns of two vertebrate slit homologs implies functional roles in CNS development and organogenesis. Mech Dev 79:57-72.

Howitt JA, Clout NJ, Hohenester E (2004) Binding site for Robo receptors revealed by dissection of the leucine-rich repeat region of Slit. EMBO J 23:4406-12.

Hu H (1999) Chemorepulsion of neuronal migration by Slit2 in the developing mammalian forebrain. Neuron 23:703-711.

Huminiecki L, Gorn M, Suchting S, Poulsom R, Bicknell R (2002) Magic roundabout is a new member of the roundabout receptor family that is endothelial specific and expressed at sites of angiogenesis. Genomics 79:547-552.

Itoh A, Miyabayashi T, Ohno M, Sakano S (1998) Cloning and expressions of three mammalian homologues of Drosophila slit suggest possible roles for Slit in the formation and maintenance of the nervous system. Brain Res Mol Brain Res 62:175-86

Jen JC, Chan WM, Bosley TM, Wan J, Carr JR, Rub U, Shattuck D, Salamon G, Kudo LC, Ou J, Lin DD, Salih MA, Kansu T, Al Dhalaan H, Al Zayed Z, MacDonald DB, Sigsby B, Plaitakis A, Dretakis EK, Gottloh I, Pieh C, Traboulsi EI, Wang Q, Wang L, Andrews C, Yamada K, Demer JL, Karim S, Alger JR, Geschwind DH, Deller T, Sicotte NL, Nelson SF, Baloh RW, Engle EC (2004) Mutations in a human ROBO gene disrupt hindbrain axon pathway crossing and morphogenesis. Science 304:1509-1513.

Jones EG, (1985) The Thalamus. Plenum Press, New York.

Jones L, López-Bendito G, Gruss P, Stoykova A, Molnár Z (2002) Pax6 is required for the normal development of the forebrain axonal connections. Development.129:5041-52.

Juriloff DM, Harris MJ, Tom C, MacDonald KB (1991) Normal mouse strains differ in the site of initiation of closure of the cranial neural tube. Teratology 44:225-33.

Karlen SJ, Krubitzer L (2006) The evolution of the neocortex in mammals: intrinsic and extrinsic contributions to the cortical phenotype. Novartis Found Symp 270:146-59; discussion 159-69. Review

Kawaguchi Y, Kubota Y (1997) GABAergic cell subtypes and their synaptic connections in the rat frontal cortex. Cereb Cortex 7:476-486.

Keleman K, Rajagopalan S, Cleppien D, Teis D, Paiha K, Huber LA, Technau GM, Dickson BJ. (2002) Comm sorts robo to control axon guidance at the Drosophila midline. Cell 110:415-27.

Keleman K, Ribeiro C, Dickson BJ (2005) Comm function in commissural axon guidance: cell-autonomous sorting of Robo *in vivo*. Nat Neurosci. 8::156-63.

Kidd T, Brose K, Mitchell KJ, Fetter RD, Tessier-Lavigne M, Goodman CS, Tear G (1998a) Roundabout controls axon crossing of the CNS midline and defines a novel subfamily of evolutionarily conserved guidance receptors. Cell 23:205-215.

Kidd T, Russell C, Goodman CS, Tear G (1998b) Dosage-sensitive and complementary functions of roundabout and commissureless control axon crossing of the CNS midline. Neuron 20:25-33.

Kidd T, Bland KS, Goodman CS (1999) Slit is the midline repellent for the robo receptor in Drosophila. Cell 96:785-94.

Kostovic I, Rakć P (1990) Developmental history of the transient subplate zone in the visual and somatosensory cortex of the macaque monkey and human brain. J Comp Neurol 297:441-70.

Kowalczyk T, Pontious A, Englund C, Daza RAM, Bedogoni F, Hodge R, Attardo A, Bell C, Huttner WB, Hevner RF (2009) Intermediate Neuronal Progenitors

(Basal Progenitors) Produce Pyramidal-Projection Neurons for All Layers of Cerebral Cortex. Cerebral Cortex Advance Access Jan 23, 2009.

Lavdas AA, Grigoriou M, Pachnis V, Parnavelas JG (1999) The medial ganglionic eminence gives rise to a population of early neurons in the developing cerebral cortex. J Neurosci. 19:7881-8.

Le TN, Du G, Fonseca M, Zhou QP, Wigle JT, Eisenstat DD (2007) Dlx homeobox genes promote cortical interneuron migration from the basal forebrain by direct repression of the semaphorin receptor neuropilin-2. J Biol Chem 282:19071-81.

Lee JS, Ray R, Chien CB (2001) Cloning and expression of three zebrafish roundabout homologs suggest roles in axon guidance and cell migration. Dev Dyn 221:216-30.

Letinic K, Zoncu R, Rakić P (2002) Origin of GABAergic neurons in the human neocortex. Nature 417:645-9.

Lewis DA, Hashimoto T, Volk DW (2005) Cortical inhibitory neurons and schizophrenia. Nat Rev Neurosci 6:312-24. Review.

Li HS, Chen JH, Wu W, Fagaly T, Zhou L, Yuan W, Dupuis S, Jiang ZH, Nash W, Gick C, Ornitz DM, Wu JY, Rao Y (1999) Vertebrate slit, a secreted ligand for the transmembrane protein roundabout, is a repellent for olfactory bulb axons. Cell 96:807-18.

Li X, Chen Y, Liu Y, Gao J, Gao F, Bartlam M, Wu JY, Rao Z (2006) Structural basis of Robo proline-rich motif recognition by the srGAP1 Src homology 3 domain in the Slit-Robo signaling pathway. J Biol Chem 281:28430-7.

Liodis P, Denaxa M, Grigoriou M, Akufo-Addo C, Yanagawa Y, Pachnis V (2007) Lhx6 activity is required for the normal migration and specification of cortical interneuron subtypes. J Neurosci 27:3078-89.

Liu JK, Ghattas I, Liu S, Chen S, Rubenstein J (1997) Dlx genes encode DNA-binding proteins that are expressed in an overlapping and sequential pattern during basal ganglia differentiation. Dev Dyn 210:498-512.

Liu Z, Patel K, Schmidt H, Andrews W, Pini A, Sundaresan V (2004) Extracellular Ig domains 1 and 2 of Robo are important for ligand (Slit) binding. Mol Cell Neurosci 26:232-240.

Long H, Sabatier C, Ma L, Plump A, Yuan W, Ornitz DM, Tamada A, Murakami F, Goodman CS, Tessier-Lavigne M (2004) Conserved roles for Slit and Robo proteins in midline commissural axon guidance. Neuron 42:213-23.

López-Bendito G, Molnár Z (2003) Thalamocortical development: how are we going to get there? Nat Rev Neurosci 4:276-289.

López-Bendito G, Cautinat A, Sánchez JA, Bielle F, Flames N, Garratt AN, Talmage DA, Role LW, Charnay P, Marín O, Garel S (2006) Tangential neuronal migration controls axon guidance: a role for neuregulin-1 in thalamocortical axon navigation. Cell 125:127-42.

López-Bendito G., Flames N, Ma L., Fouquet C, Di Meglio T, Chédotal A, Tessier-Lavigne M, Marín O (2007) Robo1 and Robo2 cooperate to control the guidance of major axonal tracts in the mammalian forebrain. J Neurosci 27:3395-3407.

López-Bendito G., Sanchez-Alcaniz JA, Pla R, Borrell V, Pico E, Valdeolmillos M, Marín O (2008) Chemokine signalling controls intracortical migration and final distribution of GABAergic interneurons. J Neurosi 28:1613-1624.

Lu W, van Eerde AM, Fan X, Quintero-Rivera F, Kulkarni S, Ferguson H, Kim HG, Fan Y, Xi Q, Li QG, Sanlaville D, Andrews W, Sundaresan V, Bi W, Yan J, Giltav JC, Wijmenga C, de Jong TP, Feather SA, Woolf AS, Rao Y, Lupski JR, Eccles MR, Quade BJ, Gusella JF, Morton CC, Maas RL (2007) Disruption of Robo2 is associated with urinary tract anomalies and confers risk of vesicoureteral reflux. Am J Hum Genet 80:616-632.

Lukaszewicz A, Savatier P, Cortay V, Giroud P, Huissoud C, Berland M, Kennedy H, Dehay C (2005) G1 phase regulation, area-specific cell cycle control, and cytoarchitectonics in the primate cortex. Neuron 47:353-64.

Lukaszewicz A, Cortay V, Giroud P, Berland M, Smart I, Kennedy H, Dehay C (2006) The concerted modulation of proliferation and migration contributes to the specification of the cytoarchitecture and dimensions of cortical areas. Cereb Cortex 16 Suppl 1:i26-34.

Luskin MB, Shatz CJ (1985a) Studies of the earliest generated cells of the cat's visual cortex: cogeneration of subplate and marginal zones. J Neurosci 5:1062-1075.

Luskin MB, Shatz CJ (1985b) Neurogenesis of the cat's primary visual cortex. J Comp Neurol 242:611-631.

Luskin MB, Pearlman AL, Sanes JR (1988) Cell lineage in the cerebral cortex of the mouse studied *in vivo* and in vitro with a recombinant retrovirus. Neuron 1:635-47.

Ma L, Tessier-Lavigne M (2007) Dual branch-promoting and branch-repelling actions of Slit/Robo signalling on peripheral and central branches of developing sensory axons. J Neurosci 27:6843–6851.

Malatesta P, Hartfuss E, Götz M (2000) Isolation of radial glial cells by fluorescent-activated cell sorting reveals a neuronal lineage. Development 127:5253-63.

Malatesta P, Hack MA, Hartfuss E, Kettenmann H, Klinkert W, Kirchhoff F, Götz M (2003) Neuronal or glial progeny: regional differences in radial glia fate. Neuron 37:751-64.

Mallamaci A, Stoykova A (2006) Gene networks controlling early cerebral cortex arealization. Eur J Neurosci 23:847-56. Review.

Mallet N, Ballion B, Le Moine C, Gonon F (2006) Cortical inputs and GABA interneurons imbalance projection neurons in the striatum of parkinsonian rats. J Neurosci 26:3875-3884.

Mambetisaeva ET, Andrews W, Camurri L, Annan A, Sundaresan V (2005) Robo family of proteins exhibit differential expression in mouse spinal cord and Robo-Slit interactions is required for midline crossing in vertebrate spinal cord. Dev Dyn 233:41-51.

Marillat V, Cases O, Nguyen-Ba-Charvet KT, Tessier-Lavigne M, Sotelo C, Chédotal A (2002) Spatiotemporal expression patterns of slit and robo genes in the rat brain. J Comp Neurol 442:130-155.

Marillat V, Sabatier C, Failli V, Matsunaga E, Sotelo C, Tessier-Lavigne M, Chédotal, A (2004) The slit receptor Rig-1/Robo3 controls midline crossing by hindbrain precerebellar neurons and axons. Neuron 43:69-79.

Marín O, Yaron A, Bagri A, Tessier-Lavigne M, Rubenstein JL (2001a) Sorting of striatal and cortical interneurons regulated by semaphorin/neuropilin interactions. Science 293:872–875.

Marín O, Anderson SA, Rubenstein JL (2001b) Origin and molecular specification of striatal interneurons.

Marín O, Plump AS, Flames N, Sánchez-Camacho C, Tessier-Lavigne M, Rubenstein JL (2003a) Directional guidance of interneuron migration to the cerebral cortex relies on subcortical Slit1/2-independent repulsion and cortical attraction. Development 130:1889-1901.

Marín O, Rubenstein JL (2003b) Cell migration in the forebrain. Annu Rev Neurosci 26:441-483.

Marín-Padilla M (1978) Dual origin of the mammalian neocortex and evolution of the cortical plate. Anat Embryol (Berl) 152:109-26.

Marín-Padilla M (1998) Cajal-Retzius cells and the development of the neocortex. Trends Neurosci 21:64-71.

McConnell SK, Ghosh A, Shatz CJ (1989) Subplate neurons pioneer the first axon pathway from the cerebral cortex. Science 245:978-82.

McConnell SK, Kaznowski CE (1991) Cell cycle dependence of laminar determination in developing neocortex. Science 254:282-5.

McManus MF, Nasrallah IM, Gopal PP, Baek WS, Golden JA (2004) Axon mediated interneuron migration. J Neuropathol Exp Neurol 63:932-41.

Métin C, Godement P (1996) The ganglionic eminence may be an intermediate target for corticofugal and thalamocortical axons. J Neurosci 16:3219-3235.

Métin C, Baudoin JP, Rakić S, Parnavelas JG (2006) Cell and molecular mechanisms involved in the migration of cortical interneurons. Eur J Neurosci 23:894-900.

Meyer G, Soria JM, Martinez-Galan JR, Martin-Clemente B, Fairen A (1998) Different origins and developmental histories of transient neurons in the marginal zone of the fetal and neonatal rat cortex. J Comp Neurol 397:493-518.

Meyer G, Goffinet AM, Fairen A (1999) What is a Cajal-Retzius cell? A reassessment of a classical cell type based on recent observations in the developing neocortex. Cereb Cortex 9:765-775.

Meyer G (2007) Genetic control of neuronal migrations in human cortical development. Adv Anat Embryol Cell Biol 189: 1-111. Review

Mione MC, Danevic C, Boardman P, Harris B, Parnavelas JG (1994) Lineage analysis reveals neurotransmitter (GABA or glutamate) but not calcium-binding protein homogeneity in clonally related cortical neurons. J Neurosci 14:107-23.

Mione MC, Cavanagh JF, Harris B, Parnavelas JG (1997) Cell fate specification and symmetrical/asymmetrical divisions in the developing cerebral cortex. J Neurosci 17:2018-29.

Misson JP, Edwards MA, Yamamoto M, Caviness VS Jr (1988) Mitotic cycling of radial glial cells of the fetal murine cerebral wall: a combined autoradiographic and immunohistochemical study. Brain Res 466:183-90.

Miyata T, Kawaguchi A, Okano H, Ogawa M (2001) Asymmetric inheritance of radial glial fibbers by cortical neurons. Neuron 31:727-41.

Miyata T, Kawaguchi A, Saito K, Kawano M, Muto T, Ogawa M (2004) Asymmetric production of surface-dividing and non-surface-dividing cortical progenitor cells. Development 131:3133-45.

Molnár Z, Adams R, Blakemore C (1998) Mechanisms underlying the early establishment of thalamocortical connections in the rat. J Neurosci 18:5723-45.

Molnár Z, Higashi S, López-Bendito G (2003) Choreography of early thalamocortical development. Cereb Cortex. 13:661-9.

Molnár Z, Métin C, Stoykova A, Tarabykin V, Price DJ, Francis F, Meyer G, Dehay C, Kennedy H (2006) Comparative aspects of cerebral cortical development. Eur J Neurosci. 23:921-34. Review

Morante-Oria J, Carleton A, Ortino B, Kremer EJ, Fairén A, Lledo PM (2003) Subpallial origin of a population of projecting pioneer neurons during corticogenesis. Proc Natl Acad Sci USA 100:12468-12473.

Morlot C, Thielens N, Ravelli RBG, Hemrika W, Romjin RA, Gros P, Cusack S, McCarthy AA (2007) Structural insights into the Slit-Robo complex. PNAS 104: 14923-14928.

Murray MJ, Whitington PM (1999) Effects of roundabout on growth cone dynamics, filopodial length, and growth cone morphology at the midline and throughout the neuropile. J Neurosci. 19:7901–7912.

Myat A, Henry P, McCabe V, Flintoft L, Rotin D, Tear G (2002) Drosophila Nedd4, a ubiquitin ligase, is recruited by Commissureless to control cell surface levels of the roundabout receptor. Neuron 35:447-59

Nadarajah B, Alifragis P, Wong RO, Parnavelas JG (2002) Ventricle-directed migration in the developing cerebral cortex. Nat Neurosci 5:218–224.

Nery S, Fishell G, Corbin JG (2002) The caudal ganglionic eminence is a source of distinct cortical and subcortical cell populations. Nat Neurosci 5:1279–1287.

Nguyen Ba-Charvet KT, Brose K, Marillat V, Kidd T, Goodman CS, Tessier-Lavigne M, Sotelo C, Chédotal A (1999) Slit2-Mediated chemorepulsion and collapse of developing forebrain axons. Neuron 22:463-473.

Nguyen-Ba-Charvet KT, Picard-Riera N, Tessier-Lavigne M, Baron-Van Evercooren A, Sotelo C, Chédotal A (2004) Multiple roles for slits in the control of cell migration in the rostral migratory stream.. J Neurosci. 24:1497-506.

Nieto M, Monuki ES, Tang H, Imitola J, Haubst N, Khoury SJ, Cunningham J, Gotz M, Walsh CA (2004) Expression of Cux-1 and Cux-2 in the subventricular zone and upper layers II-IV of the cerebral cortex.J Comp Neurol 479:168-80.

Nobrega-Pereira S, Kessaris N, Du T, Kimura S, Anderson SA, Marín O (2008) Postmitotic Nkx2.1 controls the migration of telencephalic interneurons by direct repression of guidance receptors. Neuron 59:733-745.

Noctor SC, Flint AC, Weissman TA, Dammerman RS, Kriegstein AR (2001) Neurons derived from radial glial cells establish radial units in neocortex. Nature 409:714-20.

Noctor SC, Flint AC, Weissman TA, Wong WS, Clinton BK, Kriegstein AR (2002) Dividing precursor cells of the embryonic cortical ventricular zone have morphological and molecular characteristics of radial glia. J Neurosci 22:3161-73.

Noctor SC, Martínez-Cerdeño V, Ivic L, Kriegstein AR (2004) Cortical neurons arise in symmetric and asymmetric division zones and migrate through specific phases. Nat Neurosci 7:136-44.

Noctor SC, Martínez-Cerdeño V, Kriegstein AR (2008) Distinct behaviors of neural stem and progenitor cells underlie cortical neurogenesis. J Comp Neurol 508:28-44.

Nüsslein-Volhard C, Wieschaus E, Kluding H (1984) Mutations affecting the pattern of the larval cuticle in *Drosophila melanogaster*. Roux Arch. Dev Biol 193:267-82.

Ogawa M, Miyata T, Nakajima K, Yagyu K, Seike M, Ikenaka K, Yamamotot H, Mikoshiba K (1995) The *reeler* gene-associated antigen on Cajal-Retzius neurons is a crucial molecule for laminar organization of cortical neurons. Neuron 14:899-912.

O'Rourke NA, Sullivan DP, Kaznowski CE, Jacobs AA, McConnell SK (1995) Tangential migration of neurons in the developing cerebral cortex. Development 121:2165-76.

O'Rourke NA, Chenn A, McConnell SK (1997) Postmitotic neurons migrate tangentially in the cortical ventricular zone. Development 124:997-1005.

Ozdinler PH, Erzurumlu RS, (2002) Slit2, a branching-arborization factor for sensory axons in the mammalian CNS. J Neurosci 22:4540–4549.

Park KW, Morrison CM, Sorensen LK, Jones CA, Rao Y, Chien CB, Wu JY, Urness LD, Li DY (2003) Robo4 is a vascular specific receptor that inhibits endothelial migration. Dev Biol 261:251-267.

Parnavelas JG, Edmunds SM (1983) Further evidence that Cajal-Retzius cells transform to nonpyramidal neurons in the developing rat visual cortex. J Neurocytol 12:863-871.

Parnavelas JG, Dinopoulos A, Davies SW (1989) The central visual pathways. In Björklund A, Hökfelt T, Swanson LW (eds) Handbook of Chemical Neuroanatomy. Elsevier, Amsterdam, 1-164.

Parnavelas JG, Barfield JA, Franke E, Luskin MB (1991) Separate progenitor cells give rise to pyramidal and nonpyramidal neurons in the rat telencephalon. Cereb Cortex. 1:463-8.

Peters A, Jones EG (1985) Cereb Cortex Vol 3, Visual Cortex; Vol 4, Association and Auditory Cortices. Plenum Press, New York, London.

Petilla Interneuron Nomenclature Group, Ascoli GA, Alonso-Nanclares L, Anderson SA, Barrionuevo G, Benavides-Piccione R, Burkhalter A, Buzsáki G, Cauli B, DeFelipe J, Fairén A, Feldmeyer D, Fishell G, Fregnac Y, Freund TF, Gardner D, Gardner EP, Goldberg JH, Helmstaedter M, Hestrin S, Karube F,

Kisvárday ZF, Lambolez B, Lewis DA, Marín O, Markram H, Muñoz A, Packer A, Petersen CC, Rockland KS, Rossier J, Rudy B, Somogyi P, Staiger JF, Tamas G, Thomson AM, Toledo-Rodriguez M, Wang Y, West DC, Yuste R (2008) Petilla terminology: nomenclature of features of GABAergic interneurons of the cerebral cortex. Nat Rev Neurosci. 9:557-68.

Pla R, Borrell V, Flames N, Marín O (2006) Layer acquisition by cortical GABAergic interneurons is independent of Reelin signalling. J Neurosci 26:6924-6934.

Plachez C, Andrews W, Liapi A, Knoell B, Drescher U, Mankoo B, Zhe L, Mambetisaeva E, Annan A, Bannister L, Parnavelas JG, Richards LJ, Sundaresan V (2008) Robos are required for the correct targeting of retinal ganglion cell axons in the visual pathway of the brain. Mol Cell Neurosci 37:719-730.

Pleasure SJ, Anderson S, Hevner R, Bagri A, Marín O, Lowenstein DH, Rubenstein JL (2000) Cell migration from the ganglionic eminences is required for the development of hippocampal GABAergic interneurons. Neuron 28:727-40.

Plump AS, Erskine L, Sabatier C, Brose K, Epstein CJ, Goodman CS, Mason CA, Tessier-Lavigne M (2002) Slit1 and Slit2 cooperate to prevent premature midline crossing of retinal axons in the mouse visual system. Neuron 33:219-32.

Polleux F, Whitford KL, Dijkhuizen PA, Vitalis T, Ghosh A (2002) Control of cortical interneuron migration by neurotrophins and PI3-kinase signalling. Development 129:3147–3160.

Pontious A, Kowalczyk T, Englund C, Hevner RF (2008) Role of intermediate progenitor cells in cerebral cortex development. Dev Neurosci 30:24-32. Review.

Porteus MH, Bulfone A, Liu JK, Puelles L, Lo LC, Rubenstein JL (1994) DLX-2, MASH-1, and MAP-2 expression and bromodeoxyuridine incorporation define molecularly distinct cell populations in the embryonic mouse forebrain. J Neurosci 14:6370-83.

Powell EM, Mars WM, Levitt P (2001) Hepatocyte growth factor/scatter factor is a motogen for interneurons migrating from the ventral to dorsal telencephalon. Neuron 30:79–89.

Powell EM, Campbell DB, Stanwood GD, Davis C, Noebels JL, Levitt P (2003) Genetic disruption of cortical interneuron development causes region and GABA cell type-specific deficits, epilepsy, and behavioural dysfunction. J Neurosci 23:622-631.

Price J, Thurlow L (1988) Cell lineage in the rat cerebral cortex: a study using retroviral-mediated gene transfer. Development 104:473-82.

Price DJ, Kennedy H, Dehay C, Zhou L, Mercier M, Jossin Y, Goffinet AM, Tissir F, Blakey D, Molnár Z (2006) The development of cortical connections. Eur J Neurosci. 23:910-20. Review.

Privat A (1975) Postnatal gliogenesis in the mammalian brain. Int Rev Cytol. 1975;40:281-323. Review.

Puelles L, Kuwana E, Puelles E, Bulfone A, Shimamura K, Keleher J, Smiga S, Rubenstein JL (2000) Pallial and subpallial derivatives in the embryonic chick and mouse telencephalon, traced by the expression of the genes Dlx-2, Emx-1, Nkx-2.1, Pax-6, and Tbr-1. J Comp Neurol 424:409-38.

Puelles L (2001) Thoughts on the development, structure and evolution of the mammalian and avian telencephalic pallium. Philos Trans R Soc Lond B Biol Sci. 356:1583-98. Review.

Quinn JC, Molinek M, Martynoga BS, Zaki PA, Faedo A, Bulfone A, Hevner RF, West JD, Price DJ (2007) Pax6 controls cerebral cortical cell number by regulating exit from the cell cycle and specifies cortical cell identity by a cell autonomous mechanism. Dev Biol 302:50-65.

Raedler E, Raedler A (1978) Autoradiographic study of early neurogenesis in rat neocortex. Anat Embryol (Berl) 154:267-84.

Rajagopalan S, Vivancos V, Nicolas E, Dickson BJ (2000) Selecting a longitudinal pathway: Robo receptors specify the lateral position of axons in the Drosophila CNS.

Rakić P (1974) Neurons in rhesus monkey visual cortex: systematic relation between time of origin and eventual disposition. Science 183:425-7.

Rakić P (1995) Radial versus tangential migration of neuronal clones in the developing cerebral cortex. Proc Natl Acad Sci USA 92: 11323-7. Review.

Rakić P (2000) Radial unit hypothesis of neocortical expansion. Novartis Found Symp 228:30-42; discussion 42-52. Review

Rakić S, Zecevic N (2003) Emerging complexity of layer I in human cerebral cortex. Cereb Cortex 13:1072-83

Ramón y Cajal S (1890) Textura de las circonvoluciones centrales de los manmiferos inferiors. (Nota preventive.) Gac Med Catal del 15 de diciembre.

Ramón y Cajal S (1891) Sur la structure de l'cortex cerebrale de quelques mammifères. Cellule 7:125-176.

Ramón y Cajal S (1909) Histologie du Système Nerveux de l'Homme et des Vertébrés. Maloine,Vol I, Paris.

Ramón y Cajal S (1911) Histologie du Système Nerveux de l'Homme et des Vertébrés. Maloine,Vol II, Paris.

Ramón y Cajal S (1929) Étude sur la neurogenèse de quelques vertebres. Pp. 192-211. Madrid

Reid CB, Liang I, Walsh C (1995) Systematic widespread clonal organization in cerebral cortex. Neuron 15:299-310.

Remedios R, Huilgol D, Saha B, Hari P, Bhatnagar L, Kowalczyk T, Hevner RF, Suda Y, Aizawa S, Ohshima T, Stoykova A, Tole S (2007) A stream of cells migrating from the caudal telencephalon reveals a link between the amygdala and neocortex. Nat Neurosci. 10:1141-50.

Rothberg JM, Hartley DA, Walther Z, Artavanis-Tsakonas S (1988) slit: an EGF-homologous locus of D. melanogaster involved in the development of the embryonic central nervous system. Cell 55:1047-59.

Rothberg JM, Jacobs JR, Goodman CS, Artavanis-Tsakonas S (1990) slit: an extracellular protein necessary for development of midline glia and commissural axon pathways contains both EGF and LRR domains.Genes Dev 4:2169-87.

Retzius G (1893) Die Cajal'schen Zallen des Grosshirnrinde beim Menschen und bei Saugethieren. Biol Unters 5:1-9.

Retzius G (1894) Weitere beitrage zier Kenntniss der Cajal'schen Zellen der grosshirnrinde des Menschen. Biol Unters 6:29-37.

Rubenstein JL, Beachy PA (1998) Patterning of the embryonic forebrain. Curr Opin Neurobiol. 8:18-26. Review

Rymar VV, Sadikot AF (2007) Laminar fate of cortical GABAergic interneurons is dependent on both birthdate and phenotype. J Comp Neurol 501:369-80.

Sabatier C, Plump AS, Le Ma, Brose K, Tamada A, Murakami F, Lee EY, Tessier-Lavigne M (2004) The divergent Robo family protein rig-1/Robo3 is a negative regulator of slit responsiveness required for midline crossing by commissural axons. Cell 16:157-169.

Sang Q, Wu J, Rao Y, Hsueh YP, Tan SS (2002) Slit promotes branching and elongation of neuritis of interneurons but not projection neurons from the developing telencephalon. Mol Cell Neurosci 21:250-265.

Sang Q, Tan SS (2003) Contact-associated neurite outgrowth and branching of immature cortical interneurons. Cereb Cortex 13:677-683.

Seeger M, Tear G, Ferres-Marco D, Goodman CS (1993) Mutations affecting growth cone guidance in Drosophila: genes necessary for guidance towards or away from the midline. Neuron 10: 409-426.

Shinozaki K, Miyagi T, Yoshida M, Miyata T, Ogawa M, Aizawa S, Suda Y (2002) Absence of Cajal-Retzius cells and subplate neurons associated with defects of tangential cell migration from ganglionic eminence in Emx1/2double mutant cerebral cortex. Development 129:3479-3492.

Shu T, Sundaresan V, McCarthy MM, Richards LJ (2003) Slit2 guides both precrossing and postcrossing callosal axons at the midline in vivo. J Neurosci. 23:8176-84.

Siegenthaler JA, Miller, MW (2008) Generation of Cajal-Retzius neurons in mouse forebrain is regulated by transforming growth factor beta-Fox signalling pathways. Dev Biol 313:35-46.

Simpson JH, Kidd T, Bland KS, Goodman CS (2000a) Short-range and long-range guidance by slit and its Robo receptors. Robo and Robo2 play distinct roles in midline guidance. Neuron 28:753-66.

Simpson JH, Bland KS, Fetter RD, Goodman CS (2000b) Short-range and long-range guidance by Slit and its Robo receptors: a combinatorial code of Robo receptors controls lateral position. Cell 103:1019-32.

Smart IHM: Proliferative characteristics of the ependymal layer during the early development of the mouse neocortex: a pilot study based on recording the number, location and plane of cleavage of mitotic figures (1973) J Anat 116: 67-91.

Smart IH, Dehay C, Giroud P, Berland M, Kennedy H (2002) Unique morphological features of the proliferative zones and postmitotic compartments of the neural epithelium giving rise to striate and extrastriate cortex in the monkey. Cereb Cortex 12:37-53.

Stoykova A, Gruss P (1994) Roles of Pax-genes in developing and adult brain as suggested by expression patterns. J Neurosci 14:1395-412.

Sundaresan V, Chung G, Heppell-Parton A, Xiong J, Grundy C, Roberts I, James L, Cahn A, Bench A, Douglas J, Minna J, Sekido Y, Lerman M, Latif F, Bergh J, Li H, Lowe N, Ogilvie D, Rabbitts P (1998a) Homozygous deletions at 3p12 in breast and lung cancer. Oncogene 17:1723-9.

Sundaresan V, Roberts I, Bateman A, Bankier A, Sheppard M, Hobbs C, Xiong J, Minna J, Latif F, Lerman M, Rabbitts P. The DUTT1 gene, a novel NCAM family member is expressed in developing murine neural tissues and has an unusually broad pattern of expression. (1998b) Mol Cell Neurosci 11:29-35.

Supèr H, Soriano E, Uylings HB (1998) The functions of the preplate in development and evolution of the neocortex and hippocampus. Brain Res Brain Res Rev 27:40-64. Review.

Supèr H, Del Rio JA, Martinez A, Perez-Sust P, Soriano E (2000) Disruption of neuronal migration and radial glia in the developing cerebral cortex following ablation of Cajal-Retzius cells. Cereb Cortex 10:602-613.

Sussel L, Marín O, Kimura S, Rubenstein JL (1999) Loss of Nkx2.1 homeobox gene function results in a ventral to dorsal molecular respecification within the basal telencephalon: evidence for a transformation of the pallidum into the striatum. Development 126:3359-70.

Taglialatela P, Soria JM, Caironi V, Moiana A, Bertuzzi S (2004) Compromised generation of GABAergic interneurons in the brains of Vax1-/- mice. Development 131:4239-49.

Takahashi T, Nowakowski RS, Caviness VS Jr (1995) Early ontogeny of the secondary proliferative population of the embryonic murine cerebral wall. J Neurosci. 15:6058-68.

Takahashi T, Nowakowski RS, Caviness VS (1996a) Interkinetic and migratory behaviour of a cohort of neocortical neurons arising in the early embryonic murine cerebral wall. J Neuro 16:5762-5776.

Takahashi T, Nowakowski RS, Caviness VS Jr (1996b) The leaving or Q fraction of the murine cerebral proliferative epithelium: a general model of neocortical neuronogenesis. J Neurosci 16:6183-96.

Takahashi T, Goto T, Miyama S, Nowakowski RS, Caviness VS Jr (1999) Sequence of neuron origin and neocortical laminar fate: relation to cell cycle of origin in the developing murine cerebral wall. J Neurosci 19:10357-71.

Takiguchi-Hayashi K, Sekiguchi M, Ashigaki S, Takamatsu M, Hasegawa H, Suzuki-Migishima R, Yokoyama M, Nakanishi S, Tanabe Y (2004) Generation of reelin-positive marginal zone cells from the caudomedial wall of telencephalic vesicles. J Neurosci 24:2286-2295.

Tamamaki N, Fujimori KE, Takauji R (1997) Origin and route of tangentially migrating neurons in the developing neocortical intermediate zone. J Neurosci 17:8313-23.

Tamamaki N, Nakamura K, Okamoto K, Kaneko T (2001) Radial glia is a progenitor of neocortical neurons in the developing cerebral cortex. Neurosci Res 41:51-60.

Tamamaki N, Yanagawa Y, Tomioka R, Miyazaki J, Obata K, Kaneko T (2003) Green fluorescent protein expression and colocalization with calretinin, parvalbumin, and somatostatin in the GAD67-GFP knock-in mouse. J Comp Neurol 467:60-79.

Tanaka D, Nakaya Y, Yanagawa Y, Obata K, and Murakami F (2003) Multimodal tangential migration of neocortical GABAergic neurons independent of GPI-anchored proteins. Development 130:5803-5813.

Tanaka DH, Maekawa K, Yanagawa Y, Obata K, Murakami F (2006) Multidirectional and multizonal tangential migration of GABAergic interneurons in the developing cerebral cortex. Development 133:2167-76.

Tarabykin V, Stoykova A, Usman N, Gruss P (2001) Cortical upper layer neurons derive from the subventricular zone as indicated by Svet1 gene expression. Development 128:1983-93.

Tear G, Harris R, Sutaria S, Kilomanski K, Goodman CS, Seeger MA (1996) commissureless controls growth cone guidance across the CNS midline in Drosophila and encodes a novel membrane protein. Neuron 16:501-14.

Thomaidou D, Mione MC, Cavanagh JF, Parnavelas JG (1997) Apoptosis and its relation to the cell cycle in the developing cortex. J Neurosci 17: 1075-1085.

Thompson H, Barker D, Camand O, Erskine L (2006a) Slits contribute to the guidance of retinal ganglion cell axons in the mammalian optic tract. Dev Biol. 296:476-84.

Thompson H, Camand O, Barker D, Erskine L (2006b) Slit proteins regulate distinct aspects of retinal ganglion cell axon guidance within dorsal and ventral retina. J Neurosci 26:8082-91.

Tissir F, Goffinet AM (2003) Reelin and brain development. Nat Rev Neurosci 4: 496-505

Tiveron MC, Rossel M, Moepps B, Zhang YL, Seidenfaden R, Favor J, König N, Cremer H (2006) Molecular interaction between projection neuron precursors and invading interneurons via stromal-derived factor 1 (CXCL12)/CXCR4 signalling in the cortical subventricular zone/intermediate zone. J Neurosci 26:13273-8.

Valcanis H, Tan SS (2003) Layer specification of transplanted interneurons in developing mouse neocortex. J Neurosci 23:5113-22.
Walsh C, Cepko CL (1992) Widespread dispersion of neuronal clones across functional regions of the cerebral cortex. Science 255:434-40.

Walsh C, Cepko CL (1992) Widespread dispersion of neuronal clones across functional regions of the cerebral cortex.Science 255:434-40.

Walsh FS, Doherty P (1997) Neural cell adhesion molecules of the immunoglobulin superfamily: role in axon growth and guidance. Annu Rev Cell Dev Biol 13:425-56. Review.

Wang KH, Brose K, Arnott D, Kidd T, Goodman CS, Henzel W, Tessier-Lavigne M (1999) Biochemical purification of a mammalian slit protein as a positive regulator of sensory axon elongation and branching. Cell 96:771–784.

Whitford KL, Marillat V, Stein E, Goodman CS, Tessier-Lavigne, M (2002) Regulation of cortical dendrite development by Slit-Robo interactions. Neuron 33:47-61.

Wichterle H, Garcia-Verdugo JM, Herrera DG, Alvarez-Buylla A (1999) Young neurons from medial ganglionic eminence disperse in adult and embryonic brain. Nat Neurosci 2:461-6.

Wichterle H, Turnbull DH, Nery S, Fishell G, Alvarez-Buylla A (2001) In utero fate mapping reveals distinct migratory pathways and fates of neurons born in the mammalian basal forebrain. Development 128:3759-71.

Wichterle H, Alvarez-Dolado M, Erskine L, Alvarez-Buylla A (2003) Permissive corridor and diffusible gradients direct medial ganglionic eminence cell migration to the neocortex. Proc Natl Acad Sci U SA100:727-32.

Wong K, Park HT, Wu JY, Rao Y (2002) Slit proteins: molecular guidance cues for cells ranging from neurons to leukocytes. Curr Opin Genet Dev. 12:583-91. Review.

Wu W, Wong K, Chen J, Jiang Z, Dupuis S, Wu JY, Rao Y (1999) Directional guidance of neuronal migration in the olfactory system by the protein Slit. Nature 400:331-6.

Wu SX, Goebbels S, Nakamura K, Nakamura K, Kometani K, Minato N, Kaneko T, Nave KA, Tamamaki N (2005) Pyramidal neurons of upper cortical layers generated by NEX-positive progenitor cells in the subventricular zone. Proc Natl Acad Sci USA 102:17172-7.

Xu Q, Cobos I, De La Cruz E, Rubenstein JL, Anderson SA (2004) Origins of cortical interneuron subtypes. J Neurosci 24:2612-22

Xu Q, Wonders CP, Anderson SA (2005) Sonic hedgehog maintains the identity of cortical interneuron progenitors in the ventral telencephalon. Development 132:4987-98.

Yabut O, Renfro A, Niu S, Swann JW, Marín O, D'Arcangelo G (2007) Abnormal laminar position and dendrite development of interneurons in the *reeler* forebrain. Brain Res 1140:75-83.

Yang L, Bashaw GJ (2006) Son of sevenless directly links the Robo receptor to rac activation to control axon repulsion at the midline. Neuron 52:595-607.

Yau HJ, Wang HF, Lai C, Liu FC (2003) Neural development of the neuregulin receptor ErbB4 in the cerebral cortex and the hippocampus: preferential expression by interneurons tangentially migrating from the ganglionic eminences. Cereb Cortex 13:252-64.

Yoshida M, Assimacopoulos S, Jones KR, Grove EA (2006) Massive loss of Cajal-Retzius cells does not disrupt neocortical layer order. Development 133:537-545.

Yozu M, Tabata H, Nakajima K (2005) The caudal migratory stream: a novel migratory stream of interneurons derived from the caudal ganglionic eminence in the developing mouse forebrain. J Neurosci 25:7268-77.

Yuan SS, Cox LA, Dasika GK, Lee EY (1999a) Cloning and functional studies of a novel gene aberrantly expressed in RB-deficient embryos. Dev Biol 207: 62-75.

Yuan W, Zhou L, Chen JH, Wu JY, Rao Y, Ornitz DM. (1999b) The mouse SLIT family: secreted ligands for ROBO expressed in patterns that suggest a role in morphogenesis and axon guidance. Dev Biol 212:290-306.

Yuan SS, Yeh YT, Lee EY (2002) Pax-2 interacts with RB and reverses its repression on the promoter of Rig-1, a Robo member. Biochem Biophys Res Commun. 296:1019-25.

Yue Y, Grossmann B, Galetzka D, Zechner U, Haaf T (2006) Isolation and differential expression of two isoforms of the ROBO2/Robo2 axon guidance receptor gene in humans and mice. Genomics 88:772-8.

Yung SY, Gokhan S, Jurcsak J, Molero AE, Abrajano JJ, Mehler MF (2002) Differential modulation of BMP signalling promotes the elaboration of cerebral cortical GABAergic neurons or oligodendrocytes from a common sonic hedgehog-responsive ventral forebrain progenitor species. Proc Natl Acad Sci USA 99:16273-8.

Zhu Y, Li H, Zhou L, Wu JY, Rao Y (1999) Cellular and molecular guidance of GABAergic neuronal migration from an extracortical origin to the neocortex. Neuron 23:473-485.

Zimmer C, Tiveron MC, Bodmer R, Cremer H (2004) Dynamics of Cux2 expression suggests that an early pool of SVZ precursors is fated to become upper cortical layer neurons. Cereb Cortex 14:1408-20.

Zimmer G, Garcez P, Rudolph J, Niehage R, Weth F, Lent R, Bolz J (2008) Ephrin-A5 acts as a repulsive cue for migrating cortical interneurons. Eur J Neurosci 28(1):62-73.